

**Synthetic Chemistry for**  
**Tryptophan Tryptophylquinone like**  
**Enzyme Cofactors**

Thesis submitted for the degree of  
Doctor of Philosophy

By

**William Wise**

Department of Chemistry

University of Leicester

May 2011



**University of**  
**Leicester**

## Abstract

This thesis describes studies on the synthesis of model compounds based on the tryptophan tryptophanyl quinone (TTQ) cofactor designed to probe the mechanism by which it catalyses primary amine oxidation and the role of the enzyme in assisting the TTQ-facilitated reaction. This project has begun to explore ways of investigating the mechanistic landscape going from small molecule *ortho*-quinone catalysis through to the corresponding enzymatic reaction to address the proposal that enzyme environment is directly involved in the catalytic activity of the TTQ moiety by facilitating a process known as quantum tunnelling and to determine at what point does the catalytic mechanism ‘swap’ from a classical one to a mechanism involving quantum tunnelling?

The principal goal was therefore to establish a synthetic route to novel amino acid building blocks that contained appropriate functionality that could be converted into the key *ortho*-quinone unit that would mimic TTQ. Such fragments required suitable protecting groups to allow their incorporation into peptide and protein domains. This report describes exploration of two synthetic routes to such molecules, both routes utilising 4-methylphenol that, once modified, incorporates the key *ortho*-quinone unit.

One approach is the synthesis of a novel TTQ-like amino acid that would allow for insertion into a peptide using well documented procedures. This thesis details a variety of different synthetic approaches to the preparation of such a molecule, including problems in coupling the amino acid moiety with the quinone moiety and utilisation of a range of protecting groups in an attempt to overcome these problems.

An alternative approach is also explored involving the synthesis of an *ortho*-quinone cassette that incorporates either alkyne or azide functionality and utilisation of the relatively new field of copper-catalysed click chemistry to insert this unit into an enzyme containing a non-natural amino acid with an alkyne or azide-containing side chain. Again details of a variety of different routes involved in attempting to produce such a molecule are given and although the target molecule was not produced a model system was successfully developed and inserted into an alkyne-containing amino acid.

## Acknowledgements

As with all projects, this one would have been a lot more difficult had it not have been for the support of a few key individuals. My supervisor Professor Paul Cullis and Postgraduate Tutor Katy McKenzie whose continued advice and support throughout this project has helped tremendously; all my friends who work in the Organic Synthesis Laboratory and all support staff including Gerry Griffith, Graham Eaton and Kuldip Singh. Lastly thanks to my father, mother, brother and fiancé; Rebecca Doheny-Hunt, without their support none of this would have been possible!

## Abbreviations

TPP – Thiamine pyrophosphate

PQQ – Pyrroloquinolinequinone

TTQ – Tryptophan tryptophylquinone

MADH – Methylamine dehydrogenase

AADH – Aromatic amine dehydrogenase

PDB – Protein data bank

Trp – Tryptophan

r.m.s.d – Root mean square deviation

$^1\text{H}$  NMR – Proton nuclear magnetic resonance

$^{13}\text{C}$  NMR – Carbon thirteen nuclear magnetic resonance

UV – Ultra violet

KIE – Kinetic isotope effect

TPQ – 2,4,5-Trihydroxyphenylalanine quinone

Asp – Aspartate or aspartic acid

kDa – kilodaltons

His – Histidine

MDH – Methanol dehydrogenase

CTQ – Cysteine tryptophylquinone

LTQ – Lysine tyrosylquinone

CAO – Copper-containing amine oxidase

NOE – Nuclear Overhauser Effect

HPLC – High pressure/high performance liquid chromatography

TST – Transition state theory

TS – Transition state

VEGST – Vibrationally enhanced ground state tunnelling

tRNA – Transfer ribonucleic acid

AChR – Acetylcholine receptor

AChBP – Acetylcholine binding protein

Boc – *tert*-Butyloxycarbonyl

Fmoc – 9-Fluorenylmethyloxycarbonyl

HBTU – *N,N,N',N'*-Tetramethyl-*O*-(1*H*-benzotriazol-1-yl)uronium hexafluorophosphate

TLC – Thin layer chromatography

TMS – Trimethylsilyl

Equiv – Equivalents

DIBAL – Diisobutylaluminium hydride

DMAP – 4-Dimethylaminopyridine

LiAlH<sub>4</sub> – Lithium aluminium hydride

D – Debye

HCl – Hydrochloric acid

PCC – Pyridinium chlorochromate

COD – Cyclo-octadiene

CuAAC – Copper alkyne/azide cycloaddition

NMP – *N*-Methyl-2-pyrrolidone

THF – Tetrahydrofuran

DMF – *N,N*-Dimethylformamide

TMSI – Iodotrimethylsilane

LCMS – Liquid chromatography mass spectroscopy

EDTA – Ethylenediaminetetraacetic acid

DCC – Dicyclohexylcarbodiimide

TBTA – Tris[(1-benzyl-1H-1,2,3-triazol-4-yl)methyl]amine

SBP – Sulfonated bathophenanthroline

NIST – National Institute of Standards and Technology

FTIR – Fourier transform infrared spectroscopy

ATR – Attenuated total reflectance

MH<sup>+</sup> – Molecular cation

MH<sup>-</sup> – Molecular anion

°C – Degrees celcius

D<sub>2</sub>O – Deuterated water

mL – Millilitres

mol – Moles

mmol – Millimoles

g – Grams

CD<sub>3</sub>OD – Fully deuterated methanol (D<sub>4</sub> methanol)

DMSO – Dimethylsulfoxide

M – Molar or mol dm<sup>-3</sup>

CDCl<sub>3</sub> – Deuterated chloroform

DCM – Dichloromethane

hrs – Hours

mg - Micrograms

# Contents

<b>1. INTRODUCTION .....</b>	<b>1</b>
1.1. INTRODUCTION TO ENZYME CATALYSIS .....	1
1.2. TTQ COFACTOR .....	4
1.2.1. <i>TTQ cofactor background</i> .....	4
1.2.2. <i>Biosynthesis of TTQ cofactor</i> .....	6
1.2.3. <i>Mechanism for amine oxidation within TTQ-containing enzymes</i> .....	10
1.2.4. <i>Other proteins that contain a quinone moiety</i> .....	16
1.2.5. <i>Similarities to the pyridoxal phosphate chemistry</i> .....	22
1.3. SYNTHESIS AND MECHANISTIC STUDIES ON TTQ MODELS .....	24
1.3.1. <i>TTQ models</i> .....	24
1.3.2. <i>Biomimetic studies of TTQ biosynthesis</i> .....	25
1.3.3. <i>Probing the amine oxidation mechanism with TTQ</i> .....	31
1.3.4. <i>Overall amine oxidation mechanism</i> .....	36
1.4. CATALYTIC EFFICIENCY OF <i>ORTHO</i> INDOLEQUINONES .....	38
1.4.1. <i>Catalytic efficiency of the synthetic TTQ model compound (18)</i> .....	38
1.4.2. <i>Structure-reactivity relationship studies – the role of aromaticity</i> .....	39
1.4.3. <i>Catalytic efficiency of other ortho-quinones</i> .....	41
1.4.4. <i>The role and electronic effects of C-4 substituents in ortho-indolequinones</i> .....	46
1.4.5. <i>Electronic effects of substrates</i> .....	47
1.5. QUANTUM TUNNELLING .....	48
1.5.1. <i>Classical transition-state theory (TST)</i> .....	48
1.5.2. <i>Quantum tunnelling history</i> .....	51
1.5.3. <i>Quantum tunnelling comparison for electrons vs. hydrogen</i> .....	54
1.5.4. <i>The kinetic isotope effect (KIE)</i> .....	56
1.6. HYDROGEN/PROTON TUNNELLING IN MADH .....	58
1.6.1. <i>The background of proton tunnelling in MADH</i> .....	58
1.6.2. <i>The static potential-energy barrier theory</i> .....	59
1.6.3. <i>Vibrationally enhanced ground-state tunnelling (VEGST)</i> .....	61
1.6.4. <i>The resulting dynamic barrier model</i> .....	62
1.6.5. <i>Concluding remarks on quantum tunnelling in the synthetic TTQ model compound (18) and TTQ containing enzyme</i> .....	63
1.7. INSERTION OF UNNATURAL AMINO ACIDS INTO A PROTEIN STRUCTURE.....	65
1.7.1. <i>Background to unnatural amino acid mutagenesis</i> .....	65
1.7.2. <i>Previous unnatural amino acid insertions</i> .....	66
1.7.3. <i>Limitations and advances</i> .....	68
1.8. OBJECTIVES FOR TTQ MODEL CHEMISTRY .....	70
<b>2. TTQ ANALOGUES INCORPORATING THE AMINO ACID FUNCTIONALITY .....</b>	<b>72</b>
2.1. INTRODUCTION .....	72
2.2. THE PROPOSED ROUTE TO THE TARGET COMPOUND .....	76
2.2.1. <i>Retrosynthetic analysis</i> .....	76
2.2.2. <i>Intended reaction scheme</i> .....	77
2.3. SYNTHESIS OF THE AMINO ACID FRAMEWORK .....	79
2.3.1. <i>Initial route to glutamic acid derived aldehyde</i> .....	80

2.3.2. <i>An alternative route to glutamic acid derived aldehyde</i> .....	88
2.4. SYNTHESIS OF THE QUINONE MOIETY FRAMEWORK.....	93
2.4.1. <i>Originally planned route to hydrazine derivative</i> .....	94
2.4.2. <i>Problems with conversion to the hydrazine derivative</i> .....	97
2.4.3. <i>An alternative approach to formation of quinone framework</i> .....	102
2.5. THE FISCHER INDOLE REACTION .....	105
2.5.1. <i>Using the inorganic non-acid catalysed Fischer indole</i> .....	106
2.5.2. <i>'Classic' Acid Catalysed Fischer Indole</i> .....	110
2.6. SUMMARY.....	117
<b>3. ALTERNATIVE APPROACHES TO INSERTING TTQ ANALOGUES INTO A PEPTIDE/PROTEIN BACKBONE.....</b>	<b>119</b>
3.1. NEW 'CLICK' CHEMISTRY POSSIBILITY .....	119
3.1.1. <i>Introduction to click chemistry</i> .....	121
3.1.2. <i>Click reactions in vitro and in vivo</i> .....	125
3.1.3. <i>Synthesis of target alkyne</i> .....	128
3.1.4. <i>Synthesis of target azide</i> .....	132
3.1.5. <i>Deprotection of methylether protected phenol</i> .....	137
3.1.6. <i>Summary</i> .....	144
3.2. PROOF THAT 'CLICK' CHEMISTRY IS VIABLE .....	145
3.2.1. <i>Initial problems and their solutions</i> .....	146
3.2.2. <i>The wider picture</i> .....	151
<b>4. CONCLUSIONS AND FURTHER WORK.....</b>	<b>153</b>
<b>5. EXPERIMENTAL.....</b>	<b>157</b>
5.1. GENERAL EXPERIMENTAL INFORMATION .....	157
<b>REFERENCES.....</b>	<b>230</b>
<b>7. APPENDIX.....</b>	<b>244</b>
7.1. APPENDIX 1 – X-RAY CRYSTAL DATA .....	244
7.1.1. <i>5-benzyl-1-methyl-2-(tert-butoxycarbonylamino)-pentanedioate</i> .....	244
7.1.2. <i>2-Methoxy-4-methyl-6-nitrophenol</i> .....	246
7.1.3. <i>7-methoxy-4-methyl-3-(prop-2-ynyl)-1H-indole</i> .....	248
7.1.4. <i>Methyl-2-(7-methoxy-2,4-dimethyl-1H-indol-3-yl)-acetate</i> .....	250

# 1. Introduction

## 1.1. Introduction to Enzyme Catalysis

Enzymes are normally protein-based biological molecules that act as biological catalysts. As catalysts they have the following properties:<sup>1</sup>

- They can accelerate the rate of reactions by a factor  $1 \times 10^{19}$  over the uncatalysed route<sup>2</sup> and do so under mild conditions.
- They can be highly selective for substrates and stereoselective in the reactions they catalyse.
- They may be subject to regulation i.e. the catalytic activity can be influenced by concentrations of substrate, products and other species (allosteric regulators).
- Most enzymes catalyse reactions under the same conditions.

It is because of these desirable traits that there has been some considerable work carried out to better understand how this catalytic activity/rate acceleration is achieved.

It was back in 1946, before structural information about enzymes was available, that Linus Pauling first proposed a probable reason for the fast rates of reaction observed during enzyme catalysed reactions.<sup>3</sup> He suggested that the molecules had a higher binding affinity towards the transition state than that of either the substrate or product. It was this that resulted in the activation barrier being lowered and the subsequent improvement in the rate of reaction.<sup>3</sup>

Amongst rapidly growing interest in this area an interesting publication in 1978<sup>4</sup> continued to echo the original postulation by Pauling. It reported that “the entire and sole source of catalytic power [of enzymes] is due to stabilisation of the transition

state,”<sup>4</sup> a statement that is still widely accepted. Modern concepts of transition state theory, the availability of structural, kinetic and thermodynamic data and the advent of computer simulations have resulted in the minor modification of this statement to “the entire and sole source of catalytic power of enzymes is due to the lowering of the free energy of activation and any increase in the generalised transmission coefficient, as compared to that of the uncatalysed reaction.”<sup>5</sup>

The difficulty in understanding the detailed mechanism for the reduction of the activation barrier and subsequent increase in reaction rate is due to the complexity of a many bodied system such as an enzyme in solution.<sup>5</sup> There tends to be a large number of reaction paths each having one or more ‘saddle’ points,<sup>6, 7</sup> something that differs when in comparison to a small-molecule gas-phase reaction where the potential surface often has a single valley leading to a single saddle point.<sup>5</sup>

Initially it was thought that hydrogen bonding (dominated by electrostatics) was one of the main effects used to stabilise the transition state.<sup>5</sup> However recent analysis of enzyme catalysis is beginning to provide detailed understanding of how the activation barrier is lowered and includes the contributions made by the structure and flexibility of the enzyme itself. The former provides a “pre-organised environment” that enhances catalysis<sup>8</sup> by providing a stronger stabilisation of the transition state than of the reactant state (either as bound enzyme substrate or free enzyme and substrate). However as a result of the flexibility of the enzyme the studies of enzymatic mechanisms must take into account the conformational free energy of the enzyme as well as that of the substrate, remembering that both can be different at the transition state to that of the reactant state.<sup>5</sup> Although there are now many good examples of this, one that has been well documented is that of the enormous catalytic efficiency of orotidine monophosphate decarboxylase.<sup>5, 7-12</sup> It appears that this enzyme is itself more

stable in the transition state than when it is in the reactant state which contributes to the lowering of the activation energy. It's thought that this process occurs due to the strain that is induced when the substrate binds, only being relieved at the transition state.

In addition to the electrostatic effects, if the difference between the reactant state and transition state involves substantial charge transfer (as is the case in many enzymatic reactions) then the position of particular charged groups in the enzyme must be considered.<sup>5</sup> The 'charged groups' cover a wide range of groups including metal ions and enzyme cofactors/ coenzymes/ prosthetic groups.

Cofactors are compounds that are required for biological activity of an enzyme but are rarely derived from the protein backbone. They can be divided into two categories inorganic cofactors, normally metals, and organic cofactors which are often vitamin derived compounds that are often tightly bound to the enzyme. In both cases an enzyme without its corresponding coenzyme is normally biologically inactive; such inactive enzymes are called 'apoenzyme.'<sup>13</sup>

Coenzymes vary in how strongly they bond to their corresponding enzymes, in some cases identical cofactors can be tightly bound in one enzyme but loosely bound in another enzyme.<sup>13</sup> One such example is a vitamin B1 derivative, thiamine pyrophosphate (TPP) (Figure 1) which is bound strongly in both transketolase<sup>14</sup> and pyruvate decarboxylase<sup>15</sup> and yet only weakly bound in pyruvate dehydrogenase.<sup>16</sup>

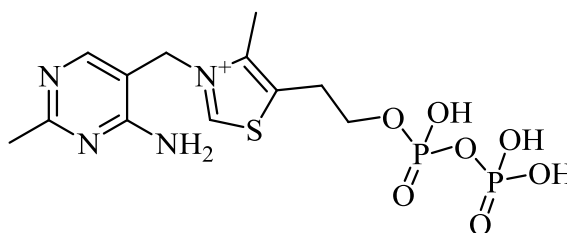


**Figure 1:** The structure of thiamine pyrophosphate.<sup>15</sup>

Another example of the varying degree to which the coenzymes bind to their corresponding enzymes is in the quinone family of coenzymes. Since the discovery, isolation and identification of the first of the cofactors that fit into this family, pyrroloquinone quinone (PQQ) (Figure 7) by Salisbury *et al.*,<sup>17</sup> this novel family of cofactors has been the focus of a great deal of research. The primary reason for initial research into PQQ was as a result of its unusual fluorescence properties and its ability to catalyse a wide variety of redox reactions. Further interest in the ‘new’ quinone was driven by the nutrition industry as cofactors are often required nutrients.<sup>18</sup> The ensuing research established the unambiguous structures of several new cofactors (including tryptophan tryptophylquinone (TTQ) shown in Figure 2) all containing the quinone moiety and sharing similar chemical/biochemical properties.<sup>18</sup> However the mechanism by which each of these cofactors is biosynthesised and incorporated into the corresponding enzymes varies greatly. Furthermore whilst the understanding of how these cofactors function as standalone molecules is now extensive, the role that the enzyme/protein plays in the catalytic cycle is understood to a much lesser extent.

## 1.2. TTQ Cofactor

### 1.2.1. TTQ cofactor background

The first published structure of the tryptophan tryptophylquinone (TTQ) cofactor (**1**) (shown below in Figure 2) was by W.S. McIntire *et al.* in 1991.<sup>19</sup> Since then the role of this cofactor has been extensively studied in both methylamine dehydrogenase (MADH),<sup>20, 21</sup> where it was originally discovered, and aromatic amine dehydrogenase (AADH).<sup>22, 23</sup> The framework consists of a 6,7-indolequinone with a covalently bound 2-indoyl group at the C-4 position.<sup>24</sup>

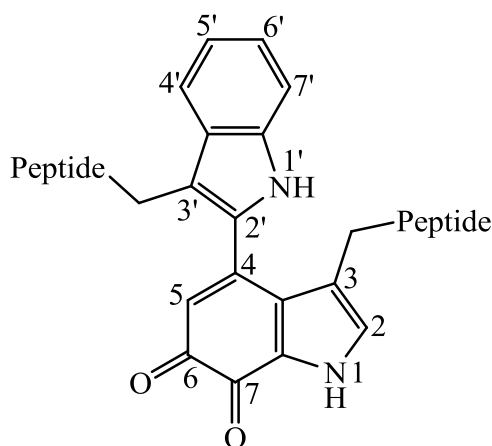
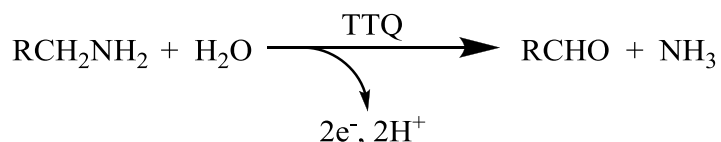


**Figure 2:** The structure of the TTQ cofactor (**1**).<sup>19</sup>

Importantly, something that the above diagram illustrates is that the TTQ cofactor (**1**) is bound covalently at the C-3 and C-3' positions to the polypeptide chain as an integral amino acid residue. This is something that separates it from other common cofactors, including some other quinone cofactors<sup>25</sup> and is also why it cannot be readily isolated intact from the enzyme matrix.<sup>26</sup>

There is now unquestionable evidence that the TTQ cofactor **1** shows redox behaviour in catalysing the oxidation of primary amines to their corresponding aldehydes, liberating ammonia.<sup>27, 28</sup> This process involves the donation of two electrons to a copper protein, amicyanin in the case of MADH<sup>29, 30</sup> and azurin in the case of AADH.<sup>31</sup> The generic equation for this oxidation of primary amines is shown below (Scheme 1):



**Scheme 1:** Generic scheme for oxidation of primary amines.<sup>19</sup>

### 1.2.2. Biosynthesis of TTQ cofactor

An important step in understanding both TTQ (**1**) and the enzymes that utilise this cofactor is to understand its biosynthesis. Even before the identification of the TTQ cofactor (**1**) much effort had been directed towards understanding the structure of MADH. Clearly the cofactor (later referred to as TTQ) is a very important, integral part of the functional enzyme and thus in an effort to investigate the biosynthesis of the TTQ cofactor (**1**) researchers had to first isolate MADH and AADH.

The enzyme MADH (Figure 3) was isolated from the bacterium *Paracoccus denitrificans* where, initially, it was wrongly assumed that the isolated enzyme contained the coenzyme pyrroloquinolinequinone (PQQ (**13**))<sup>32</sup> as opposed to TTQ (**1**) that was later identified by W.S. McIntire *et al.*<sup>19</sup> AADH (Figure 3) was isolated from the bacterium *Alcaligenes faecalis* at a much later date.<sup>22, 33</sup>

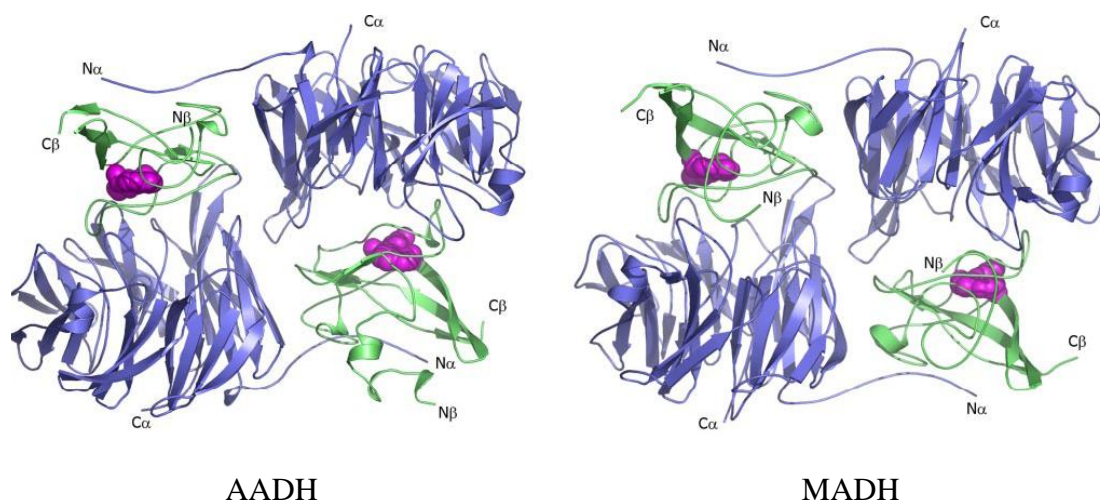


**Figure 3:** Comparison of the structures of *Alcaligenes faecalis* AADH (PDB code: 2AH1) and *Paracoccus denitrificans* MADH (PDB code: 2BBK). The TTQ cofactor (**1**) atoms are depicted as magenta spheres,  $\alpha$  subunits are depicted in blue, and the catalytic  $\beta$  subunits are shown in green.<sup>34, 35</sup>

As exemplified above, the structures of AADH and MADH (superposition of which has the PDB code 1MDA<sup>36</sup>) reveal the significant similarity between the two enzymes. This similarity extends over the entire length of the protein; both have a symmetrical tetrameric  $\alpha_2\beta_2$  structure of which the  $\beta$  subunit contains the covalently bound TTQ cofactor (**1**) and in both cases the  $\alpha$  subunit is the more substantial. In fact, similarities do not stop there; alignment of the  $\alpha\beta$  dimers of AADH and MADH reveals that 347  $C_\alpha$  atoms can be superimposed with a root mean square deviation (r.m.s.d.) of 2.3 Å. Alignment of the small subunits alone results in a much better match whereupon 105  $C_\alpha$  atoms overlap with a r.m.s.d. of 0.9 Å.<sup>34</sup>

However one notable difference between the two enzymes is the subunit molecular weights which are:<sup>22, 32, 37</sup>

AADH:  $\alpha = 39,000$ ,  $\beta = 18,000$

MADH:  $\alpha = 46,700$ ,  $\beta = 15,500$

From this information it is evident that AADH possesses a significantly smaller  $\alpha$  subunit and larger  $\beta$  subunit when compared to MADH.<sup>22</sup>

The TTQ cofactors (**1**) in both MADH and AADH are post-translationally derived from two tryptophan residues within the  $\beta$  subunit at the enzyme active site.<sup>38</sup> In the case of MADH this occurs between tryptophan residue 57 (trp57) and tryptophan residue 108 (trp108)<sup>39</sup> whereas with AADH (Figure 4) it occurs between trp109 and trp160.<sup>34</sup> In both cases only one of the tryptophan residues has been oxidised to the *o*-quinone; in MADH this is trp57<sup>40</sup> and in AADH this is trp109.<sup>34</sup>

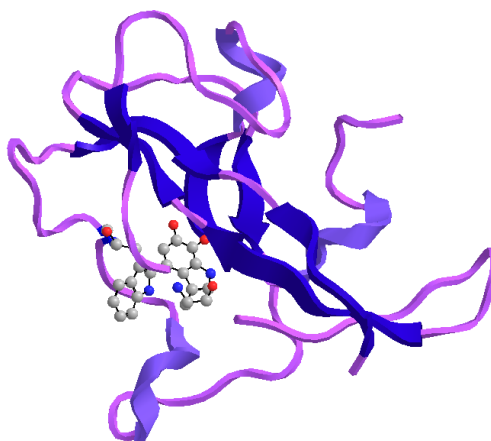
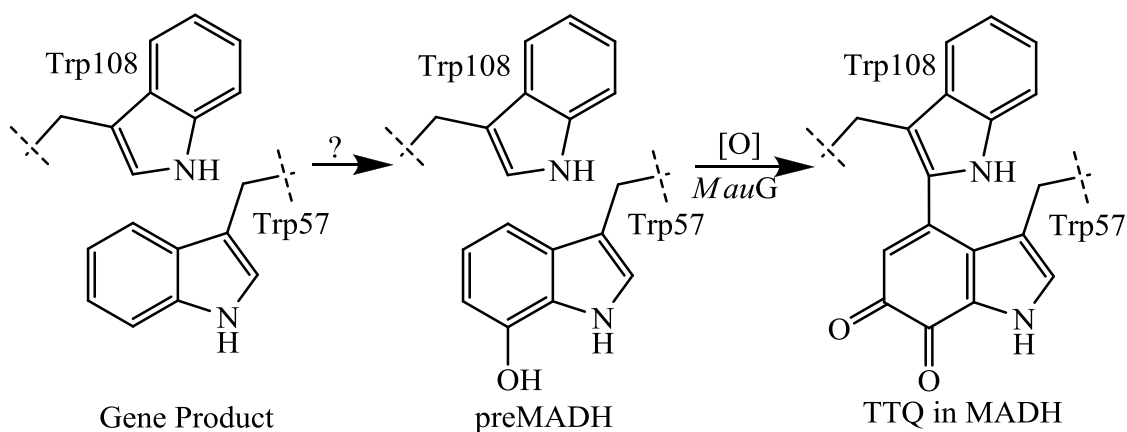


**Figure 4:** A ribbon diagram of the  $\beta$  subunit of AADH clearly showing the TTQ cofactor (**1**) in ‘ball and stick’ format.<sup>34</sup>

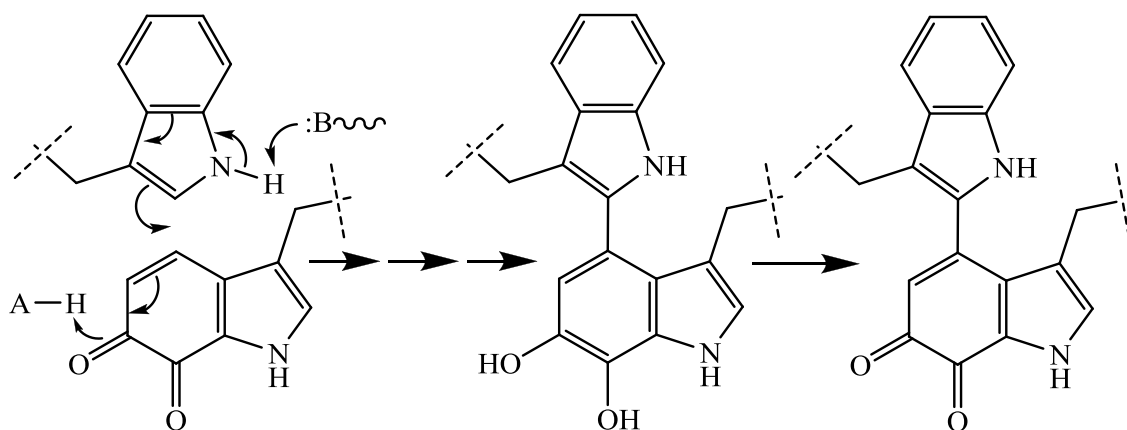
TTQ (**1**) differs from many other protein-derived enzyme cofactors in that it is not formed autocatalytically, certainly in MADH the process involves the co-expression of four other genes including, MauG, which encodes a di-heme c-type cytochrome.<sup>40</sup> This oxidation process has been proved by the *in vivo* mutation or removal of the MauG which in turn severely compromises the conversion of the tryptophan residue to the fully oxidised *o*-quinone. The oxidation steps may then be catalysed *in vitro* upon addition and incubation of the proteins product from MauG with the isolated biosynthetic intermediates.<sup>41</sup>

Even knowing that the formation of TTQ (**1**) is a MauG dependent process, it is unclear what the full mechanism for formation of TTQ (**1**) is. From isotopic studies with  $^{18}\text{O}_2$  and  $\text{H}_2^{18}\text{O}$  it has become evident that the second oxygen insertion catalysed by MauG is at C6 of the cofactor.<sup>40</sup> It is important to note however, that the source of the oxygen atom could not be ascertained and the mechanism of initial hydroxylation at C7 of  $\beta\text{Trp}57$  (within MADH) is also unknown (Scheme 2).<sup>42</sup>



**Scheme 2:** A general overview of TTQ (1) biosynthesis. Oxidation equivalents ([O]) may be provided by  $O_2$  plus an electron donor or by  $H_2O_2$ .<sup>42</sup>

In the second of these mechanistic transformations (Scheme 2) the process not only involves oxidation but also forming of the covalent bond between the two tryptophan molecules. It had been postulated by W.S. McIntire *et al*<sup>19</sup> and is now widely accepted that this takes place by the following mechanism (Scheme 3):

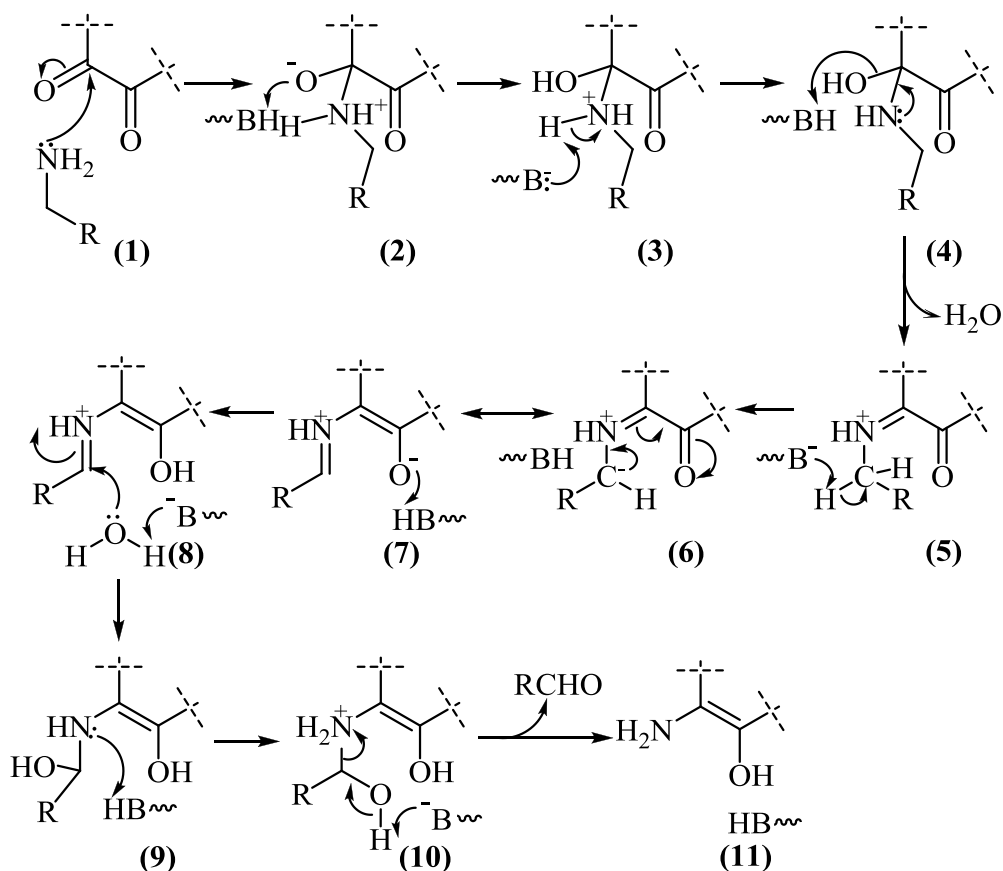


**Scheme 3:** The widely accepted mechanism by which the covalent linkage between the two tryptophan molecules is formed.<sup>19, 34, 43, 44</sup>

### 1.2.3. Mechanism for amine oxidation within TTQ-containing enzymes

There have been numerous studies throughout the years, in an effort to gain a better understanding on the mechanism of amine oxidation involving the TTQ cofactor (1).<sup>23, 26, 38, 43, 45, 46</sup> Such studies have involved the use of standard spectroscopic techniques e.g. <sup>1</sup>H NMR, <sup>13</sup>C NMR, mass spectroscopy and UV visible spectroscopy as well as Raman spectroscopy, X-ray crystallography and stopped-flow kinetics to analyse reaction intermediates. Some intermediates were also trapped by modification of the reaction substrates as well as use of inhibitors.

All of this allowed the breakdown of the mechanism into two separate reactions; a reductive half-reaction (Scheme 4) and an oxidative half-reaction (Scheme 5) resulting in an overall ‘redox’ reaction.<sup>26, 39, 39, 47</sup>



**Scheme 4:** General reductive half-equation of TTQ (1).<sup>47</sup>

Anthony proposed the above scheme which he had adapted from a mechanism originally proposed by Davidson *et al* using methylamine as the amine substrate.<sup>47</sup> The reductive half equation shown above further modifies this proposal to include all possible metabolised amines within the TTQ cofactor (**1**) containing enzymes, as the reductive half-reaction mechanism for AADH that had been proposed by Davidson *et al* is almost identical.<sup>37</sup>

The mechanism shows initial nucleophilic attack of a general amine at the C6 position of the TTQ cofactor (**1**) to form carbinolamine (**4**). This carbinolamine (**4**) then subsequently loses water to give the iminoquinone Schiff base (**5**) and subsequent abstraction of a proton from the  $\alpha$ -carbon atom of the amine substrate by the active-site base to give the carbanion intermediate (**6**). This leads to reduction of the TTQ ring system with production of an isomeric Schiff base (**7**), which is hydrolysed to the aldehyde product and the aminoquinol form of the coenzyme.

The most important feature of this mechanism (Scheme 4) is the proton abstraction from the iminoquinone Schiff base (**5**) to the carbanion (**6**) (C-H cleavage). The reason this step is of particular interest is because in these experiments, and in similar experiments using the aromatic amine dehydrogenase, an exceptionally large primary deuterium isotope effect of between 9.3-17.2 was observed.<sup>47-49</sup> This large deuterium kinetic isotope effect, measured using steady-state kinetic studies, implies that the major rate-limiting step is the abstraction of a proton from the methyl group.<sup>50</sup> Subsequent stopped-flow kinetics confirmed this suggestion and demonstrated the presence of two further kinetically significant intermediates, a relatively fast transition due to reduction of TTQ by substrate and a slower transition due to release of the aldehyde product.<sup>47</sup>

In these experiments, and the similar experiments with the aromatic amine dehydrogenase, the explanation of this large KIE was initially not clear. However it was similar to that observed in the proton abstraction step in the topa-quinone (TPQ) containing amine oxidase, which was attributed to a mechanism involving quantum-mechanical tunnelling.<sup>47</sup> This theory is further discussed in section 1.5.

Another feature of the mechanism (Scheme 4) is that there is a regioselective nucleophilic attack on the C6 carbonyl of the TTQ cofactor (**1**) by the amine. This was assumed after Huizinga *et al* presented data that established C6 of the TTQ cofactor of MADH as the reactive site at which nucleophilic attack takes place. This finding correlates well with the fact that in the structure of free MADH, C6 but not C7 is exposed to the active site pocket which is more clearly shown in Figure 5 below.<sup>45</sup>

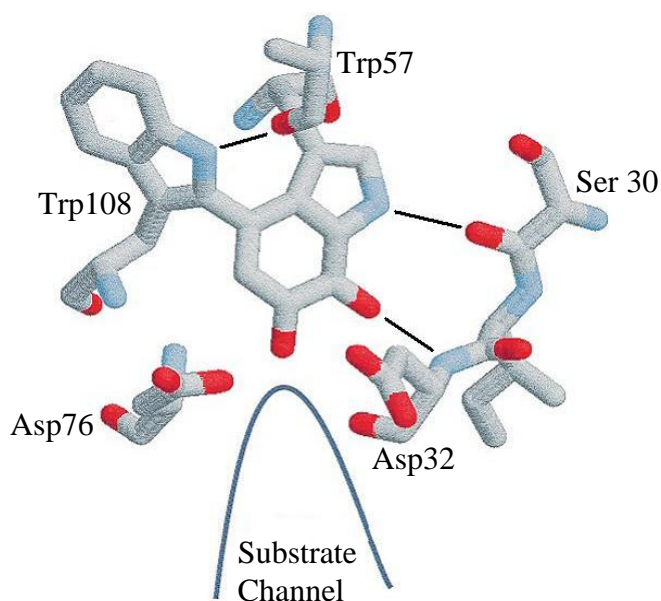
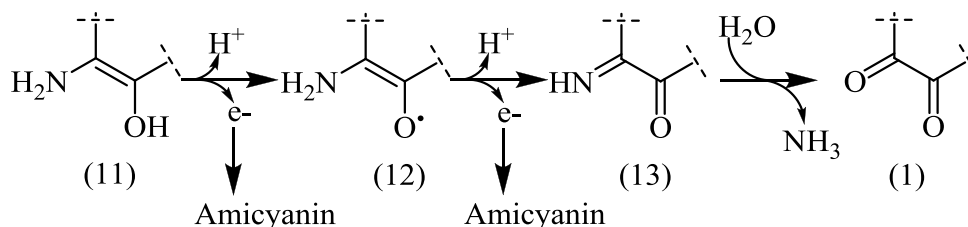


**Figure 5:** TTQ in the active site of methylamine dehydrogenase from *Paracoccus denitrificans*. The hydrogen bonds to the TTQ are shown together with Asp76, which it has been suggested is likely to be the active site base.<sup>47</sup>

Another noteworthy point in the proposed reductive half-reaction mechanism is that a base is shown to be involved in many separate steps in the overall sequence; this

may be the same base, but a second base may also be involved. The X-ray structure of the MADH (Figure 5) indicates that the base involved in the  $\alpha$  proton abstraction is probably Asp76 and that base involved in the conversion of products (7) to (8) is most likely Asp32.<sup>47</sup>

The second part of the complete mechanism is that of the oxidation half-reaction (see Scheme 5), which in conjunction with the reductive half-reaction completes the catalytic redox cycle. The purpose of this half of the catalytic cycle is rejuvenation of the catalyst TTQ (1) and release of ammonia.



**Scheme 5:** Generic oxidative half-reaction.<sup>47</sup>

The first step in this part of the catalytic cycle is the loss of a proton and an electron from the aminoquinol (11) to form a semiquinone intermediate (12). This reaction intermediate (12) is quite stable,<sup>47</sup> has been known for some time and has been confirmed by electron spin resonance (also known as electron paramagnetic resonance) and Raman spectroscopy.<sup>51</sup> It is likely that the unpaired electron in this intermediate is stabilised by delocalisation within the indole ring of the TTQ cofactor.

Further loss of another proton and an electron results in the formation of a ‘primary ketimine’ like intermediate (13). This intermediate then undergoes hydrolysis to reform the TTQ cofactor (1) and release ammonia. This is likely to involve an acid

and base at the active site, which may be the same base(s) involved in the reductive half-reaction (Scheme 4).

One of the key features of this mechanism is the loss of two single electrons; a process facilitated by two molecules of a small (11.7kDa) blue copper containing proteins called amicyanin.

Crystal structures of amicyanins from *Paracoccus versutus* (1id2.pdb) and *Paracoccus denitricans* (1aan.pdb) have been published,<sup>52, 53</sup> as has the crystal structure of the binary MADH–ami complex (1mda.pdb), the important binding interface of which is shown (Figure 6).<sup>36, 47</sup> Early studies on the amicyanin–MADH interaction had indicated that electrostatics play an important role, since the proteins associate better at low ionic strengths. However hydrophobic forces are now also thought to be important, especially since the crystal structure of the complex has mainly hydrophobic amino acids at the binding interface.<sup>54</sup>

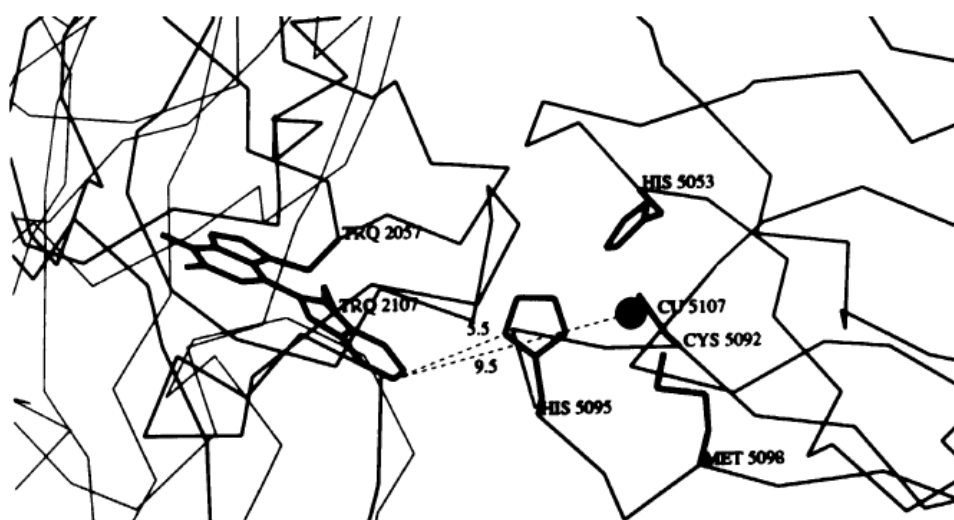


**Figure 6:** Interaction between MADH (left) and amicyanin (right), with the TTQ cofactor highlighted along with important residues within amicyanin.<sup>47</sup>

In Figure 6 above, the quinone part of the TTQ cofactor (**1**) is on Trp57 (TRQ 2057 in this scheme) and the second tryptophan ring, Trp108 (TRQ 2157 in this scheme) is shown to be nearer (9.5Å) the electron acceptor (Cu 5107) of amicyanin. The shortest distances between the TTQ and the copper atom and to the his95 (His-5095) are given in Å. His95, one of the four copper ligands, is on the surface of the protein and about half-way between the copper and the TTQ; it was therefore suggested that this histidine might mediate electron transfer between the redox centres, thus forming an electron transfer triad.<sup>36</sup>

One other noteworthy thing that Figure 6 does not clearly depict is that the two indole rings of the TTQ cofactor are not co-planar, but instead the molecule have a twisted conformation. The two tryptophan halves that make up TTQ cofactor (**1**) have a dihedral angle of approximately 42°. <sup>55</sup> The studies have shown that the delocalization of electrons into the ring system of the semiquinone is consistent with the route for departure of electrons from the indole ring that was proposed on the basis of the X-ray structure<sup>36</sup> and kinetic studies.<sup>56</sup>

This dihedral angle is consistent with molecular orbital calculations by the AM1 method which indicated that the dihedral angle of the two indole rings, defined by 5-C-4-C-2'-C-3'-C in the optimized structure of the TTQ cofactor (**1**), is 46.9°. This is interesting because the molecular geometry of TTQ (**1**) in the enzyme active site is almost tuned to that having the minimum steric energy of the molecule in spite of the existing steric restriction through space and/or through peptide bonding around the enzyme active site.<sup>57</sup>

#### 1.2.4. Other proteins that contain a quinone moiety

The TTQ cofactor (**1**) is not the only cofactor to contain a quinone. There is a family of so called quinoproteins that contain cofactors that incorporate a quinone functional group (cofactor).

Pyrrroloquinoline quinone (PQQ) (**13**) was the first of these cofactors to be found in *Bacterium anitratum* and was only the third ever prosthetic group to be identified, although at the time it was not known as PQQ.<sup>58</sup> However, despite its early discovery PQQ was not isolated and characterised until 1979 by two research groups (see Figure 7 below).<sup>17, 59</sup>

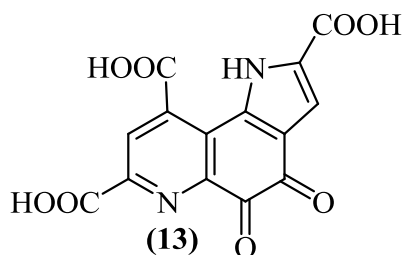


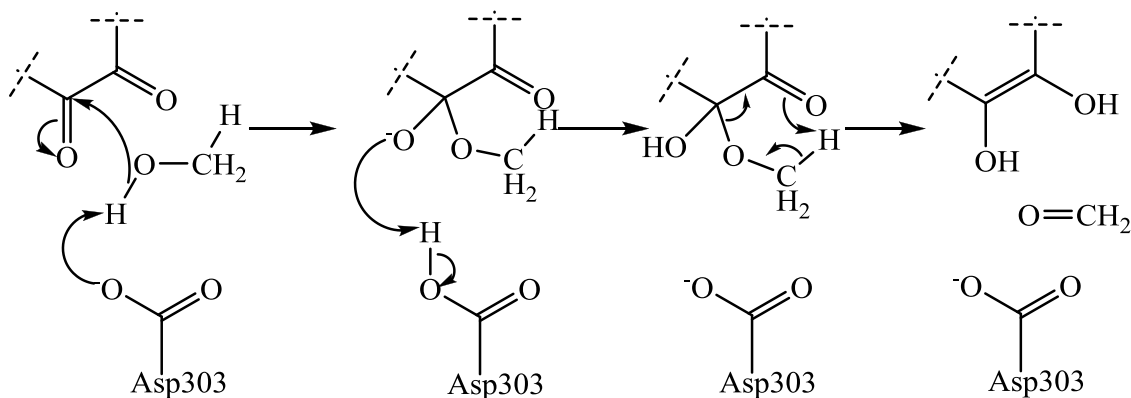
**Figure 7:** The structure of PQQ.<sup>47</sup>

Looking at the structure of PQQ (**13**) it is possible to identify similarities between it and the TTQ cofactor (**1**); obviously both have the quinone moiety, but both molecules also have the indole ring. Importantly though PQQ (**13**) has a 5, 4 quinone as opposed to the 6, 7 system in the TTQ cofactors (**1**).

It is believed that PQQ (**13**) is the only quinone containing cofactor that is tightly but not covalently bound in the enzyme active site.<sup>60</sup> PQQ (**13**) is found in bacterial enzymes where it catalyses the oxidation of a range of alcohols to their corresponding aldehydes or ketones. One such enzyme that PQQ (**13**) is found in is methanol dehydrogenase (MDH) where it catalyses the oxidation of methanol to

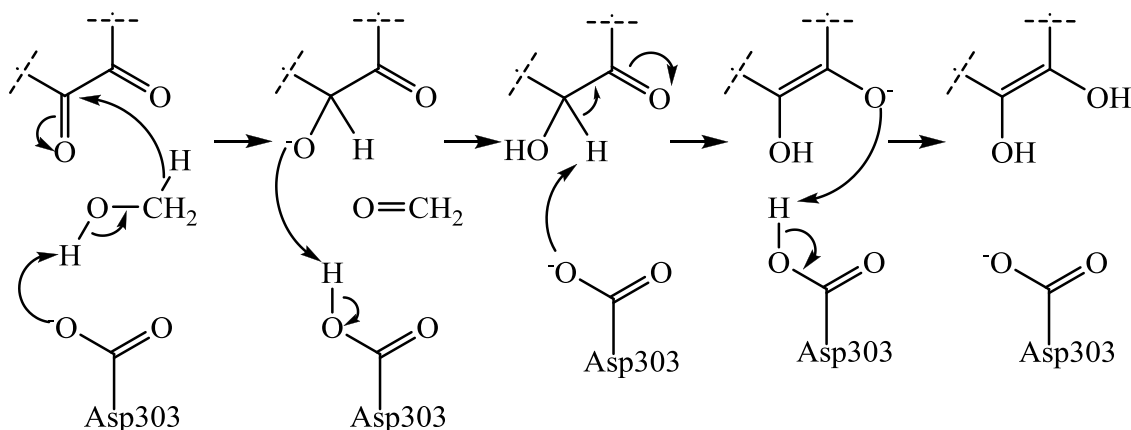
methanal (formaldehyde). As with TTQ (**1**), PQQ (**13**) has two halves to its full catalytic cycle; a reductive half-reaction (three possibilities are shown in Schemes 6, 7 and 8) and an oxidative half-reaction (shown in Scheme 15).<sup>50, 61, 62</sup>

The reaction mechanism of MDH has been more difficult to elucidate by kinetic and spectroscopic investigations than those of the other types of quinoprotein. This is because the isolated enzyme contains PQQ in the fully reduced form or as the semiquinone, and so addition of substrate (a two electron donor) does not lead to its reduction. The enzyme also becomes inactivated when oxidized with artificial electron acceptors. It is for these reasons that there have been so many proposed mechanisms for the reductive half reaction and only some of these suggestions have been disproved.<sup>47</sup>



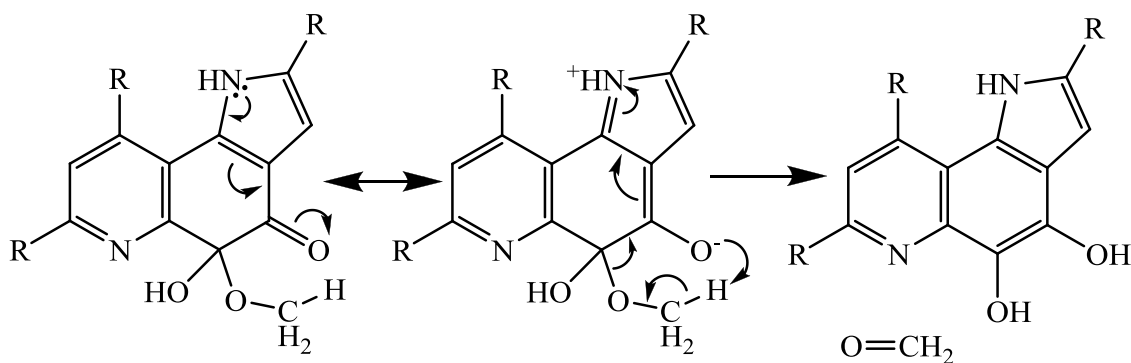
**Scheme 6:** MDH reductive half-reaction mechanism involving hemiketal intermediate.<sup>61</sup>

The first of the proposed mechanisms (Scheme 6) shows a proton abstraction by the *in situ* active site base (Asp303) resulting in a nucleophilic attack at the electrophilic C-5. This results in the hemiketal intermediate from which the methyl proton is abstracted, which in turn gives the quinol and product formaldehyde.



**Scheme 7:** MDH reductive half-reaction mechanism involving hydride transfer.<sup>61</sup>

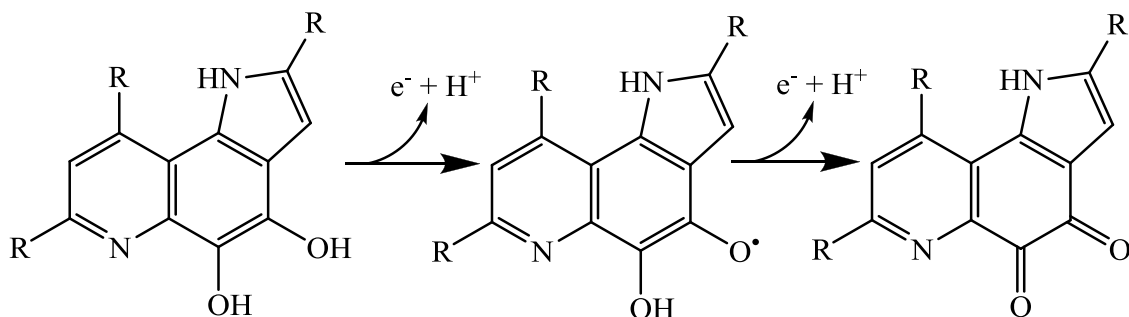
The second of the proposed mechanisms (Scheme 7) suggested as an alternative to that shown in Scheme 6. The key difference is that there is no covalent bonding of substrate. In this case the initial proton abstraction is the same, but the electrophilic C-5 is involved directly in removal of the methyl hydrogen as a hydride. The active-site base (Asp303) acts twice in the mechanism.



**Scheme 8:** MDH reductive half-reaction mechanism involving pyrrole nitrogen.<sup>47, 63</sup>

Despite its striking similarity to scheme 6, mechanism three (Scheme 8) is a further development as it directly utilises the pyrrole nitrogen to facilitate the

problematic proton abstraction from the methyl group by increasing the polarisation of the C4 carbonyl oxygen.



**Scheme 9:** MDH oxidative half-reaction mechanism.<sup>47</sup>

The oxidation step seen above (Scheme 9) is almost identical to that of TTQ (**1**), again highlighting the similarities between the two cofactors. The only real difference is that the electron acceptor which is either a dye such as phenazine ethosulphate or possibly another natural electron acceptor such as cytochrome.

In all the proposed mechanisms another similarity between PQQ (**13**) and TTQ (**1**) is shown as the mechanism involves an in situ aspartate residue which facilitates the reaction by acting as an active site base. However unlike in TTQ (**1**), it is also believed that a calcium ion contained within the MDH helps this process by coordinating to the PQQ and helping to maintain its active conformation.<sup>47</sup>

Cysteine tryptophylquinone (CTQ) (**14**) (Figure 8) is present in quinoxinohemoprotein amine dehydrogenases.<sup>64</sup>

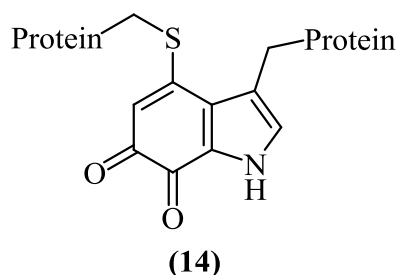


**Figure 8:** The structure of CTQ.<sup>65</sup>

CTQ (14), above, can be easily compared to TTQ (1) as they both have a similar indolequinone structure. As with TTQ (1), CTQ (14) is derived post-translationally from an active site tryptophan, however as its name suggests CTQ (14) also forms a thioether linkage with a nearby cysteine in the enzyme active site. Similarly to TTQ (1) this results in it being covalently bound to the enzyme matrix through peptide bonds. In spite of having different C-4 substituent's to that of TTQ (1), CTQ (14) catalyzes oxidative deamination of primary amines to the corresponding aldehydes.<sup>65</sup>

Lysine tyrosylquinone (LTQ) (15) is yet another quinone containing cofactor (Figure 9) although it is much smaller in size than the previously studied quinone cofactors:

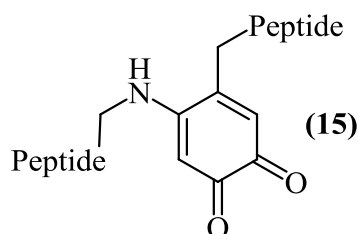


**Figure 9:** The structure of LTQ.<sup>66</sup>

It is found in one of the mammalian copper-containing amine oxidases (CAOs), lysyl oxidase. It is derived, again as its name suggests, from the cross-linking of a modified tyrosine residue to a lysine side chain. The lysyl oxidase quinoprotein plays an important role in the development of connective tissues through its catalysis to form inter- and intra-chain protein cross-linkages.<sup>66</sup>

One key and notable difference between LTQ and the other quinone cofactors studied thus far is that it does not have the 6,7-inolequinone skeleton. It is this fact that LTQ also has in common with the final quinone containing cofactor 2,4,5-trihydroxyphenylalanine quinone (TPQ) (**16**) (Figure 10) now called topa quinone.<sup>66-68</sup>

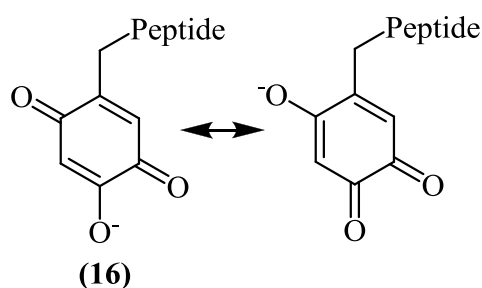


**Figure 10:** The two resonance canonicals of TPQ.

Similarly to all but PQQ (**13**) this cofactor is not dissociable from the conjugate enzyme as it is derived from a post-translational modification of a specific tyrosine residue within the protein itself and is therefore covalently bound to the protein.<sup>69</sup> Although the TPQ (**16**) molecule tends to be depicted as a *para* quinone extensive delocalisation of the electrons result in the ortho quinone resonance canonical (also shown in Figure 10).<sup>68</sup> Despite this anomaly and the molecules lack of an 6,7-inolequinone skeleton it carries out a very similar reaction to that of TTQ (**1**) whereby it catalyses the oxidative deamination of primary amines to their corresponding aldehydes and ammonia.<sup>70</sup>

Given the similarities described between these four quinone cofactors there are important questions which arise: why do these enzymes employ the redox cofactors with different C-4 substituent's and how do the C-4 substituent's affect the intrinsic reactivity of the 6,7-inolequinones?<sup>65</sup>

### 1.2.5. Similarities to the pyridoxal phosphate chemistry

These transamination reactions are not however restricted to enzymes with a quinone containing cofactor, there is another class of enzymes that carry out similar reactions using a different coenzyme namely pyridoxal phosphate (**17**) (Figure 11).<sup>71</sup>

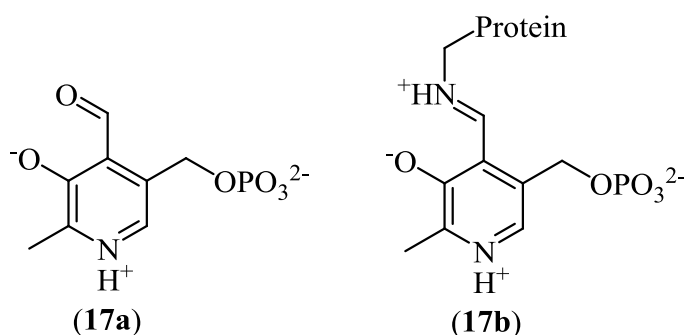
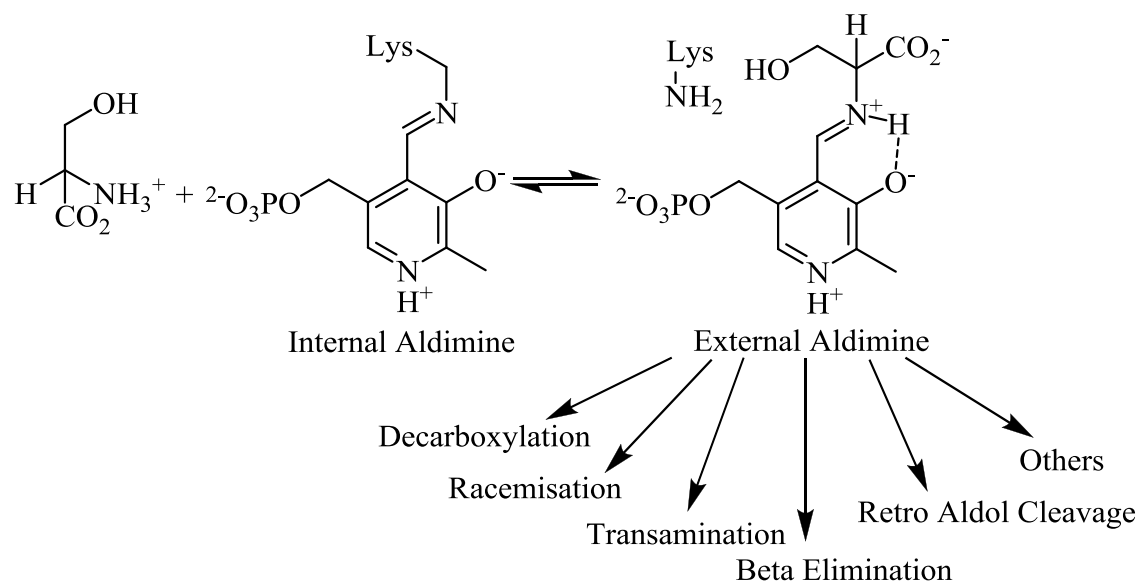


**Figure 11:** Free pyridoxal phosphate (**17a**) and bound to the enzyme as pyridoxamine phosphate (**17b**).

Pyridoxal phosphate (**17**) is derived from the catalytically inactive vitamin B6 and is located in the active site where it can exist in a number of different forms.<sup>72</sup>

Pyridoxal phosphate (**17**) is less selective than the quinone cofactors and participates in a vast range of reactions; illustrated in Scheme 10.



**Scheme 10:** Reactions that pyridoxal phosphate can facilitate.<sup>72</sup>

As is depicted above the first and common step for all pyridoxal phosphate-dependent enzyme-catalysed reactions is a Schiff base exchange reaction (transamination). This is because all known pyridoxal phosphate enzymes exist in their resting state as a Schiff base (labelled above as the ‘internal aldimine’) with an active site lysine residue, however they must be converted to an alternative Schiff base (labelled above as the ‘external aldimine’). Briefly this process involves displacement of the lysine residue by an incoming amine-containing substrate; however in real terms this is actually a multi-step process that includes several facile steps. Nevertheless the ‘external aldimine’ is a common central intermediate for all pyridoxal phosphate-catalysed reactions, enzymatic and nonenzymatic and divergence in reaction specificity occurs from this point.<sup>72</sup>

These reactions can be critical to sustaining life predominately in the biosynthesis of important neurotransmitters and heme.<sup>71-74</sup>

### 1.3. Synthesis and Mechanistic Studies on TTQ Models

#### 1.3.1. TTQ models

With TTQ (**1**) being covalently bound into the enzyme structure it has thus far been impossible to isolate it from the enzymes themselves, there has therefore been substantial effort made to develop synthetic routes to the cofactor (Figure 12).

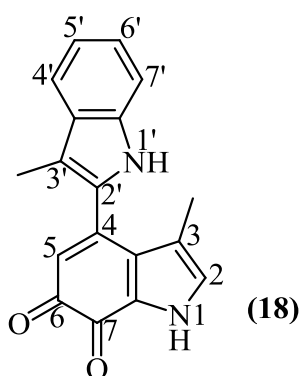


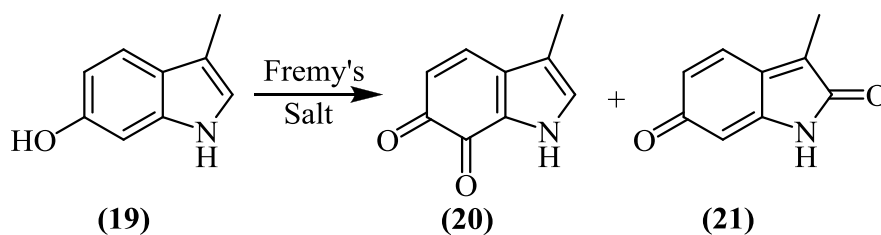
**Figure 12:** Synthetic TTQ cofactor.

Clearly this synthetic TTQ model (**18**) does not possess linkages to any peptide chains. Instead the structure of the synthetic TTQ has had its bonds to the protein chain removed and replaced by hydrogen effectively leaving just a terminal methyl groups at the 3 and 3' ends of the TTQ. Despite this, the model compound (**18**) is still a good model as it possesses similar molecular geometry, redox potential, and several spectroscopic characteristics, to that of the functional cofactor in native enzymes. This in turn indicates that model compound (**18**) is a very good structural model for MADH and AADH.<sup>38, 57</sup>

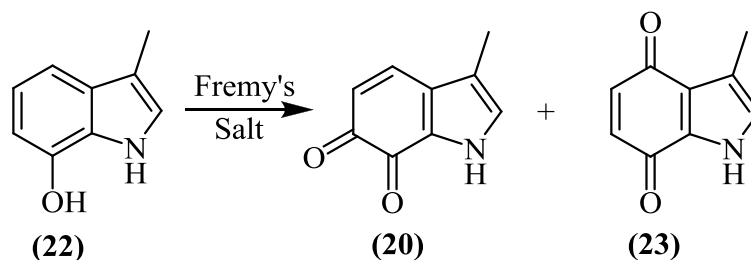
### 1.3.2. Biomimetic studies of TTQ biosynthesis

The biosynthesis of the TTQ cofactor (**1**) (Figure 2) occurs by combination of a 6,7-indolequinone derivative of tryptophan and another tryptophan residue. It has been speculated that this quinone moiety was formed from oxidation of either the 6-hydroxyindole derivative or the 7-hydroxyindole derivative and once formed it is then coupled to another tryptophan residue to form the TTQ cofactor (**1**). Itoh *et al* investigated this mechanistic proposal when they mimicked these proposed reaction steps in the synthesis of the synthetic TTQ (**18**) model.<sup>38, 44, 57</sup>

Clearly one of the key questions in this biosynthesis is whether it is the 6-hydroxyindole derivative or the 7-hydroxyindole derivative that is oxidised or indeed as to whether the proposed route was even viable. In an effort to provide evidence to support or disprove each theory, Itoh made model compounds of both hydroxyindole derivatives and then oxidised them to the quinone (Scheme 11 and 12).<sup>57</sup>

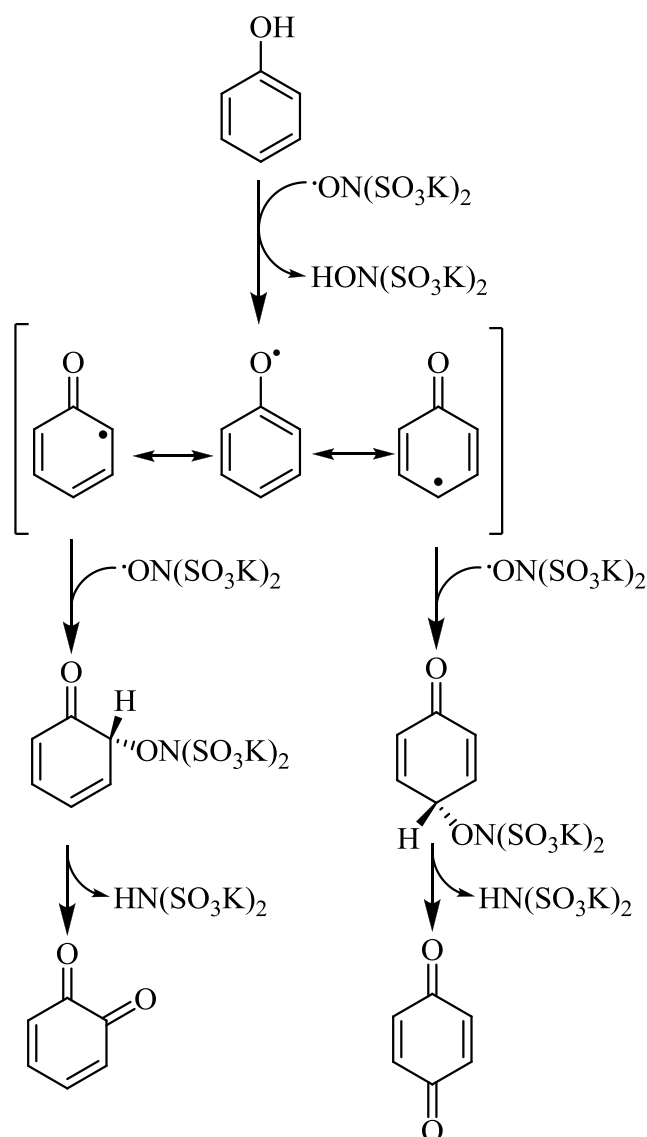


**Scheme 11:** Oxidation of the 6-hydroxyindole derivative.<sup>57</sup>



**Scheme 12:** Oxidation of the 7-hydroxyindole derivative.<sup>57</sup>

This oxidation did initially produce some unexpected results. The ortho quinone (**20**) was not the major product in either reaction; being 7% yield with the 6-hydroxyindole derivative and a marginally better 11% with the 7-hydroxyindole derivative. In both cases the major by-product was the other quinone also shown in each respective equation. However, on consideration of the reaction mechanism of this particular form of oxidation (Scheme 13), these results are perhaps easily explained.<sup>75, 76</sup>

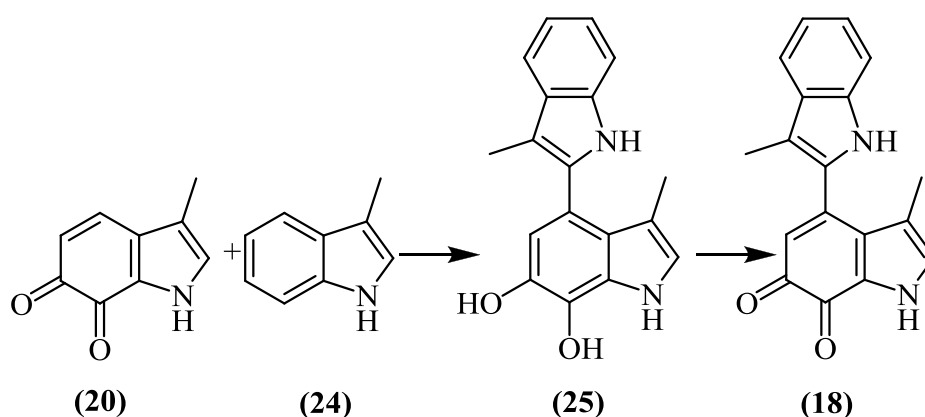


**Scheme 13:** Radical formation with Fremy's salt oxidation.<sup>76</sup>

Itoh *et al* reasoned that the formation of the *para* quinone via the *para* radical intermediate (see above) tends to be preferred due to increased electron spin density of the *para* radical.<sup>57</sup> It tends to be the case that protecting groups are used to ‘block’ this *para* position when attempting to synthesise an *ortho* quinone. As this is not the case in the synthesis of the model compound (**20**) from its corresponding hydroxyindole the ratio of desired *ortho* quinone to *para* quinone perhaps should not be unexpected.<sup>57, 76</sup>

It perhaps could be assumed that the enzyme is in some way designed to selectively produce the 6,7-indolequinone. This maybe through steric hindrance of the 2,6-dioxo indole and *para* quinone, perhaps some of the active site amino acids play an electronic role by disfavouring the by-products or perhaps enhancing the stability of the desired reaction intermediates.

Another remaining step to be explored from the biosynthesis of the TTQ cofactor (**1**) is that of the coupling between the two tryptophan molecules. Itoh *et al* had set out to cover this too; coupling the 6,7-indolequinone (**20**) with 3-methyl indole (**24**) (Scheme 14).



**Scheme 14:** Coupling of two tryptophan derivatives to form the target synthetic TTQ compound (**18**).

Scheme 14 shows that the primary product of the reaction may be the quinol form (**25**); however that can be readily oxidized by molecular oxygen to generate quinone (**18**) during the workup of the reaction. Interestingly this coupling reaction did not proceed in the absence of any additive, but upon addition of the Lewis acid,  $\text{AlCl}_3$  in a catalytic quantity the reaction proceeded and afforded the predicted compound with a relatively low yield of 18 %. The function of the  $\text{AlCl}_3$  is not currently known; normally it would coordinate to the carbonyl groups, more specifically the carbonyl on C-6 thus activating the C-4 position making it more prone to nucleophilic addition of the 3-methyl indole (**24**), however Itoh proposed that the  $\text{AlCl}_3$  may also coordinate with the 3-methyl indole (**24**) at the 1-N position, resulting in an enhancement of the nucleophilicity at the 2-position of 3-methyl indole (**24**).<sup>57</sup> The proposed mechanism for the role of the  $\text{AlCl}_3$  is shown below (Figure 13):

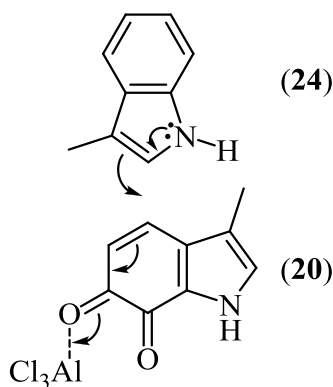
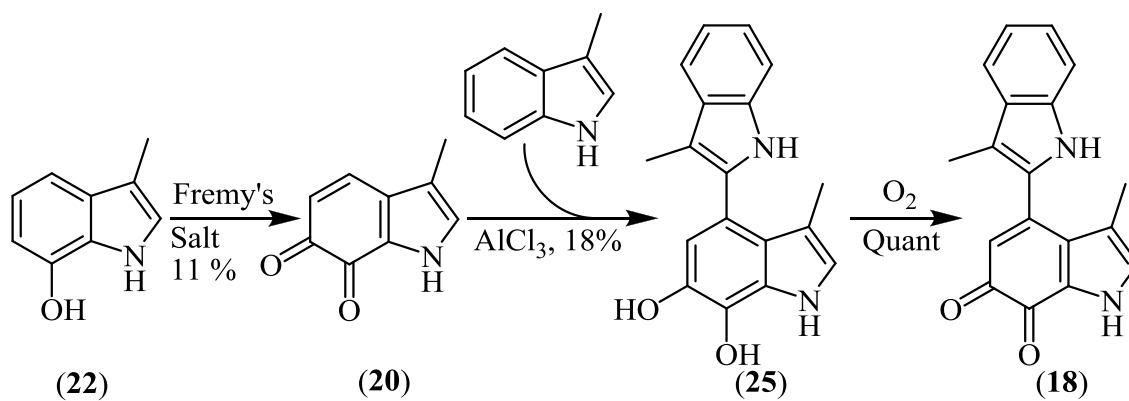


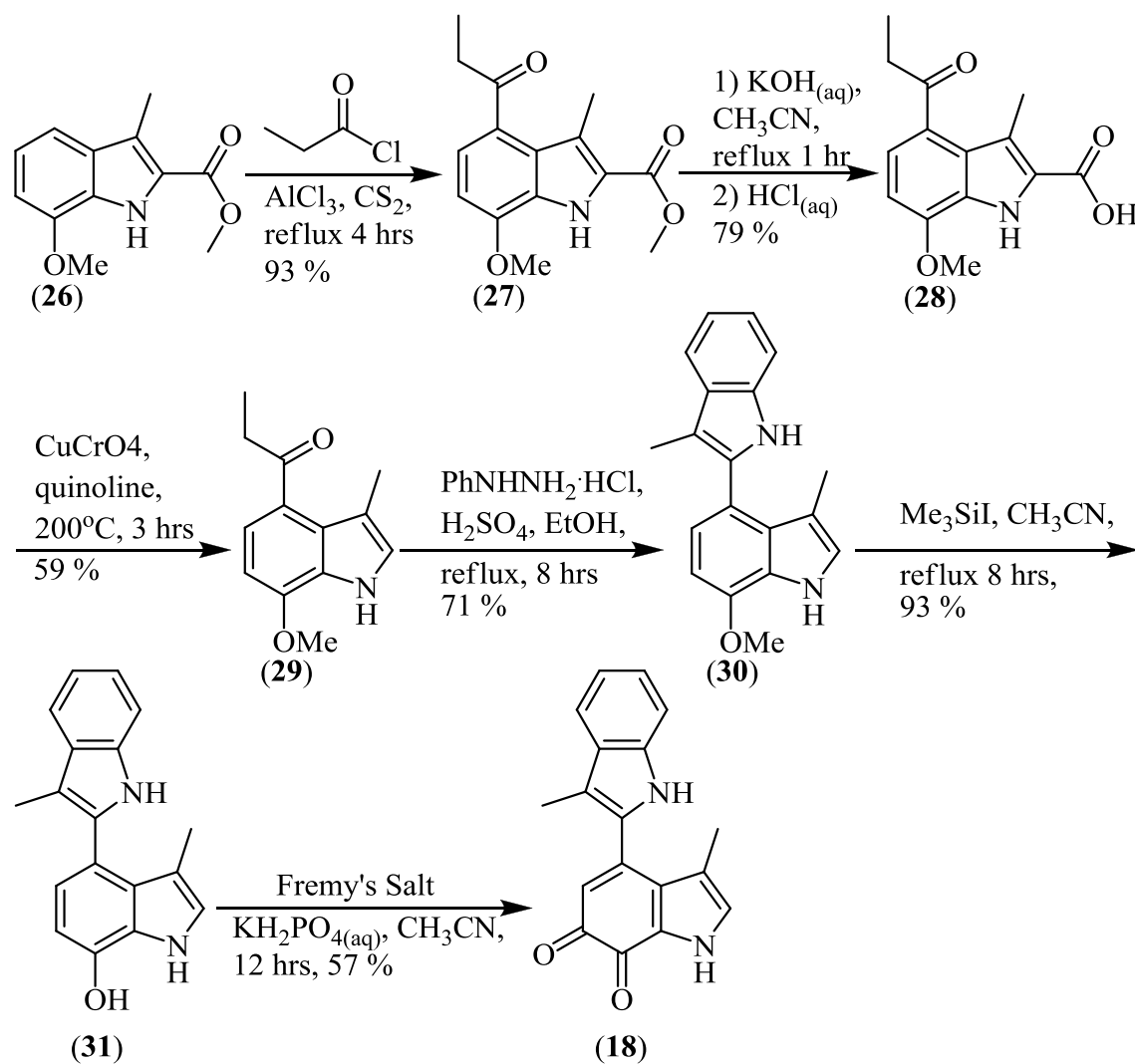
**Figure 13:** Proposed role for  $\text{AlCl}_3$ .

Itoh *et al.* have been able to provide evidence that supports the proposed biosynthetic pathway through this biomimetic synthetic work (summarised in Scheme 15 below). However it should be noted that this biomimetic pathway illustrated in this scheme was found to be highly inefficient with formation of the 6,7-indolequinone in very poor overall yields (2 %).<sup>57</sup>



**Scheme 15:** The full biomimetic pathway employed by Itoh *et al.*<sup>57</sup>

As part of this study Itoh *et al* managed to synthesise the model TTQ compound (18) with a drastically improved overall yield (16 %) by taking a different route to that of the biosynthetic pathway (Scheme 16).



**Scheme 16:** The synthetic route utilised by Itoh *et al.* to obtain the TTQ model compound (18).<sup>44</sup>

By first constructing the bis-indole framework, oxidation of the 7-hydroxyindole derivative, again using Fremy's salt, was much higher yielding as the compound was unable to form the previously seen major and unwanted by-product of the *para* substituted quinone. Because of this, despite the new synthetic pathway being eight steps as opposed to the five involved in the biomimetic pathway, it is still more efficient.

### 1.3.3. Probing the amine oxidation mechanism with TTQ

In an effort to learn more about the mechanism by which primary amines are oxidised to their corresponding aldehyde; numerous reactions have been set up between a range of amines (see Table 1) and the synthetic model TTQ molecule (**18**).<sup>38, 46, 57</sup> It was hoped that the reaction intermediates that had been isolated would provide evidence for the proposed transamination mechanism.

Reactant (a)	Reactant (b)
Synthetic TTQ compound ( <b>18</b> )	1) Ammonia
	2) Cyclopropylamine
	3) Isopropylamine
	4) <i>n</i> -propylamine
	5) Cyclohexylamine
	6) Benzhydrylamine
	7) Benzylamine

**Table 1:** Synthetic TTQ model (**18**) and the range of mechanistic probes.

Each of the above reactants had a specific reason for being used; these reasons are discussed below.

It has been reported that ammonia has an influence on the activity of MADHs as in the case of other quinoproteins<sup>51, 77, 78</sup> and thus it seems logical to start study with the interaction between the synthetic TTQ model (**18**) and ammonia. The product(s) of the reaction can be assigned to formation of the iminoquinone seen below.

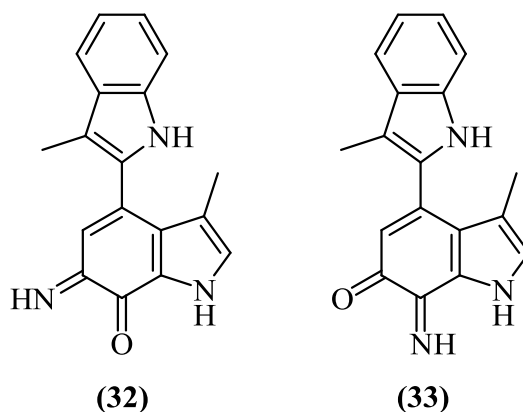


**Figure 14:** The two possible products of the reaction between synthetic TTQ (**18**) and ammonia.

Although there was satisfactory analytical data supporting the iminoquinone structure, the precise position of the nucleophilic addition has not been established and hence there are two possible products (Figure 14). Therefore there is the possibility of both the C-6 iminoquinone (**32**) or C-7 iminoquinone (**33**).<sup>57</sup>

As well as gaining more general knowledge about the kinetics and mechanism of this amine oxidation, it was hoped that by using cyclopropylamine Itoh *et al* would be able to conclusively ascertain the site of the attack by the ammonia. The two isolated intermediates are shown below (Figure 15):

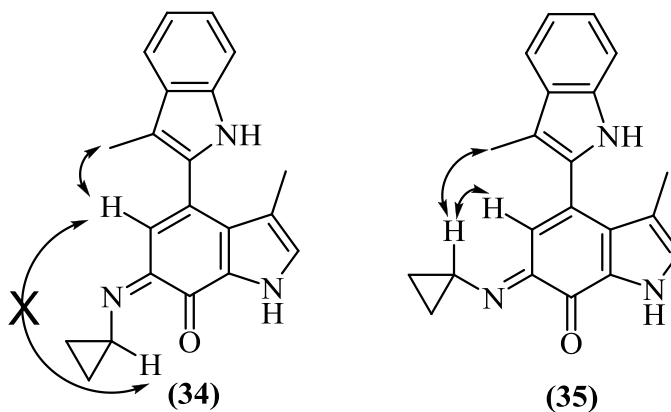


**Figure 15:** Two isolated intermediates from the reaction of synthetic TTQ (**18**) with cyclopropylamine also showing the NOE relationship.

As with ammonia the spectroscopic data revealed that the isolated intermediate was an iminoquinone derivative. The proton NMR revealed that there was a 5:1 mixture of anti-syn isomers (wrt the iminoquinone), with the major isomer being in the anti conformation (**35**). This was accounted for by a NOE enhancement in the proton NMR of two key peaks: CH<sub>3</sub>-3', 5% NOE was detected with irradiation at H-5, confirming assignment of the H-5 peak, and the cyclopropyl  $\alpha$ -CH- where 20% NOE was detected when the compound was irradiated at H-5. This confirmed that the majority of the amine had attacked the C-6 carbon.<sup>38, 46</sup>

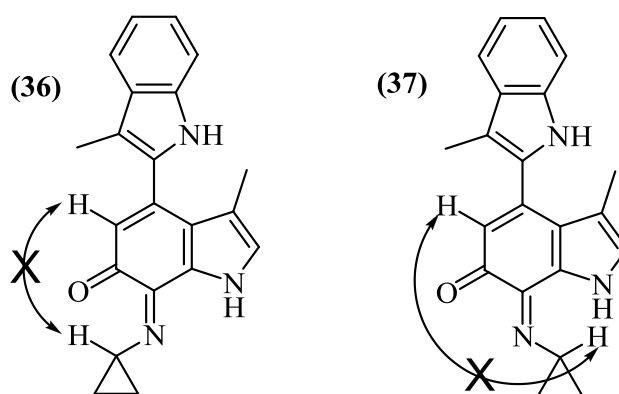


**Figure 16:** Two potential intermediates of C-7 attack by cyclopropylamine on synthetic TTQ (**18**) also showing the lack of NOE relationship between H-5 and  $\alpha$  CH.

As can be seen above (Figure 16) if the iminoquinone had been formed at the C-7 carbon then no NOE enhancement of the cyclopropyl  $\alpha$ -CH- signal would have been observed. This is because regardless of the configuration (either the syn (**36**) or the anti (**37**) wrt the iminoquinone) the  $\alpha$ -CH- signal would always be too far away from H-5 for any enhancement to be observed.

To provide unequivocal proof that both the minor and major products are stereoisomers on the C-6 carbon and not regioisomers of C-6 and the C-7 carbons, Itoh

*et al.* carried out a reduction on what was believed to be a mixture of the syn (**35**) and anti (**36**) stereoisomers with methylhydrazine; they got the single aminophenol product (**38**) shown below:<sup>38</sup>

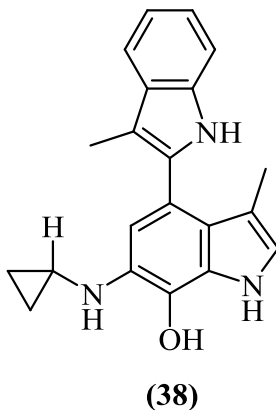


**Figure 17:** Single aminophenol product after reduction of **34/35** with methylhydrazine.<sup>38</sup>

This provides unambiguous proof that the C-6 is the point of attack and anti/syn stereoisomers are formed rather than C-6/C-7 regioisomers. If the possibility of the minor product being a C-7 regioisomer (**36/37**) were true, the reduction would also provide two C-6 and C-7 regioisomers of the aminophenol products. Thus, it can be concluded that the minor product is the syn-stereoisomer at the imine function at C-6.<sup>38, 46</sup> These findings are consistent with computational calculations carried out prior to these experiments that suggested that the C-6 adduct would be thermodynamically more stable.<sup>46</sup>

In an effort to confirm this result, a similar reaction was set up between the synthetic TTQ compound (**18**) and isopropylamine, *n*-propylamine and cyclohexylamine. These again produced similar spectral changes consistent with that of the iminoquinone formation. Further proton NMR study showed that all these adducts showed enhanced NOE with respect to H-5, again confirming that these were all sited at

the C-6 carbon. However no further information was given as to whether the anti or syn stereoisomers were the major product.<sup>38, 46</sup>

When the synthetic TTQ molecule (**18**) is reacted with benzhydrylamine as a substrate, the reaction continues from the iminoquinone stage to give the product imine (**39**) (Figure 18). This process is simply a rearrangement of the iminoquinone precursor.

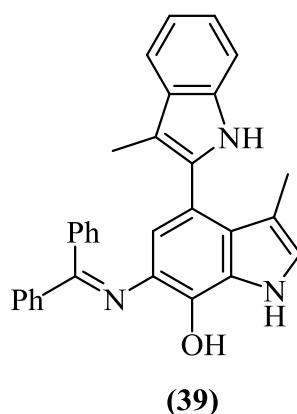
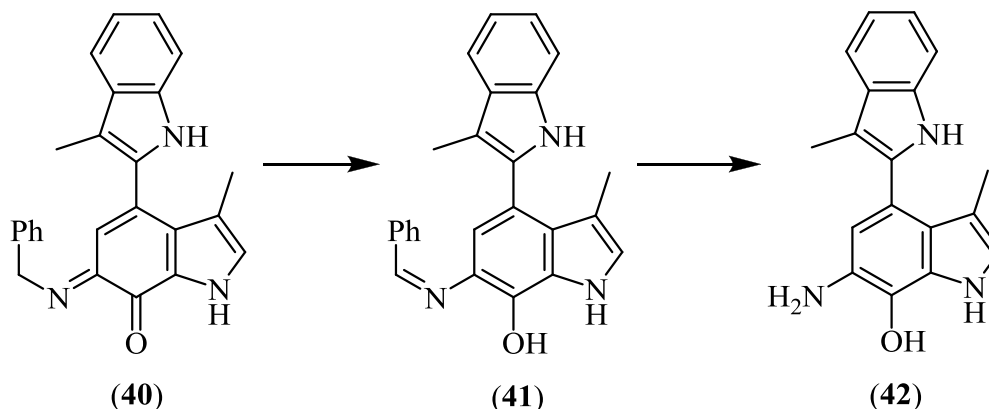


**Figure 18:** Product imine when synthetic TTQ (**18**) is reacted with benzhydrylamine.

The large NOE (27%) detected between H-5 and phenyl protons of the amine moiety indicates that the addition position of the amine is also C-6 and the direction of the imine function is trans against the C-6/C-7 double bond as illustrated in Figure 18. Further minor changes in the NMR results can all be explained when the addition position of the amine is C-6.<sup>38</sup>

One of the reasons for studying benzhydrylamine is that the product imine (**39**) is very stable, and no further reaction occurs to afford the aminophenol derivative because the imine function is conjugated with both the two phenyl rings and the indole ring. This makes benzhydrylamine a poor substrate for the catalytic reaction by the synthetic TTQ model (**18**).<sup>38, 46</sup>

A polar opposite of this reaction is that of the synthetic TTQ molecule (**18**) and the substrate benzylamine.



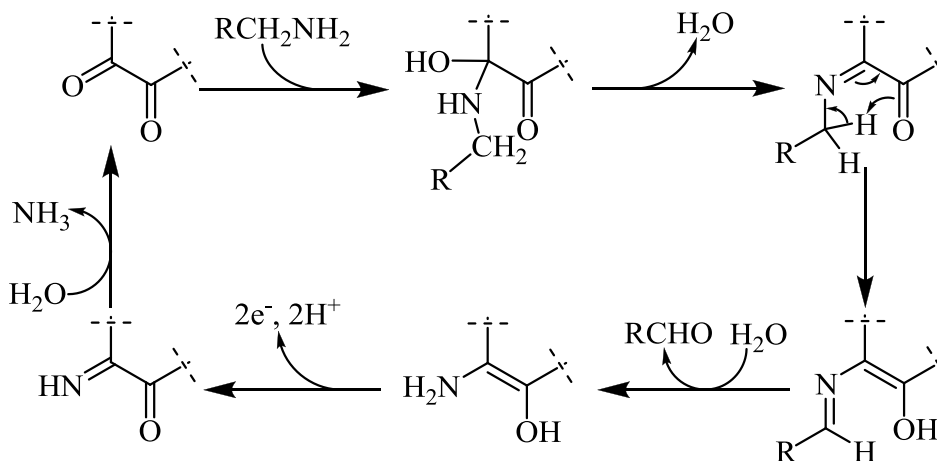
**Scheme 17:** Product aminophenol when synthetic TTQ (**18**) is reacted with benzylamine.

The final isolated product was the aminophenol (**42**), obtained quantitatively, which may be produced because of further reaction of the product imine intermediate (**41**) that was formed from iminoquinone (**40**) as shown in Scheme 17. This mechanism is confirmed by low temperature and low concentration experiments which allowed the isolation of each of the proposed intermediates.<sup>38</sup> It was proposed that imine exchange or hydrolysis was what resulted in conversion of the imine (**41**) to the aminophenol (**42**). Under the basic conditions used by Itoh *et al.* the oxidation of the aminophenol is an elementary step involving molecular oxidation.<sup>46</sup>

#### 1.3.4. Overall amine oxidation mechanism

The evidence presented in the earlier sections provides proof that the reaction mechanism for synthetic TTQ (**18**), is proceeding via the transamination mechanism; as

was originally proposed<sup>38, 46, 79</sup> and thus the natural TTQ cofactor (**1**) is probably also doing this. A full overview of the transamination mechanism is shown below (Scheme 18):



**Scheme 18:** The transamination mechanism of synthetic TTQ (**18**) and a non-specific primary amine.<sup>79</sup>

The first step involved in this mechanism is the addition of the primary amine to the C-6 carbonyl on the synthetic TTQ (**18**) forming the carbinolamine intermediate. This intermediate rapidly converts to the more stable iminoquinone with the loss of water; the iminoquinone then tautomerises to form the imine intermediate. This imine is then hydrolysed, or undergoes imine exchange (if there is a large excess of amine) to release the oxidised aldehyde and the aminophenol derivative. Finally the aminophenol is itself re-oxidised back to the quinone with the loss of ammonia.

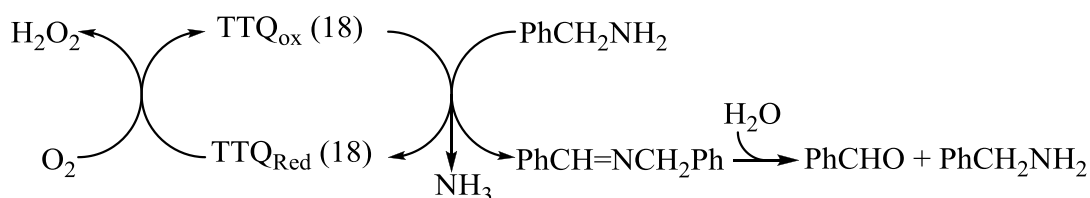
As previously mentioned it is hypothesised that the natural TTQ cofactor (**1**) oxidises primary amines via the same transamination mechanism with one key difference; it is believed that rather than a tautomerisation step that an active site base plays a role in the C-H cleavage. It is this step that has recently been postulated to proceed via a non-classical quantum tunnelling mechanism.

#### 1.4. Catalytic Efficiency of *ortho* Indolequinones

##### 1.4.1. Catalytic efficiency of the synthetic TTQ model compound (18)

Itoh *et al.* have carried out numerous studies to ascertain the catalytic efficiency of the synthetic TTQ compound (**18**) in amine oxidation.<sup>38, 46, 80</sup>

In one example, the catalytic activity of synthetic TTQ (**18**) in the amine oxidation was examined by using O<sub>2</sub> as the electron acceptor (so-called aerobic autorecycling system). It was found that treatment of benzylamine (100 mM) with a catalytic amount (1 mol %) of synthetic TTQ (**18**) in methanol under an oxygen atmosphere gave *n*-benzylidenebenzylamine (PhCH<sub>2</sub>N=CHPh), which was isolated quantitatively. Thus, the synthetic TTQ model compound (**18**) acts as an efficient catalyst in the oxidation of benzylamine by oxygen (Scheme 19), something that is not so prevalent in all other quinone containing compounds.<sup>38, 46</sup>



**Scheme 19:** Catalytic cycle in the oxidation of benzylamine by O<sub>2</sub>.<sup>38</sup>

This experiment was followed by HPLC that detected the amount of benzaldehyde being formed. This tracking of the reaction products meant that a time course plot could be made to schematically represent the catalytic activity of the synthetic TTQ molecule (**18**) (Figure 19).<sup>38</sup>

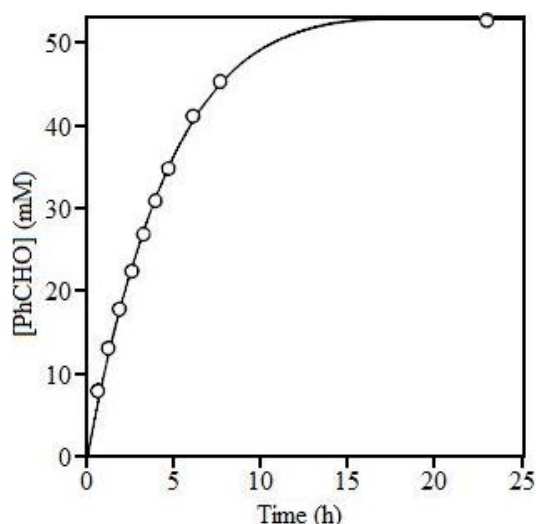


**Figure 19:** Time course plot of conversion of benzylamine to benzaldehyde.<sup>38</sup>

Figure 19 nicely depicts the take up of benzylamine and shows that the majority of conversion had taken place inside 10 hrs. These initial results show that the synthetic TTQ molecule has comparable chemical function to that of the enzyme MADH. The maximum concentration of benzylaldehyde is 50 mM, since the primary product (imine exchange), *n*-benzylidenbenzylamine, is spontaneously converted into benzylamine and benzaldehyde by hydrolysis in the HPLC column (Scheme 19).<sup>38</sup>

#### 1.4.2. Structure-reactivity relationship studies – the role of aromaticity

An important question that arises from the catalytic reaction above (section 1.4.1) is what role the second indole ring has? So far the proposed transamination mechanism for the oxidation of primary amines to their corresponding aldehydes has not involved the second indole ring.

The crystal structure of MADH and the small copper containing enzyme amicyanin alluded to a possible interaction between the two; possibly via the second indole ring of TTQ (**1**) which was located between the active site and the amicyanin.

This would suggest the role of the second indole ring was as some sort of electron transfer mediator.<sup>38, 46, 47</sup>

Itoh *et al.* made two further synthetic compounds (**43** and **44**) (Figure 20) so that structure reactivity relationships could be carried out and compared to the same catalytic oxidation of benzylamine reaction.<sup>46</sup>

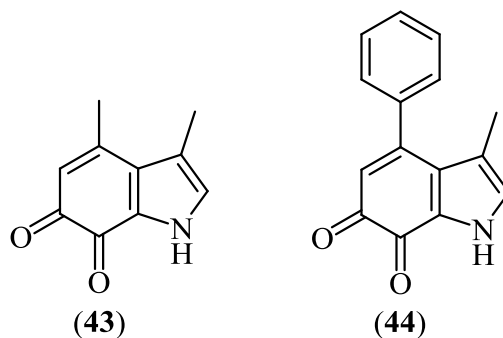


**Figure 20:** Two analogues (**43** and **44**) of synthetic TTQ (**18**) used to probe structure reactivity relationships.

The reaction was again followed by HPLC for benzaldehyde production and a time course plot made so that it could be directly compared to that of the synthetic TTQ (**18**) (Figure 21).

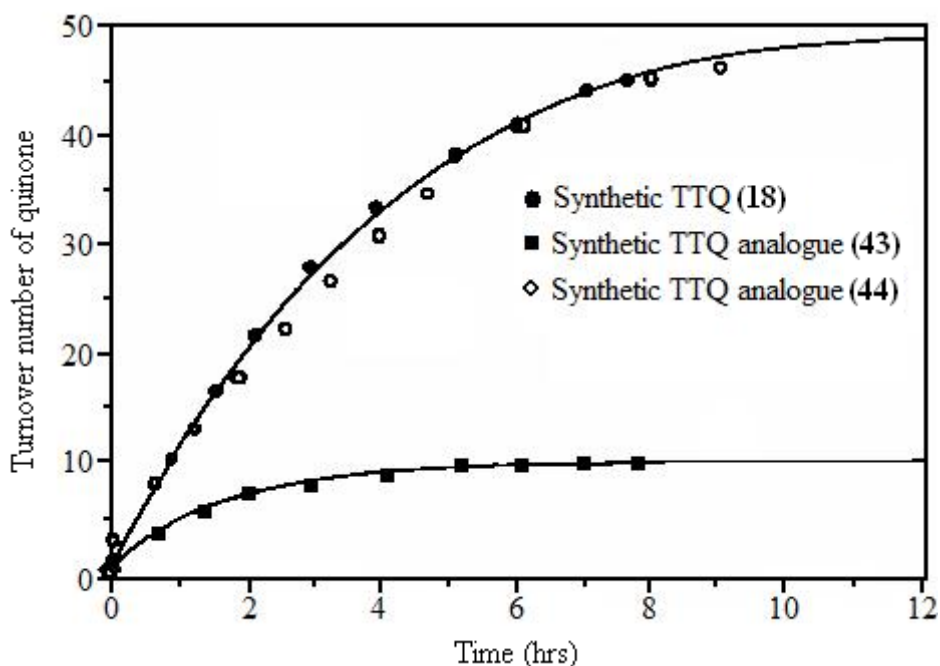


**Figure 21:** Time course plot for conversion of benzylamine to benzaldehyde by the synthetic TTQ (**18**) and its analogues (**43/44**).<sup>46</sup>

As Figure 21 illustrates the second of these TTQ analogues (**43**) was inactivated at an early stage of the reaction however the TTQ analogue (**44**) shows comparable activity to the synthetic TTQ molecule (**18**). From these results it is possible to draw the conclusion that it is important to have an aromatic substituent at the C-4 position.<sup>46</sup>

#### 1.4.3. Catalytic efficiency of other *ortho*-quinones

Further to the structure reactivity relationships; another question that arises is whether any quinone can catalyse the aerobic oxidation of benzylamine to benzaldehyde? And if any quinone did catalyse this reaction how did its catalytic activity compare to that of synthetic TTQ model? To explore this Itoh *et al* measured the catalytic conversion of benzylamine to benzaldehyde for a range of ‘ordinary’

quinones (Figure 22); 9,10-phenanthrenequinone (**45**), 1,2-naphthoquinone (**46**), 1,7-phenanthrolinequinone (**47**), 3,5-di-tert-butyl-1,2-benzoquinone (**48**), 1,4-benzoquinone (**49**):<sup>38, 46</sup>

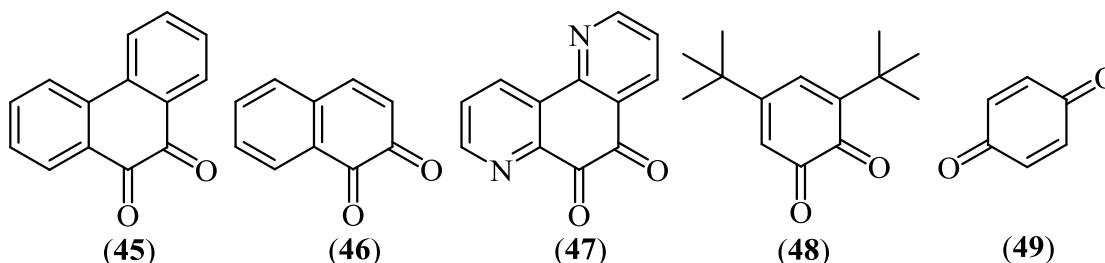


**Figure 22:** 'Ordinary' *ortho*-quinones tested by Itoh *et al.*

Quinone	Yield (%) of PhCHO
Synthetic TTQ ( <b>18</b> )	3700
9,10-phenanthrenequinone ( <b>45</b> )	50
1,2-naphthoquinone ( <b>46</b> )	0
1,7-phenanthrolinequinone ( <b>47</b> )	1600
3,5-di-tert-butyl-1,2-benzoquinone ( <b>48</b> )	600
1,4-benzoquinone ( <b>49</b> )	0

**Table 2:** Yield of PhCHO produced as a percentage of quinone used.

Looking at the values in Table 2 it can be seen that 1,7-phenanthrolinequinone (**47**) does act as a catalyst, but its catalytic efficiency is clearly lower than the synthetic TTQ molecule (**18**). It is interesting to note that 3,5-di-tert-butyl-1,2-benzoquinone (**48**), a well known reagent for amine oxidation (Corey's reagent), is a poor catalyst and

the other remaining ‘ordinary’ *ortho*- (45/46) and *para*-quinones (49) do not work at all in this system.<sup>38</sup>

These results have reinforced the structural importance of the 3,4-disubstituted 6,7-indolequinone skeleton of TTQ cofactor (1) and it was reflection upon this information that led Itoh *et al* to later make a series of *ortho*-indolequinone derivatives (Figure 23) in an effort to further investigate and probe there catalytic efficiency.

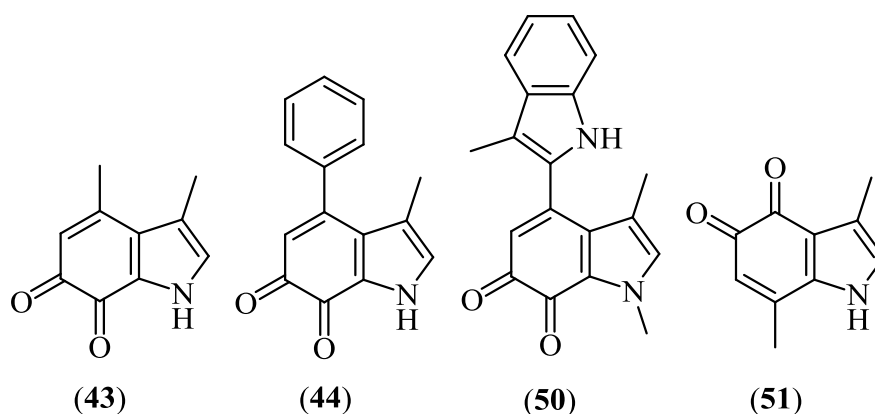


**Figure 23:** The *ortho*-indolequinone derivatives of synthetic TTQ (18).

These derivatives were all subjected to the now familiar reaction of converting benzylamine to benzaldehyde. Again the benzaldehyde formation was followed by HPLC and a time course plot (Figure 24) for each compound made.<sup>26</sup>

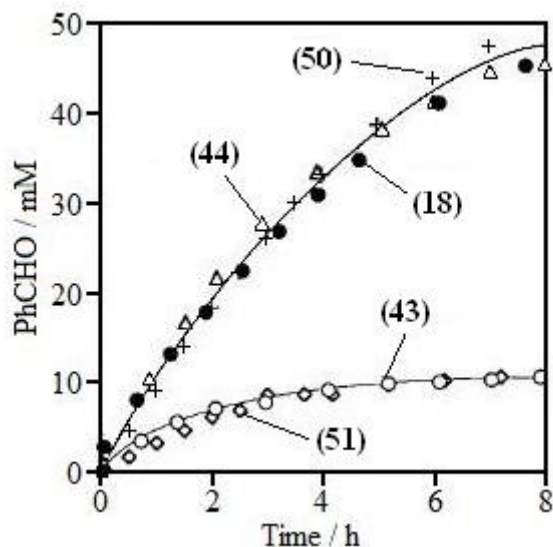


**Figure 24:** Time course plot for the production of benzaldehyde by the *ortho*-indolequinone derivatives of synthetic TTQ (**18**).<sup>26</sup>

As can be seen the oxidation of benzylamine by synthetic TTQ (**18**) proceeded until all of the substrate was consumed. Of the other *ortho*-indolequinone compounds, (**44**) and (**50**) show essentially the same high catalytic activity as the synthetic TTQ (**18**); however compounds (**43**) and (**51**) are deactivated in an early stage of the reaction.

In the case of PQQ (**13**) and other indolequinone cofactors the pyrrole proton has been shown to be important in enhancing the reactivity of the cofactor. Replacement of this proton by any alkyl group (commonly a methyl) severely reduces the reactivity of the quinone towards its substrate.<sup>80-82</sup> Interestingly this has not been the case with compound (**50**), which remained comparatively active despite replacement of this proton.<sup>26</sup>

Interestingly in the anaerobic single-turnover reaction, it has been demonstrated that the reactivities of all the quinones are almost the same in each step. Furthermore, it has been confirmed that the re-oxidation of the reduced quinone by O<sub>2</sub> is much faster than the reaction of (**18**) with benzylamine (under the basic conditions

employed).<sup>38</sup> To add, the redox potentials of the *ortho*-quinone derivatives (**43/44/50/51**) are also more negative than that of synthetic TTQ (**18**), therefore re-oxidation of these reduced species by O<sub>2</sub> must be faster than that of (**18**), suggesting that the re-oxidation step of the aminophenol by O<sub>2</sub> is not rate determining in the catalytic reaction.<sup>26</sup>

From these considerations, it can be assumed that the lower catalytic activity of the *ortho*-quinones that have the methyl group at the C-4 (**43/51**) as compared to those that have the aromatic substituent at the C-4 (**44/50**) may be attributed to the lower stability under the reaction conditions. A possible pathway in the deactivation of the catalyst is a Michael type addition of the amine substrate to the C-4 position of the quinone ring. The relatively bulky aromatic groups at C-4 may protect the quinone ring from such an undesirable addition reaction (Figure 25).<sup>26</sup>

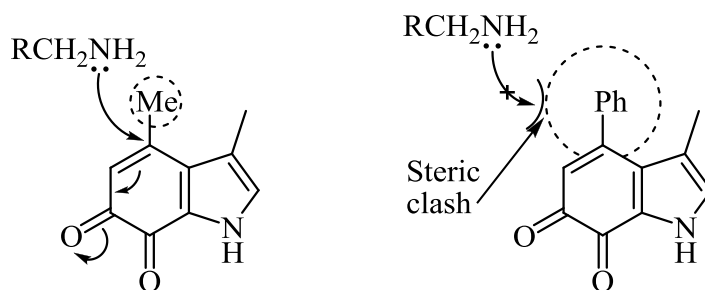


**Figure 25:** 1,4-Michael addition by a generic amine onto an *ortho*-indolequinone.

The conformation of the substituent on the C-4 carbon may also have some effect on the resistance of the compound to this 1,4-michael addition mechanism. If this substituent is planar to the main 6,7-indolequinone framework then this would make nucleophilic attack easier than if that same substituent had a twisted orientation. This may be an additional reason for the TTQ cofactor (**1**) having a twisted co-planar structure when in the protein domain.

#### 1.4.4. The role and electronic effects of C-4 substituents in *ortho*-indolequinones

So far the various C-4 substituents have all been alkyl or aryl based. However the electronic effects of a range of alternative substituents have recently been investigated (Figure 26).<sup>65, 83</sup>

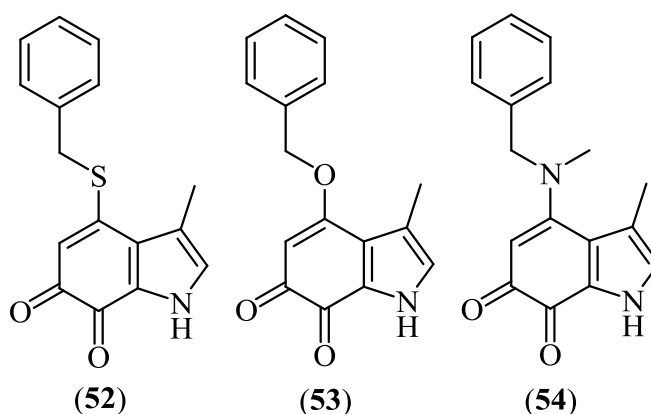


**Figure 26:** The range of TTQ derivatives used to probe the electronic effects of the C-4 substituent.

This study on the electronic effects of the C-4 substituent on the reactivity of the 6,7-indolequinone cofactors found that the reactivity of the C-4 substituent decreases in the following order:

indole (**18**) > thioether (**52**) > ether (**53**) > amine (**54**).

This pattern is thought to be in relation to the electron-donating ability of the C-4 substituents. The reactivity of the quinone with the ether substituent (**53**) toward amines is hindered due to the higher electron donor ability of the oxygen substituent in (**53**) as compared to that of the sulphur substituent in (**52**). The introduction of the

amino group at C-4 of the quinone (**54**), resulted in a further increase in the energy barrier for the iminoquinone formation process. Thus, these 6,7-indolequinones having such C-4 substituents may not be able to serve as a redox cofactor in amine dehydrogenases. Never the less as with previous reactions, it has been proved by Itoh *et al.* that the reaction of quinone compounds (**52/53/54**) with benzylamine still proceeds stepwise through the iminoquinone and the product-imine intermediates to give aminophenol as the final product as in the case of synthetic TTQ compound (**18**).<sup>65</sup>

#### 1.4.5. Electronic effects of substrates

The studies detailed above have extensively covered the effects of a variety C-4 substituents on the activity of the catalyst towards primary amine oxidation. However one further question remains and that is what effect of substituents on the amine itself have? Itoh *et al.* initially investigated this question by using a range of *para*-substituted benzylamines with varying degrees of electron donation/withdrawal (Figure 27).

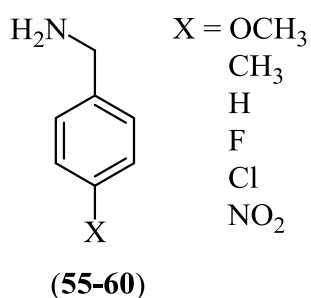


**Figure 27:** The range of *para*-substituted benzylamines tested.<sup>38</sup>

They found that the more electron donating the substituent the higher the rate of reaction for its conversion to the substituted benzaldehyde by synthetic TTQ (**18**). This means that *p*-methoxybenzylamine is more reactive than just benzylamine, which

in turn is more reactive than *p*-nitrobenzylamine. This study demonstrated a Hammett plot  $\log k_1$  and  $k_2$  versus electronic effects exhibiting a negative slope (i.e. electron donating substituents enhance rate constants).<sup>38</sup> However Cullis *et al.* found results that contradicted this. When the same *para*-substituted substrates were oxidised using AADH and the small subunit of AADH (containing TTQ (**1**) in its natural state) they showed a positive Hammett correlation.<sup>84, 85</sup>

These phenomena can be explained when considering the rearrangement step (iminoquinone to product imine) which involves  $\alpha$ -proton abstraction. The positive correlation has been attributed to enhancement of the  $\alpha$ -proton abstraction step by the electron withdrawing substituents weakening the C-H bond.<sup>37, 38</sup> The negative effect in the model system has been attributed to electron flow, from the  $\alpha$ -carbon to the quinone moiety, being more difficult in the model system than in the enzymatic system.<sup>38</sup>

It is important to recognize in any discussion of the Hammett behaviour of the synthetic TTQ centre with that of the small subunit that these differences are most likely related to a change in mechanism. The amine in the synthetic model system is also playing the role of the active site base, and in this case, there is a substituent effect on both the substrate Schiff base and the proton abstracting base. This is not the case for the small subunit in which the active site Asp residue is the probable base.<sup>85</sup>

## 1.5. Quantum Tunnelling

### 1.5.1. Classical transition-state theory (TST)

The phenomenal rate accelerations and specificities of enzymes have intrigued investigators ever since the 1830s when enzymatic activity was first observed. A major question has been how do enzymes catalyse such a wide range of reaction types with

such phenomenal rate accelerations.<sup>86</sup> A major breakthrough in understanding enzyme catalysis came through the application of transition state theory (TST) to enzymes and the reactions they catalyse.<sup>87-89</sup>

In TST, in order to pass from reactants, A, to products, B, the reaction has to pass over a potential energy barrier (Figure 28).

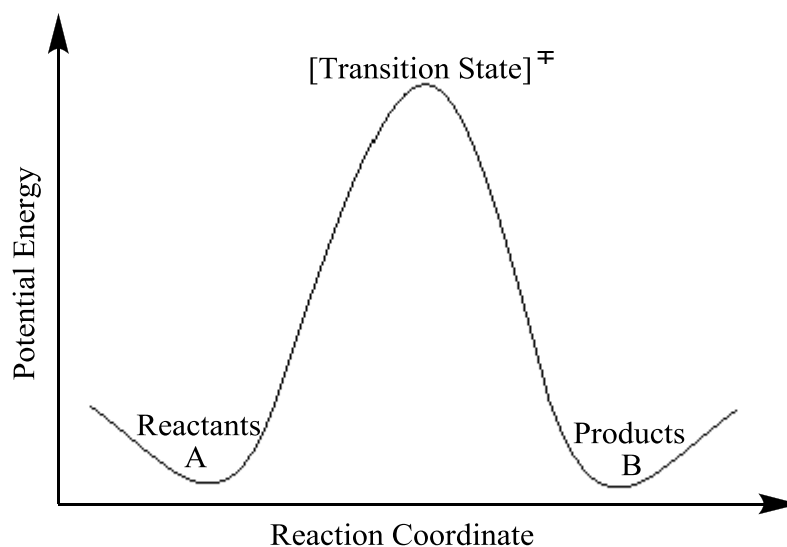


**Figure 28:** TST reaction profile graph.

This potential energy barrier involves the reactants progression through a high-energy ‘transition state’ before forming products; it is the height of this barrier that determines the rate of reaction. This is due to TST treating the absolute rate of reaction in terms of a hypothetical thermodynamic equilibrium of the ground state with the transition state and the partitioning of this hypothetical transition state species between the two ground state structures. From this treatment, the absolute rate of a reaction is related to the hypothetical concentration of the transition state and can be readily calculated by applying equilibrium thermodynamics.

TST has been applied to numerous enzymatic examples where the theory predicts a tight complex is formed between the transition state structure in the catalysed

reaction and the enzyme.<sup>86, 90</sup> As discussed in the introduction, the ability of a catalyst to enhance the rate of a reaction depends on its ability to discriminate between the substrate in the ground state and its activated form in the transition state, binding the latter species more tightly reduces the free energy of the transition state and hence lowers the activation barrier.<sup>91</sup>

The strong binding affinity of enzymes for the transition state implicit in the application of transition state theory to enzyme catalysis can be harnessed and used in the mechanistic study of enzymes by designing and developing powerful enzyme inhibitors by designing ground state structures that resemble the TS. These transition state analogues have been widely shown to be potent inhibitors providing support for transition state theory in enzyme catalysis and support for mechanistic proposals.<sup>92</sup> This was first tested by Wolfenden in 1969<sup>93</sup> in the design of the potential transition-state analogue 2-phosphoglycolate, as an inhibitor of triosephosphate isomerase. 2-Phosphoglycolate was designed to mimic the ene-diolate high energy intermediate, hence resembling the transition state more closely than the ground states and was shown to bind five times more tightly than that of the normal substrate (glyceraldehyde-3-phosphate).<sup>94</sup>

By the mid 1970's more than sixty transition state analogue inhibitors had been identified, covering a wide variety of enzymes.<sup>95</sup> These inhibitors each tested the general mechanism on which their design had been based and served as a tool to uncover the structural details of the enzyme-substrate interaction.<sup>92</sup> Several transition-state analogue inhibitors have dissociation constant values of less than  $10^{-12}$  M and some even achieving  $10^{-18}$  M, reaffirming that enzymes preferentially bind the transition state complex over that of the ground state complexes.<sup>92</sup>

### 1.5.2. Quantum tunnelling history

Although TST has been used to picture enzyme-catalysed reactions over the last 50 years,<sup>86</sup> recent developments imply that this 'textbook' illustration could be fundamentally flawed (at least in some circumstances).<sup>90</sup>

The problem is that TST considers only the particle-like properties of matter, however, matter (especially those particles with smaller mass e.g. electrons and hydrogen atoms) can also be considered as having wavelike properties: this is known as the wave-particle duality of matter. Hence an alternative picture to TST has emerged for some enzyme catalysed reactions involving electron or hydrogen transfer. One important feature of the wave-like properties of matter is that it can pass through regions that would be inaccessible if it were treated as a particle, i.e. the wave-like properties mean that matter can pass through regions where there is zero probability of finding it (Figure 29).

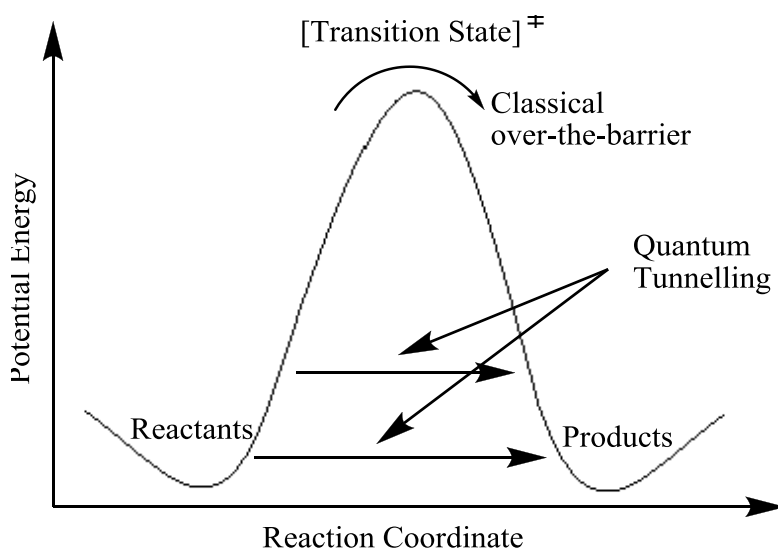


**Figure 29:** Reaction profile graph showing quantum tunnelling.

This passing through the barrier can be likened to passing from one valley to an adjacent valley via a tunnel, rather than having to climb over the mountain between. As

the analogy suggests, this significantly lowers the energy required to proceed from reactants to products. Thus, quantum tunnelling may play an important role in driving enzyme-catalysed transfer of electrons and hydrogen.<sup>90</sup>

Supporting this theory is the fact that, due to TST derivation from the Arrhenius equation, it has long been known that it is a temperature dependant process where, as temperature increases so does the rate of reaction.<sup>96</sup> In contrast quantum tunnelling has been considered to be largely temperature-independent. In spite of this, recent research has linked quantum tunnelling in enzymes to a temperature dependency. This phenomenon has been explained by the thermal vibrations in proteins (vibrationally assisted tunnelling) that reduce the tunnelling distance and, as the earlier analogy suggests, this can significantly lower the energy required to proceed from reactants to products thus increasing the probability of its occurrence.<sup>90, 96, 97</sup>

It is possible to calculate the tunnelling rate for a particle (with a known mass) as there is a directly proportional relationship (Equation 1) between the tunnelling rate ( $k$ ), reduced Planck's constant ( $\hbar$ ), the width of a barrier ( $l$ ), the height of said barrier ( $V$ ) and the mass of a particle ( $m$ ) with a kinetic energy ( $E$ ):<sup>96, 98, 99</sup>

$$k \propto \exp[(-2l\sqrt{2m(V-E)})/\hbar]$$

**Equation 1:** Tunnelling rate expression (given a rectangular potential energy barrier).<sup>98</sup>

What this equation demonstrates is that there is an exponential decrease in the tunnelling rate for a particle of a constant mass if either the width or height of the barrier is increased.<sup>98, 99</sup>

This equation can be represented graphically (Figure 30) where the tunnelling particle has a wave function ( $\psi$ ), with kinetic energy ( $E$ ):<sup>98</sup>

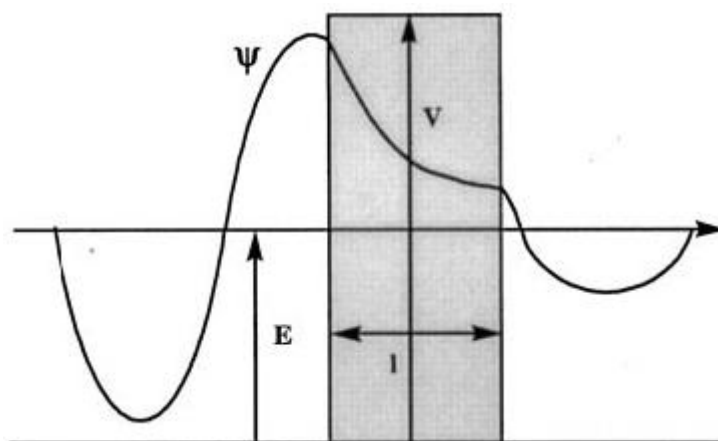


**Figure 30:** Schematic quantum tunnelling for a particle through a rectangular barrier.

This scheme perhaps better depicts the effect that narrowing or widening the width of the barrier has on tunnelling probability. However it also shows the problem with this equation is that it only applies for reactions that have a rectangular potential energy barrier. The possible role of a rectangular barrier in vibrationally assisted tunnelling has been discussed in the literature in great detail.<sup>99</sup> As a result there have been a variety of studies carried out into the different shapes of potential energy barriers, the upshot not only ruled out a rectangular potential energy barrier but also a parabolic shape too. These rectangular and parabolic barriers are appropriate (albeit crude) depictions of the potential energy surface near the top of the barrier.<sup>98</sup> Basran *et al* proposed a far less conventional shape to this barrier (Figure 31) that better fitted their experimental data.

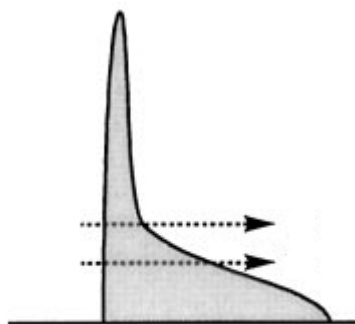


**Figure 31:** Schematic quantum tunnelling for a particle through a parabolic curve with a concave shoulder.<sup>98</sup>

In this schematic, for simplicity, it has been depicted that only the barrier width changes, and not the height, although in practice both will likely vary. The advantage of this barrier over those discussed above is that it has a concave shoulder occurring just below the likely area in which H tunnels.

### 1.5.3. Quantum tunnelling comparison for electrons vs. hydrogen

Proteins are electrical insulators; nevertheless, electrons can travel large distances (up to approx.  $3 \times 10^{-9}$  m or  $30 \text{ \AA}$ ) through proteins when being transferred from a donor to an acceptor redox centre. This apparent contradiction – of an electron passing through an electrical insulator – can be understood in terms of the wave-like properties of the electron. As explained briefly in the previous section; this is due to the electrons exhibiting wave-like properties allowing them to ‘tunnel’ through regions that would be inaccessible to matter possessing particle-like properties.<sup>100</sup> However it has been known for some time that enzyme-mediated reactions can often involve an electron tunnelling mechanism as it is required to account for experimentally observed reaction rates.<sup>97, 101-104</sup>

In contrast with electron transfer via quantum tunnelling, the quantum-mechanical transfer of other particles in enzymes has not been documented extensively. It was the ground-breaking work of Klinman *et al* in 1995 that provided the first experimental indication of hydrogen tunnelling in enzyme molecules.<sup>100, 105</sup>

As Equation 1 shows, the probability of tunnelling decreases with increasing mass of the particle, which reduces significantly the probability of hydrogen compared with electron tunnelling (the mass of the hydrogen nucleus is ~1840 times greater than that of the electron). Using the same expression (Equation 1) for proton tunnelling gives a transfer distance of 0.58Å. This distance is similar to the length of a reaction coordinate, and is thus suggestive of high tunnelling probability. The larger masses of deuterium and tritium lead to corresponding transfer distances of 0.41Å and 0.34Å, respectively, thus making kinetic isotope effect (KIE) studies attractive for the detection of H-tunnelling in enzymes.<sup>90, 100, 102</sup>

The comparatively short distance over which tunnelling of the hydrogen nucleus is effective, and the sophisticated experiments required for the detection of H-tunnelling, may account for the small number of reports on H-tunnelling in enzymes. Nevertheless, for those enzyme-catalysed reactions with a large activation energy (e.g. the breakage of stable C–H bonds in MADH and AADH), quantum tunnelling is an attractive means of transferring hydrogen from reactant to product states. Until recently, quantum tunnelling was thought to be significant only at very low (cryogenic) temperatures. However, deviations from classical TST behaviour have been seen recently with a small number of enzymes, implying that H-tunnelling may be significant in these systems at physiological temperatures.<sup>100, 106-110</sup>

#### 1.5.4. The kinetic isotope effect (KIE)

The kinetic isotope effect (KIE) in proton transfer reactions is present in all cases where the rate of proton transfer is not the same as the rate of deuterium transfer i.e.  $k_H > k_D$ . If one was to only consider classical over the barrier or transition state theory the ratio of  $k_H/k_D$  is dependent on both the temperature of the reaction and the size of the activation barrier that the reaction has to surmount.<sup>111</sup> The difference in activation energies occurs because the C–D/C–T bonds are shorter than C–H, resulting in their extra strength and ultimately leading to a higher energy required to break the C–D/C–T bond compared to the C–H bond.<sup>90</sup>

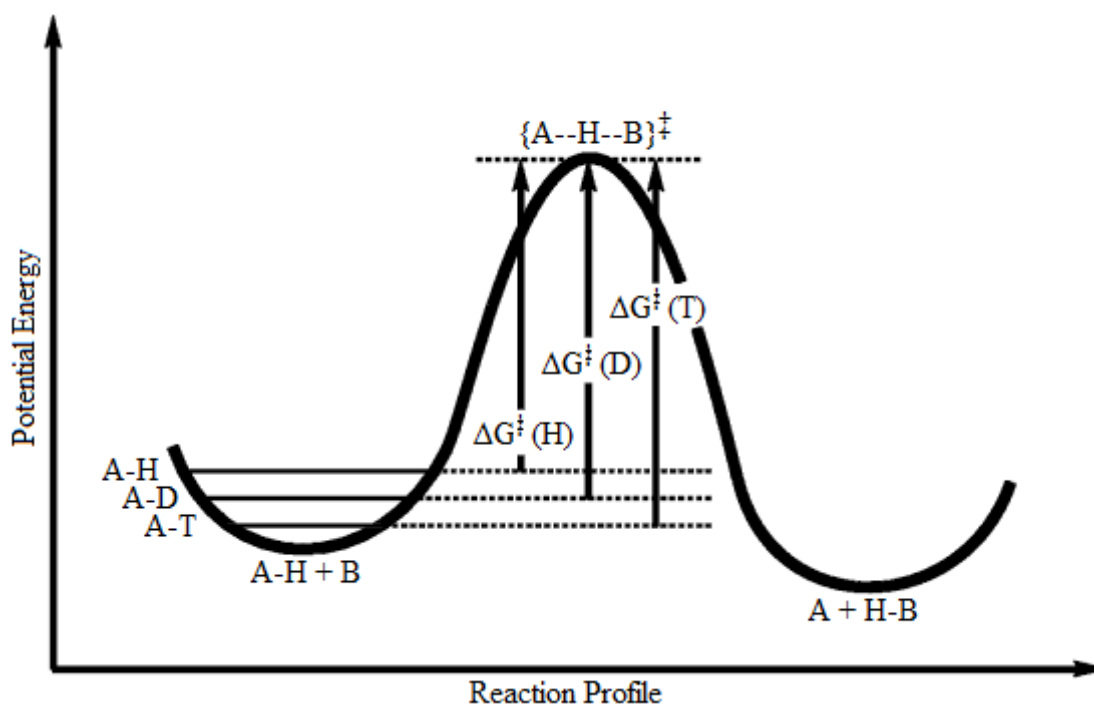


**Figure 32:** Schematic representation of the energetics for an enzyme-catalysed reaction of the reaction  $A-H + B$  to  $A + H-B$ .

By taking into account the difference in these zero point energies the maximum KIE can be calculated for a reaction involving a C–H cleavage vs. C–D/C–T cleavage. Provided only classical over the barrier or transition state theory applies this results in the values for the KIEs, which have different values depending on the isotopes being compared, being  $k_{\text{H}}/k_{\text{D}} \approx 7$  and  $k_{\text{H}}/k_{\text{T}} \approx 15$  at 25°C.<sup>90, 111, 112</sup>

Previous discussions of enzymatic hydrogen transfer most often assumed that the hydrogen's motion is (at least approximately) classical,<sup>86, 99</sup> with two experimental facts being used to justify this view:

1. When deuterons or tritons are substituted for the hydrogen the rate of transfer is typically slower by a factor roughly consistent with a classical (non-tunnelling) theory. This ratio of rate constants is not nearly as large as what might naively be expected for a tunnelling process.
2. Transfer rates and KIEs are temperature dependent, in agreement with the standard, non-tunnelling theory. In contrast, static tunnelling models suggest that rates and KIEs should be independent of temperature.<sup>99, 113</sup>

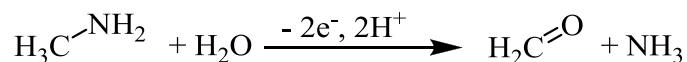
This view has now been successfully challenged and while in some circumstances it may still be true it is also possible that it may not be as 'black and white' as originally thought. Tunnelling models based on the Arrhenius equation do indeed show that for tunnelling to occur through a static potential barrier, the KIE is temperature independent. However, this is contradicted by the Kramers relationship, which takes into consideration both a dynamic potential barrier and the possible thermal vibrations of the protein. The result of this is that when considering the same proton tunnelling, the observed KIE has the potential to be temperature dependent. This means it is potentially possible to get a temperature dependent proton transfer with a KIE < 7 that still indicates it proceeds via a quantum tunnelling mechanism.<sup>99, 102, 109, 110, 114</sup>

This raises an important question; is studying KIE still a good indication as to whether a proton transfer proceeds via a classical or quantum mechanism? The answer is potentially 'no', if you were to base your conclusion solely on the size of the KIE. However if one was to concurrently measure the temperature dependency of the KIE, then potentially it is still a viable method, particularly if this is carried out in conjunction with studying protein dynamics of the enzyme. Alternatively if the measured KIE gave a value considerably higher than that expected for classical TST then it still provides a good indicator that the proton transfer might be progressing via a quantum tunnelling mechanism.

## 1.6. Hydrogen/Proton Tunnelling in MADH

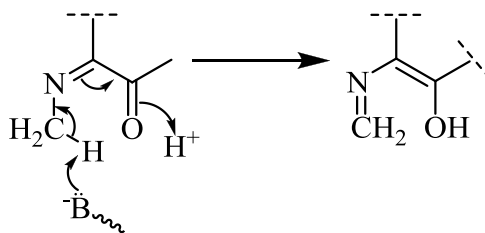
### 1.6.1. The background of proton tunnelling in MADH

As previously mentioned one of the important TTQ (1) containing enzymes is MADH. This enzyme catalyses the oxidative deamination of methylamine converting it to methanal (formaldehyde) and ammonia (see scheme 20 below).



**Scheme 20:** Deamination of methylamine by MADH.

As previously explained the excess electrons are passed through the TTQ ring system to a separate copper containing protein, amicyanin.<sup>47</sup> One of the most important steps in this mechanism, is that of the C–H cleavage (see Scheme 21).



**Scheme 21:** Proton abstraction step in MADH catalysis of methylamine.

This C–H cleavage occurs when the enzyme is moving from the iminoquinone stage to forming the tautomeric imine. It is believed that this proton abstraction is facilitated by an *in situ* active site aspartate residue (indicated by the B<sup>-</sup> in Scheme 21). This C–H cleavage was confirmed by the isolation of the reduced form of the TTQ cofactor by Itoh *et al.*<sup>38</sup> as a result the rate of C–H bond breakage can be obtained by using stopped-flow methods to monitor the kinetics of MADH reduction.<sup>100</sup>

#### 1.6.2. The static potential-energy barrier theory

The first detailed report of stopped-flow kinetic studies of the TTQ-bearing enzyme MADH was published by Brooks *et al.*<sup>48</sup> The data indicated that MADH exhibited a very large primary deuterium kinetic isotope effect which appeared to exceed the predicted classical limits. Comparison of the kinetic constants obtained with CH<sub>3</sub>NH<sub>2</sub> and CD<sub>3</sub>NH<sub>2</sub> revealed a kinetic isotope effect of 17.2, although it was noted though that this isotope effect was obtained with methylamine in which the carbon was trideuterated. This meant that a correction of this value was made to allow for the contribution of the secondary isotope effects. Using an upper limit of 1.36 for the maximum magnitude of a secondary isotope effect, the true primary deuterium isotope effect can be estimated to be in the range 9.3-17.2.<sup>48</sup> These calculations were initially modelled on the static potential barrier theory and calculations were based on the

Arrhenius equation, where such a high value suggests that the C–H cleavage proceeded via a quantum mechanical mechanism.<sup>100, 102, 109</sup>

Subsequent studies have improved on the classical Arrhenius equation and have been used to predict temperature dependence of the KIE (Figure 33).

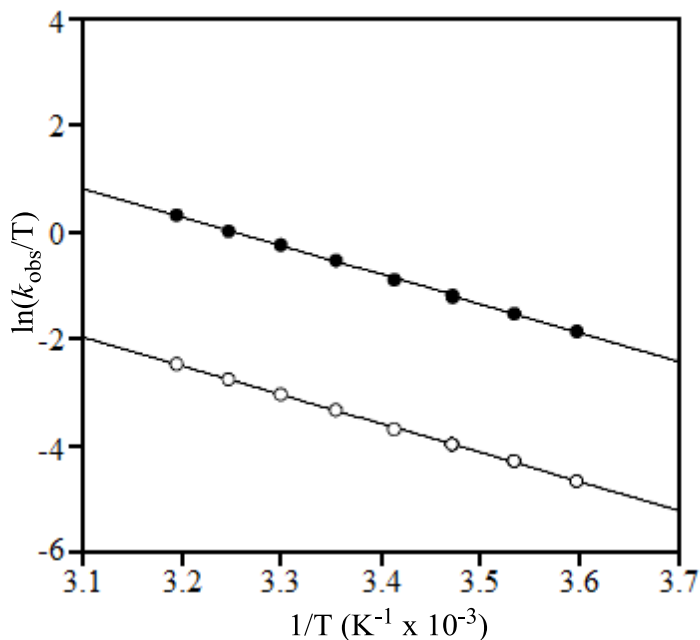


**Figure 33:** Temperature dependence plots for MADH with methylamine (closed circles) and perdeuterated methylamine (open circles) as substrates.<sup>115</sup>

This parallel relationship between proton vs. deuterium transfer implies a lack of temperature dependence on the KIE and this is therefore a good indicator that quantum tunnelling of the proton in MADH is occurring.<sup>115</sup>

The experimental results contradicted these theoretical findings and found that the predicted temperature independence of the reaction between MADH and methylamine/perdeuterated methylamine was in fact misleading as it was found that the reaction rates were strongly temperature dependent. The upshot of these findings is that they no longer fit the static potential barrier mechanism; in fact J. Basran *et al* proposed that the quantum tunnelling mechanism was driven by a thermally fluctuating potential

energy surface. This proposed barrier was later called a dynamic potential energy barrier and incorporates the vibrationally enhanced ground-state tunnelling (VEGST) theory dealt with in the section below.<sup>100, 115</sup>

### 1.6.3. Vibrationally enhanced ground-state tunnelling (VEGST)

This proposed dynamic potential energy barrier was not a new idea; a number of previous theoretical studies had suggested the presence of a temperature-dependent potential energy surface. Such thermal fluctuation in the potential energy surface is the result of fluctuations in the protein structure or fluctuations in the substrate structure, or indeed simultaneous fluctuations in both.<sup>99, 115-118</sup>

In these theoretical treatments, the only means of barrier crossing is by quantum tunnelling. In the case of MADH, it is the thermal fluctuation of the protein that predominantly drives proton transfer. Fluctuations of the substrate are not thought to contribute substantially to the proton transfer reactions since if this were the case it would give rise to different, non-zero values of the activation energies for proton and deuterium transfer, which is not supported by experimental data.<sup>115</sup> It is the fluctuation of the protein that gives rise to the dynamic-potential energy barrier which is referred to as vibrationally enhanced ground-state tunnelling (VEGST) and it is this theory that takes into account the active nature of the protein structure.<sup>90</sup> VEGST can be used to explain how proteins can facilitate this proton transfer by:

1. Reduction of mass by exclusion of water or other solvent; exclusion of water from enzyme active sites is achieved readily and documented amply in the literature.
2. An equalization of energy states for reactants and products.<sup>90, 119, 120</sup>
3. And, perhaps most importantly, the reduction of barrier width.<sup>121</sup>

#### 1.6.4. The resulting dynamic barrier model

The dynamic barrier model diagram for this hydrogen transfer step (Figure 34) uses the VEGST theory in an attempt to represent diagrammatically the relationship between the protein dynamics and the potential energy.<sup>102</sup>

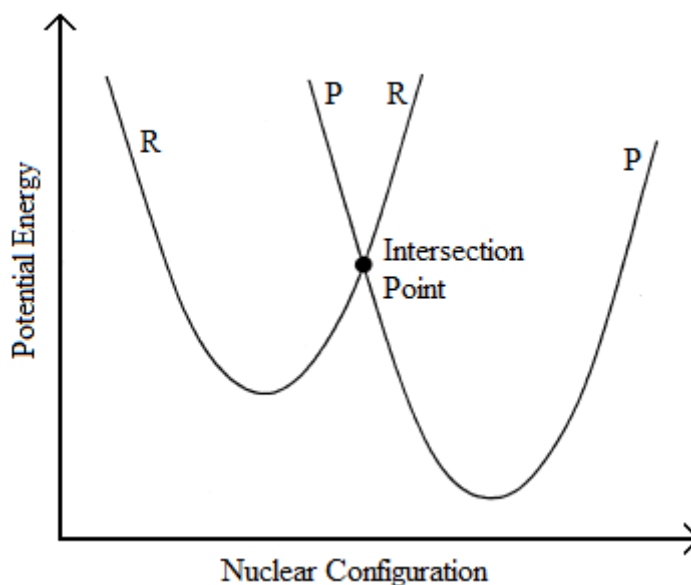


**Figure 34:** Reactant (R) and product (P) energy curves for distortion of the protein scaffold.<sup>102</sup>

This diagram shows the potential energy curves for a generic protein and is conceptually similar to long-range electron transfer in proteins.<sup>97</sup> At the intersection point of the R and P potential energy curves, the atomic positions in the protein scaffold (i.e. the nuclear component) are identical for both the R and P potential energy curves, thus allowing crossover between them. It is important to note that the thermally induced breathing of the protein may pass the nuclear geometry through the intersection point of the R and P curves many times before proton-transfer takes place. The method for proton transfer at this intersection does not necessarily have to be via quantum tunnelling, there are a range of possibilities:<sup>102</sup>

1. Classical TST method
2. Ground state tunnelling
3. Intermediate regimes

The intermediate regimes refer to a process where heavy temperature dependence is observed, the reasons for which are:<sup>102</sup>

1. partition into higher vibrational levels of the reactive C–H bond and/or
2. transfer via a combination of classical (over-the-barrier) and quantum mechanical routes.

Following the tunnelling event, rapid movement away from the intersection point along the P curve prevents coherent oscillations of the proton between the R and P curves. This progress away from the intersection point is again very similar to that of electron transfer processes. The resulting transfer reaction therefore comprises of two components: a nuclear component that reflects reorganization of the protein scaffold to a geometry compatible with proton-transfer (i.e. moving along the R curve to its intersection point with the P curve), and a subsequent tunnelling event involving proton-transfer from the R curve to the P curve.

#### 1.6.5. Concluding remarks on quantum tunnelling in the synthetic TTQ model compound (18) and TTQ containing enzyme

A major question is whether or not the synthetic TTQ compound (**18**) exhibits this quantum tunnelling phenomenon outside of the protein scaffolding? Itoh *et al's* results, whilst not directly trying to answer this, can subsequently be interpreted to answer the question. It was inadvertently investigated whilst studying the oxidation of benzylamine and its deuterated derivative by synthetic TTQ compound (**18**) under

anaerobic conditions and studying the KIE values. As previously mentioned formation of the iminoquinone adduct is followed by rearrangement to the product imine. The kinetic analysis carried out by Itoh *et al.* has revealed that this rearrangement consists of non-catalysed and general base-catalysed processes. When PhCH<sub>2</sub>NH<sub>2</sub> was replaced by PhCD<sub>2</sub>NH<sub>2</sub>, large deuterium kinetic isotope effects were obtained as 7.8 and 9.2 on both processes, respectively. As Itoh *et al.* were not considering the possibility of the small molecule exhibiting quantum tunnelling they did not go into any further detail or speculate whether these values were as a result of proton abstraction via a quantum mechanical mechanism or indeed via the more classical TST. However they did postulate that such large kinetic isotope effects were due to the product imine formation from the iminoquinone, since both non-catalysed and general base-catalysed processes involve  $\alpha$ -proton abstraction.<sup>38</sup> Considering these findings and postulations it can be concluded that the small molecule does not exhibit quantum tunnelling.

However further to these findings a number of research groups have found results indicating that quantum tunnelling during the proton abstraction step is prevalent in TTQ containing enzymes.<sup>85, 90, 102, 105, 115, 122</sup> These conclusions now lead to further unanswered questions; what role does the protein play in the facilitation of the proposed quantum tunnelling mechanism? Does it require a specific cross linking and structure? If so what does it require? At what point does the mechanism cross over from TST to quantum tunnelling? Some of these questions have been partly answered by research on the enzymes themselves; however, there remains quite a substantial gap in knowledge. If TTQ-like small molecules catalyse the oxidation of amines via a classical mechanism but when incorporated into enzymes such as MADH and AADH switch mechanisms and exploit the newly hypothesised VEGST, can this mechanistic ‘switch’ be explored by incorporating TTQ-like functionality into protein domains and recombinant

enzymes? This question can be explored using a range of new technologies to incorporate non-natural amino acids into proteins in a site-specific manner.

## **1.7. Insertion of Unnatural Amino Acids into a Protein Structure**

### **1.7.1. Background to unnatural amino acid mutagenesis**

Three groups in the 1980's were tirelessly working on expanding the genetic code to incorporate unnatural amino acids into proteins. Schultz *et al.* reported the first general method for the biosynthetic incorporation of unnatural amino acids into proteins in 1989.<sup>123, 123-126</sup> Since this point there have been steady improvements and refinements in this “unnatural amino acid mutagenesis.” Over the years many ground breaking studies have resulted in more than one hundred unnatural amino acids being incorporated into a wide range of proteins using this method.<sup>123</sup>

The natural synthesis of a protein is in the amino to carboxyl direction by the sequential addition of amino acids to the carboxyl end of the growing peptide chain. The activated precursors are ‘aminoacyl-tRNAs’ in which the carboxyl group of an amino acid is covalently attached to the 3'-OH of the tRNA via an ester linkage. The linking of the amino acid to its corresponding tRNA is a reaction that is catalysed by aminoacyl-tRNA synthetase.<sup>127</sup>

This “unnatural amino acid mutagenesis” method utilises this process to insert the unnatural amino acid into the protein chain but it does however require some key reagents:<sup>123</sup>

- The unnatural amino acid of interest.
- A suppressor tRNA charged with the unnatural amino acid and containing an anticodon that recognises the nonsense codon.

- DNA coding for the protein of interest with a nonsense codon at the desired site of the unnatural amino acid.
- A translation system containing ribosomes

This process can be schematically summarised:

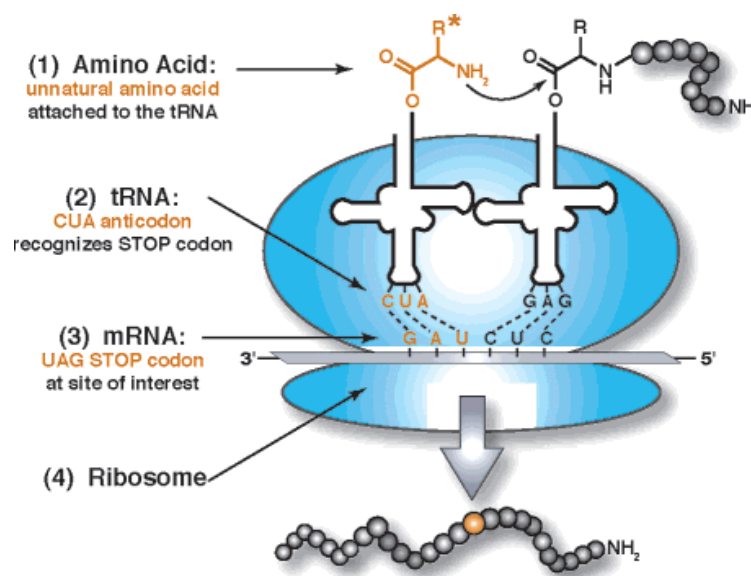


**Figure 35:** Summary of the key reagents required for incorporating unnatural amino acids into proteins using nonsense codon suppression.<sup>123</sup>

### 1.7.2. Previous unnatural amino acid insertions

As mentioned above there have been a large range of modified/unnatural amino acids inserted into proteins using this nonsense codon suppression method and importantly a large portion of these include tryptophan derivatives (Figure 36).

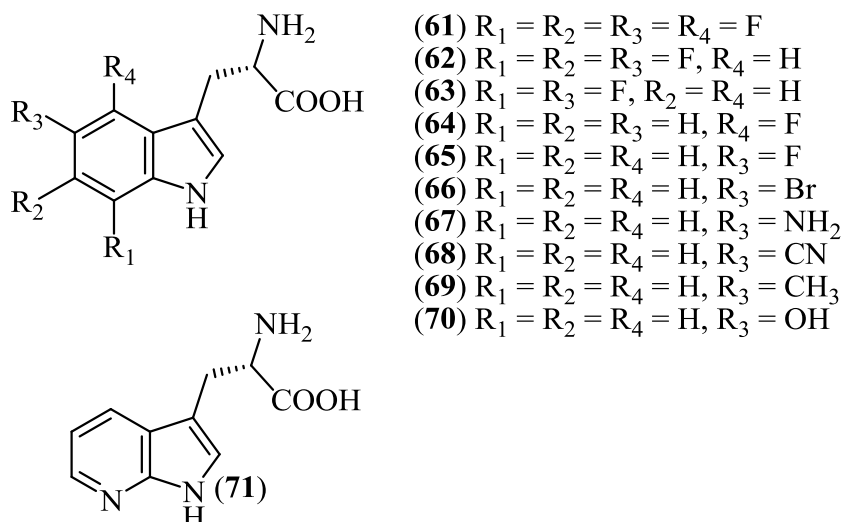


**Figure 36:** A range of tryptophan derivatives inserted into a variety of proteins.<sup>123</sup>

The derivatives (61-71) were put to good use in probing the mechanism of cation- $\pi$  interactions that had been proposed to underlie the association of acetylcholine (a quaternary amine) with the ligand binding domain of the acetylcholine receptor (nAChR).<sup>128</sup> In an effort to evaluate this hypothesis, unnatural amino acid mutagenesis was used to replace individual tryptophan residues within the nAChR binding site with a series of tryptophan analogues substituted with various electron-withdrawing groups (Figure 36 compounds 61-71).<sup>129</sup> A cation- $\pi$  interaction between the ligand and the receptor at  $\alpha$ -Trp<sup>149</sup> was clearly identified and notably, the crystal structure of an acetylcholine binding protein (AChBP) confirmed the assignment of Trp<sup>149</sup> as a key ligand binding element. Many proteins are proposed to have cation- $\pi$  interactions, and unnatural amino acid mutagenesis is a powerful technique for testing these hypotheses.<sup>123, 130</sup>

### 1.7.3. Limitations and advances

The site-specific incorporation of unnatural amino acids into proteins has clearly proven to be a powerful tool for probing protein structure and function. Still, the number of laboratories implementing this approach does not match with its effectiveness.

One of the main reasons that unnatural amino acid mutagenesis has not become a standard laboratory tool is that implementing the approach requires the combined skills of a molecular biologist, a protein biochemist, and a synthetic organic chemist. The molecular biology involves conventional site-directed mutagenesis, the biochemistry relies on standard protein purification tools and the organic synthesis uses simple, well documented procedures to produce the amino acid of choice. The actual difficulty lies in concurrently gathering each of these techniques in one laboratory.<sup>123</sup>

Another drawback associated with unnatural amino acid mutagenesis is the amount of protein that can be conveniently obtained using nonsense codon suppression. The aminoacylated tRNA is a stoichiometric reagent, the amount of full-length protein produced is limited by the amount of nonsense suppressor tRNA that can be prepared and introduced into the translation system. This is a particularly relevant concern among biochemists wishing to conduct structural studies as they need a comparatively large quantity of protein.<sup>123, 131</sup>

There have however been some recent developments and improvements in the methodology of cell translation systems in an effort to simultaneously address both of these limitations. One such development has been in a method for charging nonsense suppressor tRNAs with unnatural amino acids within *E. coli* and *Saccharomyces cerevisiae*, thus eliminating the need to chemically synthesize and subsequently

introduce the aminoacyl suppressor tRNA into the cells. The aminoacylation of the suppressor tRNA is carried out enzymatically within cells by tRNA synthetases that have been reengineered to specifically recognize and couple the unnatural amino acid of interest to the suppressor tRNA. The key here is that this method is specific and does not incorporate other amino acids and tRNAs.<sup>123, 132, 133</sup>

The reason that these methods are so important is that instead of aminoacylating a suppressor tRNA *in vitro* and delivering it to cells, these modifications rely on mutant synthetases to aminoacylate tRNAs biosynthetically and directly in living cells. This results in the aminoacylated tRNAs no longer being stoichiometric reagents because the cells produce them continuously.<sup>134</sup> This in turn results in the possibility of much larger quantities of protein being made.

The versatility of this method is exemplified by the range of unnatural amino acids that have now been inserted into proteins using this method. Figure 37 shows just a select group of tyrosine derivatives.

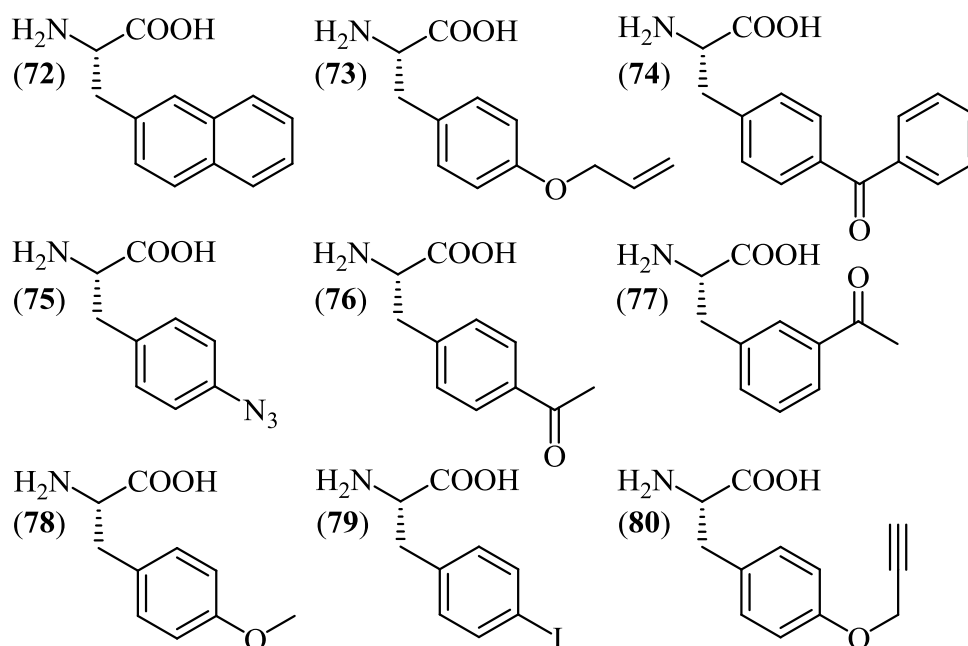


**Figure 37:** Range of tyrosine-like unnatural amino acids inserted to proteins.

Two of these molecules (**75** and **80**) incorporated into a protein structure using this, in cell aminoacylation/translation approach, are of particular importance as they again show the possibility of incorporating either an azide or alkyne into a protein. This presents the prospect of being able to utilise the rapidly expanding area of ‘click’ chemistry.<sup>123, 131, 134</sup>

### **1.8.Objectives for TTQ Model Chemistry**

The previous work by Itoh *et al.* has studied in great detail the structure, function and catalytic activity of the synthetic TTQ molecule (**18**).<sup>38, 80</sup> The improvements in X-ray crystallography have also enabled the structure of TTQ containing enzymes AADH and MADH to be known, however what still remains largely unanswered is the role of the protein as well as the joint role of the protein and the TTQ cofactor (**1**). It is hoped that by carrying out the following work we might be able to gain a better understanding into this.

The main focus of this project was therefore to develop routes to the preparation of a series of amino acid derivatives containing TTQ-like functionality and to develop TTQ-like ‘cassettes’ suitable for the site-specific incorporation into proteins and protein domains.

Insertion into a range of protein domains will explore the mechanistic transition to pathways thought to involve quantum tunnelling. It would build upon already published work (discussed in the introduction) by utilising protein domains that are ‘half way’ between the two extremes discussed above i.e. small molecule TTQ analogue studies and the fully functional natural TTQ-containing enzymes. The TTQ containing synthetic proteins can be characterised by a variety of biochemical

experimental techniques (e.g. stopped flow kinetics) to determine the role of the protein in the facilitation of the oxidative deamination.

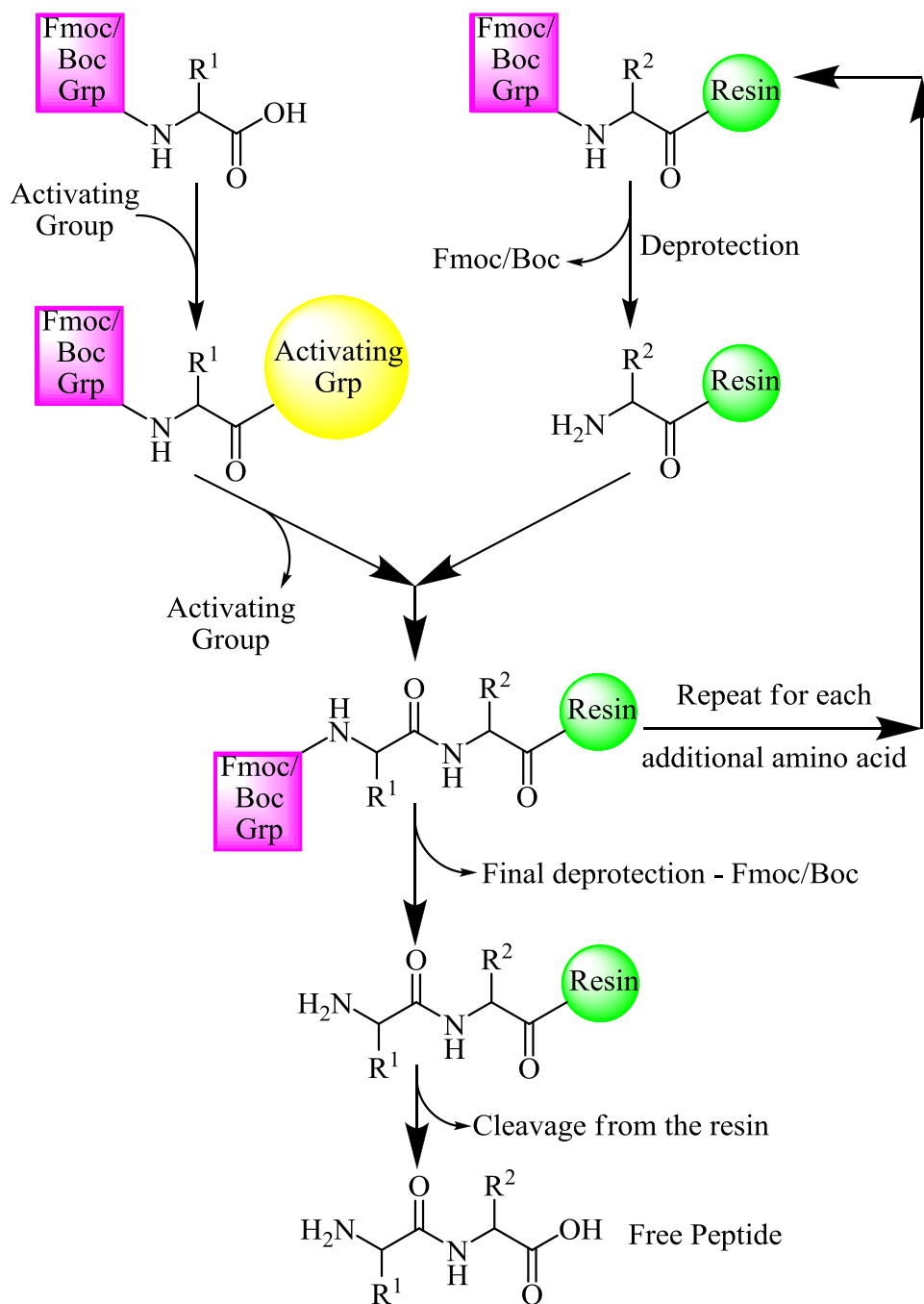
## 2. TTQ Analogues Incorporating The Amino Acid

### Functionality

#### 2.1. Introduction

There are a range of possible ways of introducing a heterocyclic compound containing the important functionality of the TTQ cofactor into a protein. This chapter concentrates more specifically on synthesising a heterocyclic compound containing the TTQ functionality which has the capability of being directly introduced into the protein backbone, either by direct peptide synthesis or site specific incorporation using genetic methods developed to allow incorporation of non-natural amino acids (see chapter 1). As discussed in the introduction this requires synthesis of the a TTQ like cofactor, however importantly, it differs from the work carried out by Itoh *et al.* in that it must incorporate a protected amino acid framework to allow peptide synthesis.

Initially, the amino acid will be inserted into a simple peptide chain using well established solid phase peptide synthesis. Suitable protection of the TTQ model amino acid would allow it to be used in this type of synthesis which was originally developed and reported by R. B. Merrifield in the early 1960s.<sup>135</sup> The classic solid phase peptide synthesis has the C-terminus of the peptide chain covalently linked to an appropriate resin bead (e.g. polystyrene) via an ester linkage, Boc or Fmoc-protected amino acids are then sequentially added to the free amino-group (scheme 22 below).



**Scheme 22:** Schematic representation of solid phase peptide synthesis.

Due to the simplicity of this cycle and modern advances in technology this process has been optimised for automation.<sup>136</sup> The usual method for this process uses Fmoc, Boc or <sup>t</sup>butyl protecting groups and some sort of coupling reagent for example HBTU (Figure 38a).<sup>137</sup>

As previously mentioned such chemistry would require the amino acid to be protected preventing unwanted side reactions occurring; these protecting groups would ideally be compatible with the chemical steps needed for the *in vitro* protein synthesis route as well as direct peptide synthesis. There are a number of protecting groups available for this purpose, however two protecting groups that have been widely used and for which there is a large amount of literature precedent are that of 9-fluorenylmethoxycarbonyl (Fmoc) (Figure 38b) and tert-butyloxycarbonyl (Boc) (Figure 38c).<sup>138</sup>

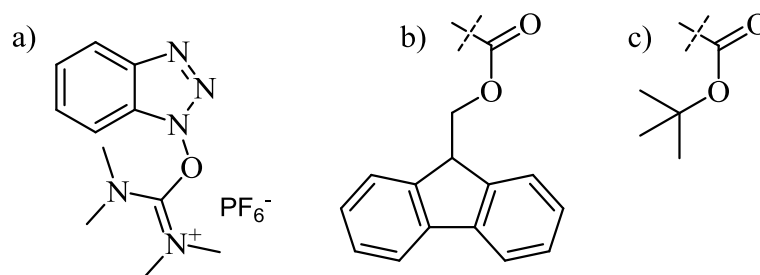


**Figure 38:** a) coupling reagent HBTU b) The Fmoc protecting group c) the Boc protecting group

These two groups are suitable as they meet a number of criteria for protecting groups in the context of peptide and protein synthesis:<sup>139</sup>

- They suppress the nucleophilic reactivity.
- Are stable to a wide variety of reaction conditions.
- Yet can be easily removed under deprotection conditions mild enough not to have an adverse effect on the rest of the molecule.

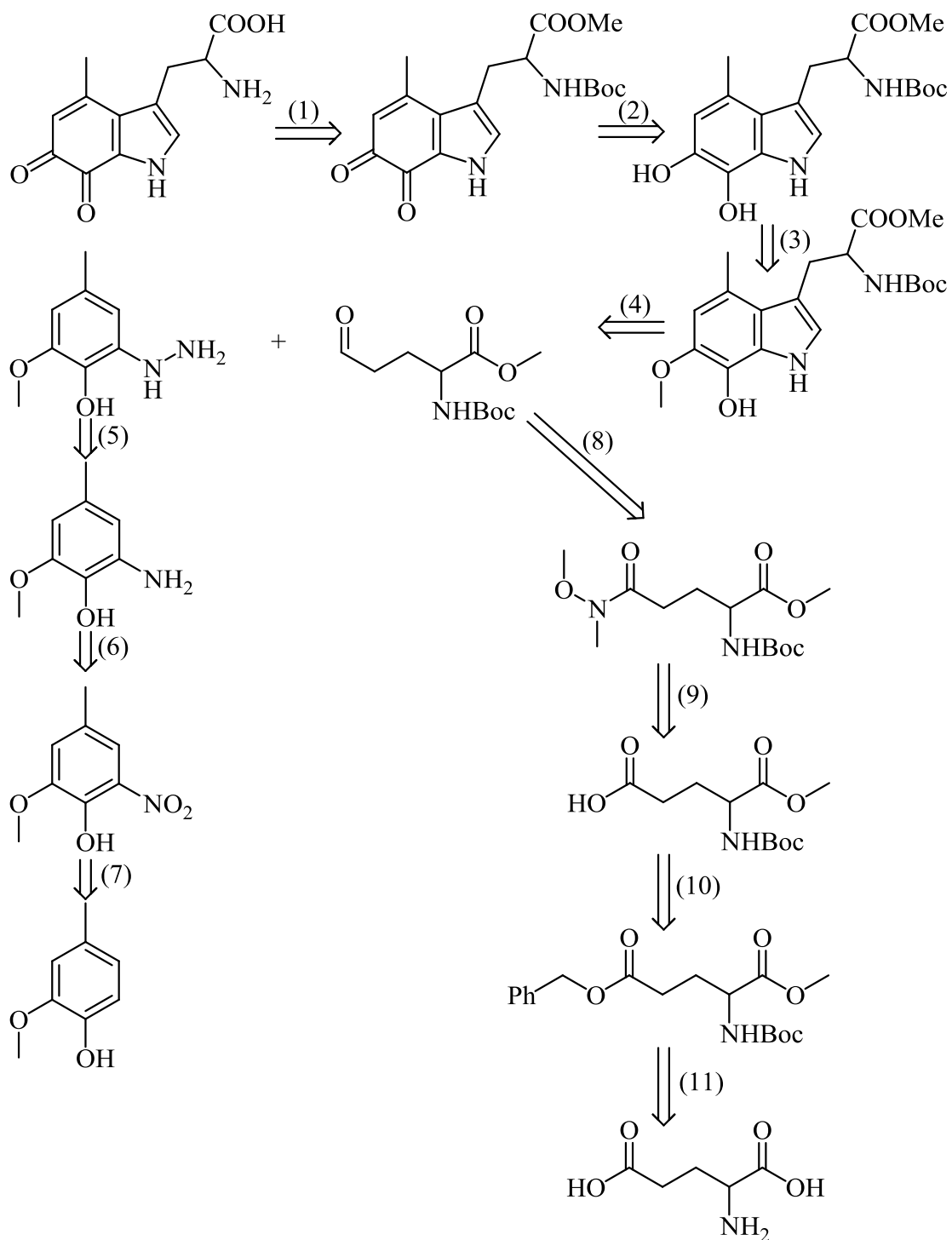
Both of these protecting groups appeared to be suitable for this application so it was decided to try and apply both in the assembly of the amino acid framework. Such

suitability is reinforced when considering their complimentary characteristics; Fmoc being base labile and Boc being acid labile.

The quinone moiety must also be masked in some way. However the protection must be easily removed after the TTQ model amino acid is inserted into a peptide/protein domain without any detrimental effects to the rest of the peptide; allowing for conversion to the ortho quinone late in the peptide/protein synthesis. One such protecting group is that of cyclic ethyl orthoformate, this protecting group has been used a number of times to protect similar groups. Suitability of this protecting group was established by Hu *et al.* who used this group to protect 3,4-dihydroxyphenylalanine and a variety of its derivatives when carrying out solid phase peptide synthesis.<sup>140</sup>

## 2.2. The Proposed Route to the Target Compound

### 2.2.1. Retrosynthetic analysis



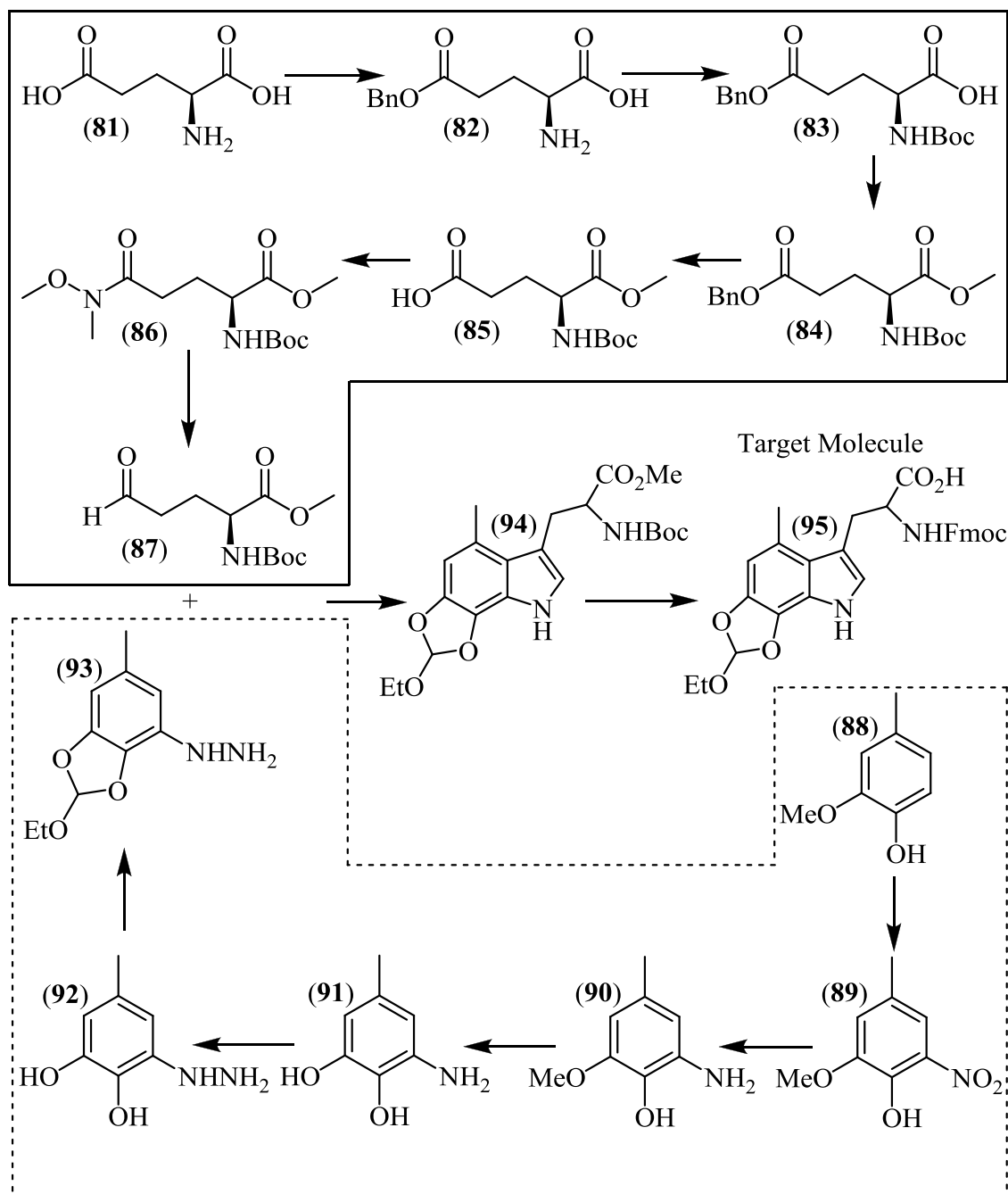
**Scheme 23:** Retrosynthetic analysis of target compound.

Taking into consideration some of the points discussed in the section above (2.1) simple retrosynthetic analysis of the target compound (**95**) is shown above. Most of the steps are simple and logical disconnections. Some of these disconnections involve more than one step so as to protect and deprotect reactive functionality and allow for high yielding reactions; these protections are not always shown.

One of the key steps in this retrosynthesis is step 4. In this step there is a separation of two halves of the compound and while this step may not at first seem to be logical disconnection it in fact would simply involve a Fischer indole reaction, for which there is a wide literature precedent. From this point on the retrosynthetic analysis then splits into two halves each molecule being independently broken down to simple readily available starting materials.

### 2.2.2. Intended reaction scheme

On the basis of the retrosynthetic analysis shown in Scheme 23, the corresponding proposed convergent synthesis is shown in Scheme 24.



**Scheme 24:** The initial overall reaction scheme as developed from the retrosynthetic analysis.

The proposed convergent synthesis aims to synthesise the amino acid framework from glutamic acid (**81**) (dealt with in section 2.3.) from which the side chain is derived from 4-methylguaiacol (**88**) (dealt with in section 2.4.). These two

fragments are coupled using a Fischer indole reaction to produce the target molecule (**95**) (dealt with in section 2.5.).

The target amino acid derivative contains the important functionality of the original synthetic TTQ molecule (**18**), including a protected quinol that once deprotected would readily oxidise to the quinone moiety. It also has a protected amino acid group that again once deprotected would allow for easy incorporation into a protein domain. It is the insertion of this modified amino acid (and other analogues) into the protein peptide that is of importance. Once inserted it is hoped that the TTQ analogues will aid the study into the role of the protein in the deamination reactions catalysed by TTQ (**1**) and its role in promoting quantum tunnelling.

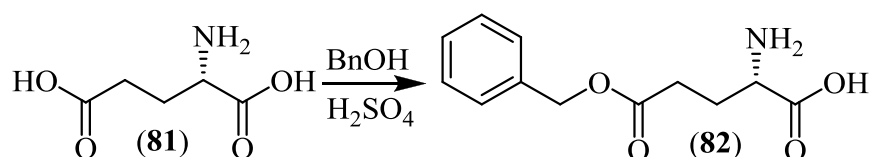
### **2.3.Synthesis of the Amino Acid Framework**

One of the important features in the overall route detailed above (Scheme 24) is the selective protection of glutamic acid to allow selective formation of the Weinreb amide at the  $\gamma$ -carbonyl group and subsequent conversion to the  $\gamma$ -aldehyde (**87**) forming the target compound for the so called ‘top route.’

Glutamic acid not only provides the  $\alpha$ -amino acid group required by the final target amino acid but also the correct functionality that can readily be converted to the aldehyde needed for the Fischer indole synthesis. In addition it is a readily available, cheap, chiral starting material.

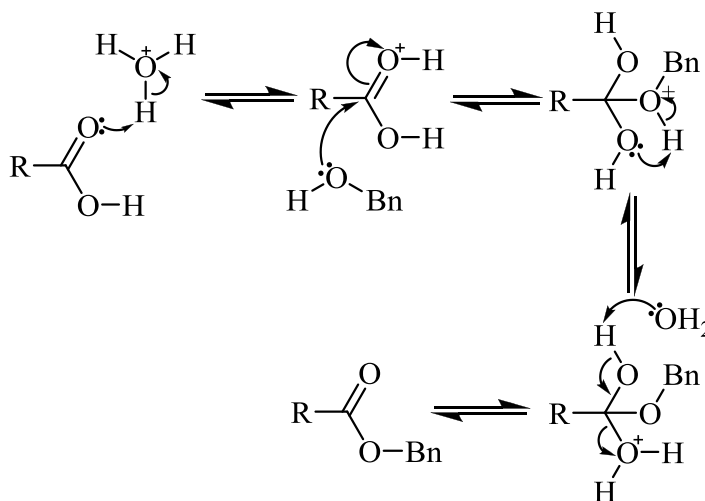
### 2.3.1. Initial route to glutamic acid derived aldehyde

As can be seen in the overall scheme (Scheme 24), the first step of the synthesis, is the selective esterification of the  $\gamma$ -carboxyl group of glutamic acid (see Scheme 25). This selective protection uses a benzyl group as the protecting group, as the starting product (benzyl alcohol) is readily available and the resultant protecting group is stable to a wide range of reaction conditions.<sup>141</sup>



**Scheme 25:** Showing the reaction scheme.

The formation of the  $\gamma$ -benzyl ester follows a standard esterification procedure and has been described in the literature previously with a 50% yield.<sup>142</sup> Initial attempts led to lower yields (31%) of the ester and subsequent attempts by the same method produced similar yields. It is believed that the reaction proceeds via a conventional esterification of a carboxylic acid mechanism (Scheme 26).



**Scheme 26:** General mechanism of esterification (in this case R is glutamic acid).

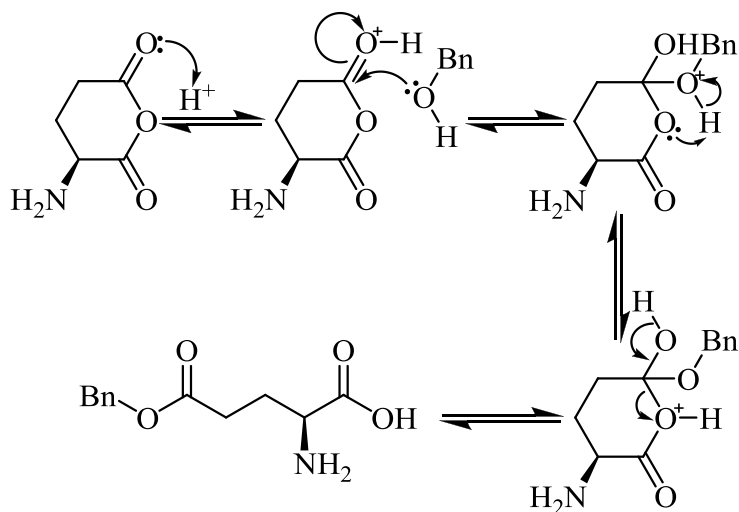
Because this is an equilibrium reaction one-way to try and improve the yield would be to remove the water produced during esterification and any additional water contained in the reactants. Any additional water content of the reagents could also be the source of discrepancy between these initial results and those published.

To explore this theory the procedure was modified whereby the reaction was initially left to stir for 7 hours before adding magnesium sulphate, to 'mop' up any residual water/water produced in the reaction. Once the reaction was filtered to remove this magnesium sulphate it was then left to stir overnight. This resulted in a much improved yield (80 %) and one that is closer to the literature values. It's important to note that this experimental value could still have been improved had more time been spent on optimising reaction conditions.

Purification of the compound proved problematic. It was largely insoluble in most solvents and because of its polar character it was very difficult to purify using the traditional method of a silica gel column chromatography. Using a 75:25 ratio of phenol and water to develop a TLC plate showed that there was still a minor impurity in the reaction mixture. On comparison with the starting material on the same plate it is likely that this is unreacted glutamic acid, but for obvious reasons a column could not be run in this solvent. The lack of solubility of the amino acids is due to them existing as a zwitterion.

One of the most intriguing questions that arose from this reaction was the regioselectivity; esterification of the  $\gamma$  acid and not the  $\alpha$  acid. The mechanism in Scheme 26 provides no answer for this. A possible mechanism that might explain this phenomenon is shown in Scheme 27, where by the reaction proceeds via the anhydride. This would mean that the  $\gamma$  C=O or  $\gamma$  acid would be the most likely to be attacked by the

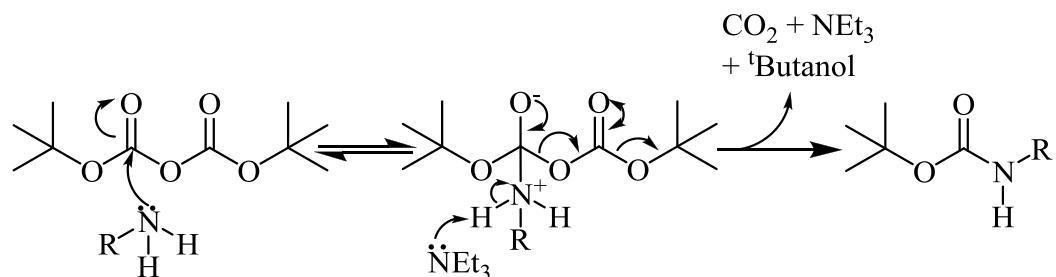
benzyl alcohol, because it is the weaker acid (i.e. stronger base) of the two potential sites of attack.



**Scheme 27:** Proposed mechanism to explain the regioselectivity of esterification.

The anhydride form of glutamic acid, so called glutamic anhydride, is something that has been well documented previously in the literature.<sup>143, 144</sup>

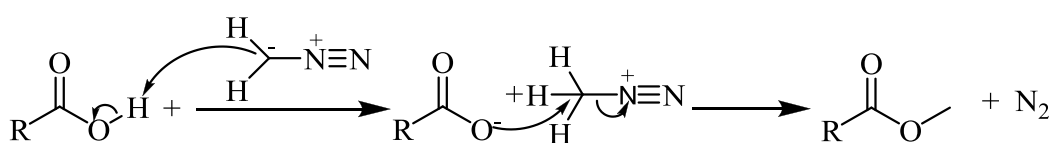
Due to the difficulties in purification of the crude benzy-glutamic acid product the simple Boc protection of the nitrogen was carried out on un-purified starting material; the method for this was taken from the literature.<sup>145</sup> The mechanism for this is shown below:



**Scheme 28:** Mechanism for Boc protection of free amine from benzyl-glutamic acid, where 'R' is  $\gamma$ -benzyl glutamic acid.

The mechanism by which the Boc protection takes place shows that simple nucleophilic attack on the carbonyl by the nitrogen results in a tetrahedral intermediate being formed. Triethylamine then acts as a base and removes a proton from the intermediate and at the same time the Boc anhydride decomposes to form the Boc protected amine, carbon dioxide and tertiary butanol. The protection of the nitrogen prevented the zwitterion formation and this drastically increased solubility as well as reducing the polarity of the compound thus allowing for improved separation with silica gel.

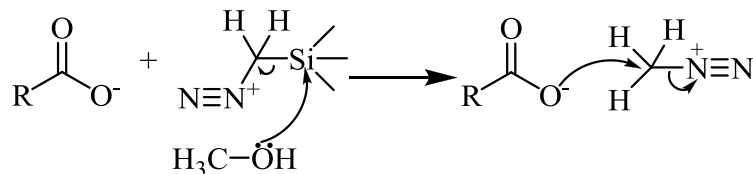
Due to the Boc group's instability in acidic conditions<sup>141</sup> standard esterification (acidic reflux) of the remaining  $\alpha$ -acid is not an option; fortunately however, a large range of alternative synthetic methods are available. One such documented procedure uses diazomethane to convert the free acid into a methyl ester; the mechanism for which can be seen below.<sup>146</sup> Despite the inherent hazards in using this compound, it is a very mild process allowing the esterification of molecules possessing either acid or base sensitive functional groups,<sup>147</sup> the mechanism is also remarkably simple:



**Scheme 29:** Mechanism for diazomethane esterification where 'R' represents Boc protected- $\gamma$ -benzyl glutamic acid.

While this reaction worked; a synthetic alternative to diazomethane was found in the form of trimethylsilyl diazomethane (TMS diazomethane). TMS diazomethane is a much more stable reagent while maintaining sufficient reactivity so as to retain the

benefits of the diazomethane molecule, a fact highlighted by the high yield of this TMS diazomethane reaction (94%).



**Scheme 30:** TMS diazomethane mechanism, where the first step (not shown) is identical to that of the diazomethane mechanism.<sup>148</sup>

The reaction mechanism (Scheme 30) is similar to that of the diazomethane mechanism with the key difference that methanol must be present to activate the TMS diazomethane. It could be considered that the methanol helps generate *in situ* diazomethane for immediate consumption. One of the protons in the resulting methyl ester originates from the diazomethane, one from the methanol, and the remaining one is the “donated” acidic proton from the carboxylic acid. The activation role of the methanol helps prevent direct nucleophilic attack of the acid on the TMS diazomethane resulting in potentially unwanted by-product shown below:

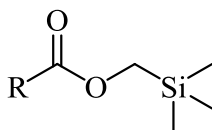


**Figure 39:** Unwanted by-product in the absence of methanol.<sup>148</sup>

Chiral high performance liquid chromatography (HPLC) showed that there was retention of configuration about the chiral centre within this modified glutamic acid as expected. This was confirmed by making the same derivative, but starting with D,L-

glutamic acid containing slightly more of the 'L' isomer. This allowed for easy assignment of the HPLC peaks for the two enantiomers.

On top of this, extra analysis of the compound was achieved by X-ray crystallography (Figure 40), which has not previously been reported.

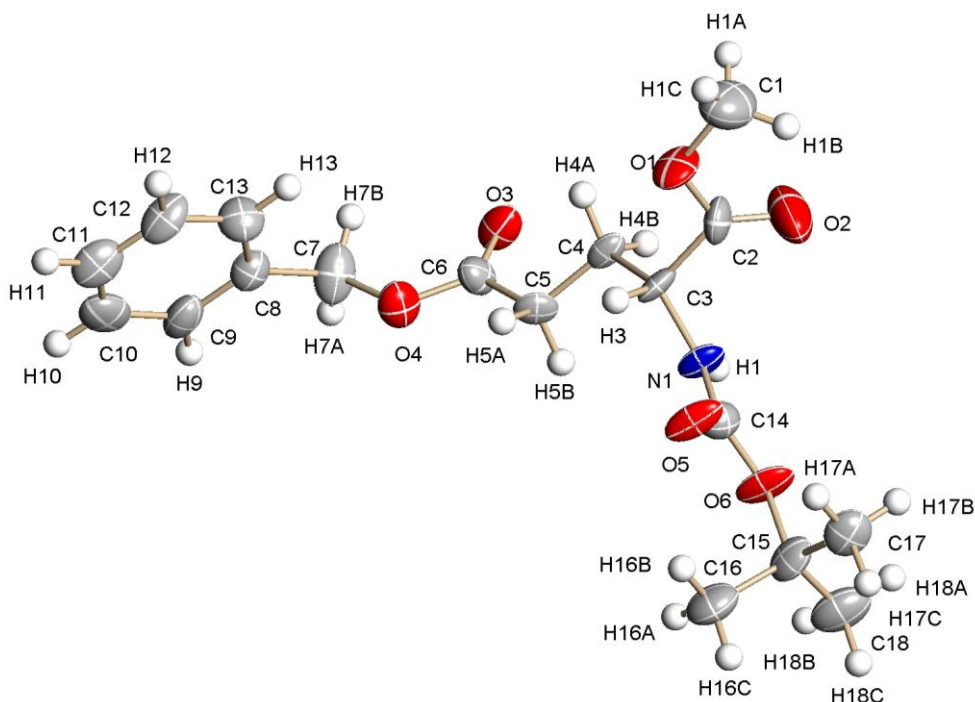


**Figure 40:** X-ray crystallography results for fully protected glutamic acid derivative (**84**) (for full set of data and parameters please see appendix 7.1.1).

Reductive cleavage of the  $\gamma$ -benzyl ester to yield (**85**) was carried out under simple hydrogenation conditions. Analysis by TLC showed that the reaction had almost gone to completion after three hours; however it was left to stir overnight to ensure the highest yield possible (yield after purification was 93 %).

The planned route was then to move onto formation of Weinreb amide (**86**) directly from the carboxylic acid. Since Nahm and Weinreb first reported on the use of

N-methoxy-N-methylamides as carbonyl equivalents,<sup>149</sup> this functional group (the Weinreb amide) has rapidly become popular in organic synthesis.<sup>150, 151</sup>

The Weinreb amide arose after decades of research into the synthesis of ketones from compounds in the carboxylic acid oxidation state via reactions with various organometallics. One major difficulty generally associated with this type of method is the propensity of reactive Grignard and organolithium reagents to over add to the substrate, producing a tertiary alcohol.<sup>149, 152</sup> The same was also true when attempting to reduce compounds in the carboxylic acid oxidation state to their corresponding aldehyde, again this often resulted in the formation of a primary alcohol. There were methods at the time that partially circumnavigated these associated problems but most required carefully controlled, low-temperature addition of one equivalent or less of the organometallic.<sup>153-156</sup>

Weinreb amides managed to combat these problems of over addition (even if a large excess of reagent was used) and did not require stringent reaction conditions to control this addition. The ease of preparation, combined with the limited side reactions during nucleophilic addition, and the selective reduction of this moiety to aldehydes has resulted in regular use of Weinreb amides within synthetic chemistry. Many of these benefits can be credited to the stability of a tetrahedral metal-chelated intermediate, which is formed when adding nucleophiles to initial Weinreb amide (Figure 41).<sup>157</sup> Such co-ordination of the metal decreases the carbon centres susceptibility to further nucleophilic attack and thus reduces the likelihood of over reduction by over addition.

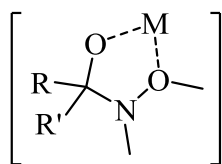
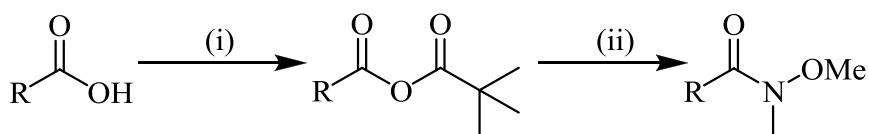


**Figure 41:** The proposed stable intermediate upon reduction of the Weinreb amide.

The Weinreb amide is formed by simple nucleophilic attack on either a suitably activated carboxylic acid or the ester from the amide.<sup>158, 159</sup> Although no literature was found for the conversion of glutamic acid directly, a range of methods are available and one using triphosgene has been used in a very wide number of systems.<sup>160</sup> This method uses the triphosgene to form an acid chloride intermediate *in situ* that is then very reactive towards the nucleophilic attack. Importantly this method uses triethylamine to mop up the hydrochloric acid that is formed as a by-product of the reaction and thus will avoid deprotection of the Boc protected amine.<sup>160</sup>

Singh *et al.* also detailed a high yielding conversion of a carboxylic acid into a Weinreb amide via an anhydride (Scheme 31).<sup>159, 161</sup>



**Scheme 31:** The conversion of a carboxylic acid to a Weinreb amide via an anhydride.

(i) 1.0 equi. of pivaloyl chloride; 1.1 equi. of triethylamine in dichloromethane at 0 °C; (ii) 1.2 equi.  $MeONHMe \cdot HCl$ ; 2.6 equi. of triethylamine.<sup>161</sup>

This reaction is carried out in basic conditions and so is unlikely to participate in secondary-Boc-deprotection reactions as well as allowing for selective amide formation due to the anhydride only forming on the  $\gamma$ -acid. They also mention that attack on the pivaloyl chloride carbonyl was not observed and suggest that this might be as a result of steric interactions.

Subsequent more detailed literature searches revealed that it is possible to form a Weinreb amide directly from an ester;<sup>162</sup> however it is unclear whether these reactions would be regioselective.

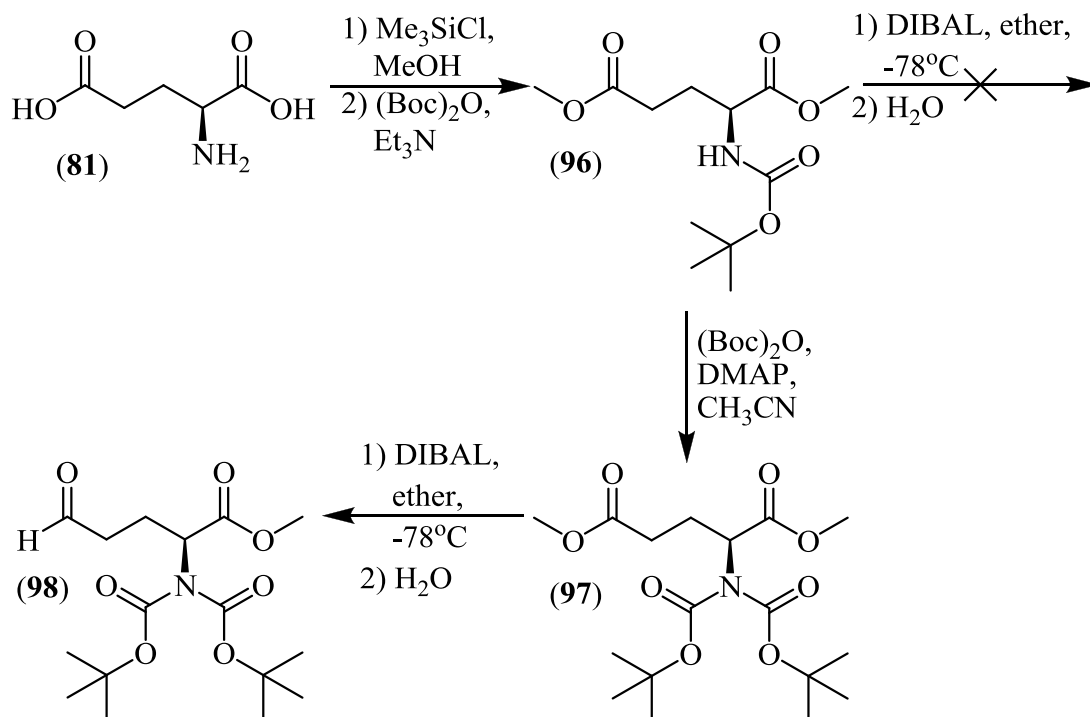
A possible further problem is the reduction of the Weinreb amide to its corresponding aldehyde (commonly using a metal hydride) as this too may also struggle to maintain regioselectivity. Again little conclusive data was found to shed light on this potential problem. All reactions which involved trying to form the Weinreb amide failed with the exception of starting material there were no identifiable reaction products. Reactions seemed only to form a sticky tar like material that could not be purified by column.

### 2.3.2. An alternative route to glutamic acid derived aldehyde

The problem with the above method is that although each individual step was optimised to provide the best yield, the overall yield was still going to be relatively low due to the number of steps involved. Up to the point of the hydrogenation to form the free  $\gamma$ -acid derivative (**85**) the overall reaction yield was 44 %. Upon searching for another suitable method for the Weinreb amide formation, and/or reasons as to why my previous attempts had failed, revealed a new route with good yields (81 %) and less steps was found.<sup>163</sup>

Padron *et al.* were looking for a special class of non-natural amino acids, the lipidic amino acids, which combine structural features of amino acids with those of lipids. They had the eventual aim of incorporating these unnatural amino acids into natural biologically active peptides.<sup>163</sup> One of the products in this published research was remarkably close to an intermediate in this project however their aims were

completely different. As part of their synthesis they required the  $\gamma$ -aldehyde derivative of glutamic acid for a Wittig type reaction. However provided their synthetic route to this derivative was reliable it offered a higher yielding, shorter and easier to follow method. This resulted in modification of the ‘top route’ (Scheme 32):

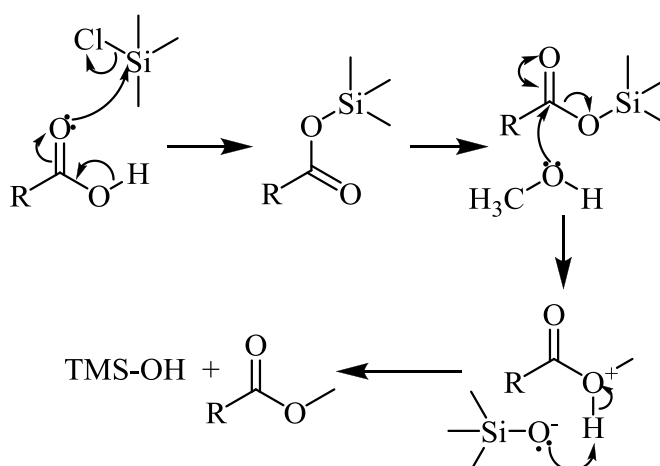


**Scheme 32:** The newly modified synthesis of  $\gamma$ -aldehyde glutamic acid derivative.

Within this new method there is an intriguing extra step where the nitrogen must be doubly-N,N-protected (97) before the selective conversion of the  $\gamma$ -ester to the  $\gamma$ -aldehyde. As can be seen from the scheme above, Padron *et al.* attempted to form the aldehyde without di-protection of the nitrogen, but had no success. This was attributed to some participation from the nitrogen and as a result the group introduced a second N-Boc group in an effort to minimize the nucleophilic power of the nitrogen by removal of the acidic N-H proton.<sup>163, 164</sup> This di-protection has been the case for other reactions involving conversion of a glutamic acid ester derivative to its corresponding  $\gamma$ -aldehyde using DIBAL.<sup>165</sup> With these reactions, as with those mentioned previously, reduction of

the  $\gamma$ -ester when the glutamic acid derivative was mono-N-protected resulted in no or very low yields of the desired  $\gamma$ -aldehyde. This di-N,N-protection is also necessary when using the DIBAL to selectively fully reduce the  $\gamma$ -ester to its corresponding alcohol.<sup>164</sup>

Although this new synthetic route involves a one pot synthesis of the dimethylester-monoBoc protected glutamic acid (**96**) this reaction still has two distinct parts to it. The first of these parts is the esterification of both the  $\alpha$  and  $\gamma$  carboxylic acids using trimethylsilyl (TMS) chloride in methanol as the methylating reagents (Scheme 33)

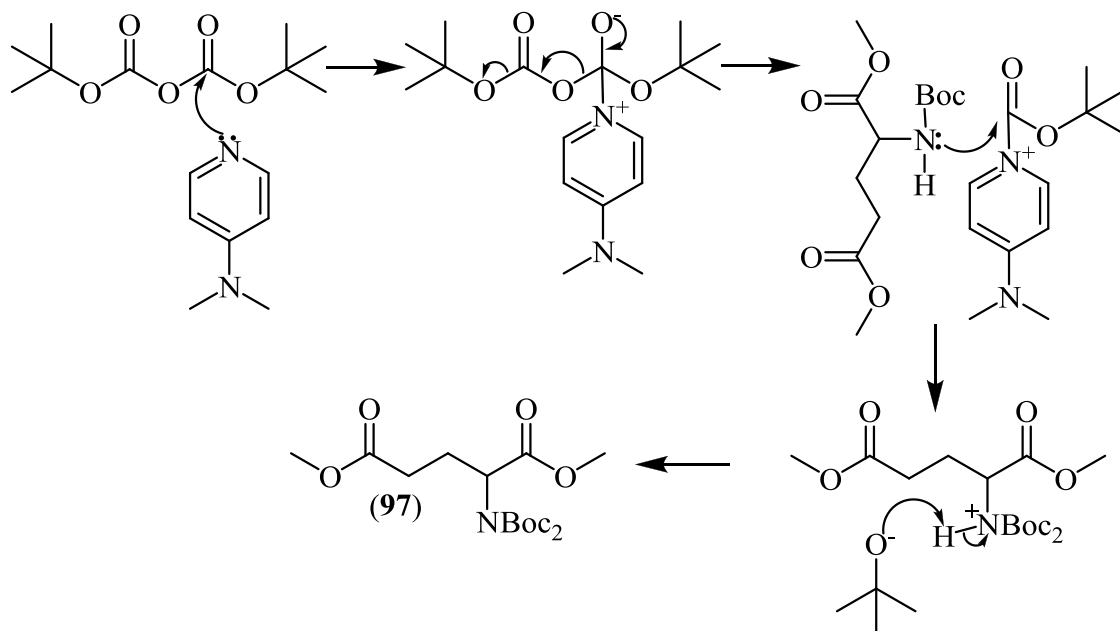


**Scheme 33:** Mechanism for esterification of glutamic acid by TMS chloride in methanol.

In this mechanism the carboxylic acid nucleophilically attacks the TMS displacing the chlorine. This process activates the carboxylic acid and it is this activation that allows the methanol to successfully attack the carbonyl and displace the TMS-O<sup>-</sup> which is a good leaving group. Simple proton transfer between the TMS-O<sup>-</sup> and the protonated ester forms the ester and TMS-alcohol. This same mechanism is clearly repeated twice; once for each acidic group in the glutamic acid molecule.

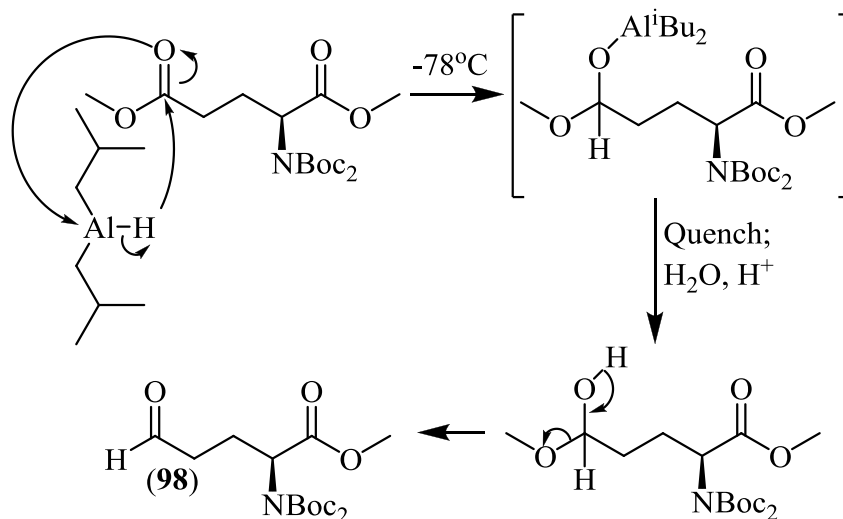
The second step is the mono N-Boc protection. In order to carry this reaction out in the ‘same pot’ as the di-methylation the hydrochloric acid produced in the first step must first be neutralised as the Boc group is not acid stable and hence the addition of excess triethylamine to the reaction. The N-Boc protection proceeds via the same mechanism as the original N-Boc protection in Scheme 28. The molecule posed no purification problems at this point and a simple flash column was enough to purify the compound with good yields (81 %).

After purification, addition of the second N-Boc group was necessary before reduction of the  $\gamma$ -ester. The conditions for this second protection were slightly more forcing in nature; requiring dimethylaminopyridine (DMAP) to activate the Boc-anhydride and facilitate the nucleophilic attack from the nitrogen lone pair on the glutamic acid derivative, as can be seen below:



**Scheme 34:** Mechanism for second N-Boc protection.

Following this protection, selective reduction of the  $\gamma$ -ester to its corresponding aldehyde can take place (reaction mechanism shown in Scheme 35). This is carried out with careful addition of only 1.1 equivalents of diisobutylaluminiumhydride (DIBAL) at  $-78\text{ }^{\circ}\text{C}$ .



**Scheme 35:** Mechanism for reduction of  $\gamma$ -ester to its corresponding aldehyde.

The reason for the selectivity of this reaction is due to a combination of DIBAL's extra reactivity in comparison to other hydride reagents, hence allowing reactions to be conducted at low temperatures, and its steric bulk which results in selectivity.

The regioselectivity is explained due to the DIBAL not delivering its hydride as a simple  $\text{H}^-$ , but instead remaining coordinated. The steric bulk of the isobutyl groups largely prevents nucleophilic attack of this species to the much more sterically hindered  $\alpha$ -ester, preferring to attack the  $\gamma$ -ester.

Perhaps more interestingly and importantly is the chemoselectivity of this reaction. Reduction of a simple ester by a more common reducing agent, for example lithium aluminium hydride ( $\text{LiAlH}_4$ ), results in complete reduction to the corresponding alcohol. The reason why DIBAL does not carry this full reduction lies in its extra

reactivity and Lewis acidity. DIBAL is a more reactive source of  $\text{H}^-$  than  $\text{LiAlH}_4$ , and it is this increased reactivity of the DIBAL which results in the reaction being carried out at  $-78^\circ\text{C}$ , something that is not easily possible with  $\text{LiAlH}_4$ . This low temperature allows the reaction to form a relatively stable intermediate where the remaining  $\text{Al}^i\text{Bu}_2$  is coordinated to the oxygen (Scheme 35). Once the reaction is quenched with acidified water and allowed to warm to room temperature any remaining active DIBAL is quenched and the tetrahedral intermediate from the first hydride addition breaks down to form the desired aldehyde. Formation of the aldehyde (85 %) was confirmed by  $^1\text{H}$  NMR which yielded a peak at 9.78 ppm and integrated to only one proton.

In comparison the  $\text{LiAlH}_4$  reaction would have to be carried out at a higher temperature ( $0^\circ\text{C}$ ) and the resulting tetrahedral intermediate is not stable and decomposes to form the aldehyde. This allows further nucleophilic attack at the carbonyl and results in further reduction to form the primary alcohol. Indeed carrying out a DIBAL reduction at higher temperatures often results in the complete reduction of the ester<sup>164</sup> which is most likely to be a direct result of the instability of the tetrahedral intermediate as in  $\text{LiAlH}_4$  reduction.

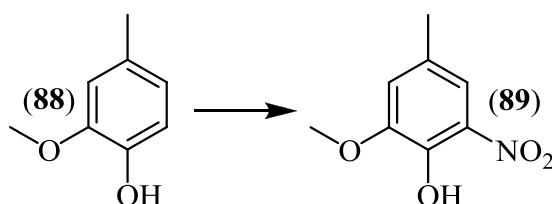
#### 2.4. Synthesis of the Quinone Moiety Framework

Both halves of this reaction scheme have different roles before they converge; the top route is responsible for synthesis of the amino acid framework needed to insert the unnatural amino acid into a protein, the bottom route incorporates the quinone moiety as is present in TTQ. There is a methyl group at the C-4 position in the final product, however this is a model system and once a synthetic route for the target

compound has been found then it will be possible to modify this to an alternative analogue for example those containing an aromatic ring.

#### 2.4.1. Originally planned route to hydrazine derivative

The initial synthetic route for the synthesis of the quinone framework can be found in Scheme 24. The original plan was to start from a readily available starting material, 2-methoxy-4-methylphenol (**88**) as it already contained the appropriate functionality needed to form the quinone moiety. However in order to converge the two fragments from the two routes this product had to contain a hydrazine moiety thus allowing for Fischer Indole reaction.



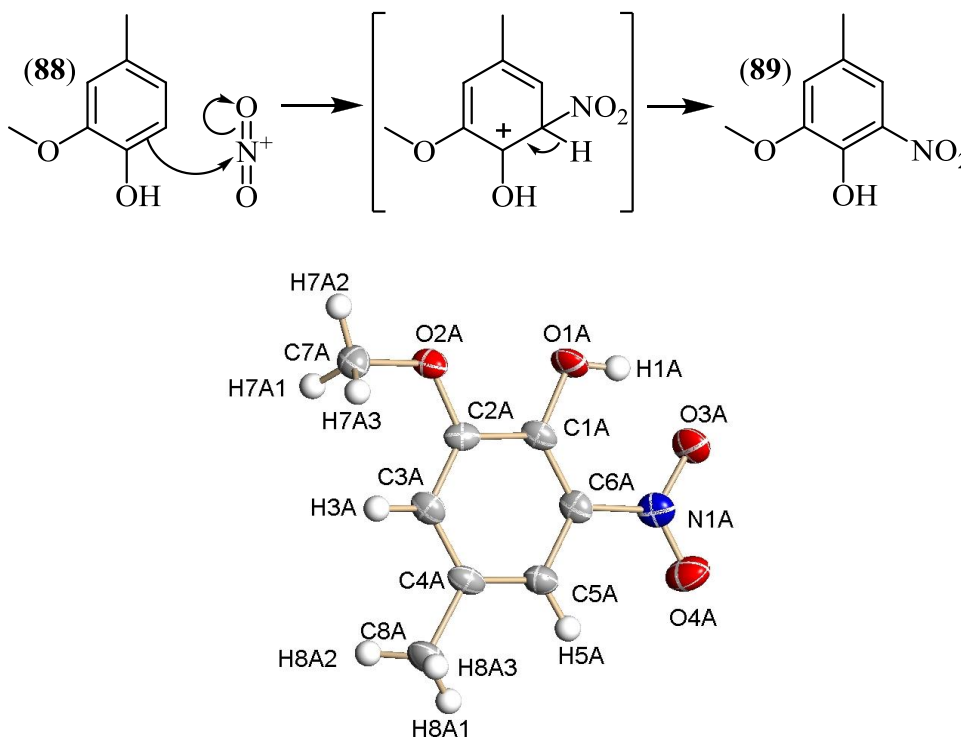
**Scheme 36:** Original starting material (**88**) and its nitrated product (**89**).

The synthesis of the hydrazine derivative began with the introduction of the nitrogen ortho to the hydroxyl substituent by nitration. However there were a number of problems encountered during this reaction. As a result a range of nitration conditions were attempted but all proved largely unsuccessful, leaving a black tar which contained a number of unidentifiable products. However, some material was recovered from the reactions with the best achieved yield being 17%.

It has been shown in the literature that nitration of phenol (and analogues) with concentrated nitric acid or mixed acids can be problematic, often resulting in over

nitration, a range of oxidised products and unspecified resinous tarry material resulting from the oxidative cleavage of the substrate.<sup>166, 167</sup> Over nitration is an increasing problem with growing activation of the ring which increases the probability of the electrons within the ring attacking an electrophilic species such as the nitronium ion (Scheme 37). However despite this being a potential issue in molecule (**88**), it is unlikely as the hydroxyl group is ortho-para directing and all other positions are blocked. Also once one nitro-group is added it is strongly deactivating which tends the molecule towards addition at the meta position (in relation to the nitro-group), and again both of these positions are also blocked. It is also noted that as a consequence of side reactions if any product is formed the typical yields rarely exceed 60%.<sup>168</sup>

The proposed mechanism for this nitration (Scheme 37) proceeds via a nitronium ion.



**Scheme 37:** Top: the possible mechanism for nitration of (**88**).<sup>158</sup> Bottom: the X-ray crystallography structure of the product (**89**) (for full set of data and parameters please see appendix 7.1.2).

In this mechanism the nitronium ion is formed when the nitric acid is combined with the acetic acid prior to addition to the reaction. This nitronium ion is then attacked by the electron rich aromatic ring at the site most likely to stabilise the resulting positively charged intermediate; as could be imagined this is *ortho* to the hydroxyl substituent. Simple elimination of a proton then regenerates the aromaticity and forms the product.

Although the yield was low (17 %) enough material was produced to continue further along the proposed synthetic route. Some material was also subjected to X-ray crystallography (Scheme 37) so that further confirmation of the products could be obtained.

Synthesis of the amine was achieved by simple hydrogenation of the nitro-group. However the amine product (**90**) was fairly unstable and decomposed if left at room temperature overnight. It was found that storage as the acidified hydrochloric acid salt (**90a**) at -18°C prolonged life time. This hydrochloric acid salt did not require liberation before the next step as the hydrazination was carried out under very strongly acidic conditions.

One possible way to reduce the problems associated with the initial nitration step is to protect the free hydroxyl group. So as to reduce complexity, one of the simplest ways to protect the phenol is with methyl ether as is the case with the other hydroxyl substituent. It was hoped that such protection would allow for easy deprotection i.e. same deprotection conditions for both protecting groups. The proposed synthetic route was still the same as is shown in Scheme 24 with the exception of the initial extra protection.

Protection of the phenol is a fairly simple and high yielding reaction using methyl iodide as the methylating agent. The product is also cheaply commercially available further making it a suitable starting material.

The nitration of 1,2-dimethoxy-4-methylbenzene (**103**) (aka 3,4-dimethoxytoluene) should only occur once due to other sites being blocked and the deactivating nature of the nitro group. The reaction conditions took a while to optimise, with early attempts seemingly still suffering from ‘over-oxidation’ and returning only ‘tar’ consisting of unidentifiable products. However once the reaction conditions were optimised it returned modest yields (56 %) that were vastly improved on the corresponding hydroxyl analogue (17 %). The mechanism of this is analogous to that previously proposed for the free phenol (Scheme 37).

Reduction of the nitro group (**99**) to its corresponding amine (**100**) again proceeded under normal mild hydrogenation conditions and gave the amine in the expected high yields. The loss of material was probably through mechanical loss in the work up of the reaction and subsequent purification.

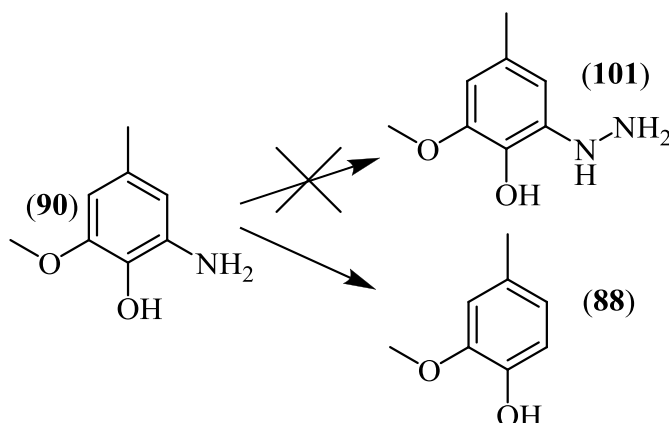
#### 2.4.2. Problems with conversion to the hydrazine derivative

Conversion of the free phenol compound (**90**) to the hydrazine derivative (**101**) was attempted several times and with a range of different reaction conditions, however none of the reaction conditions yielded any of the desired compound (Table 3).

Time with NaNO <sub>2</sub>	Temp. with NaNO <sub>2</sub>	Stirring Method	Reducing Agent (RA)	Time with RA	Temp. with RA
5 mins	0 °C	Glass rod	Na <sub>2</sub> SO <sub>3</sub>	Overnight	60-70 °C
5 mins	0 °C	Magnetic bar	Na <sub>2</sub> SO <sub>3</sub>	Overnight	60-70 °C
5 mins	0 °C	Mechanical	Na <sub>2</sub> SO <sub>3</sub>	Overnight	60-70 °C
60 mins	0 °C	Mechanical	Na <sub>2</sub> SO <sub>3</sub>	Overnight	60-70 °C
5 mins	0 °C	Magnetic bar	SnCl <sub>2</sub> ·2H <sub>2</sub> O	60 mins	0 °C
5 mins	0 °C	Mechanical	SnCl <sub>2</sub> ·2H <sub>2</sub> O	60 mins	0 °C
30 mins	0 °C	Mechanical	SnCl <sub>2</sub> ·2H <sub>2</sub> O	Overnight	Room temp.
30 mins	-35 °C	Mechanical	SnCl <sub>2</sub> ·2H <sub>2</sub> O	Overnight	Room temp.
30 mins	-35 °C	Mechanical	SnCl <sub>2</sub> ·2H <sub>2</sub> O	Overnight	-35 °C

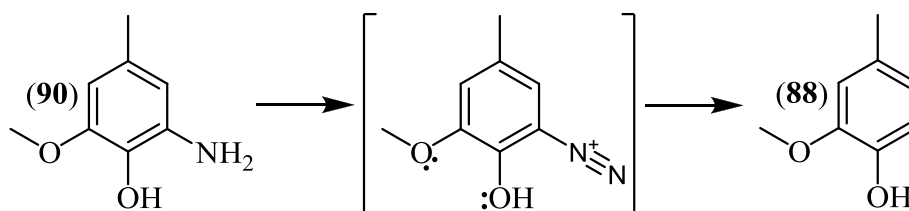
**Table 3:** The range of reaction conditions tried in an attempt to form the hydrazine derivative (**101**).

In all cases the primary by-product of the reaction was the deaminated analogue of the starting material (**88**) (Scheme 38).



**Scheme 38:** Intended conversion of amine (**90**) to hydrazine (**101**) and the actual deaminated by-product (**88**) isolated from the hydrazination reaction.

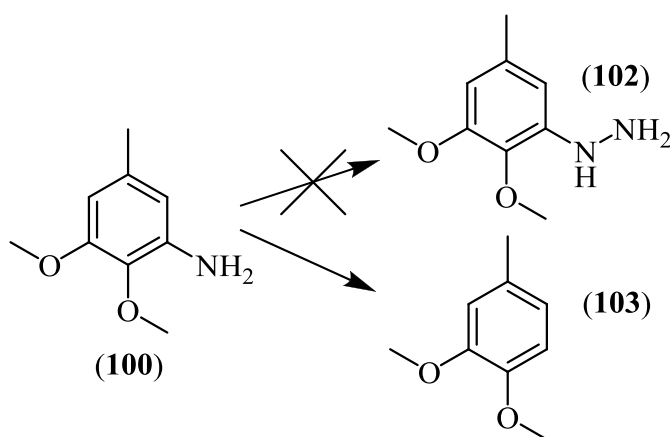
Initially it was thought that this might be as a consequence of localised heating upon addition of sodium nitrite solution (highly exothermic reaction) to the acidified paste and as a consequence a variety of stirring methods and temperatures were tried. The observation may also be explained when considering the mechanism for the formation of the hydrazine (Scheme 39) which proceeds via a diazonium salt.<sup>158</sup> As this scheme shows the aromatic ring could potentially lose nitrogen gas in an entropically favourable reaction something that could explain the experimental observations of effervescence during the addition of the sodium nitrite.



**Scheme 39:** Proposed mechanism for formation of diazonium salt and subsequent loss of nitrogen.

Aryl deaminations via the diazonium salt have been documented previously in the literature and on occasion have been deliberately used as part of a synthetic route.<sup>147, 169-171</sup> However despite its wide use in synthetic chemistry, there has been limited investigations into the mechanism.<sup>172</sup> There are two possible mechanisms that have been proposed; one involves decomposition of the diazonium salt to an intermediate aryl radical, which later accepts hydrogen from a donor.<sup>171</sup> The second involves the diazo-group simply being reduced;<sup>171</sup> such reduction has been documented using sodium stannite, a similar reducing agent to the stannous chloride used in this reaction.<sup>172</sup>

The further protection of the phenol as its methyl ether, originally used in an effort to optimise the initial nitration reaction, might have the additional benefit of activating the electron rich aromatic ring to a lesser extent in comparison with the free hydroxyl and thus reduce the possibility of the above mechanism taking place. The extent to which the aromatic ring is activated by a group has a correlation with the electron donating or electron withdrawing influence of the substituents, as measured by molecular dipole moments. This being the case phenol has an electron donating (activating) dipole moment of  $1.50 \text{ D}^{173}$  whereas when protected as a methyl ether, e.g. anisole it has a lower electron donating dipole moment of  $1.22 \text{ D}^{174}$ .



**Scheme 40:** Intended reaction route from amine (**100**) to the hydrazine (**102**) and the actual deaminated by-product (**103**).

Subsequent reactions with both hydroxyl groups protected (**100**) still yielded the deaminated by-product (**103**). This was again attributed to the electron rich aromatic ring facilitating the loss of nitrogen in a similar mechanism to that shown in Scheme 39.

Formation of the hydrazine was due to be one of the final steps in the bottom route synthesis (Scheme 24), with only protection of the quinone to follow. One idea

given some consideration might have been to use the planned ethyl orthoformate protecting group to further reduce the activity of the aromatic ring in comparison to that of the methyl ether protected hydroxyl groups.

Ethyl orthoformate is used as a common protecting group for catechols due to its stability under basic conditions.<sup>140, 141</sup> This stability makes it particularly compatible with the Boc chemistry related to the amino acid framework. But if the ethyl orthoformate protected quinone could be inserted at a suitable stage in the synthesis then it would also be compatible with the Fmoc chemistry, allowing for selective deprotection of either moiety. However it had been reported in the literature that such a protecting group was not stable to the strongly acidic reaction conditions needed for the hydrazine formation.<sup>141</sup> An easy to make test compound (**104**) (Figure 42) was therefore subjected to similar reaction conditions.

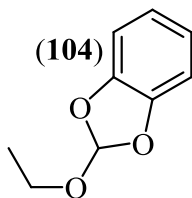


**Figure 42:** Test compound for stability tests of the ethyl orthoformate protecting group.

The tests confirmed the literature findings that this protecting group would be unsuitable for protection prior to formation of the hydrazine. Clearly there would also be little point in trying these reactions with both phenols in an unprotected form (**105**).

These results required a rethink for the synthesis of the quinone moiety framework. The question was: is there a way of forming the quinone moiety without starting with it in a protected or unprotected form?

### 2.4.3. An alternative approach to formation of quinone framework

Having invested a large amount of time and effort on the glutamic acid derived aldehyde it was important that the Fischer indole route was still used. Obviously this still requires hydrazine formation as part of the bottom route, importantly though the possibility of a molecule not containing a protected form of the quinone is to be considered. Once such possibility (**106**) is shown below (Figure 43):

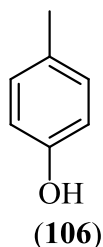
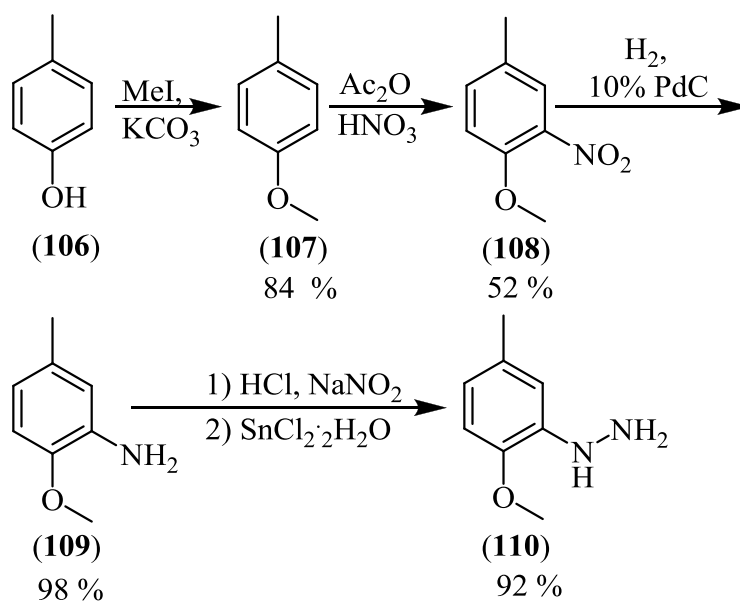


**Figure 43:** Possible new starting material in the synthesis of the hydrazine component.

Itoh *et al.* have previously shown that it is possible to oxidise a free phenol to the corresponding *ortho*-quinone using Frémy's salt. This step was one of the last in their synthesis of the synthetic TTQ molecule (**18**).<sup>26</sup> It was hoped that this step could be repeated with this new possibility after the Fischer indole reaction to join the two halves of the reaction. The mono-methoxy compound would be less electron rich than its counterparts and hence the deamination reaction may be less problematic when forming the hydrazine; a process thought to have happened previously. This molecule further fulfilled the criteria initially set out, as it was very cheap to buy and readily available and as can be seen (Scheme 41) follows a simple synthetic route.



**Scheme 41:** The new synthetic route for the hydrazine component.

The majority of the reactions followed very similar methods as used in the previous route; first protection of the phenol, followed by nitration and then reduction of the nitro group. These steps were all fairly easy and were consistently high yielding as can be seen in Scheme 41, once again the exception being the nitration.

Although the nitration step was still the poorest yielding, it was much higher than the results that were obtained for the dihydroxy starting material (**88**). Previously only one *ortho* position was available for nitration; one concern with this particular molecule was that it might be possible to nitrate the molecule twice. However there was literature precedent for this not being the case.<sup>175</sup> As discussed previously this is probably due to the strong deactivating effect of the nitro group.

The conversion to the hydrazine was however still highly problematic. Initial reactions did produce some of the hydrazine, albeit in a very low yield. However once isolated from the reaction mixture, it was found that the hydrazine decomposed very quickly at room temperature a process that probably involves the elimination of nitrogen.<sup>176</sup>

Once formed the hydrazine is sufficiently unstable that it instantly begins to decompose and has a half life of approximately three hours at room temperature, shown by NMR spectroscopy. The result was that it was very difficult to purify the crude material as normal purification methods either use heat (increasing the thermal degradation) or take a comparatively long time e.g. column chromatography. The time needed to run a column meant that the product had begun to decay before it was isolated resulting in it only being about as pure as when the column was started. Column chromatography had been attempted in the cold room (approx  $-5^{\circ}\text{C}$ ), but unfortunately this still did not work efficiently enough so as to obtain pure product. A recrystallisation from benzene was found for a similar compound (*para*-methoxyphenylhydrazine)<sup>177</sup> however this also failed as it never recrystallised, this could have been simply due to solubility issues but could also possibly have been due to thermal degradation.

The upshot of these results meant that the reaction had to be optimised so as to obtain as close to 100% yield of product as possible so that no further purification was needed. After many attempts the eventual reaction conditions were dropwise addition of aqueous sodium nitrate solution to a paste of the amine (**109**) in concentrated hydrochloric acid at  $-35^{\circ}\text{C}$ . After 30 mins a solution of tin(II) chloride dehydrate in concentrated hydrochloric acid was added and the resultant precipitate left to warm to room temperature whilst standing for 15 hrs. These reaction conditions had to be stuck to rigidly; at  $-40^{\circ}\text{C}$  the HCl used as both reagent and solvent begins to freeze; when this happens it is very difficult to maintain efficient stirring and localised hotspots result on addition of the sodium nitrite. The localised heating within the reaction then facilitates the deamination of the starting material thus returning the major product as (**107**) in a similar reaction mechanism to that of previous reactions (Scheme 39). At temperatures

higher than  $-35^{\circ}\text{C}$  the intermediate diazonium salt begins to degrade (although at a far reduced rate to that experienced at room temp), resulting in contamination of the final compound.

As a result, the reaction has to be kept as cold as possible but prevented from freezing. The resulting reaction parameters are difficult to adhere to as the addition of the sodium nitrite solution is an extremely exothermic reaction which can result in varied product purity.

### **2.5. The Fischer Indole Reaction**

With both halves of the target molecule now complete the two fragments had to be joined together. It was planned to do this using a Fischer indole synthesis; joining the aldehyde from the amino acid framework to the hydrazine of the quinone framework. As previously demonstrated by Itoh *et al*<sup>26</sup> formation of the quinone moiety would take place after this by oxidation of the free phenol by Fremy's salt.

Acid labile protecting groups aside, classic acid catalysed Fischer indole reactions used to form indole structures are notoriously poor yielding reactions. Due to this, some consideration was given to a palladium-catalysed indole formation. However as a review by Cacchi and Fabrizi demonstrates, while there are regular examples of indoles with substitution at the two position, there are very, very few examples of this kind of reaction where the only substitution is at the 3 position.<sup>178</sup> Importantly the few examples of palladium catalysed Fischer indole couplings that result in only substitution at the three position, do not occur between an aromatic hydrazine and a carbonyl. Any of the palladium-catalysed Fischer indole reactions that involve a coupling between a

hydrazine and a carbonyl, result in substitutions in both the two and three positions as the carbonyl in question is always a ketone.<sup>178, 179</sup>

### 2.5.1. Using the inorganic non-acid catalysed Fischer indole

A classic acid-catalysed Fischer indole synthesis was discounted because of the acid labile Boc protecting groups. As previously discussed, palladium catalysed reactions were also not a viable option; however, there were examples of non-acid catalysed Fischer indole reactions which used low catalyst loadings of rhodium to form an indole between an aldehyde and a hydrazine.<sup>180</sup> The group had used a variety of aldehydes and ketones, but maintained the simplest aromatic hydrazine (phenylhydrazine). It was therefore unclear if the reaction would work with a more complex aromatic system.

Initially this reaction was tried without starting material from the top route, instead it used the more readily available and easy to produce pentanal (**111**) (from pentan-1-ol using pyridinium chlorochromate (PCC)). This initial ‘test’ reaction would combine this simple aldehyde with the hydrazine (**110**); the desired product of which (**112**) (shown below in Figure 44) could be used to test other reactions, such as deprotection of the phenol.

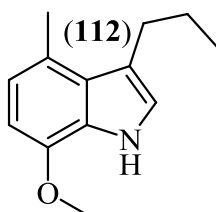


**Figure 44:** The potential indole product from the rhodium catalysed Fischer indole reaction.

The paper in which the procedure is detailed,<sup>180</sup> used a rhodium cyclo-octadiene (COD) complex, however it did also mention that a range of other rhodium complexes including  $\text{RhCl}_3 \cdot 3\text{H}_2\text{O}$ ,  $\text{RhCl}_3\text{Py}_3$ ,  $\text{RhCl}(\text{PPh}_3)_3$ , and  $[\text{RhCl}(\text{NBD})]_2$  could also be used and showed comparable catalytic activity. It was therefore decided to use the simplest of these complexes,  $\text{RhCl}_3 \cdot 3\text{H}_2\text{O}$  as this was a readily available compound.

The reaction itself was carried out at a very high temperature, well above the boiling point of the solvent and therefore was conducted in a sealed high pressure apparatus (Figure 45) under an inert nitrogen atmosphere.

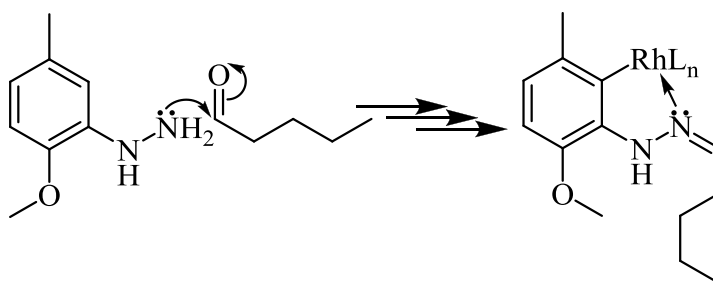


**Figure 45:** High pressure apparatus used for the rhodium-catalysed Fischer indole reaction.

This initial test reaction was a success albeit with a fairly low yield (29 %). The yield could be the result of the high temperature ‘decomposing’ the hydrazine. The catalysis of this reaction must be rapid in an effort to avoid the problems associated with the high temperatures i.e. react with hydrazine to form product before the hydrazine has decomposed. The possibility of carrying the reaction out at different temperatures was

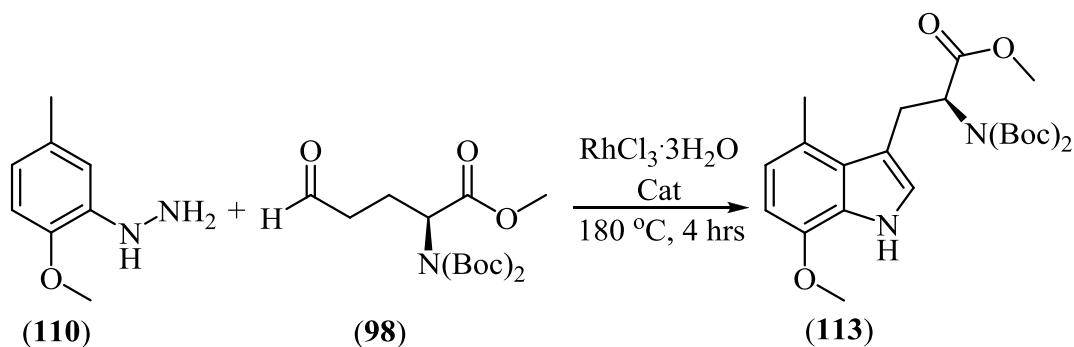
ruled out by this paper which suggested that reactions carried out at lower (or higher) temperatures had a detrimental effect on the reaction yield.<sup>180</sup>

It was suggested in the initial paper that the mechanism for this process (Scheme 42) proceeded via some sort of *ortho*-metalation.<sup>180</sup> Interestingly and perhaps surprisingly, this novel reaction has been very rarely used for other such applications.



**Scheme 42:** Possible mechanism for rhodium-catalysed indole formation.<sup>180</sup>

In the classic acid catalysed mechanism, an amine-imine type intermediate has been reported for an acid-catalysed Fischer indole reaction.<sup>181</sup> The proposed mechanism shown above (Scheme 42) for the present reaction, includes a proposed *ortho*-metallation step to form a rhodium containing intermediate. *Ortho*-metallated complexes are already known in reactions between N-containing compounds such as azobenzene and metal complexes.<sup>182, 183</sup> This reaction proved to be higher yielding (21%) when compared to that of the classical acid catalysed Fischer indole synthesis (16%) discussed later (section 2.5.2).



**Scheme 43:** Rhodium catalysed Fischer indole reaction between the hydrazine (**110**) and the glutamic acid derivative (**98**) which incorporates the essential amino acid functionality.

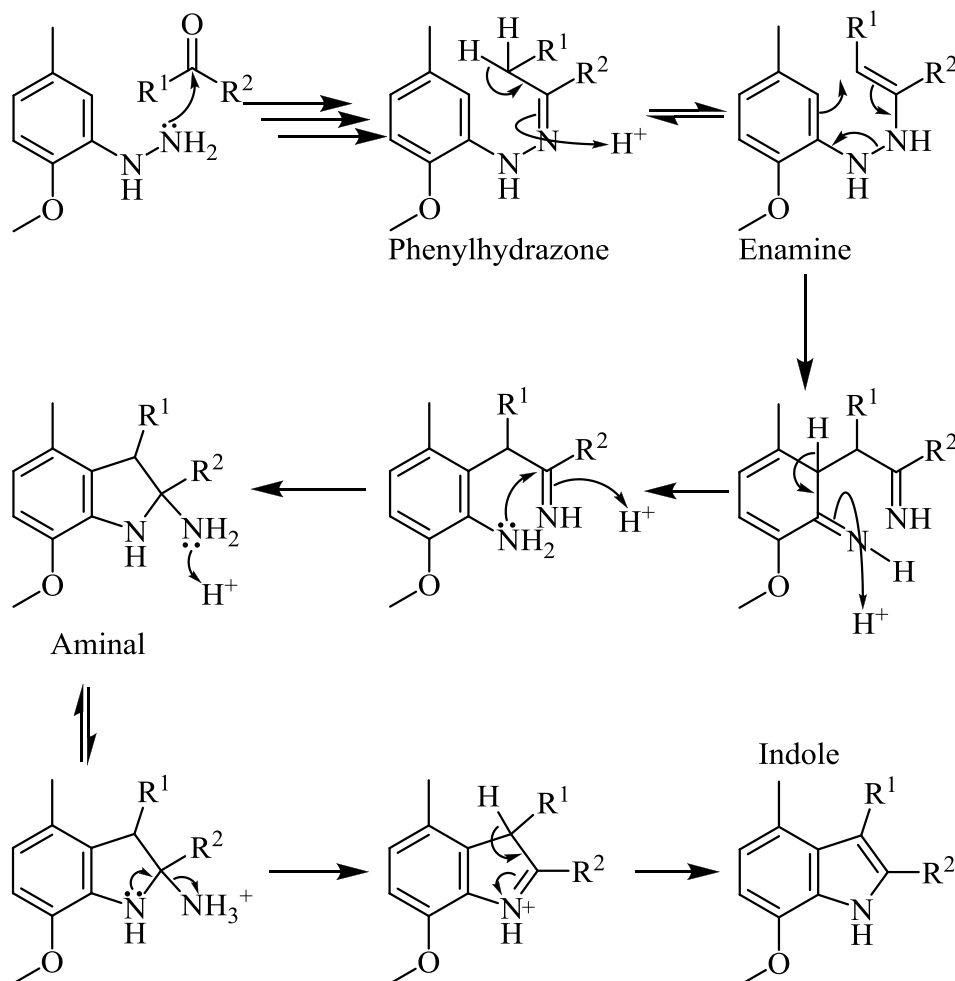
Now that the process had been established in a test reaction it was to be applied to the glutamic acid derivative (**98**) (reaction scheme shown above in Scheme 43). Unfortunately this time the reaction proved to be unsuccessful with none of the desired product (**113**) detected. It is unclear why this is the case; however one possibility is that the starting material (**98**) might have coordinated in some way to the metal. This coordination could have been while it was in the protected form (as starting material) or in a deprotected form as a direct result of the heating. There is literature evidence that some materials using N-Boc protection begin to decompose and ‘lose’ their protection when heated to high temperatures i.e. 100 °C upwards.<sup>184</sup> These literature claims were supported by subsequent reactions in which the glutamic acid derivative (**98**) was placed under identical reaction conditions (180 °C, ethanol, in sealed reaction vessel) but in the absence of the hydrazine (**110**) or rhodium catalyst. The reaction did not return the expected starting material (**98**) but a large quantity of unidentifiable products. It was conceivable that one of these by-products might be the ethanol acetal of the aldehyde. To eliminate this possibility the same test was carried out but using

tetrahydrofuran as the solvent instead of ethanol, however this reaction returned similar unidentifiable results.

One of the reasons that this coordination might be a particular problem is due to the simplicity of the rhodium catalyst used. The potentially polydentate starting material offers a more stable complex than that of the monodentate chlorine and water in an entropically driven process known as the ‘chelate effect.’<sup>185</sup> The result is that the rhodium is never free to carry out the *ortho*-metalation that is thought to be paramount to the reaction mechanism. This coordination process might be prevented or at least slowed by the coordination of the rhodium to another ligand such as those detailed in the original paper. As previously mentioned and detailed in the original paper, experimenting with reaction temperatures was unlikely to have an effect on the reaction yield.<sup>180</sup>

#### 2.5.2. ‘Classic’ Acid Catalysed Fischer Indole

With the rhodium catalysed method no longer a possibility attention had to return to the more classical acid catalysed Fischer indole reaction (Scheme 44).



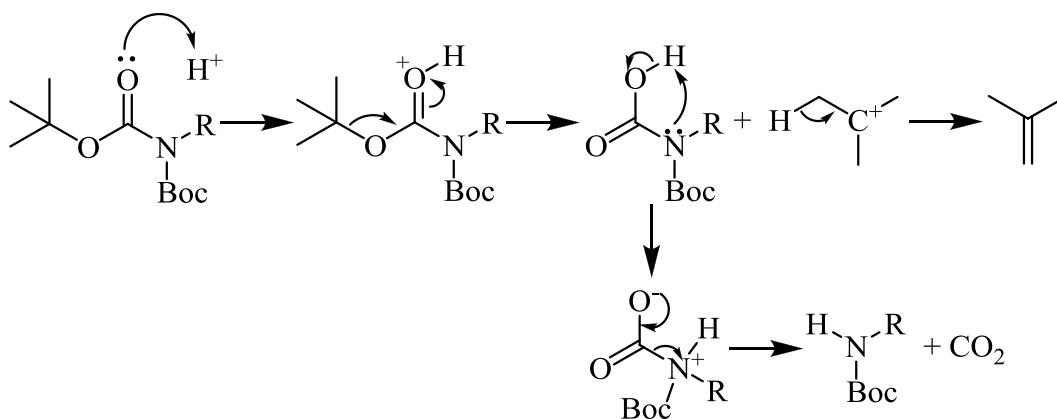
**Scheme 44:** The general mechanism for classical acid-catalysed Fischer indole synthesis.<sup>158</sup>

The first step in this mechanism is formation of the phenylhydrazone (an imine) from the ketone via a well known mechanism. This imine then tautomerises to the enamine which is followed by a key step; the rearrangement of the enamine to form a strong carbon-carbon bond and concerted cleavage of the nitrogen-nitrogen single bond, in an example of 3,3-sigmatropic rearrangement. This sigmatropic rearrangement destroys the aromaticity and subsequent re-aromatisation (tautomerisation that is facilitated by the acidic reaction conditions) of the benzene ring creates an aromatic amine, which acts as a nucleophile and attacks the other imine forming an amination.

This aminal undergoes acid decomposition with the loss of ammonia and a proton, in a mechanism that is similar to acid decomposition of an acetal, to form the indole.<sup>158</sup> As there is only one ortho-position (with respect to the hydrazine) available for attack, there should only be one possible product formed.

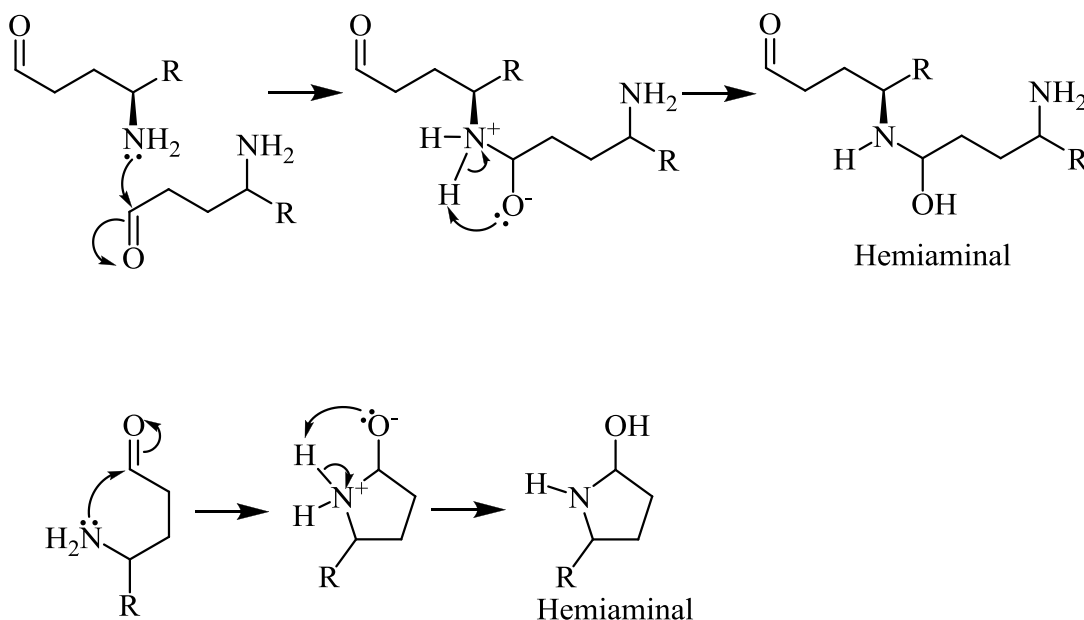
As with previous attempts, the acid catalysed Fischer indole reaction was first optimised using pentanal (**111**) as the starting aldehyde, producing a simple TTQ derivative (**112**). This reaction initially produced very little product (less than 1 %), as too much acid rapidly darkened the mixture in an exothermic reaction. However optimisation of the reaction by reducing the quantity (and thus the concentration) of acid increased the overall yield (16 %). Purification of the product was still particularly difficult; TLC of the crude mixture revealed more than 16 individual spots. The resultant purification by silica gel column chromatography was painstakingly slow and the 'semi-purified' product obtained had to be further purified by recrystallisation to yield the pure desired compound (**112**).

Once the acid-catalysed reaction had been optimised with pentanal, attention turned to the more complex glutamic acid derivative. However one potentially important problem arose; as previously stated, the Boc protected glutamic acid derivative (**98**) would not be acid stable. This would most likely result in a deprotection of the amino group, the mechanism for which is shown below (Scheme 45):



**Scheme 45:** Mechanism for acid deprotection of Boc protecting group where ‘R’ is the remaining part of the glutamic acid derivative.<sup>158</sup>

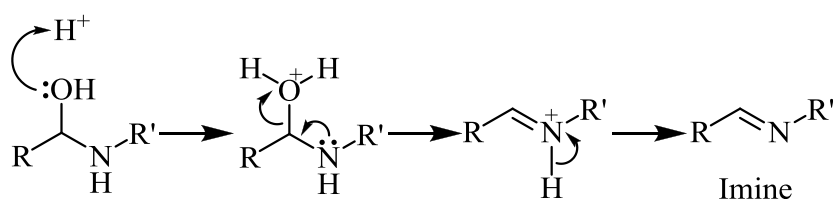
The problem with this deprotection then is that it frees the lone pair of electrons up on the nitrogen to allow nucleophilic attack. This nucleophilic attack could be either intermolecular or intramolecular attack on the aldehyde, forming a hemiaminal intermediate (Scheme 46).



**Scheme 46:** Intermolecular (top) and intramolecular (bottom) attack of the deprotected amine nitrogen to the aldehyde where ‘R’ in both cases is a methylester.

Importantly the intermolecular mechanism could further continue this nucleophilic attack as in either its hemiaminal or imine form it still contains the reactive functional groups. The result of this could be uncontrolled polymerisation of the glutamic acid derivative.

Due to the acidic nature of the reaction conditions, in both cases the hemiaminal is likely to decay further, forming the product imine (Scheme 47).

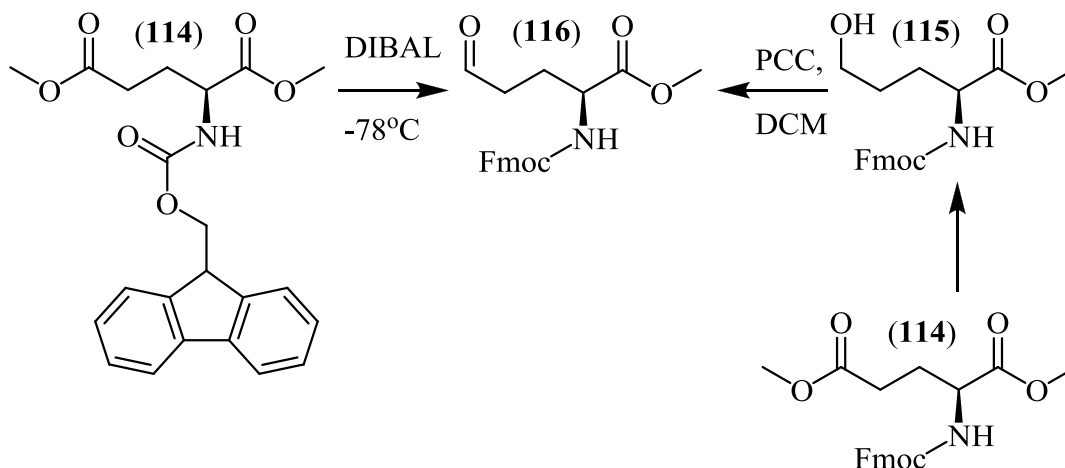


**Scheme 47:** General mechanism for decay of hemiaminal in acidic conditions to form an imine.

The results of the acid catalysed Fischer indole reaction on the Boc protected glutamic acid derivative (**98**) were inconclusive as it returned only unidentifiable products and was unclear which, if either, of these reaction mechanisms had taken place. However what was clear was that the reaction had not been successful and none of the desired product was detected.

Alongside the development of the N,N-diBoc protected glutamic acid was the development of an acid stable derivative. As discussed in the introduction to this chapter, one such protecting group that provides a possible solution to this problem and is still compatible with peptide synthesis is the Fmoc (9-fluorenylmethyl carbamate) group. Importantly, this group is still easily removed, non-hydrolytically, by the addition of simple amines; this could be important for easy removal of the protecting group prior to insertion into a protein domain.

Formation of the mono-Fmoc derivative (**114**) (Scheme 48) of glutamic acid was fairly easy; the protocol of which can be found in the experimental.



**Scheme 48:** Mono-Fmoc derivative of glutamic acid (**116**).

A variety of attempts to form derivative (**116**) failed. Scheme 48 shows the two different routes attempted; in each case a variety of concentrations and temperatures were tried in an effort to directly and selectively form the  $\gamma$ -aldehyde (**116** Scheme 48). Due to time constraints little time was spent on optimising these reactions and as a consequence the target compound (**116**) was never made.

There are a number of possible reasons for this; one of the most obvious could be related to a previously discussed topic; the nitrogen is only mono-protected and previous literature attempts to form the aldehyde with a mono-protected amine all failed. It was suggested that this was due to some sort of participation by the nitrogen.<sup>163</sup> These results as well as those for the mono-Boc protected amine provide supporting evidence for this.

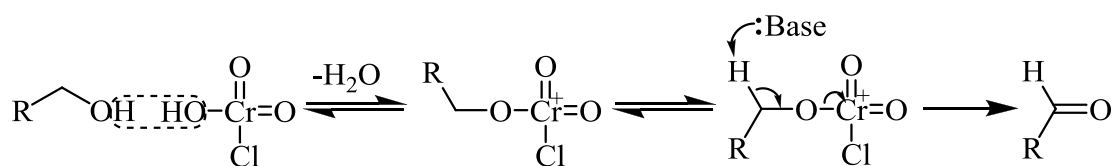
One of the possible ways around this problem would be to N,N-diFmoc protect the glutamic acid derivative, however literature searching showed that there were no

protocols for the N,N-diFmoc protection of any amino acid. This lack of literature suggested that this di-protection was not possible, or at least was potentially very difficult; due to time constraints and the potential complexity of the problem it was decided not to further explore this idea.

An alternative possibility could be related to the steric bulk of the Fmoc protecting group. DIBAL is not just an H<sup>-</sup> supplier, in that it only becomes a reducing agent after forming a Lewis acid-base complex.<sup>158, 186</sup> This being the case it might be that the steric bulk of the Fmoc protecting group preventing, or at least hindering, the complex formation.

The latter of these two proposals would better explain the experimental data. It was reported by Padron *et al.*,<sup>163</sup> that when an attempt to reduce the ester of a mono-N-protected glutamic acid derivative (**96**) was made, there was a mixture of unidentifiable compounds. This was not the case when attempting to reduce the Fmoc derivative (**114**) as the reaction predominately returned starting material, with other minor by-products including the over-reduced product alcohol (**116**).

The alcohol was an unexpected by-product; however enough of it was isolated to attempt an alternative route to the aldehyde; selective partial oxidation using pyridinium chlorochromate (PCC). The mechanism for PCC oxidation (Scheme 49) shows first, formation of a chromic ester by elimination of water followed by an ‘E2 like’ elimination using a base (pyridine) to remove a proton.<sup>147</sup>

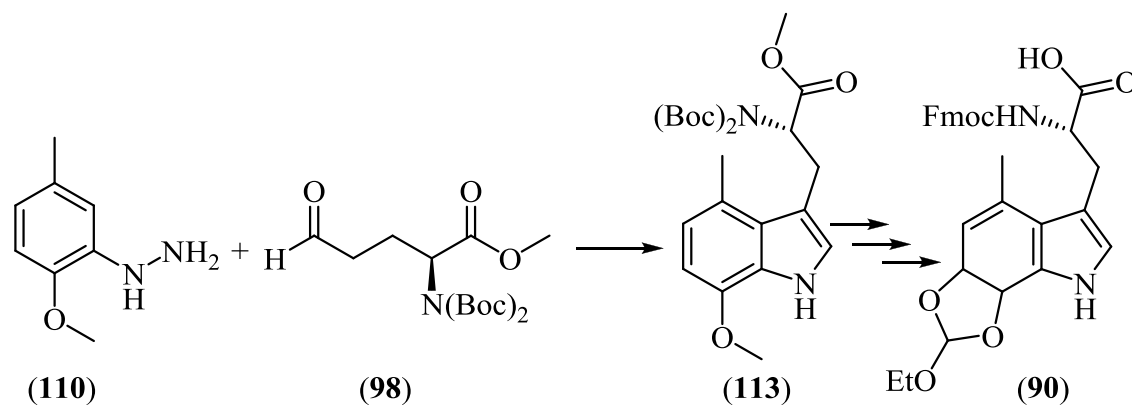


**Scheme 49:** General scheme for the oxidation of a primary alcohol to its corresponding aldehyde.<sup>147, 187, 188</sup>

Unfortunately no desired aldehyde was detected and no starting material was recovered. This could possibly be again due to steric hindrance from the Fmoc protecting group, because, while the mechanism (Scheme 49) seems fairly simple what has to be considered is that the chromate ion is large. However there are no reported examples of this problem in the literature.

## 2.6. Summary

This chapter has detailed the successful synthesis of a glutamic acid derivative (**98**) that it was hoped could be used in the synthesis of the final target molecule (**90**) which incorporates the desired amino acid functionality (Scheme 50). The chapter also details synthesis of the hydrazine (**110**) that was utilised to incorporate the quinone moiety into the final compound.



**Scheme 50:** The intended overall Fischer indole reaction between the glutamic acid derivative (**98**) and the hydrazine (**110**) to form the indole (**113**) which can undergo a variety of protection and deprotection steps to form the target compound (**90**).

In both the synthesis of the glutamic acid derivative (**98**) and of the hydrazine (**110**) the chapter also details failed syntheses that resulted in the production of unwanted reaction products and continues to elaborate on possible reasons for each specific problem encountered. As a part of this discussion the chapter details reactions designed to circumnavigate these problems and discusses the outcome of these reactions including whether they supported or disproved earlier theories. This discussion is important for anyone who wishes to carry out follow on work from this project. The new synthetic routes resulted in deviations from the originally proposed synthetic route that had been derived from retrosynthetic analysis.

Regardless of the synthetic approach tried in this chapter there were problems with one of the last steps which utilised a Fischer indole reaction to join an aldehyde (containing the amino acid functionality) to a hydrazine (containing methyl ether that could later be oxidised to the quinone). These problems were not overcome in this project and as a result research was focused a completely different way of introducing the TTQ analogue into a peptide/protein.

### 3. Alternative Approaches to Inserting TTQ Analogues into a Peptide/Protein Backbone

#### 3.1. New 'click' chemistry possibility

The problems described above indicated increasing difficulties to the proposed target compound and although there were still a number of options that could be pursued it was decided to explore an alternative approach in parallel.

Rather than trying to synthesise an unnatural amino acid containing the preformed ortho-quinone and insert it into a protein chain, one option was to synthesise a molecule with the desired functionality of TTQ (**1**) that could be inserted into a protein domain at a later date using appropriate chemistry. Such an approach would make the protein synthesis potentially less problematic because it would involve inserting a far simpler modified amino acid into a protein chain and attaching the functional heterocycle at a later date. This has the added bonus that simple modified amino acids e.g. those that contain alkyne functionality in their side chain, have already been shown to have been inserted into a protein domain.<sup>123</sup>

Within this chemistry there are two obvious possibilities; the first only requires modification of the amino acid sequence within the protein domain so that a cysteine residue can be present in the active site i.e. no need to insert an unnatural amino acid. With such an amino acid present at the active site, the target molecule (**117**) (Figure 46) could be designed to incorporate a simple alkyl halide allowing for an S<sub>N</sub>2 type reaction. In this molecule the addition of a  $\beta$ -ketone to the alkyl halide increases the electrophilicity of the compound and thus increases its chances of nucleophilic attack from a cysteine residue.

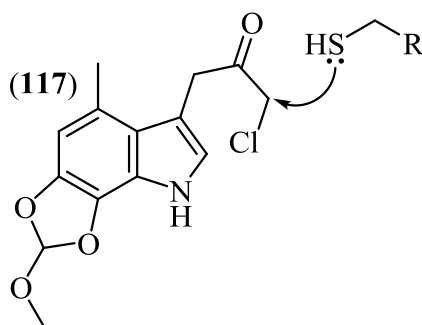


**Figure 46:** A proposed target alkyl halide depicting nucleophilic attack from a cysteine residue where ‘R’ is the remaining part of cysteine.

As can be seen this molecule incorporates the important features of the TTQ (1) molecule; the indole frame work with a protected 6,7-quinone structure and possessing the additional functionality needed to insert it into a protein domain. However forming such a compound does have a number of problems, for example the ketone would have to be protected in some way so as to avoid the Fischer indole reaction occurring at two potentially different sites. This protection and subsequent deprotection increases the number of synthetic steps and would decrease overall yield. There would also be problems associated with deprotecting the methylether-protected phenol (this problem is addressed in 3.1.5) as one possible method involves the use of thiophenol. There could also be selectivity issues; there would be more than one cysteine residue within a protein domain, all of which might have the same reactive potential towards the alkyl halide.

The second possibility was to make either of the target compounds shown in Figure 47, which could then undergo a copper catalysed cycloaddition to an azide or alkyne counterpart in a so-called ‘click’ reaction. The counterparts would be side-

chains of unnatural amino acids inserted into the protein backbone by the ‘unnatural amino acid mutagenesis’ process discussed in Chapter 1 (Section 1.7.1).

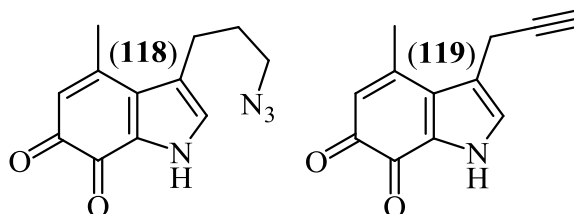


**Figure 47:** Two further proposed target molecules.

There are some problems associated with producing these target molecules; however, there are not as many problems as with the previously suggested molecule. An advantage of this route is that one of the University of Leicester’s strong research areas is ‘click’ chemistry; this could help to provide welcome expertise and guidance. Further to this, inserting molecules into proteins by ‘click’ chemistry is proven chemistry with many methods available.<sup>189</sup>

### 3.1.1. Introduction to click chemistry

The term ‘click’ chemistry was coined by Sharpless *et al.* in 2001 and encompasses a large variety of reactions; however such reactions have to fit a defined set of stringent criteria.<sup>190</sup> The reaction must be:

- wide in scope;
- give very high yields;
- generate only inoffensive by-products that can be removed by non-chromatographic methods;
- be stereospecific (but not necessarily enantioselective);

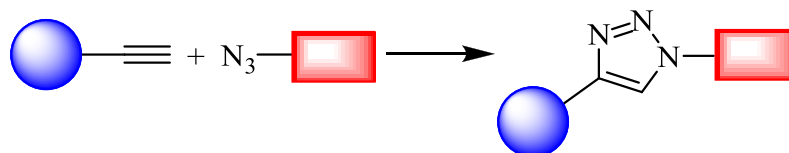
- involve only simple reaction conditions (ideally, the process should be insensitive to oxygen and water);
- use readily available starting materials and reagents;
- use no solvent or a solvent that is benign (such as water) or easily removed, and simple product isolation;
- purification if required must be by non-chromatographic methods, such as crystallization or distillation;
- the product must be stable under physiological conditions.

It has to be said that many of these criteria are subjective and even if measurable and objective criteria could be agreed upon, it is unlikely that any reaction will be perfect for every situation and application. However, several reactions have been identified which fit the bill better than others:<sup>190</sup>

- Cycloadditions of unsaturated species, especially 1,3-dipolar cycloaddition reactions, but also the Diels-Alder family of transformations.
- Nucleophilic substitution chemistry, particularly ring-opening reactions of strained heterocyclic electrophiles such as epoxides, aziridines, aziridinium ions, and episulfonium ions.
- Carbonyl chemistry of the 'non-aldol' type, such as formation of urea's, thiourea's, aromatic heterocycles, oxime ethers, hydrazones, and amides.
- Additions to carbon-carbon multiple bonds, especially oxidative cases such as epoxidation, dihydroxylation, aziridination, and sulfenyl halide addition, but also Michael additions of Nu-H reactants.

However of this wide variety of possibilities, of particular interest in this project, is the reaction between an azide and an alkyne in a copper catalysed Huisgen

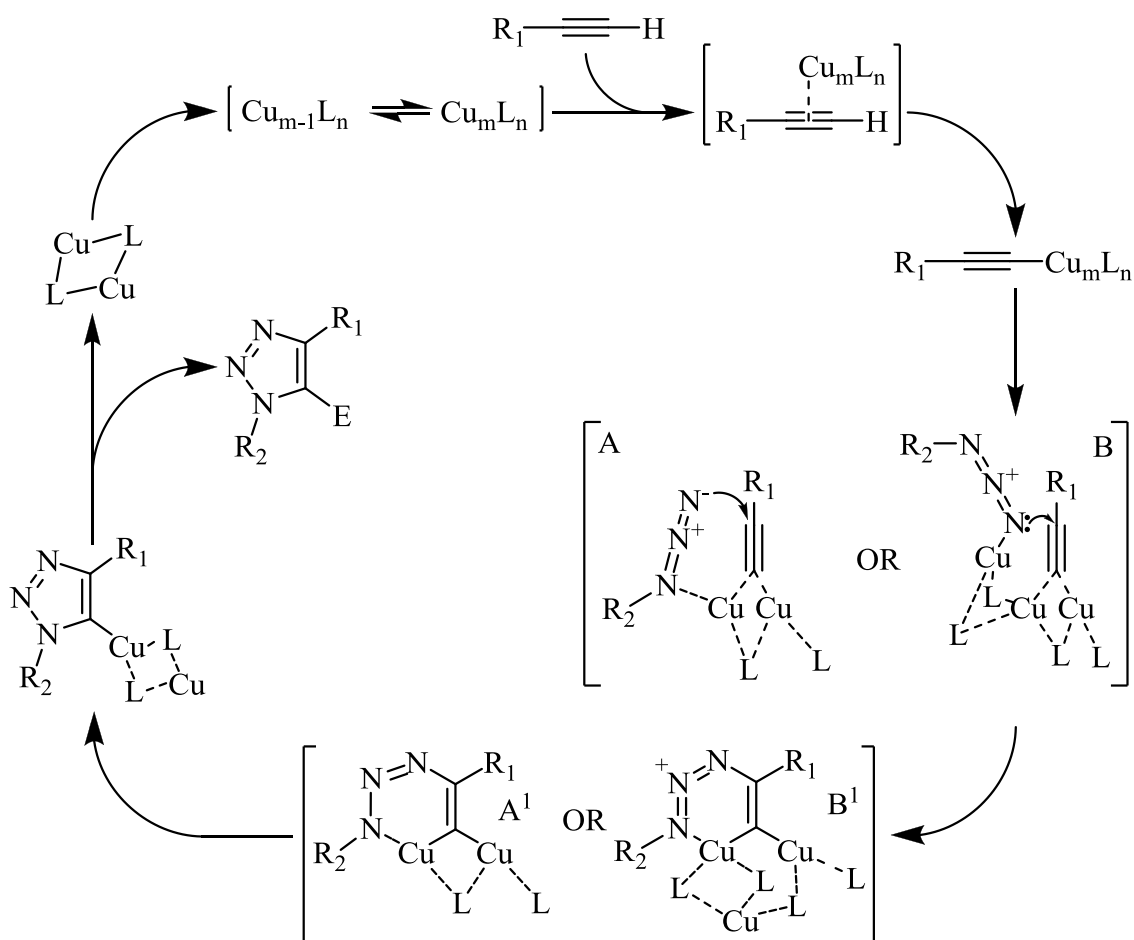
1,3-dipolar cycloaddition (scheme 51). This is possibly one of the most common ‘click’ chemistry reactions, and is so popular that it is often referred to simply as the “click reaction.”<sup>191</sup>



**Scheme 51:** A non-specific depiction of a copper-catalysed reaction between a general terminal alkyne and a general azide.

This copper catalysed variant was concurrently, yet independently, developed by both Meldal *et al.*<sup>192</sup> and Sharpless *et al.*<sup>193</sup> and offered a significant improvement over a similar reaction investigated in detail and presented by Huisgen in 1961<sup>194</sup> after its discovery by Michael in 1893.<sup>195</sup> The problem with this initial process (developed by Huisgen) is that both organic azides and alkynes are kinetically stable; the result is that the reaction has to be carried out at high temperatures. The vast improvement reported; due to the addition of the copper catalyst, lowered the reaction temperature (to room temperature) but also the reaction time too. This Cu(I) catalysis of the Huisgen reaction is more broadly known as the CuAAC reaction (copper alkyne/azide cycloaddition).

The mechanism for this reaction (Scheme 52) is still a point of intense scientific debate. However, considering the second order kinetics for the [Cu(I)] observed by Rodionov *et al.*,<sup>196</sup> on top of increasing structural evidence, it is unlikely that a single Cu(I) atom aligned with the C-C bond of the alkyne is responsible for catalysis. Moreover it has also been suggested that, as in Scheme 52, the acetylide and the azide are not necessarily coordinated to the same Cu atom in the transition state.<sup>197</sup>



**Scheme 52:** A proposed mechanism of a general CuAAC reaction.<sup>197</sup>

Within this mechanism there are two proposed intermediates; ‘A’ and ‘B.’ Intermediate A is generally assumed to be the intermediate; however, it fails to explain adequately many of the observations concerning the reaction; therefore an alternative intermediate B has been proposed by Meldel *et al* which could explain most observations.<sup>197</sup> As can be seen from this mechanism (Scheme 52), the copper catalysed click chemistry exclusively forms a 1,4-disubstituted-1,2,3-triazole ring system (also Scheme 51). It is however important to note that while copper-catalysed click chemistry forms the 1,4 system, a ruthenium-catalysed click reaction can alter the

reaction intermediate in such way as to exclusively produce a 1,5 disubstituted-1,2,3-triazole ring system.<sup>198</sup>

### 3.1.2. Click reactions *in vitro* and *in vivo*

One of the major uses of copper catalysed click chemistry was its use in bioconjugation. Bioconjugation encompasses a broad area of science at the border between molecular biology and chemistry. Bioconjugation techniques generally involve the covalent attachment of synthetic labels to a biomolecular framework. Examples include the modification of proteins and nucleic acids by incorporation of fluorophores, ligands, chelates, radioisotopes and affinity tags; or modifications such as fusing two or more proteins together or linking a complex carbohydrate with a peptide.<sup>199</sup>

As discussed earlier the use and application of the copper catalysed click chemistry was first hinted at by Meldal *et al.* in their first click chemistry paper. They had discovered “mild” reaction conditions in the formation of peptidotriazoles that were also fully compatible with Fmoc and Boc peptide chemistry.<sup>192, 197</sup> Subsequent development of this reaction in water realised the reactions’ potential for introducing a wide variety of functionality into a biomolecular environment and has now proved to be very useful in the study of biological molecules.

Whilst the list of potential biological molecules suitable for such chemistry is vast, of particular interest to this project is the use of chemistry in relation to ligation and decoration of peptides. One particular group had been able to demonstrate this kind of chemistry; Eichler *et al.* performed ligation of peptides to form assembled (ligation of two protein fragments) as well as scaffolded (peptide fragments ligated on to a

multivalent peptide scaffold as shown in Figure 48) peptides. Importantly though they discovered that this technique was compatible with several different functionalities within the peptide additionally pointing out that this method offered the possibility of easily creating combinatorial libraries of assembled and scaffolded proteins.<sup>200</sup>

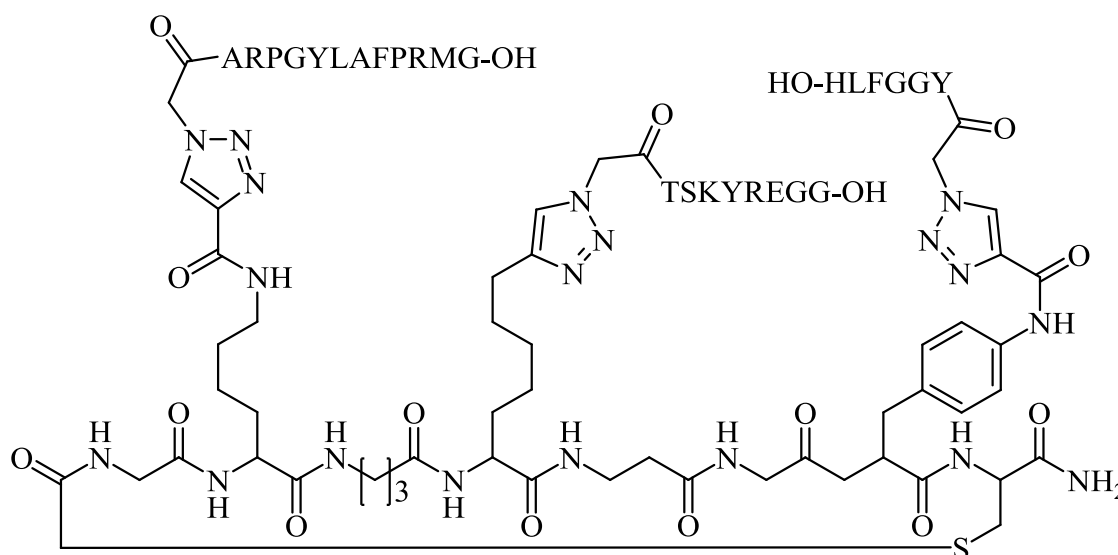


**Figure 48:** An example scaffolded peptide formed using click chemistry.<sup>200</sup>

Another example of *in vitro* click chemistry demonstrated by Chaikof *et al.* was the immobilisation of protein molecules onto a solid surface.<sup>201</sup> This important and useful step forward had a large range of applications because at the time there were only a few reliable methods available for the immobilisation of biomolecules onto solid surfaces. The reasons for such a restriction in applicable methods was due to a range of limiting factors such as: reduction in biomolecular activity attributed to denaturation, random orientation of the biomolecules on the surface, and detrimental reactions at or near the active site.<sup>199, 201</sup> The most important feature about the utilisation of a copper catalysed click reaction in this research was that not only did the immobilisation of the

protein occur with an almost quantitative yield but it also maintained its biological activity;<sup>201</sup> something that is essential in this project.

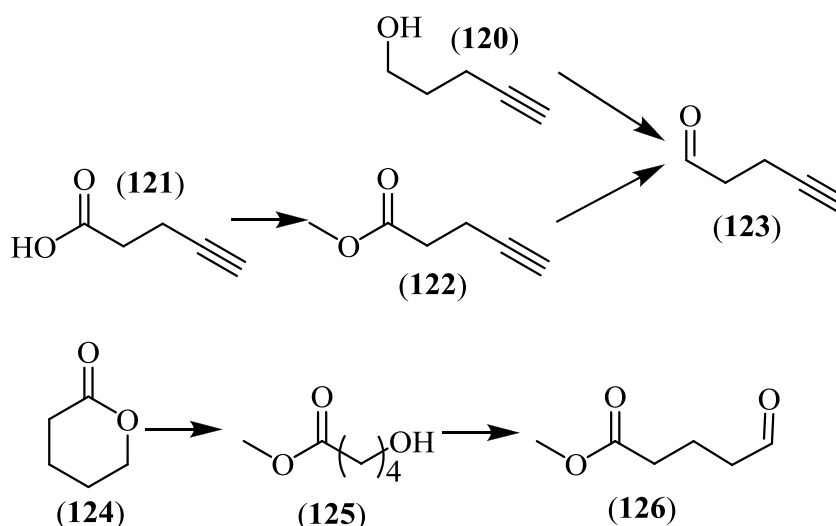
Both these early examples and subsequent more complex examples which utilise copper catalysed click chemistry prove that it is possible to use such chemistry *in vitro* without major complications. The result is that the ultimate challenge is selectively interconnecting two molecules in an extra- or intracellular environment. Until the use of copper catalysed click chemistry, the reactions that could carry out such chemistry were very limited.<sup>197, 202</sup>

Whilst research into the *in vivo* interconnection of two macro-biomolecules is still in its infancy, reported *in vivo* introduction of the smaller molecules involved in fluorescence labelling is now extensive.<sup>197</sup> One of the earliest developments of this chemistry was reported by Speers and Cravatt in 2004.<sup>203</sup> They used alkyne or azide benzenesulfonates to react with the active site of a variety of enzymes within living cancer cells or mice, it was then after lysis of the cells that the probe was labelled with a fluorophore.<sup>203, 204</sup> Whilst this step didn't involve full *in vivo* click chemistry it was an important step forward the principles of which researchers still utilise; *in vivo* tagging of the enzyme or protein followed by *in vitro* analysis using bulkier 'reporter' tags which had been 'clicked' onto the initial tag.

True *in vivo* copper catalysed click chemistry is very challenging due to the toxicity of the metal which precludes its use in the presence of live cells or organisms; a problem which has as yet not been overcome.<sup>199, 205</sup> True *in vivo* click chemistry utilises a copper free, ring strain promoted process, developed and reported by Bertozzi *et al.*<sup>206, 207</sup> and is something that is not suitable at the early stage of this project.

### 3.1.3. Synthesis of target alkyne

The new tack for insertion of a molecule into a protein domain required the synthesis of two different target molecules (**118** and **119**) (Figure 47). In the new synthesis the route to the quinone framework would remain the same, using the same hydrazine molecule as produced previously, however the amino acid framework would change so that either the alkyne or azide functionality could be incorporated instead of the amino acid (Scheme 53).



**Scheme 53:** The two possible routes to the alkyne or azide framework prior to the Fischer indole reaction; top, to produce alkyne functionality (**123**) and below to produce the ester functionality which will be converted to an azide after the Fischer indole reaction (**126**).

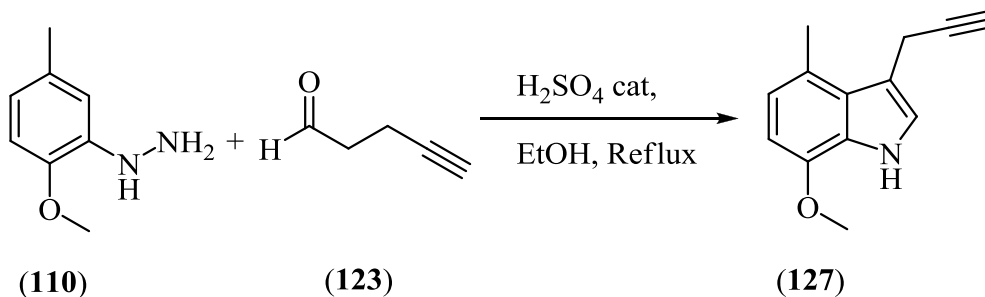
An important note is that the majority of synthetic modification required to produce the azide functionality takes place after the Fischer indole reaction.

The required target necessary to produce the alkyne functionality (**123**) was obtained by means of a PCC oxidation of the corresponding alcohol. The reaction material was filtered through a pad of silica to remove as much of the chromium salts as possible but a suitable method was never found for further purification (crude yield 98%). One paper that had previously made the target compound purified it by distillation at atmospheric pressure, and made no reference to any impurities that were difficult to remove.<sup>208</sup> Attempts to distil the compound at either atmospheric pressure or under vacuum failed to remove impurities as did column chromatography. The impurities can be clearly identified in the NMR spectrum, and initially it was thought that they were primarily comprised of starting material, however further analysis by NMR (addition of starting material to sample) showed this was not the case.

Similar reaction impurities were identified in the production of pentanal (**111**) used for the production of an earlier molecule (**112** Figure 44). In both cases a range of reaction conditions were attempted in an effort to optimise the reaction thus producing close to 100% yield so that purification was not necessary. These attempts also failed to remove the impurities and maintained a similar or worse yield.

Attempts were also made to produce the aldehyde derivative by an alternative method (also shown in Scheme 53). It was hoped that conversion of the readily available pentynoic acid to the methyl ester and subsequent reduction to its corresponding aldehyde (again using DIBAL) would negate the use of PCC and may result in purer starting material. However the reduction with DIBAL was very poor yielding with less than 1 % detected by HPLC. Due to this result, the additional steps and subsequent purification involved in this process the reaction route was not pursued further. The result of these investigations and those detailed above (oxidation of the

alcohol using PCC) was that the aldehyde material (**123**) was used in an un-purified form.



**Scheme 54:** The acid catalysed Fischer indole reaction between the hydrazine (**110**) and the aldehyde (**123**) which was used to incorporate the alkyne functionality into the target molecule (**127**).

The subsequent acid catalysed Fischer indole reaction (shown above in Scheme 54) worked as previously and returned very similar poor yields (11 %). However after purification the sample produced very long needle like crystals that were sufficiently pure to obtain an X-ray crystallography image (Figure 49).

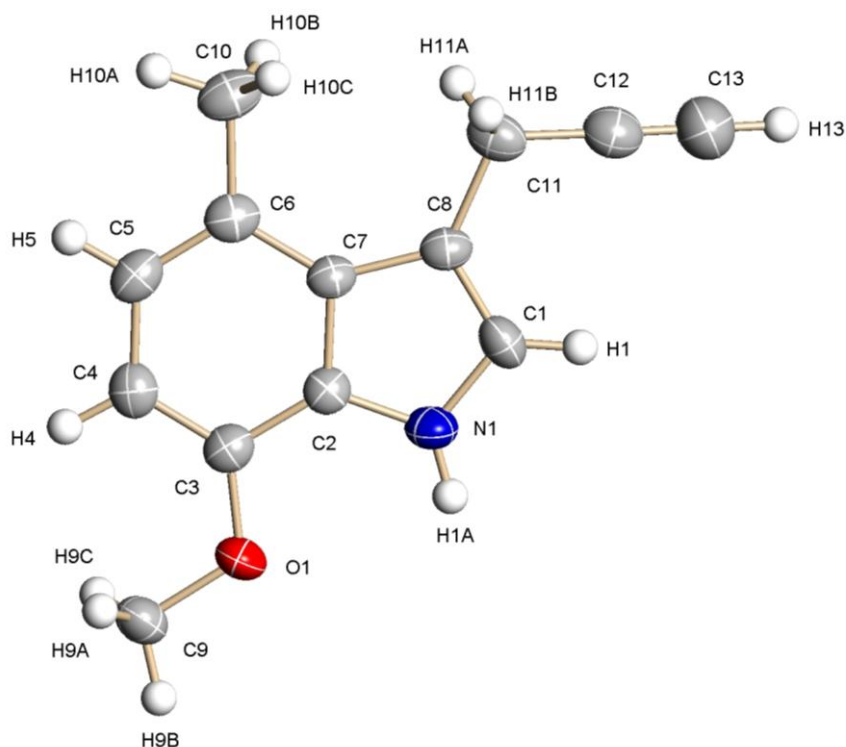


**Figure 49:** X-ray crystallography image of alkyne derived TTQ analogue (**127**) (for full set of data and parameters please see appendix 7.1.3).

In both cases (**112** and **127**) it is very reasonable to assume that the impure aldehyde starting material (and to a much lesser extent the hydrazine) will have contributed to the low yields obtained during the Fischer indole steps. Furthermore (as with (**112**)), purification of the desired product was again difficult with TLC analysis of the crude material returning a large quantity of spots. However, by following a similar procedure of purification as for that of (**112**) the desired product was obtained. The long and drawn out purification undoubtedly contributed to the low yields obtained from this reaction.

### 3.1.4. Synthesis of target azide

Production of the azide (**118**) was planned to progress via tosylation of an alcohol and then subsequent conversion to the azide by nucleophilic attack from sodium azide. However the planned route required selective oxidation of an alcohol to an aldehyde, thus allowing for the Fischer indole. This meant that one of the alcohol groups had to be selectively protected, which could be easily removed at a later date.

There was very limited literature precedent for selective mono-protection/esterification of a diol similar to this one, however a literature method was found for the production of the aldehyde (**126** Scheme 53) from the starting material valerolactone.<sup>209</sup> As this paper highlights, the biggest problem with the alcohol intermediate, prior to conversion to the aldehyde, is that it readily relactonises. This relactonisation is extensive when the compound is heated for distillation purposes and thus it tends to be oxidised without further purification.

This method was attempted, but unfortunately failed. Further literature searching into valerolactone showed that it had two possible isomers (Figure 50).

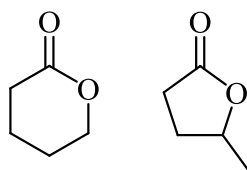


**Figure 50:** Two possible isomers for valerolactone.

The method in the paper used the 6 membered ring form and uses a catalytic amount of sulphuric acid in methanol to ring open the compound. Further inspection of the valerolactone used revealed it was exclusively the five membered ring isomer. Had it been possible to ring open this isomer then it would have resulted in formation of the

corresponding ketone and not the desired aldehyde. However, even with this in mind, there was little evidence of this product by NMR.

It was decided to attempt the proposed synthetic route using a more readily available starting material (**128** Figure 51) derived from the  $\gamma$ -valerolactone.

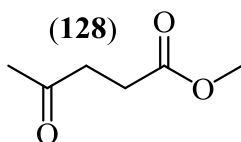


**Figure 51:** More readily available starting material.

This starting material was more stable, making it easy to work with and would allow development of the synthetic route to form the desired azide (**128**) albeit one carbon shorter in the alkyl chain to the azide. If this route was successful and the desired compound could be coupled to a corresponding alkyne by the copper catalysed ‘click’ chemistry method discussed previously, then further investigations could be made into the formation of the desired aldehyde.

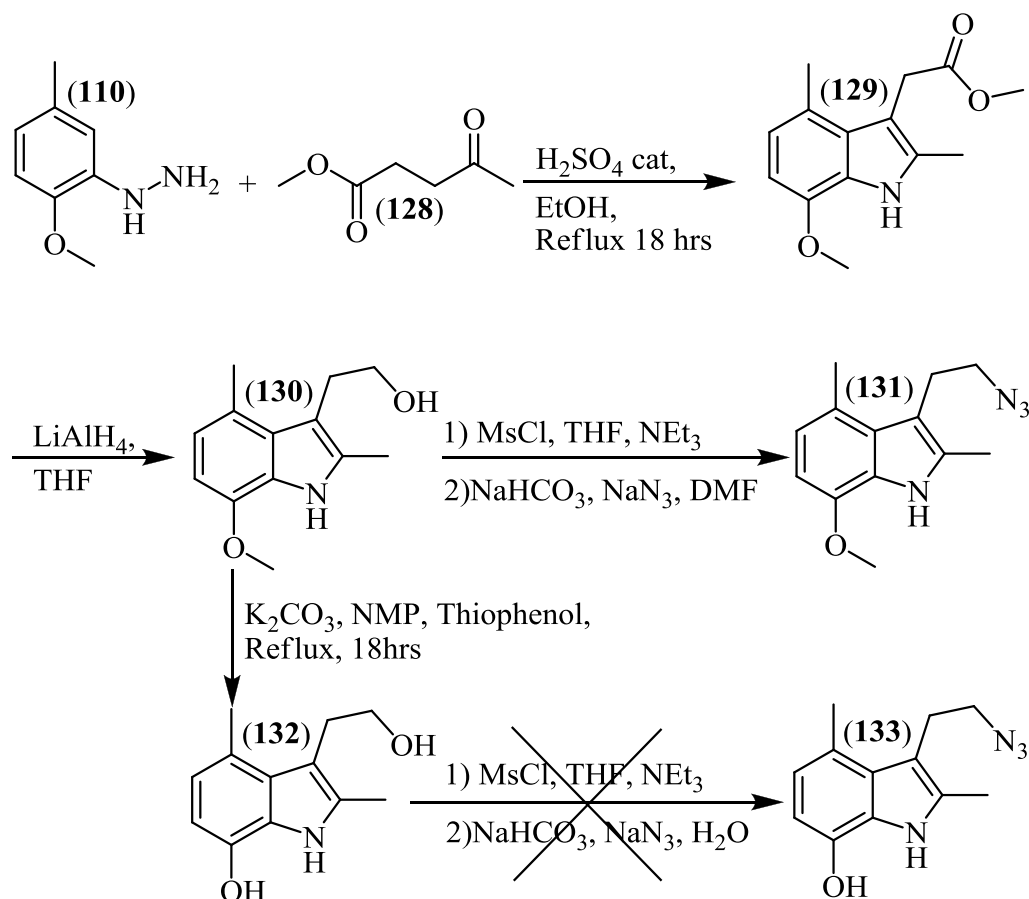
This new starting material was almost identical to the target starting material; one of the alcohols was protected in an ester form (helping to prevent cyclisation) and there was a free carbonyl to undergo the Fischer indole reaction (see Scheme 55).

The Fischer indole reaction behaved as previously with a typical yield of 15% of purified material, a minor improvement on previous Fischer indole reactions, and with a difficult separation between a considerable variety of spots varying widely in their polarity. As before the compound required further purification by recrystallisation after the column.

The small increase in the yield could be as a direct result of slightly more pure starting material. As discussed earlier, the previous starting materials had problems

with purification (pentanal (**111**) and (**123**) Scheme 53), this was not the case with the starting material used in this reaction as it was bought in a pure form.

This successful Fischer indole reaction continued the real and promising possibility of a new synthetic route to an azide TTQ derivative (Scheme 55).



**Scheme 55:** The new synthetic pathway to a TTQ derivative.

Crystals obtained after the Fischer indole of the target compound (**129**) were sufficiently well developed that X-ray crystallography could be used to further confirm its identity (Figure 52).

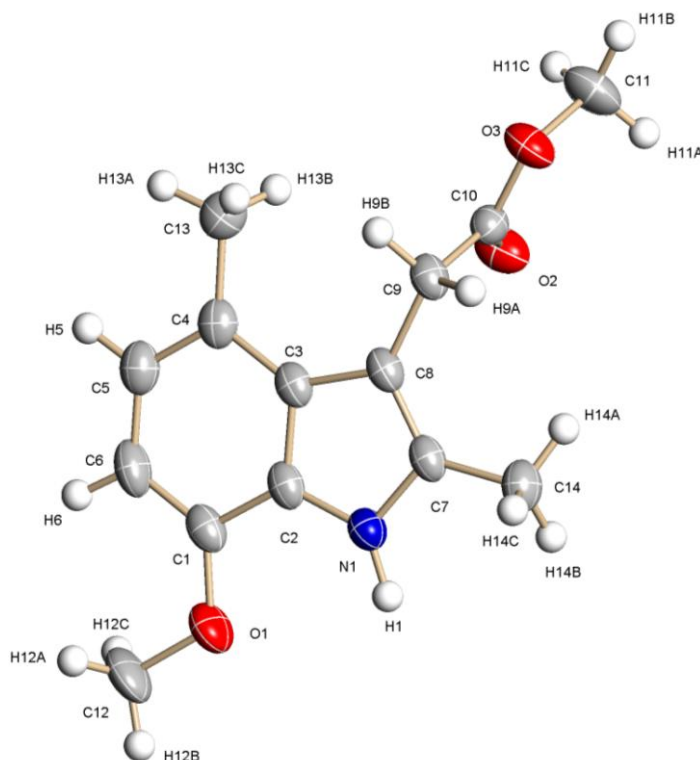


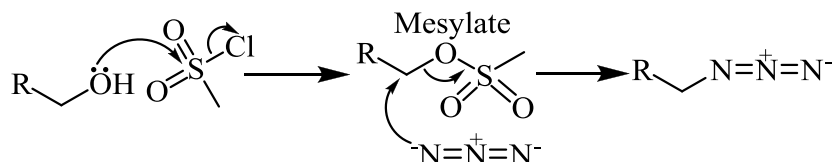
**Figure 52:** X-ray crystallographic structure of Fischer indole product (**129**) (for full set of data and parameters please see appendix 7.1.4).

After the product from the Fischer indole reaction was isolated (**129**) (15 %), the ester was subjected to a standard reduction by lithium aluminium hydride to its corresponding primary alcohol (**130**). This reaction was easy, worked well and was high yielding (91 %) with little evidence of unwanted by-products.

The synthetic pathway then diverged into two slightly different routes. The first of these was to remove the ether protection of the hydroxyl group at this stage (**132**) (Scheme 55). Deprotection of the ether was likely to involve some quite harsh reaction conditions, one of the downsides to being a very effective protecting group. Deprotection will be discussed in more detail in the next section (3.1.5.), but it was successfully deprotected in a very high yielding reaction (96 %) involving *N*-methyl-2-

pyrrolidone (NMP) and thiophenol. The second route was to continue to work on the protected phenol and deprotect at a later time.

The resultant primary alcohols (**130** and **132**) then separately underwent one pot synthesis to first form a mesylate and then the corresponding azide (Scheme 56).



**Scheme 56:** The mechanism for mesylation and subsequent attack by sodium azide where R would be the remaining alkyl chain and indole ring.

The mesylation mechanism is identical to the tosylation mechanism whereby the alcohol nucleophilically attacks the sulphur displacing the chlorine atom. The mesylate is then an ideal leaving group and allows for easy nucleophilic attack of the azide on the carbon.

This method was adapted from Susumu *et al.*<sup>210</sup> who used the same process to form an azide derivative of poly(ethylene glycol). This method first used tetrahydrofuran (THF) as the solvent in which to form the mesylate and then water as the solvent to form the azide and displace the mesylate group. This method initially threw up some issues; although the mesylated compounds were easily formed in THF they were insoluble in water, the overall result was that after the prescribed overnight reflux in water the initial attempt to form an azide failed. Interestingly though, starting material was not isolated from the reaction; instead a range of unidentifiable by-products were obtained.

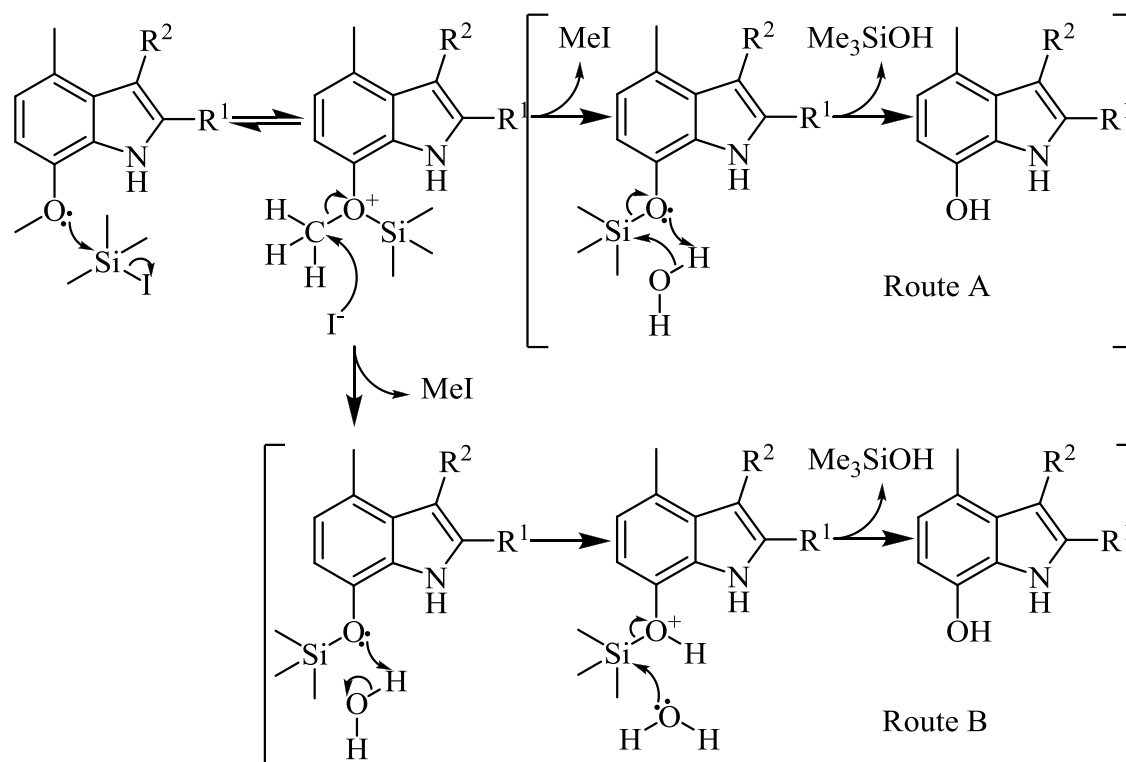
An alternative solvent was then found so that the ‘one pot’ synthesis could be carried out in DMF. The reaction was therefore tried again, following the same method,

but with the conversion to the azide being carried out in DMF instead. This new solvent was only trialled on the methyl ether protected phenol (**130**), as there were some difficulties in reproducing the deprotected form (**132**). There were also some potential additional issues with the deprotected phenol; it is an acidic group and thus the protection may be unsuccessful. As a result of the difficulties it was decided to mitigate these potential problems by simply concentrating on the methyl ether protected compound (**130**) rather than that of the deprotected form (**132**) and the second of these possible routes to obtain the deprotected azide (**133**) was not explored any further.

Concentrating on one route only proved to be highly successful and produced the desired azide with reasonable yields (55 %). Due to the purity of the target compound on TLC it is conceivable that at least a portion of the desired compound was lost in the purification stages of such a small scale reaction.

### 3.1.5. Deprotection of methylether protected phenol

With both the target compounds (**127** and **131**) that had so far successfully undergone the Fischer indole reaction, the penultimate step was deprotection of the methylether-protected phenol before oxidation to the quinone. It was initially thought that such a deprotection could easily be accomplished with the use of iodotrimethylsilane (TMSI) as Itoh *et al.* had shown this to be effective in deprotecting a methylether-protected phenol in systems that were very similar in design.<sup>26</sup> The deprotection mechanism would proceed as shown below (Scheme 57):



**Scheme 57:** The proposed mechanism by which TMSI deprotects ether protected alcohol and the two possible routes for hydrolysis of the silylether.<sup>211</sup>

The suggested, rather straightforward mechanism for this process involves the ether nucleophilically attacking the iodotrimethylsilane in a fast and reversible step to produce the silylated oxonium ion which is then converted to the silyl ether by nucleophilic attack of iodide at the methyl. Subsequent hydrolysis of this silyl ether liberates the free phenol and silyl alcohol.<sup>211</sup>

The normal method for liberating an alcohol is by methanolysis,<sup>212</sup> however the Itoh method did not use methanol, instead preferring an aqueous workup with sodium thiosulphate to remove iodine traces. It is therefore unclear whether the subsequent hydrolysis of the silylether proceeds via a concerted S<sub>N</sub>2 mechanism (route A) or by route B.

The method used by Itoh *et al.*,<sup>26</sup> however, did not deprotect any of the compounds, nor did the reaction return any starting material. The reaction was very ‘messy’, as shown by TLC, and even after a difficult purification the by-products were unable to be identified by either mass spectrum or <sup>1</sup>H NMR.

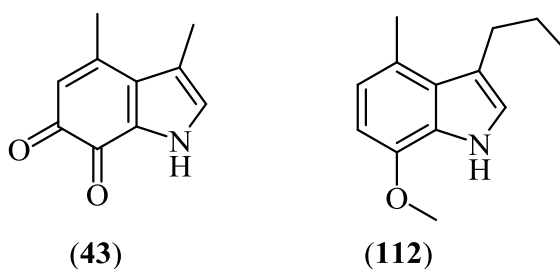


**Figure 53:** One of Itoh’s quinone compounds (**43**) the precursor to which used TMSI to deprotect the methyl ether and one of the more simple compounds used in this project (**112**) in an attempt to optimise the TMSI conditions.

This methyl ether deprotection reaction was attempted using a range of increasingly simple substrates in an attempt to identify whether it was the substrate that was the problem; however these reactions also failed. The substrates included one of the molecules produced while attempting to optimise the Fischer indole reaction (**112**) (Figure 53). This molecule is very similar to one of the TTQ analogues that had been synthesised by Itoh *et al.* (**43**) (also Figure 53) using this method of deprotection; the only difference being that (**112**) has a longer alkyl chain at the 3 position of the indole framework.

This had been a problem previously for a co-worker on a similar project;<sup>213</sup> Parmar was also attempting to follow Itoh’s method for preparation of the TTQ analogues, however, he too failed to get the iodotrimethylsilane to deprotect the phenol. Instead he also obtained a range of products, none of which were the target compound

or any starting material and in fact he reported several spots on TLC that were “more polar than starting material,” just as was observed in similar reactions within this project. Parmar had attributed this to possible decomposition of the TMSI due to its reactivity towards moisture and problems with stability; these problems would have been compounded by the fact that he was using old reagents.<sup>213</sup> The findings in this work do not support this hypothesis; the reactions were attempted with TMSI had been freshly bought in, stored over copper (to stabilise it) and had remained in a sealed glass ampoule until it was required.

There are a range of reported reaction conditions using TMSI for deprotection of aromatic ethers;<sup>141</sup> but it is maybe the case that with these molecules the reaction conditions have to be more precisely met for the reaction to be successful.

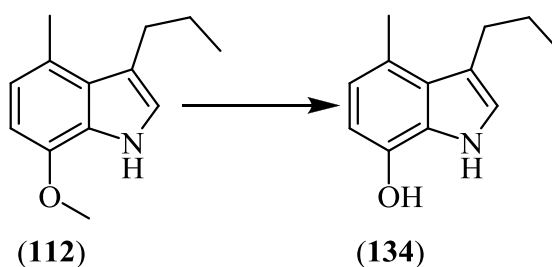
An alternative possibility for the reactions unwillingness to produce the desired phenol could be due to the ‘over active’ TMSI. It might be that due to a lack of degradation of the TMSI because of its storage conditions the concentration of the active TMSI (as opposed to degraded/decomposed TMSI that Parmar cited as a possibility) was much higher than in the experiments carried out by Itoh *et al.* Also worth considering is that given that the reaction mechanism utilises the iodide ion to abstract the methyl group (Scheme 57), perhaps ‘old’ TMSI would have sufficient concentration of these iodide ions to kick start the reactions.

Different methods to that published by Itoh *et al.* were investigated as possible alternatives for the deprotection of both (**127**) and (**130**). Deprotection of aromatic ethers is a common reaction in many synthetic schemes, with a plethora of reactions available to the modern chemist.<sup>141</sup>

One of the more common methods uses boron tribromide, but following the production of only unidentifiable by-products, no attempts were made to

improve/optimize the protocol. It is possible the reaction did not work due to an unfavourable interaction between the alkyne target molecule and  $\text{BBr}_3$ .

Another method that seemed to be extremely simple and is quoted in the literature as giving 100% yield was a radical reaction involving potassium and 18-crown-6 utilising toluene as the solvent. Initially a complex is set up between the potassium and the polyether (18-crown-6), forming an ionic salt which is given the generic name of an alkali. When this complexation is carried out in aromatic solvents, the arene radical anions are formed as a secondary species through electron transfer from the initially produced alkalis to the solvent molecules.<sup>214</sup>



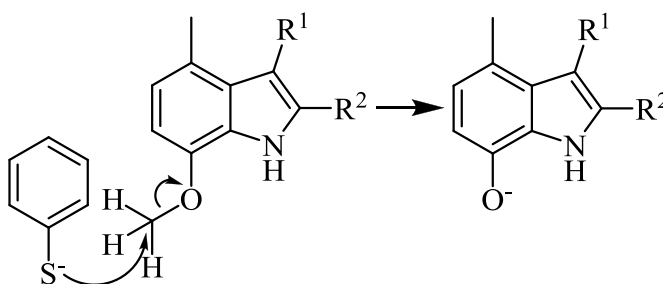
**Scheme 58:** The molecule originally produced when optimising the Fischer indole reaction (**112**) used later to optimise deprotection of the aromatic methyl ether forming (**134**).

This radical reaction worked well for the test compound (**134**) (Scheme 58), however upon attempting it on the alkyne material (**127**) there was no reaction at all. The only identifiable product of the reaction was that of starting material (89%), suggesting that the reaction was incompatible with an alkyne functional group. The most likely reason for this is some sort of radical quenching mechanism by the alkyne.

Subsequent reactions by this method on both (**112**), (**129**) and (**130**) showed that this reaction was a distinctly unreliable way of demethylating methyl ether

protected phenols. Sometimes the reaction would be high yielding and in other reactions, seemingly run under identical reaction conditions, no reaction was observed at all, quantitatively returning starting material.

An alternative route was optimised by Nayak *et al.*<sup>215</sup> using thiophenol and potassium carbonate (Scheme 59).



**Scheme 59:** Nucleophilic attack by thiophenolate anion to methyl ether in an S<sub>N</sub>2 reaction which liberates the phenol anion.

In this mechanism the thiophenol is deprotonated by the potassium carbonate, the resulting thiophenolate anion then nucleophilically attacks the methyl group liberating the phenol anion. An acidic aqueous work up then protonates the phenol.<sup>215</sup>

Again this reaction worked well for the test compound (**134**) with just a simple alkyl chain in place of 'R<sup>1</sup>', but failed with the introduction of an alkyne at this position. Although no identifiable compounds were obtained it is possible that the unwanted by-products of the reaction are a consequence of thermal degradation. The original paper stated that attempts to carry out this reaction at lower temperatures considerably reduced the reaction yield. They also mentioned that attempts to carry out the reaction in other solvents also failed.<sup>215</sup>

There are possibilities that present themselves of dealing with this deprotection at a different stage; some of which were described earlier. One such example was

spoken about in the production of the azide i.e. prior to formation of the azide, the phenol could be deprotected. Such deprotection is possible, as it had already been developed in the project but the material had been lost in an attempt to form the azide using water as the solvent. This meant it was impossible to confirm whether formation of the mesylate and subsequent formation of the azide was possible in the presence of an acidic phenol. The visual appearance of this reaction had shown some promising signs; the mesylation had later been proved to be successful in the methylether protected derivative (**131**) and the visual appearance of this mesylation reaction with the deprotected hydroxyl (**133**) was comparable.

One of the possible problems involved in the use of the mesylate intermediate in the presence of the free phenolic hydroxyl group is that the phenolic hydroxyl may be preferentially protected in a mechanism similar to that shown in Scheme 59. This is a real possibility as the pKa of the free phenolic hydroxyl is likely to be between nine and ten<sup>216</sup> and as a result it is likely to be in a deprotonated form given the basic medium used. The fact that other research groups had been able to mesylate aromatic hydroxyl groups using methods very similar to that used in this project supports this hypothesis.<sup>217</sup> Allowances could be made during synthesis of the azide by adding substantially more than two equivalents of methanesulfonyl chloride. This possible solution would result in both hydroxyl groups becoming mesylated something of limited concern as the phenol cannot easily undergo further nucleophilic attack by the azide. It is plausible that the visual observation could have been due to mesylation of both groups as 2.3 equivalents of methanesulfonyl chloride were added.

### 3.1.6. Summary

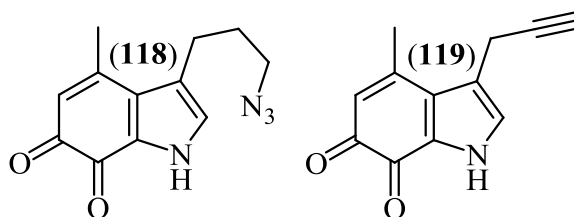
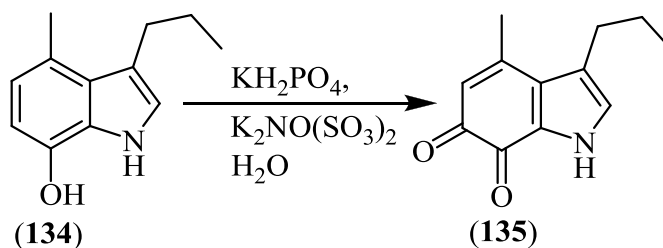


**Figure 54:** The two target molecules proposed in this chapter which will allow easy incorporation into peptides/proteins by click chemistry

The preliminary results in this chapter look promising. Whilst the final target compounds (**118**, **119**) (Figure 54) were never obtained, the research has made some important initial findings. The work so far has shown that the reaction schemes are predominately high yielding (with the exception of the Fischer indole reaction) for synthesis of both the azide (**118**) and alkyne (**119**) derivatives of TTQ.

There are many, more possible routes for deprotection of the methyl ether, all providing an alternative to the routes tried. The information that these experiments provide allows further study/experimentation to be more targeted. For example alternative methods to those involving a radical mechanism might be considered for deprotection of the alkyne and similarly any reactions that use high temperatures should be avoided as they may cause polymerisation.

Perhaps more importantly than providing direction on other methods of deprotection, this chapter shows a deprotection method that works. This deprotection occurred before the formation of the important azide functionality and is definitely a route that should be explored further. This is particularly the case as further more detailed literature based research has suggested that initial concerns over the stability of the mesylate intermediate in the presence of the phenol are unsubstantiated.



**Scheme 60:** Oxidation of the free phenol to the quinone using Frémy's Salt was a simple reaction, proved by conversion of the test compound **(134)** to **(135)**.

Once the deprotection has been achieved it is possible to easily oxidise the free phenol to the quinone moiety using Frémy's salt (Scheme 60). This reaction had been proven to work efficiently by first deprotecting the test compound **(134)** and then converting the free phenol into the quinone moiety **(135)**. The yield for the latter oxidation was 75%, and may have been higher if it were not for loss of compound in the purification.

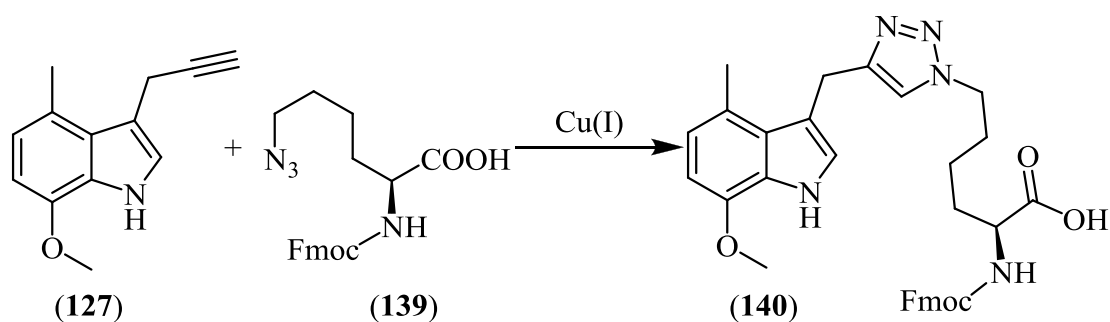
### 3.2. Proof that 'click' chemistry is viable

The azide and alkyne compounds were sufficiently close to the final target compounds to have a realistic attempt at trying to couple it to a non-natural amino acid. These attempts would highlight the potential for the 'click' chemistry as a realistic and easily applied method for coupling the target TTQ-like functionality to a protein chain. These reactions would also draw attention to and deal with any possible problems in advance of the reaction being tried with much larger peptides and finally proteins.

Due to the amount of starting material available, the initial experiments were conducted on the alkyne TTQ derivative only, it was intended that once these reactions were optimised, a similar attempt would be made on the azide TTQ derivative. It was

hoped that the two reactions would work under very similar conditions allowing for easy insertion of either derivative into a protein without extensive development of the reaction protocol.

### 3.2.1. Initial problems and their solutions



**Scheme 61:** The copper catalysed reaction between a TTQ like molecule (**127**) and an azide containing unnatural amino acid (**139**) forming an amino acid/synthetic TTQ like compound linked by a triazole (**140**).

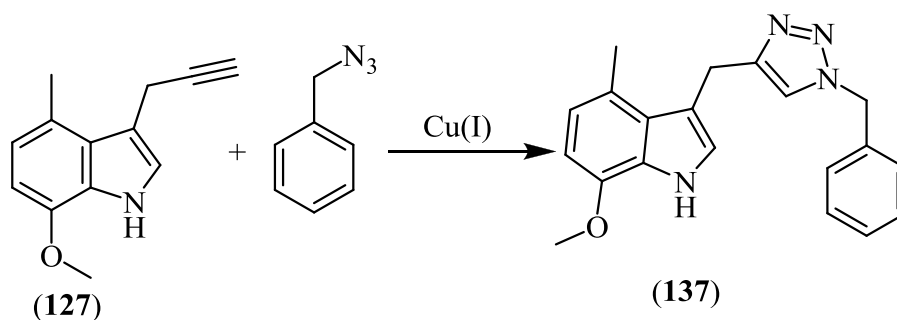
Initially the ‘click’ chemistry was attempted in its simplest form; this involved a very simple reaction by which one equivalent of copper(II) sulphate and sodium ascorbate (to reduce the copper(II) to copper(I)) are combined in one pot, to which the alkyne TTQ derivative (**127**) and unnatural amino acid azide (**139**) are added (Scheme 61). This simple form of ‘click’ chemistry was unsuccessful with none of the desired compound being detected.

One possible explanation for these results is that the copper may have strongly chelated to the amino acid. This chelation may have been before the cycloaddition step of the reaction or after; nevertheless the net result was no obtainable product being formed. Chelation may also account for the observations of a considerable amount of

insoluble precipitate in the reaction. Unfortunately due to the copper(I)'s ability to become easily oxidised to copper(II) which exhibits paramagnetic behaviour,<sup>185</sup> NMR of the material was very difficult and shed no light on what might have happened. However the appearance of the NMR spectrum did provide supporting evidence that copper was present in the molecules.

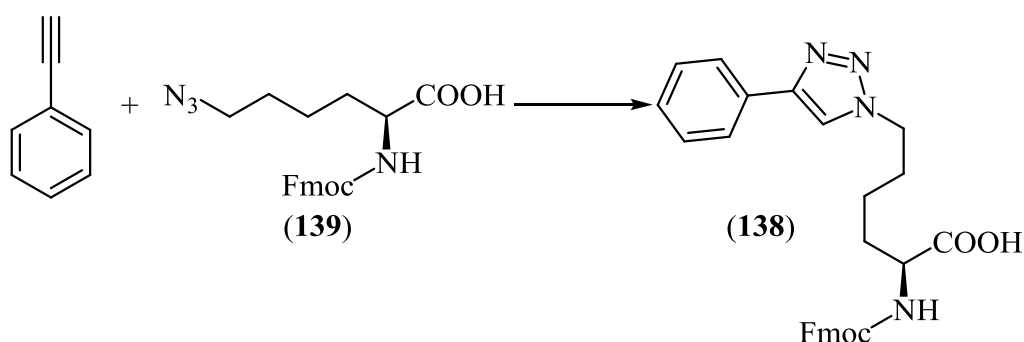
The potential for chelation should not be a surprise as copper is known to readily chelate to a vast range of nitrogen and oxygen containing compounds.<sup>185</sup> Indeed chelation of the metal in copper catalysed 'click chemistry' has also been previously reported. Ornelas *et al.* had reported their problems when also using copper(II) sulphate and sodium ascorbate in a click reaction involving large polyamide dendrimers.<sup>218</sup> The group had attempted several different work-up procedures in an effort to remove the copper metal from the reaction products but all such attempts failed. Their work-up procedures were also followed in this project in case, due to the comparative simplicity of the molecules being used, the copper could be removed. Unfortunately, just as in the paper, such attempts failed.

The problem initially faced, was that it was unclear as to whether the chelation of the copper was to the synthetic TTQ analogue or, more likely, to the amino acid. A simple reaction was devised to test this theory; reacting the synthetic TTQ analogue (**127**) with one of the most simple forms of azide; (azidomethyl)benzene (Scheme 62).



**Scheme 62:** A test reaction between a TTQ analogue (**127**) and a simple azide.

This reaction worked, as LCMS showed clear evidence for product (**137**). However, even with an aqueous ethylenediaminetetraacetic acid (EDTA) work-up only a small quantity of the desired product could be isolated copper free. Interestingly the unnatural amino acid was also reacted with a simple alkyne in an attempt to address whether the alkyne was the problem (Scheme 63).



**Scheme 63:** Another test reaction between the unnatural amino acid azide (**139**) and a simple alkyne.

As before this reaction worked and formed product (**138**), however again, only a small quantity of the desired product could be isolated copper free. These results suggested that both molecules had some complexation capabilities but that it was the combination of both molecules in the initial ‘click’ reaction that became very problematic.

Ways around such contamination were considered for their specific merits and it was while carrying out such literature based research that the work of a research group, who had also previously reported copper contamination of the products of their reactions, was discovered.<sup>219</sup> The contamination of the polymeric nanostructures they were developing drove them to developing a copper free ‘click chemistry’ approach; relying on a strain-promoted mechanism instead as initially reported by Bertozzi *et*

*al.*<sup>206, 207</sup> Time constraints on this project meant that this approach could not be trialled as it was not possible to quickly develop a new synthetic pathway that would allow for insertion of the strained alkyne ring system that is required to facilitate such a mechanism.

There remained two possible solutions around this potential problem: protecting the unnatural azide containing amino acid in such a way that it was no longer such a strong chelator or chelate the copper to a specific ligand prior to the reaction taking place.

The protection of the amino acid uses known procedures and chemistry that is relatively un-complex. The unnatural azide containing amino acid bought in for these test ‘click’ reactions was already partially protected by an Fmoc group; however there was still a free carboxylic acid group. It was thought that this could be protected as a methylester under mild conditions using methanol and dicyclohexylcarbodiimide (DCC). This protection would prevent dissociation and formation of carboxylate ion as might be the case with the free carboxylic acid, which in turn would reduce its chelation properties.

However, regardless of method, such protection does require extra steps in the reaction. It would also not be possible to carry out such reactions when using the CuAAC reaction to attach the synthetic TTQ analogue (**119**) to a much more complex protein. It was therefore decided that in the interests of time and simplicity to attempt to use the latter of the two possibilities (copper ligand(s)).

Copper ligands are regularly used in ‘click chemistry’ as they help with the stability and solubility of the copper(I) as well as preventing the chelation of the metal to reagents in the reaction and often result in an increase in turnover. Utilising ligands

is also the method that Ornelas *et al* used when attempting to get around their problems too.<sup>218</sup>

The ligand first complexed with copper, prior to the ‘click’ reaction, was tris[(1-benzyl-1H-1,2,3-triazol-4-yl)methyl]amine (TBTA) (Figure 55) chosen because it is readily available with easy to follow preparation methods.

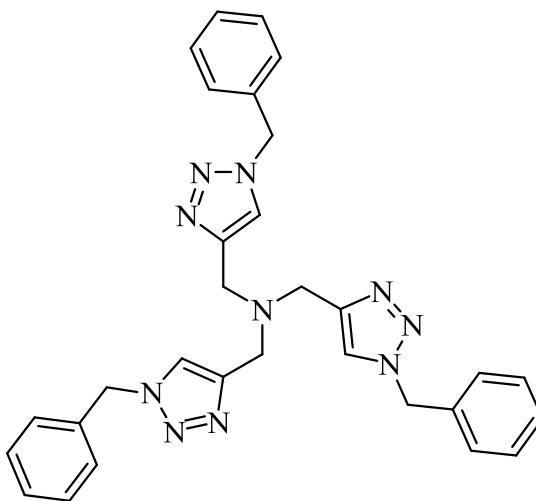
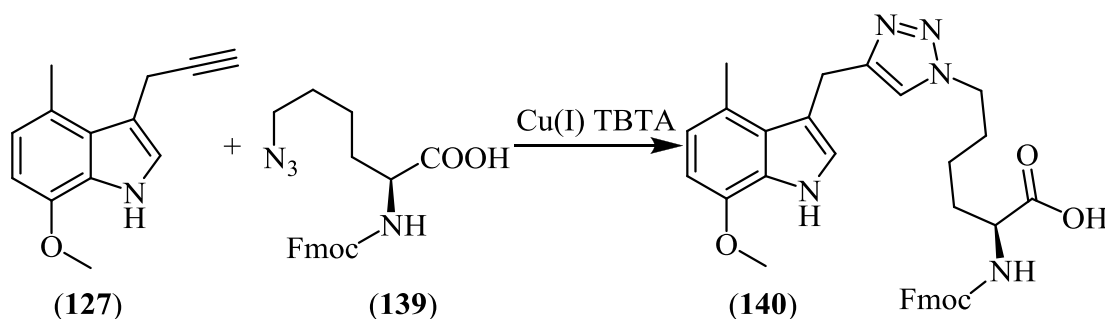


**Figure 55:** The TBTA ligand.<sup>220</sup>

The common method of using Cu(II) salts with ascorbate has been shown to be problematic in this project, however the TBTA ligand has been shown by others to effectively enhance the copper-catalyzed cycloaddition without damaging biological scaffolds;<sup>220</sup> something that could be important when considering the overall aim of this work. Another important feature of TBTA is that it is a ‘strongly’ coordinating ligand, which over the short period of time needed for the ‘click’ reaction should largely prevent its displacement by the amino acid or alkyne.

The first of the preparative methods found began by using Cu(I) directly, in the form of copper bromide, however, the copper bromide was largely insoluble in the solvent system being used and thus even with heating never formed the TBTA complex.

As a result it was decided to try and form the complex using the much more soluble copper(II) sulphate and then later reduce the complex with sodium ascorbate as in previous reactions.



**Scheme 64:** Showing the triazole product (**140**) of the reaction between a TTQ analogue (**127**) and an unnatural amino acid azide (**139**), but this time using the TBTA complexed copper (I) as the catalyst.

Having formed the copper TBTA complex the ‘click’ reaction was attempted once more (Scheme 64); this time with moderate success. LCMS was once more used to highlight the formation of the product (**140**) and approximate its purity. Although LCMS is not quantitative it did still provide evidence that the major product formed in the reaction was that of the desired amino acid/synthetic TTQ linked by a triazole (**140**) (Scheme 64), however it was clear from the NMR spectrum that the reaction products still contained copper and as with previous reactions could not be purified to remove the copper.

### 3.2.2. The wider picture

The results detailed above are still very exciting. They confirm that ‘click chemistry’ is a viable way of attaching the TTQ analogues to an amino acid and thus

potentially a protein. These results and their potential open up the whole project and could provide the realisation of the overall goal of being able to insert this cofactor into protein domains in order to further probe mechanisms thought to involve quantum tunnelling and establish the effect of the protein itself in facilitating this.

Despite the excitement, optimisation of the reaction must first be carried out as the desired products are, at the moment, insufficiently pure. As with any optimisation of a reaction this could centre on concentrations, times, temperatures or even purification methods and with the continuing development of CuAAC chemistry there is constant developments and improvements on current methodology. Within these improvements are a constant flow of newly developed ligands, all of which have specific attributes. With such a raft of new and old copper catalysed click reaction ligands, the optimisation of this reaction should initially centre around utilisation of these ligands to try and improve the reaction. One such ligand worth trying is that of sulfonated bathophenanthroline (SBP) (Figure 56) as this was the ligand that was used by Ornelas *et al.*<sup>218</sup> to try and solve their continuing issues with copper chelation. In their particular system it did not completely solve the issues with chelation, but it did dramatically reduce the contamination.

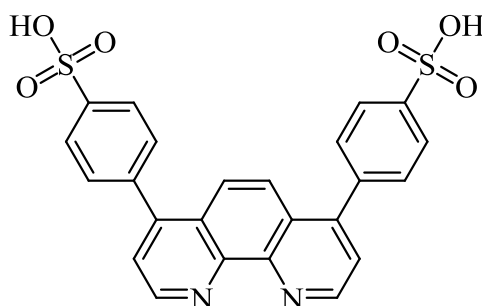
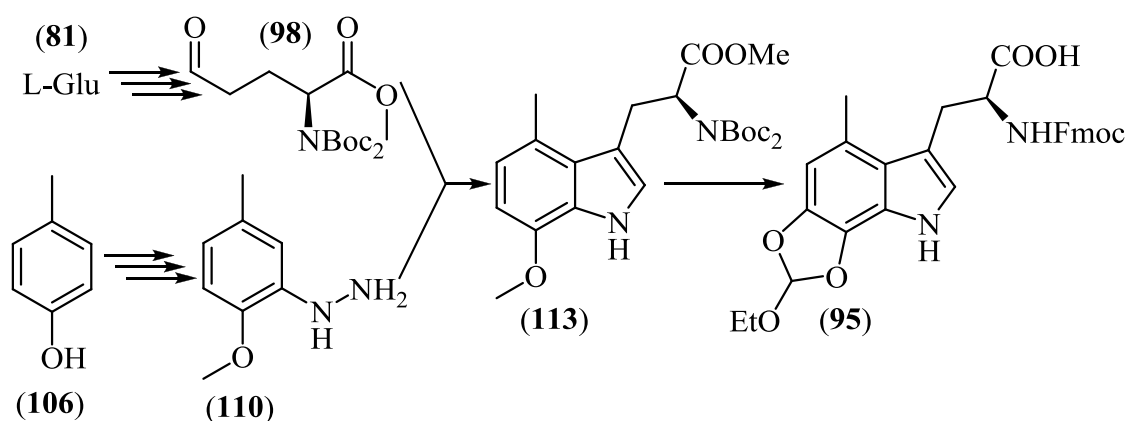


**Figure 56:** The sulfonated bathophenanthroline (SBP) ligand.

## 4. Conclusions and Further Work

The overall outlook on this project is a positive one. Although the target compounds were not made, there are a number of suggestions as to why each reaction did not work and the possible ways around each problem.

The synthetic route to the initial target molecule (**95**) which involves a protected glutamic acid derivative was well developed (Scheme 65).



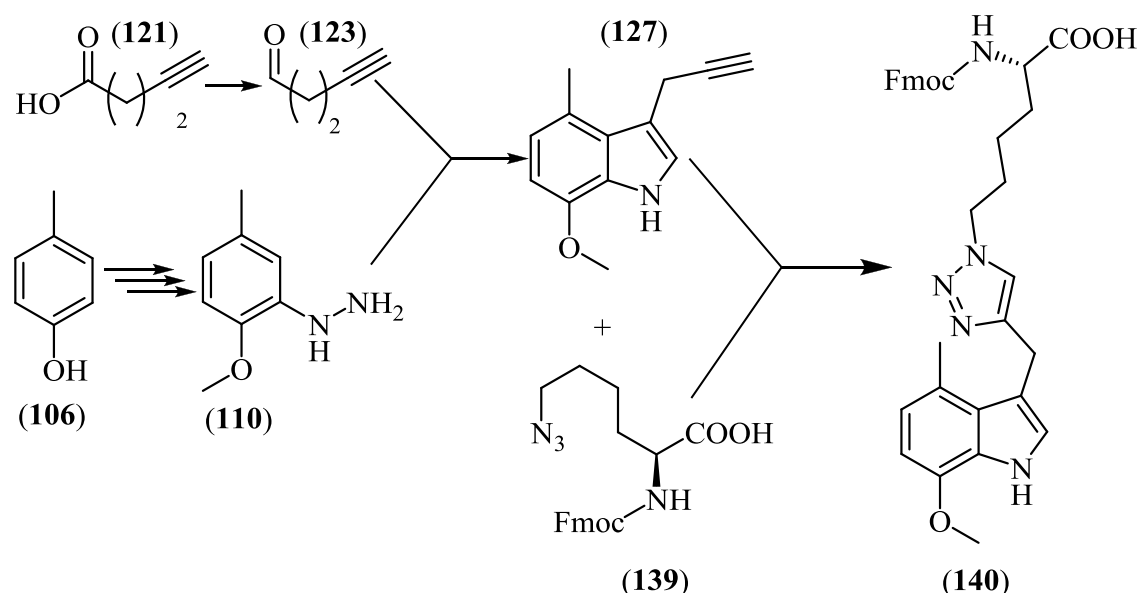
**Scheme 65:** A summary of the initial synthetic route to an amino acid functionalised TTQ analogue (**95**).

If problems with coupling the glutamic acid derivative (**98**) and the hydrazine (**110**) can be overcome then there is only one more step to surmount before the compound would be ready for insertion. The non-acid metal catalysed Fischer indole reaction is still worth exploring for this coupling reaction as all avenues of enquiry were not completely closed in an effort to move the project on beyond this stumbling block. The areas worth exploring are:



and the amine and can then be selectively deprotected at the  $\gamma$ -acid to form the aldehyde using DIBAL.<sup>165</sup> In this example the benzyl protecting group was used, which might also be suitable in this application too, as it is acid stable until the pH is below 1.<sup>141</sup>

A further alternative would be to once more explore a route initially proposed in this project; selective protection of the amino acid and then proceeding via the Weinreb amide to the aldehyde. Similar problems to that found in this project may be encountered in formation of the aldehyde if the amine is not N,N-diprotected.



**Scheme 66:** Reaction between alkyne (123) and the hydrazine (110) forms the indole (127) which contains the alkyne functional group necessary for the click reaction with the azide (139) forming the triazole compound (140).

The ‘click’ chemistry route adopted later in the project (Scheme 66 above) has clearly shown promise. Formation of the indole ring system was completed and a derivative of the target compound (only missing the quinone moiety) was able to be inserted into an unnatural azide containing amino acid (139). For these reasons it is paramount that any further research is concentrated in this area.

Further attempts must be made to efficiently deprotect the phenol so that it can be easily oxidised to the quinone. With respect to the alkyne TTQ derivative, the deprotection attempts made in this project were unsuccessful, however with such a vast range of deprotection methods available it is highly likely that a successful method can be found. With respect to the azide TTQ derivative, exploration should be made into deprotecting the phenol before formation of the azide. Early results in this project proved that such deprotection was possible; however, it was unclear whether formation of the azide was then possible. With this molecule it might even be possible to go one step further and form the quinone moiety before formation of the azide.

The possibility of attaching the TTQ analogue to the amino acid chain of a protein by nucleophilic attack from a cysteine residue into a 'β-keto-α-chloro' containing version of the TTQ analogue was also mentioned in this project. Although no attempt was made to form this analogue in this project, it could still clearly be a target molecule. This would provide another possible mechanism of insertion for the TTQ analogues into a protein chain.

The development of a range of synthetic pathways has been detailed in this project to a range of molecules. Once the final deprotection of the phenol has been addressed the synthetic pathway can be repeated, creating a library of structures that could be used to address the role and probe the mechanism by which a protein facilitates the conversion of primary amines to their corresponding aldehydes.

## 5. Experimental

### 5.1. General Experimental Information

Solvents were evaporated at reduced pressure using a *Buchi*<sup>®</sup> Rotavapor rotary evaporator.

Unless otherwise stated, anhydrous solvents were dispensed from a *Pure Solv*<sup>™</sup> solvent purification system. The solvent was collected in a round bottom flask containing 4 Å molecular sieves.

Thin layer chromatography of compounds was carried out using *Merck*<sup>®</sup> silica gel 60 F<sub>254</sub> thin layer chromatography plates. Column chromatography to purify compounds was carried out using *Fluka*<sup>®</sup> silica gel 60.

Low resolution electrospray mass spectra were recorded using a *Micromass*<sup>™</sup> Quattro-LC using electrospray ionisation from solution and a Quadrupole analyser.

High resolution fast atom bombardment spectra were recorded using a *Kratos*<sup>™</sup> Concept IIIH 2-sector mass spec, using xenon as the fast atom bombardment gas and *m*-nitro benzyl alcohol as the matrix (unless otherwise stated) with 8 kV as accelerating voltage and a resolution of @2000[10 % valley] for nominal spectra. Accurate mass determination was achieved using a 'peak matching' technique against polyethylene glycol as reference and a resolution of @10000 [10 % valley].

Other high resolution spectra (electrospray) were recorded using a *Waters*<sup>™</sup> Xevo Q-time of flight instrument using electrospray ionisation from solution. The instrument was pre-calibrated using sodium iodide and had a 'lock mass' of leucine enkephalin. This enabled a mass accuracy of @2ppm at a resolution of @10000 [full width at half maximum]

Gas chromatography mass spectrum (electron ionisation) spectra were recorded using a *Perkin Elmer*<sup>®</sup> Turbo Mass, using a pre-calibrated single quad analyser, with electron ionisation giving nominal mass spectra, with searchable NIST<sup>™</sup> database. Gas chromatography (flame ionization detector) spectra were recorded using a *Perkin-Elmer*<sup>®</sup> Clarius 500 Gas Chromatograph instrument.

Infra red spectra were recorded using a *Perkin Elmer*<sup>®</sup> Spectrum One FTIR Spectrometer with a Universal ATR Sampling Accessory, operating with *Perkin Elmer*<sup>®</sup> Spectrum software.

Nuclear magnetic resonance spectra were recorded using one of the instruments below:

- *Bruker Biospin*<sup>®</sup> DPX300 – 5mm QNP probe (<sup>1</sup>H/<sup>13</sup>C) with Z axis gradient, XWIN-NMR v 3.5-pl0, <sup>1</sup>H=299.90 MHz, <sup>13</sup>C=75.41 MHz
- *Bruker Biospin*<sup>®</sup> DRX400 – 5mm QNP probe (<sup>1</sup>H/<sup>13</sup>C), XWIN-NMR v 3.5-pl6, <sup>1</sup>H=400.13 MHz, <sup>13</sup>C=100.61 MHz
- *Bruker Biospin*<sup>®</sup> AV500 – 5mm BBO probe with Z axis gradient, TOPSPIN v 2.1, <sup>1</sup>H=500.13 MHz, <sup>13</sup>C=125.76 MHz

<sup>1</sup>H NMR Chemical shifts are reported in ppm using TMS or the residual proton signal from the solvent as an internal reference.

High performance liquid chromatography analyses were performed using a *Perkin Elmer*<sup>®</sup> Series 200 System, operating with *Perkin Elmer*<sup>®</sup> TotalChrom software. The columns used were CHIRALCEL OD-H, CHIRALCEL OJ, CHIRALPAK AD and CHIRALPAK AS manufactured by *Daicel Technologies*<sup>™</sup>. All were 250mm × 4.6mm. All programs were twenty minutes long with isocratic 1 % propanol in hexane as the solvent.

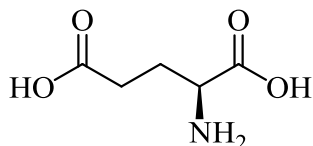
X-ray structures were recorded using a *Bruker*<sup>®</sup> Apex 2000 instrument.

Melting points of compounds were carried out using Reichert apparatus in an uncorrected format.

The high-pressure apparatus was a Roth laboratory autoclave model 1.

Purification of some stated compounds used a Chromatotron Model 7924T, manufactured by *Harrison Research*<sup>®</sup>, USA.

### Spectral Analysis of Glutamic Acid (81)



The white crystalline solid had spectral analysis carried out on it for comparison against other reactions.

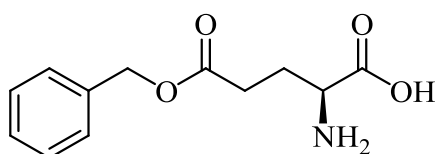
Melting point = 203-204 °C (lit 204.5 °C<sup>221</sup>)

MS (ES): 148 (MH<sup>+</sup>), and 146 (MH<sup>-</sup>), C<sub>5</sub>H<sub>9</sub>NO<sub>4</sub> requires 148.13 (MH<sup>+</sup>) and 146.13 (MH<sup>-</sup>)

IR (neat): 1638 cm<sup>-1</sup> (C=O), 3013 cm<sup>-1</sup> (O-H)

<sup>1</sup>H NMR (400 MHz, D<sub>2</sub>O) δ: 2.02-2.18 (2H, m, CH<sub>2</sub>CH<sup>1</sup>H<sup>2</sup>CHNH<sub>2</sub>), 2.44-2.57 (2H, m, CH<sub>2</sub>CH<sup>1</sup>H<sup>2</sup>CHNH<sub>2</sub>), 3.74-3.78 (1H, app t, CH<sub>2</sub>CH<sup>1</sup>H<sup>2</sup>CHNH<sub>2</sub>, J<sub>A</sub> = 6.4 Hz)

## 2-Amino-5-(benzyloxy)-5-oxopentanoic acid (**82**)



### Method 1

Concentrated sulfuric acid (188 mmol, 10 mL) was very slowly added to anhydrous diethyl ether (100 mL), followed by addition of benzyl alcohol (100 mL, 0.95 mol). The warm solution was reduced to thick, clear, colourless oil under vacuum at a rotary evaporator and L-glutamic acid (**81**) (14.8 g, 100 mmol) added in several portions under an atmosphere of nitrogen. After complete addition of the glutamic acid, the solution was left to stir for 18.5 hours at room temperature (25 °C). Ethanol (200 mL) and pyridine (50 mL) was then added to the resultant solution which was left to cool in an ice bath. The white precipitate formed was collected by suction filtration. The resultant crude white crystalline solid was resuspended in ether and gently stirred for approximately 15 mins, before being filtered and dried (13.92 g, 59 %).<sup>142</sup>

This method did yield the desired product (**82**) however it was poor yielding as TLC showed the crude mixture to predominately consist of L-glutamic acid (**81**).

### Method 2

Method as above, however after complete addition of the L-glutamic acid (**81**), the solution was stirred for 7 hours at room temperature (25 °C) after which anhydrous magnesium sulfate was added to the solution with continued stirring before being filtered off. The clear filtrate was then stirred at room temperature (25 °C) for a further 11.5 hours after which it was worked up as described above to yield crude 2-amino-5-

(benzyloxy)-5-oxopentanoic acid (**82**) as a white crystalline solid (18.964 g, 80 %).<sup>142</sup>

Due to high polarity of the compound it was not possible to purify this compound by column chromatography, however TLC and <sup>1</sup>H NMR showed a much higher conversion of the L-glutamic acid (**81**) to the benzyl protected product (**82**) so the crude product was used un-purified in subsequent reactions.

Melting point = 155-156 °C (impure) (lit 160-162 °C<sup>222</sup>)

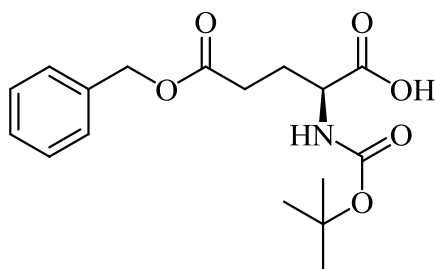
MS (ES): 238 (MH<sup>+</sup>), and 236 (MH<sup>-</sup>), C<sub>12</sub>H<sub>15</sub>NO<sub>4</sub> requires 238.25 (MH<sup>+</sup>) and 236.25 (MH<sup>-</sup>)

MS (ES): 238.1078 (MH<sup>+</sup>), C<sub>12</sub>H<sub>15</sub>NO<sub>4</sub> requires 238.1080

IR (neat): 1722 cm<sup>-1</sup> (C=O), 2947 cm<sup>-1</sup> (O-H)

<sup>1</sup>H NMR (300 MHz, CD<sub>3</sub>OD) δ: 1.95-2.15 (2H, m, CH<sub>2</sub>CH<sup>1</sup>H<sup>2</sup>CHNH<sub>2</sub>), 2.45-2.57 (2H, m, CH<sub>2</sub>CH<sup>1</sup>H<sup>2</sup>CHNH<sub>2</sub>), 3.59 (1H, app t, CH<sub>2</sub>CH<sup>1</sup>H<sup>2</sup>CHNH<sub>2</sub>, J<sub>A</sub> = 6.4 Hz), 5.04 (2H, s, PhCH<sub>2</sub>OOC), 7.17-7.30 (5H, m, 5×Ar-H)

<sup>13</sup>C NMR (125 MHz, DMSO) δ: 24.6 (CH<sub>2</sub>CH<sub>2</sub>CHNH<sub>2</sub>), 29.0 (CH<sub>2</sub>CH<sub>2</sub>CHNH<sub>2</sub>), 54.7 (CH<sub>2</sub>CH<sub>2</sub>CHNH<sub>2</sub>), 62.8 (PhCH<sub>2</sub>OOC), 126.4 (Ph), 127.5 (Ph), 128.0 (Ph), 128.4 (Ph, quaternary carbon), 174.4 (PhCH<sub>2</sub>OOC), 177.0 (HNCHCOOH).

**5-(Benzyloxy)-2-(tert-butoxycarbonylamino)-5-oxopentanoic acid (83)**

To a vigorously stirred suspension of 2-amino-5-(benzyloxy)-5-oxopentanoic acid (**82**) (0.50 g, 2.11 mmol) in anhydrous dimethylformamide (10.5 mL), anhydrous triethylamine (1.2 mL) was added at room temperature (25 °C) under an atmosphere of nitrogen. To the reaction vessel di-*tert*-butyl-dicarbonate (0.92 g, 4.2 mmol) was added and the solution heated to 60 °C for 0.5 hours, after which the volatile materials were removed *in vacuo*. The residue was treated with aqueous hydrochloric acid (50 mM, 30 mL) at 0 °C for 15 minutes. Extraction of the acidified material was then performed twice with ethyl acetate (2 × 20 mL) and evaporation of the organic layer *in vacuo* afforded a yellow oil. Toluene was added to this crude oil and then removed *in vacuo* so as to azeotropically distil traces of dimethylformamide. The resultant crude material was purified by flash column chromatography on silica gel (10: 90 ethyl acetate: petroleum ether (40/60 °C)) to yield 5-(benzyloxy)-2-(*tert*-butoxycarbonylamino)-5-oxopentanoic acid (**83**) as white crystals (0.533 g, 75 %).<sup>145</sup>

Melting point = 67-68 °C (lit 64 °C<sup>145</sup>)

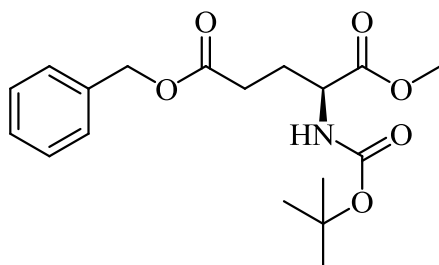
MS (ES): 338.1603 (MH<sup>+</sup>), C<sub>17</sub>H<sub>23</sub>NO<sub>6</sub> requires 338.1604 (MH<sup>+</sup>)

IR (neat): 1696  $\text{cm}^{-1}$  (C=O amide), 1733  $\text{cm}^{-1}$  (C=O)

$^1\text{H}$  NMR (300 MHz,  $\text{CD}_3\text{OD}$ )  $\delta$ : 1.44 (9H, s,  $^t\text{Bu}$ ,  $3\times\text{CH}_3$ ), 1.84-2.00 (1H, m,  $\text{CH}_2\text{CH}^1\text{H}^2\text{CHNH}_2$ ), 2.10-2.27 (1H, m,  $\text{CH}_2\text{CH}^1\text{H}^2\text{CHNH}_2$ ), 2.49 (2H, app t,  $\text{CH}_2\text{CH}^1\text{H}^2\text{CHNH}_2$ ,  $J_{\text{A}}=7.5\text{Hz}$ ), 4.17 (1H, dd,  $\text{CH}_2\text{CH}^1\text{H}^2\text{CHNH}_2$ ,  $J_{\text{A}}=9.1\text{Hz}$ ,  $J_{\text{B}}=4.9\text{Hz}$ ), 5.13 (2H, s,  $\text{Ph-CH}_2\text{-OOC}$ ), 7.27-7.39 (5H, m,  $5\times\text{Ar-H}$ )

$^{13}\text{C}$  NMR (75 MHz,  $\text{CD}_3\text{OD}$ )  $\delta$ : 28.0 ( $\text{CH}_2\text{CH}_2\text{CHNH}_2$ ), 28.7 ( $^t\text{Bu}$ ,  $3\times\text{CH}_3$ ), 31.4 ( $\text{CH}_2\text{CH}_2\text{CHNH}_2$ ) 54.1 ( $\text{CH}_2\text{CH}_2\text{CHNH}_2$ ), 67.4 ( $\text{Ph-CH}_2\text{-OOC}$ ), 80.6 (Boc C( $\text{CH}_3$ ) $_3$ ), 129.2 (Ar-C), 129.4 (Ar-C) 129.6 (Ar-C), 137.6 (Ar-C), 158.1 (Boc-C-NH), 174.2 ( $\text{PhCH}_2\text{OOC-CH}_2$ ), 175.6 ( $\text{NHCHCOOH}$ )

### 5-Benzyl-1-methyl-2-(*tert*-butoxycarbonylamino)-pentanedioate (**84**)



#### Method 1

5-(Benzyloxy)-2-(*tert*-butoxycarbonylamino)-5-oxopentanoic acid (**83**) (0.51 g, 1.5 mmol) was dissolved in chloroform (5.75 mL) and then methanol (0.122 mL, 3 mmol) was added followed by a catalytic amount of sulfuric acid (0.2 mL). This solution was refluxed for 15 hrs, cooled and a saturated solution of sodium hydrogen carbonate (15 mL) was added followed by ethyl acetate (15 mL). The resulting two

layers were separated, the organic phase washed with brine and dried over anhydrous magnesium sulfate. The resultant suspension was vacuum filtered to remove the anhydrous drying agent before being concentrated *in vacuo*.

Analysis of the crude mixture by NMR, TLC and mass spectrometry detected none of the desired product. Further analysis of the isolated fractions by TLC, mass spectrometry and  $^1\text{H}$  NMR revealed a mixture of starting material, material from which the Boc protecting group had been removed and a range of unidentifiable products, but none of the desired methylated product.<sup>223</sup>

## Method 2

To a stirred solution of 5-(benzyloxy)-2-(*tert*-butoxycarbonylamino)-5-oxopentanoic acid (**83**) (0.51 g, 1.51 mmol) in anhydrous diethyl ether (10 mL) at 0 °C was added an ethereal solution of trimethylsilyldiazomethane (2 M) drop-wise until a slight yellow colour persisted. After the mixture had stirred for 15 min at room temperature (25 °C), nitrogen was passed through the solution until the yellow colour disappeared. The remaining solvent was evaporated under reduced pressure to give crude 5-benzyl-1-methyl-2-(*tert*-butoxycarbonylamino)-pentanedioate (**84**) as a clear yellow oil (0.525 g, 99 %). The crude material was purified by flash column chromatography on silica gel (5: 95 ethyl acetate: petroleum ether (40/60 °C)) to yield (**84**) as a clear pale yellow oil (0.497 g, 94 %).<sup>224</sup>

MS (ES): 352 ( $\text{MH}^+$ ),  $\text{C}_{18}\text{H}_{25}\text{NO}_6$  requires 352.39 ( $\text{MH}^+$ )

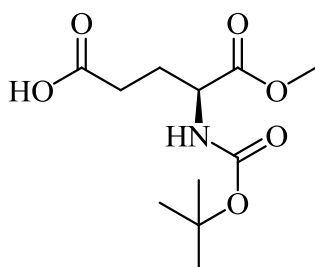
IR (neat): 1682  $\text{cm}^{-1}$  and 1728  $\text{cm}^{-1}$  (C=O), 3366  $\text{cm}^{-1}$  (NH)

This experiment was repeated on starting material containing a biased mixture of L and D isomers (containing slightly more L isomer) to test for retention of configuration. HPLC (1 : 99 – propanol : hexane) (Chiralpak AD) : 15.5 mins L isomer, 16.2 mins D isomer.

$^1\text{H}$  NMR (300 MHz,  $\text{CDCl}_3$ )  $\delta$ : 1.36 (9H, s,  $^t\text{Bu}$ ,  $3\times\text{CH}_3$ ), 1.82-1.96 (1H, m,  $\text{CH}_2\text{CH}^1\text{H}^2\text{CHNH}$ ), 2.06-2.20 (1H, m,  $\text{CH}_2\text{CH}^1\text{H}^2\text{CHNH}$ ), 2.29-2.48 (2H, m,  $\text{CH}_2\text{CH}^1\text{H}^2\text{CHNH}$ ), 3.66 (3H, s,  $\text{OMe}$ ), 4.27 (1H, m,  $\text{CH}_2\text{CH}^1\text{H}^2\text{CHNH}$ ), 5.05 (3H, br s,  $\text{Ph-CH}_2\text{-OOC}$  and  $\text{CH}_2\text{CH}_2\text{CHNH}$ ), 7.22-7.33 (5H, m,  $5\times\text{Ar-H}$ )

$^{13}\text{C}$  NMR (75 MHz,  $\text{CDCl}_3$ )  $\delta$ : 27.8 ( $\text{CH}_2\text{CH}_2\text{CHNH}$ ), 28.3 ( $^t\text{Bu}$ ,  $3\times\text{CH}_3$ ), 30.3 ( $\text{CH}_2\text{CH}_2\text{CHNH}$ ) 52.5 ( $\text{OMe}$ ), 52.8 ( $\text{CH}_2\text{CH}_2\text{CHNH}$ ), 66.5 ( $\text{Ph-CH}_2\text{-OOC}$ ), 80.1 ( $^t\text{Bu-C}(\text{CH}_3)_3$ ), 128.3 ( $2\times\text{Ar-C}$ ), 128.6 ( $\text{Ar-C}$ ), 135.7 ( $\text{Ar-C}$ ), 155.4 ( $^t\text{Bu-OOCNH}$ ), 172.5 ( $\text{PhCH}_2\text{OOC-CH}_2$ ), 172.7 ( $\text{NHCHCOOH}$ )

#### 4-(*tert*-Butoxycarbonylamino)-5-methoxy-5-oxopentanoic acid (**85**)



A sealed anhydrous nitrogen flushed round bottomed flask was charged with 5-benzyl-1-methyl-2-(*tert*-butoxycarbonylamino)-pentanedioate (**84**) (200 mg, 0.57 mmol) in methanol (25 mL) to which 10 % palladium on charcoal catalyst (c.a. 15 mg)

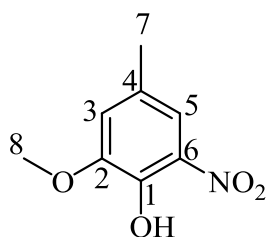
was added. The flask was evacuated and back filled with hydrogen gas, the reaction was then vigorously stirred under an atmosphere of hydrogen for or 24 hrs; the reaction was monitored for completion by TLC. A further 15mg of 10 % palladium on charcoal catalyst was added and the mixture vigorously stirred for a further 8 hrs with continued positive pressure of hydrogen. The solution was vacuum filtered to remove the heterogeneous 10 % palladium on charcoal catalyst. The volatile materials were removed *in vacuo* to yield 4-(*tert*-butoxycarbonylamino)-5-methoxy-5-oxopentanoic acid (**85**) as a pale yellow oil (0.140 g, 93 % yield).

MS (ES): 261 ( $MH^+$ ),  $C_{11}H_{19}NO_6$  requires 261.27 ( $MH^+$ )

IR (neat): 1728  $cm^{-1}$  (C=O), 2997  $cm^{-1}$  (O-H)

$^1H$  NMR (300 MHz,  $CD_3OD$ )  $\delta$ : 1.34 (9H, s,  $^tBu$ ,  $3 \times CH_3$ ), 1.71-1.86 (1H, m,  $CH_2CH^1H^2CHNH$ ), 1.94-2.08 (1H, m,  $CH_2CH^1H^2CHNH$ ), 2.29-2.48 (2H, app t,  $CH_2CH^1H^2CHNH$ ,  $J_A=7.4Hz$ ), 3.62 (3H, s,  $OMe$ ), 4.07 (1H, dd,  $CH_2CH^1H^2CHNH$ ,  $J_A=8.8Hz$ ,  $J_B=5.1Hz$ ),

$^{13}C$  NMR (75 MHz,  $CDCl_3$ )  $\delta$ : 27.9 ( $CH_2CH_2CHNH$ ), 28.8 ( $^tBu$ ,  $3 \times CH_3$ ), 31.3 ( $CH_2CH_2CHNH$ ), 52.8 ( $OMe$ ), 54.5 ( $CH_2CH_2CHNH$ ), 80.7 ( $^tBu-C(CH_3)_3$ ), 158.1 ( $^tBu-OOCNH$ ), 174.5 ( $CHCOOMe$ ), 176.5 ( $CH_2COOH$ )

**2-Methoxy-4-methyl-6-nitrophenol (89)**

A range of reaction conditions were explored for the nitration of 4-methylguaiacol with the following method found to be optimal.

A solution of 4-methylguaiacol (**88**) (1 mL, 7.8 mmol) in chloroform (20 mL) was stirred and cooled to  $-40\text{ }^{\circ}\text{C}$  and fuming nitric acid (3.1 mL) in acetic acid (5 mL) added whilst maintaining the reaction temperature below  $-35\text{ }^{\circ}\text{C}$ . After 2 mins, water (20 mL) was added and the chloroform layer isolated, dried and evaporated *in vacuo* to give the crude mixture as very dark red/brown thick oil. This material was purified by column chromatography (1:1 ethyl acetate: petroleum ether ( $40/60\text{ }^{\circ}\text{C}$ )) to yield 2-methoxy-4-methyl-6-nitrophenol (**89**) as bright orange/red crystals (0.243 g, 17 % yield).

Melting point =  $78\text{-}80\text{ }^{\circ}\text{C}$  (lit  $80\text{ }^{\circ}\text{C}$ <sup>225</sup>)

MS (ES): 184 ( $\text{MH}^+$ ), and 182 ( $\text{MH}^-$ ),  $\text{C}_8\text{H}_9\text{NO}_4$  requires 184.16 ( $\text{MH}^+$ ) and 182.16 ( $\text{MH}^-$ )

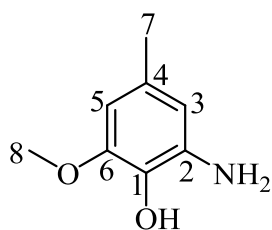
MS (FAB): 183.05279 ( $\text{M}^+$ ),  $\text{C}_8\text{H}_9\text{NO}_4$  requires 183.05316

IR (neat):  $1315\text{ cm}^{-1}$  (N=O),  $1536\text{ cm}^{-1}$  (N=O),  $3163\text{ cm}^{-1}$  (O-H)

$^1\text{H}$  NMR (300MHz,  $\text{CDCl}_3$ )  $\delta$ : 2.26 (3H, s, Ar-Me<sup>7</sup>), 3.85 (3H, s, OMe<sup>8</sup>), 6.88 (1H, app d, Ar-H,  $J_A=7.3\text{Hz}$ ), 7.39-7.41 (1H, m, Ar-H), 10.53 (1H, s, Ar-OH).

$^{13}\text{C}$  NMR (75 MHz,  $\text{CDCl}_3$ )  $\delta$ : 21.0 (Ar-Me<sup>7</sup>), 56.6 (OMe<sup>8</sup>), 115.3 (Ar-CH), 119.3 (Ar-CH), 129.0 (Ar-C<sup>4</sup>-Me), 133.5 (Ar-C<sup>1</sup>-OH), 144.4 (Ar-C<sup>6</sup>-NO<sub>2</sub>), 149.6 (Ar-C<sup>2</sup>-OMe).

### 2-Amino-6-methoxy-4-methylphenol (90)



#### Method 1

A solution of 2-methoxy-4-methyl-6-nitrophenol (**89**) (0.223 g, 1.21 mmol) in ethyl acetate (10 mL) was treated with tin(II) chloride dihydrate powder (1.54 g, 6.82 mmol) and heated under reflux for 2 hrs. The reaction mixture was cooled (25 °C) and treated with saturated aqueous sodium hydrogen carbonate (25 mL), with vigorous stirring to break up lumps formed. The organic layer was separated from the aqueous layer and solids which were further extracted with ethyl acetate (4 × 35 mL). The combined organic layers were dried over anhydrous magnesium sulfate, filtered and evaporated *in vacuo* to give the crude product.

Analysis of the crude by NMR, TLC and mass spectrometry indicated none of the desired product was present. Subsequent purification of the residue by column

chromatography on silica gel (30:70 ethyl acetate: petroleum ether (40/60 °C)) and analysis of these isolated fractions by TLC, mass spectrometry and  $^1\text{H}$  NMR revealed a mixture of starting material, tin(II) chloride dihydrate powder, unidentifiable compounds and no presence of the desired amine compound.

## Method 2

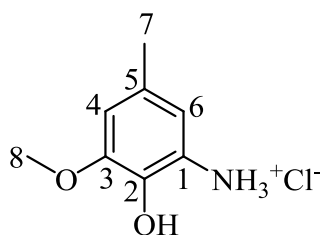
A solution of 2-methoxy-4-methyl-6-nitrophenol (**89**) (0.2 g, 1.09 mmol) and 10 % palladium on charcoal catalyst (0.10 g) in methanol (15 mL) was added to a vessel previously dried and flushed with nitrogen, which was then filled with hydrogen by means of a balloon and needle and vigorously stirred. This was stirred overnight ( $\approx$  12 hrs) before the mixture was filtered using Hirsch funnel and filter paper keeping the filtered 10 % palladium on charcoal catalyst wet with methanol. The resultant solution was concentrated *in vacuo* to yield 2-amino-6-methoxy-4-methylphenol (**90**) as a purple/grey powder (0.162 g, 97 %).

Melting point = 66 °C decomp

MS (ES): 154 ( $\text{MH}^+$ ),  $\text{C}_8\text{H}_{11}\text{NO}_2$  requires 154.18 ( $\text{MH}^+$ )

$^1\text{H}$  NMR (300MHz,  $\text{CD}_3\text{OD}$ )  $\delta$ : 2.18 (3H, s, Ar-Me<sup>7</sup>), 3.80 (3H, s, OMe<sup>8</sup>), 6.21- 6.26 (2H, m,  $2 \times$  Ar-H).

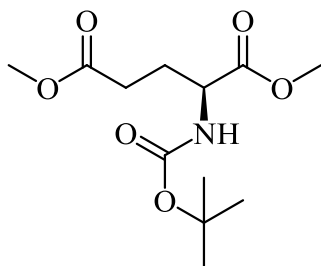
$^{13}\text{C}$  NMR (75 MHz,  $\text{CDCl}_3$ )  $\delta$ : 21.3 (Ar-Me<sup>7</sup>), 56.0 (OMe<sup>8</sup>), 102.4 (Ar-CH), 109.8 (Ar-CH), 133.8 (ArC<sup>1</sup>-OH), 138.1 (ArC<sup>2</sup>-NH<sub>2</sub>), 144.6 (ArC<sup>4</sup>-Me), 150.9 (ArC<sup>6</sup>-OMe).

**2-Hydroxy-3-methoxy-5-methylbenzenaminium chloride (90a)**

A solution of 2-methoxy-4-methyl-6-nitrophenol (**89**) (0.2 g, 1.09 mmol) and 10 % palladium on charcoal catalyst (0.10 g) in methanol (15 mL) was added to a vessel previously dried and flushed with nitrogen, which was then filled with hydrogen by means of a balloon and needle and vigorously stirred. This was stirred overnight ( $\approx$  12 hrs) before the mixture was filtered using Hirsch funnel and filter paper keeping the filtered 10 % palladium on charcoal catalyst wet with methanol. The resultant solution had anhydrous hydrochloric acid bubbled through it the resulting salt solution (**90a**) was then reduced to a purple/grey powder *in vacuo* (0.201 g, 97 %).

$^1\text{H}$  NMR (300MHz,  $\text{CD}_3\text{OD}$ )  $\delta$ : 0.96 (3H, s, Ar-Me<sup>7</sup>), 2.55 (3H, s, OMe<sup>8</sup>), 5.36 (1H, s, Ar-H), 5.53 (1H, s, Ar-H).

Insufficient sample dissolved in solvent to record a  $^{13}\text{C}$  NMR spectrum.

**Dimethyl-2-(*tert*-butoxycarbonylamino)-pentanedioate (96)**

To a stirred suspension of L-glutamic acid (**81**) (1.47 g, 1 mmol) in anhydrous methanol (33 mL, 0.3 M) in an ice bath was slowly added iodotrimethylsilane (5.6 mL, 44 mmol, 4.4 equiv). The ice bath was removed once the addition was complete and the reaction stirred overnight until TLC analysis of the reaction showed complete conversion. Triethylamine (9 mL, 65 mmol, 6.5 equiv) and di-*tert*-butyl dicarbonate (2.4 g, 11 mmol, 1.1 equiv) were added sequentially. The mixture was stirred until TLC analysis showed complete protection had been achieved. The solvent was removed under reduced pressure and the resultant residue triturated and washed with diethyl ether (3 × 150 mL) before filtering through a pad of Celite. The combined organic layers were evaporated and the resulting crude dimethyl-2-(*tert*-butoxycarbonylamino)-pentanedioate (**96**) (2.643 g, 96 %) was purified by flash column chromatography on silica gel (20:80 ethyl acetate: petroleum ether (40/60 °C)) to yield dimethyl-2-(*tert*-butoxycarbonylamino)-pentanedioate (**96**) as an oil (2.236g, 81 %).<sup>163</sup>

MS (ES): 276 (MH<sup>+</sup>) and 298 (MNa<sup>+</sup>), C<sub>12</sub>H<sub>21</sub>NO<sub>6</sub> requires 276.15 (MH<sup>+</sup>) and 298.13 (MNa<sup>+</sup>)

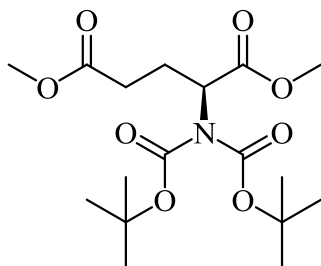
MS (ES): 276.1451 ( $\text{MH}^+$ ) and 298.1264 ( $\text{MNa}^+$ ),  $\text{C}_{12}\text{H}_{21}\text{NO}_6$  requires 276.1448 ( $\text{MH}^+$ ) and 298.1266 ( $\text{MNa}^+$ )

IR (neat):  $1712\text{ cm}^{-1}$  and  $1737\text{ cm}^{-1}$  (C=O),  $3375\text{ cm}^{-1}$  (N-H)

$^1\text{H}$  NMR (300 MHz,  $\text{CDCl}_3$ )  $\delta$ : 1.43 (9H, s,  $^t\text{Bu}$ ,  $3\times\text{CH}_3$ ), 1.87-2.01 (1H, m,  $\text{CH}_2\text{CH}^1\text{H}^2\text{CHNH}$ ), 2.11-2.24 (1H, m,  $\text{CH}_2\text{CH}^1\text{H}^2\text{CHNH}$ ), 2.31-2.50 (2H, m,  $\text{CH}_2\text{CH}^1\text{H}^2\text{CHNH}$ ), 3.67 (3H, s,  $\text{CH}_2\text{COOMe}$ ), 3.74 (3H, s,  $\text{NHCHCOOMe}$ ), 4.33 (1H, dd,  $\text{NHCHCOOMe}$ ,  $J_A=12.7\text{Hz}$ ,  $J_B=7.5\text{Hz}$ ), 5.12 (1H, s,  $\text{CH}_2\text{CH}_2\text{CHNH}$ )

$^{13}\text{C}$  NMR (75 MHz,  $\text{CDCl}_3$ )  $\delta$ : 27.8 ( $\text{CH}_2\text{CH}_2\text{CHNH}$ ), 28.3 ( $^t\text{Bu}$ ,  $3\times\text{CH}_3$ ), 30.0 ( $\text{CH}_2\text{CH}_2\text{CHNH}$ ), 51.8 ( $\text{CH}_2\text{CH}_2\text{COOMe}$ ), 52.4 ( $\text{NHCHCOOMe}$ ), 52.8 ( $\text{CH}_2\text{CH}_2\text{CHNH}$ ), 80.0 ( $^t\text{Bu}-\text{C}(\text{CH}_3)_3$ ), 155.3 ( $\text{NHCOOC}(\text{CH}_3)_3$ ), 172.6 ( $\text{CH}_2\text{CH}_2\text{COOMe}$ ), 173.1 ( $\text{NHCHCOOMe}$ ).

### Dimethyl-2-(bis(*tert*-butoxycarbonyl)amino)-pentanedioate (**97**)



To a stirred solution of the dimethyl-2-(*tert*-butoxycarbonylamino)-pentanedioate (**96**) (1.6 g, 5.8 mmol) and dimethylaminopyridine (140 mg, 1.15 mmol, 0.2 equiv.) in anhydrous acetonitrile (150 mL, 1.5 M) was added di-*tert*-butyl-

dicarbonate (1.408g, 6.45 mmol, 1.1 equiv) at room temperature (25 °C); the reaction became slightly red with gas evolution. The mixture was stirred for 2 hrs, when TLC showed some starting material still remained. More di-*tert*-butyl-dicarbonate (0.633 g, 2.9 mmol, 0.5 equiv.) was added and the mixture stirred overnight (12 hrs). The solvent was evaporated, and the crude material purified by flash column chromatography on silica gel (15:85 ethyl acetate: petroleum ether (40/60 °C)) to afford dimethyl-2-(bis(*tert*-butoxycarbonyl)amino)-pentanedioate (**97**) as a clear pale yellow oil (1.697 g, 78 %).<sup>163</sup>

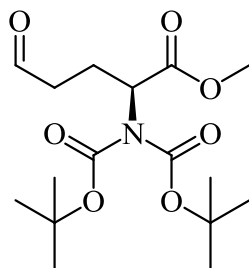
MS (ES): 376 (MH<sup>+</sup>) and 398, C<sub>17</sub>H<sub>29</sub>NO<sub>8</sub> requires 376.41 (MH<sup>+</sup>) and 398.41 (MNa<sup>+</sup>)

MS (ES): 376.1979 (MH<sup>+</sup>), C<sub>17</sub>H<sub>29</sub>NO<sub>8</sub> requires 376.1972 (MH<sup>+</sup>)

IR (neat): 1732 cm<sup>-1</sup>, 1754 cm<sup>-1</sup> and 1778 cm<sup>-1</sup> (C=O)

<sup>1</sup>H NMR (300 MHz, CDCl<sub>3</sub>) δ: 1.50 (18H, s, 2×(<sup>t</sup>Bu, 3×CH<sub>3</sub>)), 2.13-2.28 (1H, m, CH<sub>2</sub>CH<sup>1</sup>H<sup>2</sup>CHNH), 2.32-2.56 (3H, m, CH<sub>2</sub>CH<sup>1</sup>H<sup>2</sup>CHNH and CH<sub>2</sub>CH<sup>1</sup>H<sup>2</sup>CHNH), 3.68 (3H, s, CH<sub>2</sub>COOMe), 3.72 (3H, s, N(Boc)<sub>2</sub>CHCOOMe), 4.94 (1H, dd, NHCHCOOMe, J<sub>A</sub>=9.5Hz, J<sub>B</sub>=4.7Hz),

<sup>13</sup>C NMR (75 MHz, CDCl<sub>3</sub>) δ: 25.2 (CH<sub>2</sub>CH<sub>2</sub>CHN(Boc)<sub>2</sub>), 28.0 (<sup>t</sup>Bu, 6×CH<sub>3</sub>), 30.6 (CH<sub>2</sub>CH<sub>2</sub>CHN(Boc)<sub>2</sub>), 51.7 (CH<sub>2</sub>CH<sub>2</sub>COOMe), 52.2 (N(Boc)<sub>2</sub>CHCOOMe), 57.4 (CH<sub>2</sub>CH<sub>2</sub>CHN(Boc)<sub>2</sub>), 83.3 (2×(Boc-C(CH<sub>3</sub>)<sub>3</sub>)), 151.9 (N(COOC(CH<sub>3</sub>)<sub>3</sub>)<sub>2</sub>), 170.8 (N(Boc)<sub>2</sub>CHCOOMe), 173.1 (CH<sub>2</sub>CH<sub>2</sub>COOMe).

**Methyl-2-(bis(*tert*-butoxycarbonyl)amino)-5-oxopentanoate (98)**

To a stirred solution of the dimethyl-2-(bis(*tert*-butoxycarbonyl)amino)-pentanedioate (**97**) (1 g, 2.7 mmol) in anhydrous diethyl ether (27 mL, 0.1 M) was added dropwise diisobutylaluminium hydride (3 mL, 1.0 M in hexane, 3 mmol, 1.1 equiv) at -78 °C. This was stirred for 5mins before being quenched with water (0.4 mL,  $\approx 7$  equiv.), stirred for a further 30mins, dried over anhydrous magnesium sulfate, and filtered through a pad of Celite. The solvent was removed *in vacuo*, and the crude purified by flash column chromatography on silica gel (10:90 ethyl acetate: petroleum ether (40/60 °C)) to afford methyl-2-(bis(*tert*-butoxycarbonyl)amino)-5-oxopentanoate (**98**) as an oil (0.781 g, 85 % yield).<sup>163</sup>

The phases in subsequent larger scale reactions were separated to remove water, dried over anhydrous magnesium sulfate and filtered before removal of volatile materials *in vacuo*.

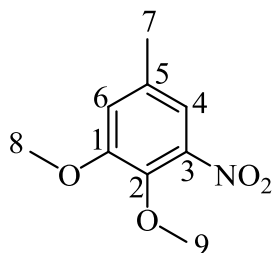
MS (ES): 346 ( $\text{MH}^+$ ) and 344 ( $\text{MH}^-$ ),  $\text{C}_{16}\text{H}_{27}\text{NO}_7$  requires 346.39 ( $\text{MH}^+$ ) and 344.39 ( $\text{MH}^-$ )

IR (neat): 1698  $\text{cm}^{-1}$  (aldehyde C=O), 1744  $\text{cm}^{-1}$  (C=O)

$^1\text{H}$  NMR (300 MHz,  $\text{CDCl}_3$ )  $\delta$ : 1.50 (18H, s,  $^t\text{Bu}$ ,  $6 \times \text{CH}_3$ ), 2.10-2.26 (1H, m,  $\text{CH}_2\text{CH}^1\text{H}^2\text{CHN}(\text{Boc})_2$ ), 2.41-2.69 (3H, m,  $\text{CH}_2\text{CH}^1\text{H}^2\text{CHN}(\text{Boc})_2$  and  $\text{CH}_2\text{CH}^1\text{H}^2\text{CHN}(\text{Boc})_2$ ), 3.73 (3H, s,  $\text{N}(\text{Boc})_2\text{CHCOOMe}$ ), 4.85-4.98 (1H, m,  $\text{N}(\text{Boc})_2\text{CHCOOMe}$ ), 9.78 (1H, app t,  $\text{OHCCH}_2\text{CH}_2\text{N}(\text{Boc})_2$ ,  $J_A=0.1\text{Hz}$ ).

$^{13}\text{C}$  NMR (75 MHz,  $\text{CDCl}_3$ )  $\delta$ : 22.3 ( $\text{CH}_2\text{CH}_2\text{CHN}(\text{Boc})_2$ ), 27.7 ( $^t\text{Bu}$ ,  $6 \times \text{CH}_3$ ), 40.2 ( $\text{CH}_2\text{CH}_2\text{CHN}(\text{Boc})_2$ ), 52.0 ( $\text{N}(\text{Boc})_2\text{CHCOOMe}$ ), 57.1 ( $\text{CH}_2\text{CH}_2\text{CHN}(\text{Boc})_2$ ), 83.1 ( $^t\text{Bu}-\text{C}(\text{CH}_3)_3$ ), 151.8 ( $2 \times \text{N}(\text{COOC}(\text{CH}_3)_3$ ), 170.5 ( $\text{N}(\text{Boc})_2\text{CHCOOMe}$ ), 200.7 ( $\text{HOCCH}_2\text{CH}_2\text{CHN}(\text{Boc})_2$ ).

### 1,2-Dimethoxy-5-methyl-3-nitrobenzene (**99**)



A solution of 1,2-dimethoxy-4-methylbenzene (**103**) (1.051 g, 1 mL, 6.9 mmol) in chloroform (20 mL) was stirred and cooled to  $-40\text{ }^\circ\text{C}$  before a solution of -fuming nitric acid (3.1 mL) in glacial acetic acid (5 mL) was added maintaining a reaction temperature not above  $-35\text{ }^\circ\text{C}$ . After 2 mins, water (20 mL) was added and the organic phase extracted before all solvent was removed *in vacuo*. The crude 1,2-dimethoxy-5-methyl-3-nitrobenzene (**99**), a very dark red/brown thick oil (1.352 g, 99 %) was purified by flash column chromatography on silica gel (1:1 ethyl acetate:

petroleum ether (40/60 °C)) to yield 1,2-dimethoxy-5-methyl-3-nitrobenzene (**99**) as bright orange solid (0.767 g, 56 %).

Melting point = 53-55 °C (lit 52-55 °C<sup>226</sup>)

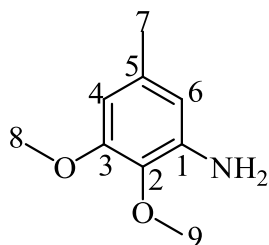
MS (FAB): 198 (MH<sup>+</sup>), C<sub>9</sub>H<sub>11</sub>NO<sub>4</sub> requires 198.19 (MH<sup>+</sup>)

IR (neat): 1582 cm<sup>-1</sup> (N=O)

<sup>1</sup>H NMR (300MHz, CDCl<sub>3</sub>) δ: 2.61 (3H, s, Ar-Me<sup>7</sup>), 3.93 (3H, s, OMe), 3.97 (3H, s, OMe), 6.73 (1H, s, Ar-H), 7.64 (1H, s, Ar-H).

<sup>13</sup>C NMR (75 MHz, CDCl<sub>3</sub>) δ: 21.3 (Ar-Me<sup>7</sup>), 56.2 (OMe), 56.3 (OMe), 108.0 (Ar-CH), 114.0 (Ar-CH), 129.0 (Ar-C<sup>5</sup>-Me), 141.0 (Ar-C-OMe), 147.0 (Ar-C-NO<sub>2</sub>), 152.9 (Ar-C-OMe).

### 2,3-Dimethoxy-5-methylaniline (**100**)



A sealed round bottomed flask was charged with 1,2-dimethoxy-5-methyl-3-nitrobenzene (**99**) (1.383 g, 7 mmol) in methanol (15 mL) and 10 % palladium on

charcoal catalyst (c.a. 10 mg) was added. The vessel, previously dried and flushed with nitrogen, was back filled with hydrogen. The reaction was vigorously stirred with a positive pressure of hydrogen for 65 hours. The solution was filtered through a pad of Celite and the combined organic phases had volatile materials removed *in vacuo* to yield 2,3-dimethoxy-5-methylaniline (**100**) as a purple/grey powder (1.073 g, 92 %).<sup>227</sup>

Melting point = 95-97 °C

MS (ES): 168 (MH<sup>+</sup>), C<sub>9</sub>H<sub>13</sub>NO<sub>2</sub> requires 168.10 (MH<sup>+</sup>)

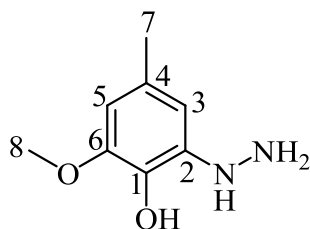
MS (ES): 168.1022 (MH<sup>+</sup>), C<sub>9</sub>H<sub>13</sub>NO<sub>2</sub> requires 168.1025 (MH<sup>+</sup>)

IR (neat): 3389 cm<sup>-1</sup> and 1615 cm<sup>-1</sup> (N-H)

<sup>1</sup>H NMR (300MHz, CD<sub>3</sub>OD) δ: 2.10 (3H, s, Ar-Me<sup>7</sup>), 3.73 (3H, s, OMe), 3.76 (3H, s, OMe), 6.46 (1H, s, Ar-H), 6.66 (1H, s, Ar-H).

<sup>13</sup>C NMR (75 MHz, CD<sub>3</sub>OD) δ: 16.8 (Ar-Me<sup>7</sup>), 56.5 (OMe), 57.7 (OMe), 102.9 (Ar-CH), 116.2 (ArC-OMe), 117.3 (ArCH), 140.3 (ArC<sup>1</sup>-NH<sub>2</sub>), 143.2 (ArC<sup>5</sup>-Me), 149.6 (ArC-OMe).

## 2-Hydrazinyl-6-methoxy-4-methylphenol (101)



### Method 1

Concentrated hydrochloric acid (0.5 mL, 32 %) was placed in a round bottom flask with cracked ice and further cooled in an ice bath (0 °C) to which, 2-amino-6-methoxy-4-methylphenol (**90**) (0.153 g, 1 mmol) was added slowly maintaining 0 °C. Keeping the temperature as near to 0 °C as possible, sodium nitrite (0.069 g, 1 mmol) in water (3 mL) was added dropwise with vigorous stirring.

A solution of sodium sulfite (5 mmol) was prepared by dissolving sodium hydroxide pellets (0.2 g, 5 mmol) in a round bottomed flask with water (20 mL); 1 drop of phenolphthalein solution was added and sulfur dioxide was passed through until an acid solution was indicated.

The sodium sulfite solution was cooled to approximately 5 °C with ice before the diazonium salt solution was rapidly added with vigorous stirring. The solution was allowed to warm (25 °C) until the sodium sulfite (which had separated at the lower temperature) had re-dissolved. The solution was warmed to 60-70 °C for 1 hr before enough hydrochloric acid was added to make the solution acidic to litmus paper. It was returned to heat until the solution became clear (12 hrs). Hydrochloric acid (32 %) was added to the hot, clear solution and the reaction slowly cooled to 0 °C to precipitate the hydrazine as its hydrochloride salt. The free base could have been liberated by adding

aqueous sodium hydroxide (25 %) and the 2-hydrazinyl-6-methoxy-4-methylphenol (**101**) then extracted into benzene.

Analysis of the crude mixture by NMR, TLC and mass spectrometry detected none of the desired product. Further analysis of the isolated fractions by TLC, mass spectrometry and  $^1\text{H}$  NMR revealed a mixture of starting material and unidentifiable compounds and showed no presence of the desired hydrazine compound.

## Method 2

A solution of sodium nitrite (0.759 g in 0.39 mL water, 1.1 mmol) at 0 °C was added dropwise to a suspension of 2-amino-6-methoxy-4-methylphenol (**90**) (0.153 g, 1 mmol) in concentrated hydrochloric acid (5 mL, 32 %) also cooled to 0 °C. To this mixture was added dropwise a solution of tin(II) chloride dihydrate in concentrated hydrochloric acid (5 mL, 32 %) before being stirred for 1hr at 0 °C. The reaction mixture was then basified by addition of aqueous sodium hydroxide (10 mL, 50 %), further diluted with water (5 mL), treated with another portion of aqueous sodium hydroxide (3.3 mL, 50 %) and then crushed ice (30g). The reaction mixture was extracted with diethyl ether (4 × 50 mL) and the combined organic fractions were washed with saturated aqueous sodium chloride solution, dried over anhydrous anhydrous magnesium sulfate and vacuum filtered. A small amount of the filtrate was removed for analysis and the remaining filtrate was acidified by adding anhydrous hydrochloric acid. The precipitate was collected by suction filtration and then dried under reduced pressure after which flash column chromatography on silica gel was used to purify the crude (5 %: 95 % ethyl acetate: petroleum ether (40/60 °C)).

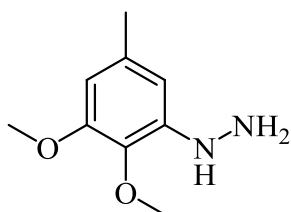
Analysis of the crude mixture by NMR, TLC and mass spectrometry detected none of the desired product. Further analysis of the isolated fractions by TLC, mass

spectrometry and  $^1\text{H}$  NMR revealed a mixture of starting material, deaminated by-product, unidentifiable compounds and showed no presence of the desired hydrazine compound.<sup>228</sup>

### Method 3

2-Amino-6-methoxy-4-methylphenol (**90**) (0.153 g, 1 mmol) was mixed with concentrated hydrochloric acid (5 mL, 32 %) at  $-35^\circ\text{C}$ . To this semi-crystalline paste, sodium nitrite (0.069 g, 1 mmol) in water (0.5 mL) was added while vigorously stirring with a mechanical stirrer at  $-35^\circ\text{C}$ . A cooled solution of tin(II) chloride dihydrate (0.564g, 2.5 mmol) in concentrated hydrochloric acid (5 mL, 32 %) was added and the resultant yellow/white precipitate was left to stand for 15 hrs at room temperature. The solid was collected by vacuum filtration, thoroughly pressed and shaken with aqueous sodium hydroxide (30 mL, 25 %) and diethyl ether (30 mL). The organic layer was separated and the aqueous layer extracted with diethyl ether ( $3 \times 30$  mL). The organic fractions were combined, dried over anhydrous magnesium sulfate, filtered and the volatiles evaporated *in vacuo*. The crude material was purified by flash column chromatography on silica gel (1:19 ethyl acetate: petroleum ether ( $40/60^\circ\text{C}$ )).

Analysis of the crude mixture by NMR, TLC and mass spectrometry detected none of the desired product. Further analysis of the isolated fractions by TLC, mass spectrometry and  $^1\text{H}$  NMR revealed a mixture of starting material, deaminated by-product, unidentifiable compounds and confirmed no presence of the desired hydrazine compound.

**(2,3-Dimethoxy-5-methylphenyl)-hydrazine (102)****Method 1**

A mechanically stirred suspension of 2,3-dimethoxy-5-methylaniline (**100**) (0.167g, 1 mmol) in concentrated hydrochloric acid (32 %, 5 mL) was cooled to 0 °C, a solution of sodium nitrite (0.0759g in 0.39 mL water 1.1 mmol), also cooled to 0 °C, was added dropwise. After stirring for 30mins a solution of tin(II) chloride dihydrate in concentrated hydrochloric acid (32 %, 5 mL) was added and stirring continued for a further 1hr at 0 °C after which the reaction mixture was basified with aqueous sodium hydroxide (50 %,10 mL). The reaction was further diluted with water (5 mL), treated with another portion of aqueous sodium hydroxide (50 %,10 mL) and then crushed ice (approximately 30g). The resultant mixture was extracted with diethyl ether (4 × 50 mL) and the combined organic fractions washed with brine, dried over anhydrous magnesium sulfate and filtered. A small amount of filtrate was removed for analysis and the remaining filtrate was acidified by adding anhydrous hydrochloric acid. The precipitate was collected by suction filtration and dried under reduced pressure before being purified by column chromatography (5:95 ethyl acetate: petroleum ether (40/60 °C)).<sup>228</sup>

Analysis of the crude mixture by NMR, TLC and mass spectrometry detected none of the desired product. Further analysis of the isolated fractions by TLC, mass

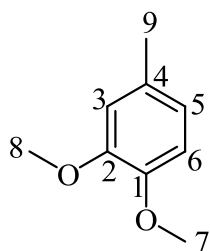
spectrometry and  $^1\text{H}$  NMR revealed a mixture of starting material, deaminated material, unidentifiable compounds and showed no presence of the desired hydrazine compound.

Further attempts were made following this procedure but altering one variable at a time (i.e temperature) with no success.

## Method 2

2,3-Dimethoxy-5-methylaniline (**100**) (1.67g, 10 mmol) in concentrated hydrochloric acid (approx. 32 %, 40 mL) was cooled to 0 °C. To this semi-crystalline paste was added dropwise a solution of sodium nitrite (0.759g, 11 mmol) in water (4 mL), also cooled to 0 °C, whilst being stirred vigorously. After 30mins, a cooled solution of tin(II) chloride dihydrate in concentrated hydrochloric acid (32 %, 23 mL) was added and a yellow/white precipitate separated and was left to stand overnight (25 °C). The solid was collected by vacuum filtration, thoroughly pressed and shaken with aqueous sodium hydroxide (25 %, 38 mL) and diethyl ether (50 mL). The organic layer was separated and the aqueous layer extracted a further three times with diethyl ether (3 × 50 mL), the organic fractions were combined, dried with anhydrous magnesium sulfate, filtered and volatiles removed *in vacuo*. The remaining oil was purified by column chromatography (10:90 ethyl acetate: petroleum ether (40/60 °C)).

Analysis of the crude mixture by NMR, TLC and mass spectrometry detected none of the desired product. Further analysis of the isolated fractions by TLC, mass spectrometry and  $^1\text{H}$  NMR revealed a mixture of starting material, deaminated by-product, unidentifiable compounds and showed no presence of the desired hydrazine compound.

**1,2-Dimethoxy-4-methylbenzene (103)**

A mixture of 2-methoxy-4-methylphenol (0.252 mL, 0.276 g, 2 mmol, 1 equiv.), anhydrous potassium carbonate (1.382 g, 10 mmol, 5equiv.) and iodomethane (1.244 mL, 2.838 g, 20 mmol, 10equiv.) in acetone (10 mL) was heated under reflux overnight (15 hrs). After cooling, the mixture was filtered to remove the potassium carbonate. The resultant filtrate was then washed with water (10 mL) and extracted with chloroform (3 × 15 mL). Volatiles were removed under reduced pressure to yield 1,2-dimethoxy-4-methylbenzene (**103**) as a colourless oil (0.286 g, 94 %). The product was used without further purification.

MS (ES): 153 (MH<sup>+</sup>), C<sub>9</sub>H<sub>12</sub>O<sub>2</sub> requires 153.16 (MH<sup>+</sup>)

GCMS (EI): GC peak at 7.32 mins, with 152 (M<sup>+</sup>), C<sub>9</sub>H<sub>12</sub>O<sub>2</sub> requires 152.16 (M<sup>+</sup>)

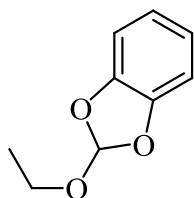
MS (FAB): 152.08337 (M<sup>+</sup>), C<sub>9</sub>H<sub>12</sub>O<sub>2</sub> requires 152.08373

IR (neat): Absence of phenolic OH

$^1\text{H}$  NMR (300MHz,  $\text{CDCl}_3$ )  $\delta$ : 2.29 (3H, s, Ar-Me<sup>9</sup>), 3.82 (3H, s, OMe), 3.84 (3H, s, OMe), 6.62 – 6.81 (3H, m, Ar-H<sup>3,5,6</sup>).

$^{13}\text{C}$  NMR (75 MHz,  $\text{CDCl}_3$ )  $\delta$ : 21.0 (Ar-Me<sup>9</sup>), 55.9 (OMe), 56.7 (OMe), 111.3 (Ar-CH), 112.5 (Ar-CH), 120.8 (Ar-CH), 130.4 (ArC<sup>4</sup>-Me), 146.9 (ArC-OMe), 148.7 (ArC-OMe).

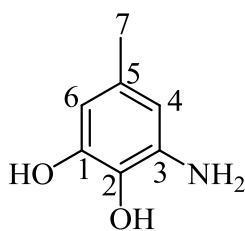
### 2-ethoxybenzo-1,3-dioxole (104)



Pyrocatechol (0.22 g, 2 mmol), triethoxymethane (0.444 g, 0.394 ml, 1.5 mmol), *para*-toluenesulphonic acid (0.05 g, 0.29 mmol), powdered 4 Å molecular sieves (0.2 g) in dry benzene (40 ml with a further 5×20 ml portions added during process) were heated in a distillation apparatus until approximately 120 ml of the benzene/EtOH azeotrope (bp 67-75 °C). The cooled dark red mixture was filtered and distilled to yield 2-ethoxybenzo-1,3-dioxole (**104**) (0.297 g, 89 %) as a colourless liquid.

$^1\text{H}$  NMR (300MHz,  $\text{CDCl}_3$ )  $\delta$ : 1.25 (3H, t, CH<sub>3</sub>,  $J_{\text{A}}=7.1\text{Hz}$ ), 3.71 (2H, q, CH<sub>2</sub>,  $J_{\text{A}}=7.1\text{Hz}$ ), 6.77 – 6.84 (5H, m, Ar-H and CH).

### 3-Amino-5-methylbenzene-1,2-diol (105)



#### Method 1

Aluminium triiodide was synthesised by placing aluminium powder (0.108 g, 4 mmol) and iodine crystals (0.812 g, 6.4 mmol) into anhydrous acetonitrile (10 mL) and heating this mixture under reflux until the characteristic red colour of the iodine had completely disappeared.

To a cooled solution of the aluminium triiodide (1.661 g, 4 mmol) in acetonitrile (10 mL) a solution of 2-amino-6-methoxy-4-methylphenol (**90**) (0.511 g, 3.3 mmol) and tetrabutylammonium iodide (0.012 g, 0.03 mmol) in acetonitrile (3.3 mL) was added dropwise before heating under reflux for 0.5 hr and hydrolysis with water (35 mL). The mixture was concentrated *in vacuo* and the residue partitioned between water (30 mL) and benzene (30 mL). The benzene fraction was washed with water (2 × 20 mL), the combined aqueous fractions were further extracted with ethyl acetate (6 × 25 mL). The combined organic phases were dried over anhydrous magnesium sulfate and the solvent evaporated to give a crude yield which was purified by column chromatography (1:1 ethyl acetate: petroleum ether (40/60 °C)).

Analysis of the crude product by NMR, TLC and mass spectrometry suggested none of the desired product had been formed. Further analysis of the isolated fractions by TLC, mass spectrometry and <sup>1</sup>H NMR revealed a mixture of starting material and

unidentifiable compounds and confirmed no presence of the desired demethylated compound.

## Method 2

To a solution of 2-amino-6-methoxy-4-methylphenol (**90**) (0.153 g, 1.0 mmol, 2M in chloroform) was added iodotrimethylsilane (0.26 g, 0.185 mL, 1.3 mmol, 1.3 equiv.). The reaction was stirred at 25 °C and monitored by TLC until it showed complete conversion; at this point the reaction intermediates were hydrolysed and the iodotrimethylsilane neutralised by adding methanol (2 mL, 4 equiv.). All volatile components were removed *in vacuo* and the resultant crude material purified immediately by flash column chromatography on silica gel (1:1 ethyl acetate: petroleum ether (40/60 °C)).

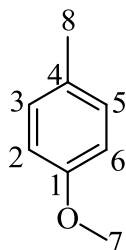
Analysis of the crude product by NMR, TLC and mass spectroscopy suggested none of the desired product had been formed. Further analysis of the isolated fractions by TLC, mass spectroscopy and <sup>1</sup>H NMR revealed a mixture of starting material and unidentifiable compounds and confirmed no presence of the desired demethylated compound.

A large number of further attempts (Table 4) were made at the demethylation following a similar procedure, each time altering one variable (e.g. temperature, time, concentration of starting materials and reagents) but none were successful.

Substrate	Concentration of TMSI	Temperature	Time
Amine ( <b>90</b> )	1.3 eq TMSI in CDCl <sub>3</sub>	Room Temp.	16 hrs
Amine ( <b>90</b> )	3.5 eq TMSI in CDCl <sub>3</sub>	Room Temp.	16 hrs
Amine ( <b>90</b> )	3.5 eq TMSI in MeCN	Room Temp.	16 hrs
Amine ( <b>90</b> )	Neat TMSI	Room Temp.	16 hrs
Amine ( <b>90</b> )	Neat TMSI	50 °C	16 hrs
Nitro ( <b>89</b> )	3.5 eq TMSI in MeCN	Room Temp.	16 hrs
Nitro ( <b>89</b> )	3.5 eq TMSI in CDCl <sub>3</sub>	Room Temp.	16 hrs
Nitro ( <b>89</b> )	Neat TMSI	Room Temp.	16 hrs
Nitro ( <b>89</b> )	Neat TMSI	50 °C	16 hrs
Nitro ( <b>89</b> )	Neat TMSI	50 °C	24 hrs
Nitro ( <b>89</b> )	Neat TMSI	50 °C	72 hrs

**Table 4:** A list of reaction conditions tried in an attempt to remove the methyl ether from the target compound all on a 1 ml scale.

### 1-Methoxy-4-methylbenzene (**107**)



A mixture of 4-methylphenol (**106**) (0.216 g, 2 mmol, 1 eq), anhydrous potassium carbonate (1.382 g, 10 mmol, 5 eq) and iodomethane (1.244 mL, 2.838 g, 20

mmol, 10 eq) in acetone (10 mL) was heated under reflux overnight (15hrs). After cooling the mixture was filtered to remove the potassium carbonate. The resultant filtrate was washed with water (10 mL) and extracted with chloroform ( $3 \times 15$  mL). Volatiles were removed *in vacuo* to yield 1-methoxy-4-methylbenzene (**107**) as a colourless oil (0.206 g, 84 %). The product was used without further purification.

Mass spectrum (ES): 123 ( $\text{MH}^+$ ),  $\text{C}_8\text{H}_{10}\text{O}$  requires 123.16 ( $\text{MH}^+$ )

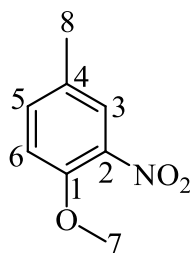
Mass spectrum (ES): 123.0811,  $\text{C}_8\text{H}_{10}\text{O}$  requires 123.0811 ( $\text{MH}^+$ )

IR (neat): Absence of phenolic OH

$^1\text{H}$  NMR (300MHz,  $\text{CDCl}_3$ )  $\delta$ : 2.39 (3H, s, Ar-Me<sup>8</sup>), 3.86 (3H, s, O-Me<sup>7</sup>), 6.86 – 7.22 (4H, m, Ar-H).

$^{13}\text{C}$  NMR (75 MHz,  $\text{CDCl}_3$ )  $\delta$ : 20.5 (Ar-Me<sup>8</sup>), 55.3 (O-Me<sup>7</sup>), 113.8 (Ar-CH<sup>2, 6</sup>) 129.9 (Ar-C<sup>4</sup>-Me), 130.0 (Ar-CH<sup>3, 5</sup>), 157.6 (Ar-C<sup>1</sup>-OMe).

### 1-Methoxy-4-methyl-2-nitrobenzene (**108**)



## Method 1

A solution of 4-methylanisole (**107**) (4.845g, 5 mL, 39.7 mmol) in chloroform (100 mL) was stirred and cooled to -40 °C before a solution of fuming nitric acid (15.5 mL) in glacial acetic acid (25 mL) was added never letting the reaction temperature rise above -35 °C. After 2mins water (100 mL) was added and the chloroform layer extracted; the water was extracted twice more with chloroform (2 × 100 mL). The combined chloroform layers were dried over magnesium sulphate before all solvent was removed *in vacuo*. The crude reaction mixture was purified by flash column chromatography on silica gel (5: 95 ethyl acetate: petroleum ether (40/60 °C)).

Analysis of the crude mixture by NMR, TLC and mass spectrometry detected none of the desired product. Further analysis of the isolated fractions by TLC, mass spectrometry and <sup>1</sup>H NMR revealed a mixture of nitrated/demethylated product and unidentifiable compounds and showed only a very small amount of the desired 1-methoxy-4-methyl-2-nitrobenzene (0.068g, 1 %), however no starting materials remained.

A large number of further attempts following this procedure were made each time altering one variable (eg. temperature, time), however none were successful.

## Method 2

A solution of 4-methylanisole (**107**) (5.63 mL, 5.46 g, 44.5 mmol) in acetic anhydride (4.20 mL 4.54 g, 44.5 mmol) was added dropwise with stirring at -40°C over 30mins to a nitrating mixture prepared from nitric acid (3.7 mL, 5.6 g, 89 mmol) and acetic anhydride (18.2 g, 178 mmol). After complete addition, the mixture was stirred for 30mins at -40°C before transferring into a three neck round bottom flask containing diethyl ether (150 mL) at -78°C. Ammonia was condensed into the mixture until the

temperature had returned to  $-78^{\circ}\text{C}$  and the reaction remained alkaline to litmus paper. At this point the excess ammonia was removed on an aspirator and the temperature allowed to rise to  $0^{\circ}\text{C}$ ; the mixture was neutral to litmus paper. Diethyl ether (100 mL) was added to this mixture and the ethereal layer decanted into a separating funnel. The remaining residue was washed with more diethyl ether (150 mL) and the combined ethereal layer washed with cold water ( $4 \times 50$  mL), dried over anhydrous magnesium sulfate and filtered, before removal of the diethyl ether under reduced pressure. The crude material (6.501 g, 87 %) was purified using flash column chromatography on silica gel (1:9 ethyl acetate: petroleum ether ( $40/60^{\circ}\text{C}$ )) to yield 1-methoxy-4-methyl-2-nitrobenzene (**108**) as a dark orange oil (3.876g, 52 %).<sup>229</sup>

GCMS (DCM) (EI): 15.03min (single peak), 167 ( $\text{M}^+$ ),  $\text{C}_8\text{H}_9\text{NO}_3$  requires 167.16 ( $\text{M}^+$ )

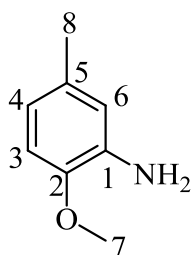
MS (ES): 168 ( $\text{MH}^+$ ),  $\text{C}_8\text{H}_9\text{NO}_3$  requires 168.16 ( $\text{MH}^+$ ),

MS (ES): 168.0663 ( $\text{MH}^+$ ),  $\text{C}_8\text{H}_9\text{NO}_3$  requires 168.06552 ( $\text{MH}^+$ )

IR (neat):  $1525\text{ cm}^{-1}$  (N=O),

$^1\text{H}$  NMR (300 MHz,  $\text{CDCl}_3$ )  $\delta$ : 2.27 (3H, s, ArC-Me<sup>8</sup>), 3.86 (3H, s, OMe<sup>7</sup>), 6.91-7.58 (3H, m,  $3 \times$  Ar-CH).

$^{13}\text{C}$  NMR (75 MHz,  $\text{CDCl}_3$ ): 20.0 (ArC-Me<sup>8</sup>), 56.5 (Ar-OMe<sup>7</sup>), 113.5 (ArC<sup>6</sup>H), 125.6 (ArC<sup>3</sup>H), 130.1 (ArC<sup>4</sup>-Me), 134.9 (Ar-C<sup>5</sup>H), 139.2 (ArC<sup>2</sup>-NO<sub>2</sub>), 150.9 (ArC<sup>1</sup>-OMe).

**2-Methoxy-5-methylaniline (109)**

A solution of 1-methoxy-4-methyl-2-nitrobenzene (**108**) (5.015 g, 4.162 mL, 30 mmol) and 10 % palladium on charcoal catalyst (0.10g) in methanol (200 mL) was added to a vessel previously dried and flushed with nitrogen. The vessel, then back filled with hydrogen, was vigorously stirred overnight ( $\approx$  14 hrs). The mixture was filtered using a Hirsch funnel and filter paper keeping the filtered 10 % palladium on charcoal catalyst wet with methanol. The resultant solution was then concentrated to a dark purple/brown powder under vacuum (4.049g, 98 %). The 2-methoxy-5-methylaniline (**109**) was used as crude without further purification.<sup>227</sup>

Melting Point: 49-51 °C

GCMS (DCM) (EI): 12.45min (single peak), 137 ( $M^+$ ),  $C_8H_{11}NO=137.18$  ( $M^+$ )

MS (ES): 138 ( $MH^+$ ),  $C_8H_{11}NO$  requires 138.18 ( $MH^+$ ),

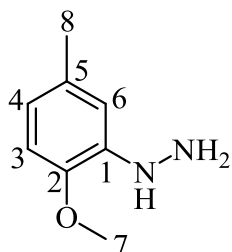
MS (ES): 138.0918 ( $MH^+$ ),  $C_8H_{11}NO$  requires 138.09134 ( $MH^+$ )

IR (neat): 3300  $cm^{-1}$  (NH)

$^1\text{H}$  NMR (300 MHz,  $\text{CDCl}_3$ )  $\delta$ : 2.15 (3H, s, ArC-Me<sup>8</sup>), 3.64 (2H, br s,  $\text{NH}_2$ ), 3.74 (3H, s, OMe<sup>7</sup>), 6.42-6.64 (3H, m,  $3\times$ Ar-CH).

$^{13}\text{C}$  NMR (75 MHz,  $\text{CDCl}_3$ )  $\delta$ : 20.7 (ArC-Me<sup>8</sup>), 55.6 (Ar-OMe<sup>7</sup>), 110.5 (ArC<sup>3</sup>H), 116.0 (ArC<sup>6</sup>H), 118.7 (ArC<sup>4</sup>H), 130.5 (ArC<sup>5</sup>Me), 135.9 (ArC<sup>1</sup>NH<sub>2</sub>), 145.3 (ArC<sup>2</sup>-OMe).

### (2-Methoxy-5-methylphenyl)-hydrazine (110)



#### Method 1

2-Methoxy-5-methylaniline (**109**) (1.303 g, 9.5 mmol) in hydrochloric acid (6M, 4 mL) was stirred at 0°C to which a solution of sodium nitrite (0.74 g, 10.07 mmol) in water (2 mL) was added dropwise over a period of 30 mins and the resultant solution left to stir for an additional 30mins at -35 °C. A solution of tin(II) chloride (11.06g, 58.33 mmol) in concentrated hydrochloric acid (12 mL of 32 %) was added to the mixture (2 hrs, 0°C). The resulting mixture was stirred for an additional 1hr. The resulting paste was poured into a solution of aqueous sodium hydroxide (12.54 g, 32ml, 9.8 M, 0°C), filtered to remove any black precipitates and the resulting filtrate extracted with benzene (4 × 50 mL). The combined organic fractions were dried over anhydrous magnesium sulfate, filtered and then concentrated *in vacuo*. The crude material was

purified by column chromatography (1:19 ethyl acetate: petroleum ether (40/60 °C)) to isolate some of the reaction by-products.<sup>230</sup>

Analysis of the crude mixture by NMR, TLC and mass spectrometry detected none of the desired product. Further analysis of these isolated fractions by TLC, mass spectrometry and <sup>1</sup>H NMR revealed a mixture of deaminated material, unidentifiable compounds and confirmed no presence of the desired hydrazine compound.

## Method 2

2-Methoxy-5-methylaniline (**109**) (5.624 g, 41 mmol) was mechanically mixed with concentrated hydrochloric acid (42 mL, 32 %) at 0 °C. To this semi-crystalline paste sodium nitrite (2.83 g, 41 mmol) in water (12 mL) was added whilst stirring vigorously at 0 °C. A cooled solution of tin(II) chloride dihydrate (23.00 g, 0.102mol) in concentrated hydrochloric acid (23 mL, 32 %) was added and a yellow/white precipitate separated which was left to stand for 15hrs. The solid was collected by vacuum filtration, thoroughly pressed and shaken with aqueous sodium hydroxide (38 mL, 25 %) and diethyl ether (50 mL). The organic layer was separated and the aqueous layer extracted with diethyl ether (3 × 50 mL), organic fractions combined, dried over anhydrous magnesium sulfate, filtered and volatiles evaporated *in vacuo* to yield (2-Methoxy-5-methylphenyl)-hydrazine (**110**) as a light brown precipitate (5.732 g, 92 %). The crude product was used without further purification.

Melting Point: 41-43 °C

GCMS (DCM) (EI): 10.61min (single peak), 152 (M<sup>+</sup>), C<sub>8</sub>H<sub>12</sub>N<sub>2</sub>O=152.19 (M<sup>+</sup>)

MS (ES): 153 (MH<sup>+</sup>), C<sub>8</sub>H<sub>12</sub>N<sub>2</sub>O requires 153.20 (MH<sup>+</sup>),

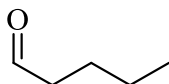
MS (ES): 153.1534 (MH<sup>+</sup>), C<sub>8</sub>H<sub>12</sub>N<sub>2</sub>O requires 153.10224 (MH<sup>+</sup>)

IR (neat): 3392 cm<sup>-1</sup> (NH)

<sup>1</sup>H NMR (300 MHz, CDCl<sub>3</sub>) δ: 2.22 (3H, s, ArC-Me<sup>8</sup>), 3.45 (2H, v. br s, NH<sub>2</sub>), 3.72 (3H, s, OMe<sup>7</sup>), 5.45 (1H, v. br s, NH), 6.42-6.72 (3H, m, 3×Ar-CH).

<sup>13</sup>C NMR (75 MHz, CDCl<sub>3</sub>) δ: 21.2 (ArC-Me<sup>8</sup>), 55.6 (Ar-OMe<sup>7</sup>), 109.7 (ArC<sup>3</sup>H), 111.7 (ArC<sup>6</sup>H), 118.7 (ArC<sup>4</sup>H), 130.6 (ArC<sup>1</sup>), 140.8 (ArC<sup>5</sup>-Me), 144.7 (ArC<sup>2</sup>-OMe).

### Synthesis of Pentanal (**111**)



To a stirred solution of pyridinium chlorochromate (3.233g, 15 mmol, 1.5eq) in dichloromethane (30 mL) was slowly added pentan-1-ol (0.882g, 1.09 mL, 10 mmol, 1eq) at room temperature (25 °C). Stirring continued at 25°C for 12hrs before the mixture was filtered through a silica gel pad. The residue was washed through the pad of silica with portions of diethyl ether (50 mL) until no more material was eluted. The solvent from the combined organic fractions was then removed *in vacuo* to yield crude pentanal (**111**).<sup>231</sup>

Attempts to purify the crude material by column chromatography (20: 80 ethyl acetate: petroleum ether (40/60 °C)) proved to be difficult and unsuccessful. All

characterisation was therefore on the crude material containing some unreacted starting material (approx 10-15 %)

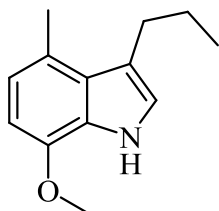
GCMS (EI): peak at 2.27mins, 86 ( $M^+$ ),  $C_5H_{10}O$  requires 86.13

IR (neat):  $1727\text{ cm}^{-1}$  (C=O),

$^1\text{H}$  NMR (300 MHz,  $\text{CDCl}_3$ )  $\delta$ : 0.85 (3H, t,  $\text{OCHCH}_2\text{CH}_2\text{CH}_2\text{CH}_3$ ,  $J_A=7.4\text{Hz}$ ), 1.29 (2H, s,  $\text{OCHCH}_2\text{CH}_2\text{CH}_2\text{CH}_3$ ), 1.55 (2H, p,  $\text{OCHCH}_2\text{CH}_2\text{CH}_2\text{CH}_3$ ,  $J_A=7.4\text{Hz}$ ), 2.35 (2H, td,  $\text{OCHCH}_2\text{CH}_2\text{CH}_2\text{CH}_3$ ,  $J_A=7.4\text{Hz}$   $J_B=1.9\text{Hz}$ ), 9.69 (1H, t,  $\text{OCHCH}_2\text{CH}_2\text{CH}_2\text{CH}_3$ ,  $J_A=1.9\text{Hz}$ ).

$^{13}\text{C}$  NMR (75 MHz,  $\text{CDCl}_3$ )  $\delta$ : 14.2 ( $\text{CH}_3\text{CH}_2\text{CH}_2\text{CH}_2\text{CHO}$ ), 22.3 ( $\text{CH}_3\text{CH}_2\text{CH}_2\text{CH}_2\text{CHO}$ ), 24.5 ( $\text{CH}_3\text{CH}_2\text{CH}_2\text{CH}_2\text{CHO}$ ), 43.9 ( $\text{CH}_3\text{CH}_2\text{CH}_2\text{CH}_2\text{CHO}$ ), 203.1 ( $\text{CH}_3\text{CH}_2\text{CH}_2\text{CH}_2\text{CHO}$ ).

### 7-Methoxy-4-methyl-3-propyl-1H-indole (112)



## Method 1

Ethanol was added to calcium hydride and stirred for 12hrs. The suspension was distilled through a Vigreux column at 80°C and collected in a quick fit conical flask containing 4Å molecular sieves.

The (2-methoxy-5-methylphenyl)-hydrazine (**110**) (4.656 g, 30.6 mmol) was dissolved in the anhydrous absolute ethanol (50 mL). Pentanal (**111**) (3.252 g, 4.014 mL, 30.6 mmol) was added to this solution, followed by sulfuric acid (0.9 mL, 1.656 g, 16.875 mmol) and the resultant mixture refluxed at 85 °C for 18 hrs. The mixture was cooled and quenched with saturated sodium hydrogen carbonate (300 mL) and extracted with diethyl ether (3 × 300 mL). The organic fractions were combined, dried over anhydrous magnesium sulfate, filtered and the volatiles evaporated *in vacuo*. The crude product was purified by column chromatography (1:39 ethyl acetate: petroleum ether (40/60 °C)). After the volatiles were removed *in vacuo*, the semi-purified material was recrystallised (petroleum ether (80/100)) yielding 7-methoxy-4-methyl-3-propyl-1H-indole (**112**) as off-white needle-like crystals (0.986g, 16 %).

## Method 2

A mixture of the (2-methoxy-5-methylphenyl)-hydrazine (**110**) (0.609g, 4 mmol) with pentanal (**111**) (0.345g, 0.595 mL, 4 mmol) and rhodium(III) chloride trihydrate (0.002g, 7.59µmol, approx 0.002eq) in ethanol (20 mL) was stirred under nitrogen at 180°C for 4hrs using a sealed metal reaction chamber. The volatiles were removed *in vacuo* and the remaining products purified by flash column chromatography on silica gel (1:39 ethyl acetate: petroleum ether (40/60 °C) (fractions 1-60) increasing to 1:19 (fractions 61-120) 1:9 (fractions 121-180)). Fractions 36 to 50 were combined and the volatiles removed *in vacuo*, leaving dark red crystals and an oil. This mixture

was recrystallised from petroleum ether (80/100) yielding 7-methoxy-4-methyl-3-propyl-1H-indole (**112**) as off-white needle-like crystals (0.236g, 29 %).

Melting Point: 68-69 °C

GCMS (DCM) (EI): 14.93 min (single peak), 203 ( $M^+$ ),  $C_{13}H_{17}NO$  requires 203.13 ( $M^+$ )

MS (ES): 204 ( $MH^+$ ), 202 ( $M^+$ ),  $C_{13}H_{17}NO$  requires 204.14 ( $MH^+$ ), 202.13 ( $M^+$ )

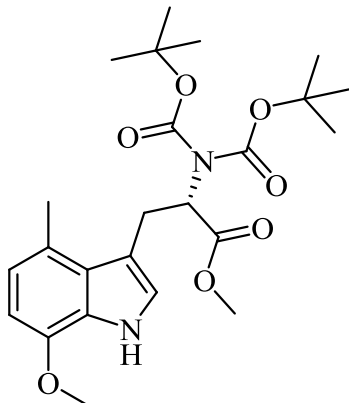
MS (ES): 204.1383 ( $MH^+$ ),  $C_{13}H_{17}NO$  requires 204.1389 ( $MH^+$ ),

IR (neat): 3429  $cm^{-1}$  (N-H indole)

$^1H$  NMR (300 MHz,  $CDCl_3$ )  $\delta$ : 1.04 (3H, t, ArC-CH<sub>2</sub>CH<sub>2</sub>CH<sub>3</sub>,  $J_A=7.4$ Hz), 1.72 (2H, sex, ArC-CH<sub>2</sub>CH<sub>2</sub>CH<sub>3</sub>,  $J_A=7.4$ Hz), 2.65 (3H, app d, Ar-Me,  $J_A=0.8$ Hz), 2.88 (2H, td, ArC-CH<sub>2</sub>CH<sub>2</sub>CH<sub>3</sub>,  $J_A=7.4$ Hz,  $J_B=0.8$ Hz), 3.94 (3H, s, OMe), 6.49-6.76 (2H, m, 2×Ar-CH), 6.91-6.93 (1H, m, indole Ar-CH), 8.13 (1H, br s, NH).

$^{13}C$  NMR (75 MHz,  $CDCl_3$ )  $\delta$ : 14.1 (ArC-CH<sub>2</sub>CH<sub>2</sub>CH<sub>3</sub>), 19.6 (Ar-Me), 24.6 (ArC-CH<sub>2</sub>CH<sub>2</sub>CH<sub>3</sub>), 29.1 (ArC-CH<sub>2</sub>CH<sub>2</sub>CH<sub>3</sub>), 55.3 (OMe), 101.4 (Ar-CH-COMe), 118.4 (Ar-NHCH), 120.2 (Ar-CH-CMe), 121.0 (Indole Ar-CH), 123.4 (Ar-C-Me), 127.0 (Ar-C), 127.2 (Ar-C), 144.5 (Ar-C-OMe).

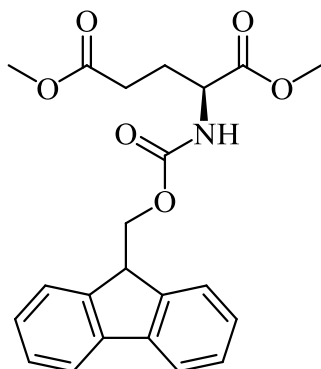
**Methyl-2-(bis-(*tert*-butoxycarbonyl)-amino)-3-(7-methoxy-4-methyl-1H-indol-3-yl)-propanoate (113)**



A mixture of (2-methoxy-5-methylphenyl)-hydrazine (**110**) (0.529 g, 4 mmol), methyl 2-(bis(*tert*-butoxycarbonyl)amino)-5-oxopentanoate (**98**) (1.217 g, 3.47 mmol) and rhodium(III) chloride trihydrate (0.002 g, 7.59  $\mu\text{mol}$ , approx 0.002 eq) in ethanol (30 mL) was stirred under nitrogen at 180 °C for 4 hrs using a sealed metal reaction chamber. Volatiles were removed *in vacuo* and the remaining products purified by flash column chromatography on silica gel (2:8 ethyl acetate: petroleum ether (40/60 °C)).

Analysis of the crude mixture by NMR, TLC and mass spectrometry detected none of the desired product. Further analysis of the isolated fractions by TLC, mass spectrometry and  $^1\text{H}$  NMR revealed a mixture of unidentifiable compounds and confirmed no presence of the desired compound, however no starting materials remained.

A large number of further attempts following this procedure were made, each time altering one variable (e.g. temperature, time, solvent); however no further attempts at this procedure were successful.

**Dimethyl-2-(((9H-fluoren-9-yl)methoxy)-carbonylamino)-pentanedioate (114)****Method 1**

*N*-(Fluoren-9-ylmethoxycarbonyl)succinimide (0.603 g, 1.79 mmol) in 1,4-dioxane (5 mL) was added to a stirred solution of the hydrochloric acid salt of dimethyl-2-aminopentanedioate (0.474 g, 2.24 mmol) in sodium hydrogen bicarbonate (4.5 cm<sup>3</sup>, 9 % aqueous) cooled to 0 °C. The reaction mixture was allowed to warm to room temperature and left to stir overnight (14 hrs) before water (10 mL) was added and the aqueous solution washed with ethyl acetate (2 × 25 mL). The remaining aqueous phase was acidified by addition of concentrated hydrochloric acid (32 %) and extracted into diethyl ether (25 mL). The combined organic phases were dried over anhydrous anhydrous magnesium sulfate and concentrated *in vacuo* to yield crude as a colourless oil (0.591 g, 83 %).

Although the crude NMR and mass spectrometry showed positive results, Method 2 (below), which was being run in parallel, provided better yields and results.

**Method 2**

To a stirred suspension of *N*-(fluoren-9-ylmethoxycarbonyl)succinimide protected L-glutamic acid (**81**) (1.847 g, 5 mmol) in anhydrous methanol (20 mL), at 0

°C, was slowly added iodotrimethylsilane (2.8 mL, 22 mmol, 4.4 equiv). The ice bath was removed after the addition was complete and the reaction stirred overnight (12 hrs) where TLC analysis showed complete conversion. The combined organic layers were evaporated *in vacuo* and the resulting crude material was purified by flash column chromatography on silica gel (100 % ethyl acetate) to yield dimethyl-2-(((9H-fluoren-9-yl)methoxy)-carbonylamino)-pentanedioate (**114**) as a white solid (1.776 g, 89 %)

Melting point: 141-143 °C

MS (ES): 398 (MH<sup>+</sup>) and 420 (MNa<sup>+</sup>), C<sub>22</sub>H<sub>23</sub>NO<sub>6</sub> requires 398.42 (MH<sup>+</sup>) and 420 (MNa<sup>+</sup>)

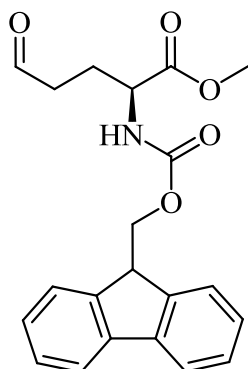
IR (neat): 1683 cm<sup>-1</sup> and 1728 cm<sup>-1</sup> (C=O), 3317 cm<sup>-1</sup> (N-H)

<sup>1</sup>H NMR (300MHz, CDCl<sub>3</sub>) δ: 1.85-2.00 (1H, m, CH<sub>2</sub>CH<sup>1</sup>H<sup>2</sup>CHNH<sub>2</sub>), 2.09-2.23 (1H, m, CH<sub>2</sub>CH<sup>1</sup>H<sup>2</sup>CHNH<sub>2</sub>), 2.25-2.44 (2H, m, CH<sub>2</sub>CH<sup>1</sup>H<sup>2</sup>CHNH<sub>2</sub>), 3.59 (MeOOCCH<sub>2</sub>CH<sup>1</sup>H<sup>2</sup>), 3.68 (NHCHCOOMe), 4.14 (1H, t, Fmoc, CH<sub>2</sub>CH-Ar J<sub>A</sub>=6.9Hz), 4.27-4.48 (3H, m, CH<sub>2</sub>CH-Ar and NHCHCOOMe), 5.41 (1H, d, CHNH<sup>H</sup>Fmoc, J<sub>A</sub> = 8.1Hz), 7.17-7.71 (8H, m, Ar-H).

<sup>13</sup>C NMR (75 MHz, CDCl<sub>3</sub>) δ: 27.6 (CH<sub>2</sub>CH<sup>1</sup>H<sup>2</sup>CHNH<sub>2</sub>), 30.0 (CH<sub>2</sub>CH<sup>1</sup>H<sup>2</sup>CHNH<sub>2</sub>), 47.2 (Fmoc, CH<sub>2</sub>CH-Ar), 51.8(OMe), 52.6(OMe), 53.3 (CH<sub>2</sub>CH<sup>1</sup>H<sup>2</sup>CHNH<sub>2</sub>), 67.1 (Fmoc, CH<sub>2</sub>CH-Ar), 120.0 (Fmoc, ArCH), 125.1 (Fmoc, ArCH), 127.1 (Fmoc, ArCH), 127.3 (Fmoc, ArCH), 141.3 (Fmoc, Ar-C-CH), 143.8 (Fmoc, Ar-C-CH), 155.9 (Fmoc, NH-CO-OCH<sub>2</sub>), 172.3 (NHCHCOOH), 173.1 (NHCHCH<sub>2</sub>CH<sub>2</sub>COOH).

This method was repeated but with purification by recrystallisation from diethyl ether; this gave lower yields than isolation by column chromatography.

### Methyl-2-(((9H-fluoren-9-yl)methoxy)carbonylamino)-5-oxopentanoate (116)

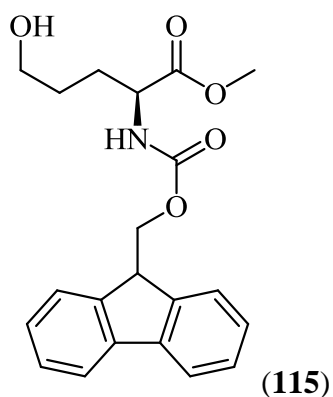


#### Method 1

To a stirred solution of dimethyl-2-(((9H-fluoren-9-yl)methoxy)-carbonylamino)-pentanedioate (**114**) (0.519 g, 1.35 mmol) in anhydrous tetrahydrofuran (13 mL, 0.1 M) was added dropwise diisobutylaluminium hydride (1.5 mL, 1.0 M in hexane, 1.5 mmol, 1.1 equiv.) at -78 °C. The reaction was stirred for 5mins before quenching with water (0.2 mL,  $\approx$  7 equiv.), stirring for a further 30mins, anhydrous over anhydrous magnesium sulfate, filtering through a pad of Celite and removing the solvent *in vacuo*. The crude product was purified by flash column chromatography on silica gel (1:1diethyl ether: hexane).<sup>163</sup>

Analysis of the crude mixture by NMR, TLC and mass spectrometry detected none of the desired product. Further analysis of the isolated fractions by TLC, mass spectrometry and <sup>1</sup>H NMR spectroscopy revealed a mixture of starting material and unidentifiable products, but none of the desired aldehyde product.

A range of reaction conditions were attempted following a similar method, however all yielded similar results. Warming the reaction resulted in both esters being attacked, however leaving the reaction for an increased amount time (66 hrs) at  $-78\text{ }^{\circ}\text{C}$  resulted in selective reduction of the  $\gamma$  ester to the alcohol by-product (**115**) (shown below with  $^1\text{H}$ NMR data)



$^1\text{H}$  NMR (300MHz,  $\text{CDCl}_3$ )  $\delta$ : 1.46-2.20 (4H, m,  $\text{CH}_2\text{CH}^1\text{H}^2\text{CHNH}_2$  and  $\text{CH}_2\text{CH}^1\text{H}^2\text{CHNH}_2$ ), 2.40 (1H, br s,  $\text{OHCH}_2\text{CH}_2\text{CH}^1\text{H}^2$ ), 3.64 (2H, t,  $\text{OHCH}_2\text{CH}_2\text{CH}^1\text{H}^2$ ,  $J_A = 6.0\text{Hz}$ ), 3.73 (3H, s,  $\text{NHCHCOOMe}$ ), 4.21 (1H, t, Fmoc,  $\text{CH}_2\text{CH-Ar}$   $J_A = 6.9\text{Hz}$ ), 4.35-4.53 (3H, m,  $\text{CH}_2\text{CH-Ar}$  and  $\text{NHCHCOOMe}$ ), 5.76 (1H, d,  $\text{CHNH Fmoc}$ ,  $J_A = 8.2\text{Hz}$ ), 7.26-7.77 (8H, m, Ar-H).

MS (ES): 370 ( $\text{MH}^+$ ) and 392 ( $\text{MNa}^+$ ),  $\text{C}_{22}\text{H}_{23}\text{NO}_6$  requires 370.41 ( $\text{MH}^+$ ) and 392 ( $\text{MNa}^+$ )

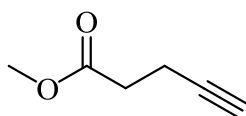
## Method 2

To a cooled ( $0\text{ }^{\circ}\text{C}$ ) and stirred solution of pyridinium chlorochromate (0.1 g, 0.464 mmol, 1.72 eq) in dichloromethane (30 mL) was slowly added methyl 2-(((9H-fluoren-9-yl)methoxy)carbonylamino)-5-hydroxypentanoate (**115**) (0.100 g, 0.27 mmol,

1 eq). The solution was stirred for a further 4 hrs at room temperature (25 °C) before being suction filtered through a silica gel pad; the residue and filter pad were washed with portions of diethyl ether (6 × 50 mL). The combined organic phases were reduced *in vacuo*. The crude was purified using column chromatography (1:1 diethyl ether: petroleum ether (40/60 °C)).<sup>231</sup>

Analysis of the crude mixture by NMR, TLC and mass spectrometry detected none of the desired product.

### Methylpent-4-ynoate (122)



#### Method 1

4-Pentynoic acid (**121**) (100 mg, 1.02 mmol, 1eq) was dissolved in anhydrous methanol (5 mL) and anhydrous sulfuric acid (0.15 g) and the solution heated to reflux for 12hrs. This was extracted with dichloromethane (5 mL) and the combined organic extract was washed with saturated sodium hydrogen carbonate solution (10 mL) before the organic phase was concentrated by rotary evaporator and the residue purified by column chromatography (25:75 ethyl acetate: petroleum ether (40/60 °C)).<sup>232</sup>

Analysis of the crude mixture by NMR, TLC and mass spectrometry detected none of the desired product.

## Method 2

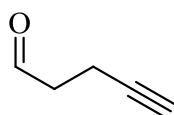
4-Pentynoic acid (**121**) (100 mg, 1.02 mmol, 1 eq) was dissolved in anhydrous methanol (1 mL) and anhydrous acetonitrile (9 mL). The solution was cooled to 0°C and trimethylsilyldiazomethane (1.2 mL, 2.04 mmol, 2 eq) added dropwise over 5 mins before stirring for 2 hrs and allowing to warm to room temperature (25 °C). All solvent was then removed by rotary evaporator and the residue purified by column chromatography (20:80 ethyl acetate: petroleum ether (40/60 °C)) to yield methylpent-4-ynoate (**122**) as a colourless liquid (0.044 g, 39 %).<sup>233</sup>

MS (ES): 113.0601 (MH<sup>+</sup>), C<sub>6</sub>H<sub>8</sub>O<sub>2</sub> requires 113.1344 (MH<sup>+</sup>)

<sup>1</sup>H NMR (300MHz, CDCl<sub>3</sub>) δ: 1.91 (1H, t, MeOOCCH<sub>2</sub>CH<sub>2</sub>CCH, *J*<sub>A</sub> = 2.5Hz), 2.40-2.54 (4H, m, MeOOCCH<sub>2</sub>CH<sub>2</sub>CCH), 3.64 (2H, m, MeOOCCH<sub>2</sub>CH<sub>2</sub>CCH).

<sup>13</sup>C NMR (75 MHz, CDCl<sub>3</sub>) δ: 14.3 (MeOOCCH<sub>2</sub>CH<sub>2</sub>CCH), 33.1 (MeOOCCH<sub>2</sub>CH<sub>2</sub>CCH), 51.8 (MeOOCCH<sub>2</sub>CH<sub>2</sub>CCH), 69.0 (MeOOCCH<sub>2</sub>CH<sub>2</sub>CCH), 82.4 (MeOOCCH<sub>2</sub>CH<sub>2</sub>CCH), 172.2 (MeOOCCH<sub>2</sub>CH<sub>2</sub>CCH).

## Pent-4-ynal (**123**)



## Method 1

To a stirred solution of methylpent-4-ynoate (**122**) (0.3 g, 2.68 mmol) in anhydrous diethyl ether (20 mL) was added dropwise diisobutylaluminium hydride (3 mL, 1.0 M in hexane, 3 mmol, 1.1 equiv.) at  $-78^{\circ}\text{C}$  and the reaction stirred for 5mins before quenching with water (0.8 mL,  $\approx 7$  equiv.). The mixture was stirred for a further 30mins, dried over anhydrous magnesium sulfate and filtered through a pad of Celite before the solvent was evaporated *in vacuo* to yield a crude liquid.

Analysis of the crude mixture by NMR, TLC and mass spectrometry showed that the desired product had been formed; however the reaction was not clean and overall was very low yielding ( $> 1\%$ ).

## Method 2

To a cooled and stirred solution of pyridinium chlorochromate (3.233 g, 15 mmol, 1.5eq) in dichloromethane (30 mL) was slowly added pent-4-yn-1-ol (**120**) (0.841 g, 0.930 mL, 10 mmol, 1eq). The solution was stirred at room temperature ( $25^{\circ}\text{C}$ ) for a further 4 hrs. The mixture was suction filtered through a silica gel pad before both the residue and the silica pad were washed with portions of diethyl ether ( $6 \times 50$  mL). The solvent from the combined organic phases removed *in vacuo* at room temperature ( $25^{\circ}\text{C}$ ) to yield crude pent-4-ynal (**123**) (98 %).

Steps to purify the crude material failed due to its volatility and similar boiling point to starting material, therefore all NMRs and IRs were carried out on crude material.

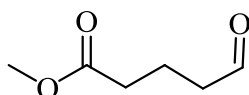
G CMS (EI): peak at 8.47mins, 82 ( $\text{M}^+$ ),  $\text{C}_5\text{H}_6\text{O}$  requires 82.10

IR (neat): 1735  $\text{cm}^{-1}$  (C=O), 2126  $\text{cm}^{-1}$  (C $\equiv$ C)

$^1\text{H}$  NMR (300MHz,  $\text{CDCl}_3$ )  $\delta$ : 1.93 (1H, t, OCHCH $_2$ CH $_2$ CCH,  $J_A=2.7\text{Hz}$ ), 2.45 (2H, tdd, OCHCH $_2$ CH $_2$ CCH,  $J_A=7.1\text{Hz}$ ,  $J_B=2.7\text{Hz}$ ,  $J_C=1\text{Hz}$ ), 2.64 (2H, app tt, OCHCH $_2$ CH $_2$ CCH,  $J_A=7.1\text{Hz}$ ,  $J_B=1\text{Hz}$ ), 9.74 (1H, t, OCHCH $_2$ CH $_2$ CCH)

$^{13}\text{C}$  NMR (75 MHz,  $\text{CDCl}_3$ )  $\delta$ : 11.6 (OCHCH $_2$ CH $_2$ CCH), 42.3 (OCHCH $_2$ CH $_2$ CCH), 69.3 (OCHCH $_2$ CH $_2$ CCH), 82.3 (OCHCH $_2$ CH $_2$ CCH), 200.2 (OCHCH $_2$ CH $_2$ CCH).

### Methyl-5-oxopentanoate (**126**)



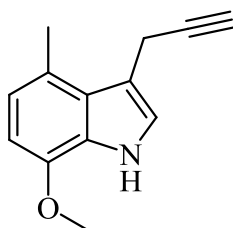
Concentrated sulfuric acid (3 drops, 98 %) was added to a stirred solution of 5-methyldihydrofuran-2(3H)-one (**124**) (a.k.a.  $\gamma$ -valerolactone) (3.0036 g, 2.862 mL, 30 mmol) in freshly distilled methanol (60 mL), the mixture was heated to reflux until TLC analysis showed no starting material remained. The mixture was cooled in an ice bath, sodium hydrogen carbonate (0.5 g) added and the mixture stirred for a further 10mins before the excess solid was removed by filtration. The solvent was removed *in vacuo* (25°C) to yield the reaction intermediate methyl-5-hydroxypentanoate (**125**).<sup>209</sup> The following oxidation step was carried out immediately on this crude intermediate.

Pyridinium chlorochromate (9.699 g, 45 mmol, 1.5 eq) in anhydrous dichloromethane (36 mL) was stirred and a solution of methyl-5-hydroxypentanoate (**125**) (3.996 g, 30 mmol, 1eq) in anhydrous dichloromethane (24 mL) added in one

portion and stirred for 2hrs (25 °C) before anhydrous diethyl ether (60 mL) was added. The resultant residue was triturated with anhydrous diethyl ether (3 × 15 mL) and the resultant organic fractions were combined, filtered through a small pad of silica and the solvent removed *in vacuo*. The remaining oil was vacuum distilled (c.a. 10mmHg) to give a colourless liquid (boiling point range 90-98°C).<sup>209</sup>

Analysis by NMR, TLC and mass spectrometry, showed none of the desired product in this distillate.

### 7-Methoxy-4-methyl-3-(prop-2-ynyl)-1H-indole (127)



Ethanol was added to calcium hydride and stirred for 12 hrs. The suspension was distilled at 80 °C through a Vigreux column and ethanol collected in a quick fit conical flask containing 4Å molecular sieves.

The (2-methoxy-5-methylphenyl)-hydrazine (**110**) (3.104 g, 20.4 mmol) was dissolved in the anhydrous ethanol (50 mL) and pent-4-ynal (**123**) (1.672 g, 20.4 mmol) added, followed by sulfuric acid (98 %, 0.6 mL, 7.5 mmol, 0.736 g). The resultant mixture which was heated to reflux (85 °C) for 18 hrs, was cooled, quenched with saturated sodium hydrogen carbonate (200 mL) and extracted with diethyl ether (3 × 200 mL). The organic fractions were combined, dried over anhydrous magnesium sulfate, filtered and the volatiles evaporated *in vacuo*. The crude product was purified by column chromatography (1:1 dichloromethane: petroleum spirit (40/60 °C)) followed

by a recrystallisation from petroleum ether (80/100) to yield 7-methoxy-4-methyl-3-(prop-2-ynyl)-1H-indole (**127**) as pale red needle-like crystals (0.451g, 11 %).

Melting Point: 87-88 °C

GCMS (DCM) (EI): 23.35 min (single peak), 199 ( $M^+$ ),  $C_{13}H_{13}NO$  requires 199.10 ( $M^+$ )

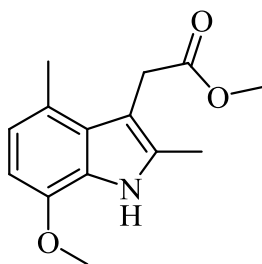
MS (ES): 200 ( $MH^+$ ), 198 ( $M^+$ ),  $C_{13}H_{13}NO$  requires 200.10 ( $MH^+$ ), 198.10 ( $M^+$ )

MS (ES): 200.1074 ( $MH^+$ ),  $C_{13}H_{13}NO$  requires 200.1076 ( $MH^+$ )

IR (neat): 3301  $cm^{-1}$  (C-H alkyne), 3397  $cm^{-1}$  (N-H indole), 2119  $cm^{-1}$  (C≡C)

$^1H$  NMR (300 MHz,  $CDCl_3$ )  $\delta$ : 2.18 (1H, t, ArC-CH<sub>2</sub>CCH,  $J_A=2.7Hz$ ), 2.66 (3H, app s, ArC-Me), 3.88 (2H, dd, ArC-CH<sub>2</sub>CCH,  $J_A=2.7Hz$ ,  $J_B=1.0Hz$ ), 3.93 (3H, s, OMe), 6.49-6.76 (2H, m, 2×Ar-CH), 7.16-7.19 (1H, m, indole Ar-CH), 8.20 (1H, br s, NH).

$^{13}C$  NMR (75 MHz,  $CDCl_3$ )  $\delta$ : 17.2 (ArC-CH<sub>2</sub>CCH), 19.4 (Ar-Me), 55.4 (OMe), 69.5 (ArC-CH<sub>2</sub>CCH), 83.2 (ArC-CH<sub>2</sub>CCH), 101.8 (Ar-CH-COMe), 112.4 (Ar-NHCHC), 120.6 (Ar-CH-CMe), 122.0 (Indole Ar-CH), 122.9 (Ar-C-Me), 126.3 (Ar-C), 127.5 (Ar-C), 144.6 (Ar-C-OMe).

**Methyl-2-(7-methoxy-4-methyl-1H-indol-3-yl)-acetate (129)**

Ethanol was added to calcium hydride and stirred for 12hrs. The suspension was distilled through a Vigreux column at 80°C and collected in a quick fit conical flask containing 4Å molecular sieves.

The (2-methoxy-5-methylphenyl)-hydrazine (**110**) (0.776 g, 5.1 mmol) was dissolved in the anhydrous absolute ethanol (10 mL) and methyl levulinate (0.664 g, 0.632 mL, 5.1 mmol) added, followed by concentrated sulfuric acid (98 %, 0.2 mL, 3.75 mmol, 0.368 g) and the whole refluxed at 85°C for 18hrs. The mixture was cooled, quenched with saturated sodium hydrogen carbonate (50 mL) and extracted with diethyl ether (3 × 50 mL). The organic fractions were combined, dried over anhydrous magnesium sulfate, filtered and volatiles evaporated *in vacuo*. The crude product was purified by column chromatography (1:4 dichloromethane: petroleum ether (40/60 °C)) before being recrystallised (petroleum ether 80/100) to yield methyl-2-(7-methoxy-4-methyl-1H-indol-3-yl)-acetate (**129**) as off white needle-like crystals (0.189g, 15 %).

Melting Point: 145-146 °C

GCMS (DCM) (EI): 27.88min (single peak), 247 (M<sup>+</sup>), C<sub>14</sub>H<sub>17</sub>NO<sub>3</sub> requires 247.29 (M<sup>+</sup>)

MS (ES): 248 (MH<sup>+</sup>), 246 (M<sup>+</sup>), C<sub>14</sub>H<sub>17</sub>NO<sub>3</sub> requires 248.29 (MH<sup>+</sup>), 246.29 (M<sup>+</sup>)

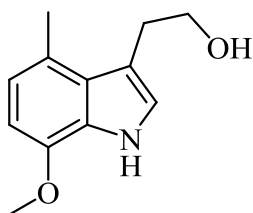
MS (ES): 248.1281 (MH<sup>+</sup>), C<sub>14</sub>H<sub>17</sub>NO<sub>3</sub> requires 248.1287 (MH<sup>+</sup>)

IR (neat): 1722 cm<sup>-1</sup> (C=O ester), 3373 cm<sup>-1</sup> (N-H indole)

<sup>1</sup>H NMR (300 MHz, CDCl<sub>3</sub>) δ: 2.40 (3H, s, Indole ArC-Me), 2.60 (3H, app d, ArC-Me), 3.68 (3H, s, ArCCH<sub>2</sub>COOMe), 3.84 (2H, s, ArCCH<sub>2</sub>COOMe), 3.91 (3H, s, OMe), 6.44-6.73 (2H, m, 2×Ar-CH), 8.09 (1H, br s, NH).

<sup>13</sup>C NMR (75 MHz, CDCl<sub>3</sub>) δ: 11.7 (Indole ArC-Me), 19.3 (Ar-Me), 31.3 (ArCCH<sub>2</sub>COOMe), 51.9 (ArCCH<sub>2</sub>COOMe), 55.4 (ArC-OMe), 101.1 (Ar-CH-COMe), 105.5 (ArC-CH<sub>2</sub>COOMe), 120.9 (Ar-CH-CMe), 122.0 (Ar-C-Me), 127.7 (2×Ar-C), 132.4 (Indole Ar-C-Me), 144.0 (Ar-C-OMe), 173.0 (ArCCH<sub>2</sub>COOMe).

### 2-(7-Methoxy-2,4-dimethyl-1H-indol-3-yl)-ethanol (130)



In a anhydrous two-neck round bottom flask under nitrogen equipped with a water condenser, a suspension of lithium aluminium hydride (0.048 g, 1.212 mmol, 1.5 eq) in anhydrous tetrahydrofuran (40 mL) was made. A solution of methyl-2-(7-

methoxy-4-methyl-1H-indol-3-yl)-acetate (**129**) (0.2 g, 0.808 mmoles, 1 equiv.) in anhydrous tetrahydrofuran (40 mL) was added dropwise via a pressure equalising dropping funnel and the reaction mixture stirred (25 °C) until TLC showed consumption of starting materials. Water (4 mL) was added slowly via the condenser and when effervescence had stopped, aqueous sodium hydroxide solution (3 M, 4 mL) was added via the condenser followed by a further portion of water (12 mL). The mixture was filtered through Celite and the cake was washed with tetrahydrofuran (3 × 100 mL); the combined organic fractions were removed *in vacuo*. Purification of the colourless oil by chromatography column (49:1 dichloromethane: methanol) yielded 2-(7-methoxy-2,4-dimethyl-1H-indol-3-yl)-ethanol (**130**) as a colourless oil (0.161 g, 91 %).

GCMS (DCM) (EI): 17.39 min, 219 (M<sup>+</sup>), C<sub>13</sub>H<sub>17</sub>NO<sub>2</sub> requires 219.1259 (M<sup>+</sup>)

MS (ES): 220.1333 (MH<sup>+</sup>), C<sub>13</sub>H<sub>17</sub>NO<sub>2</sub> requires 220.1338 (MH<sup>+</sup>)

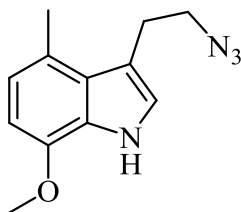
IR (neat): 3380 cm<sup>-1</sup> (OH)

<sup>1</sup>H NMR (300 MHz, CDCl<sub>3</sub>) δ: 1.64 (1H, br s, OH), 2.28 (3H, s, Indole Ar-Me), 2.52 (3H, s, Ar-Me), 2.99 (2H, t, ArC-CH<sub>2</sub>CH<sub>2</sub>OH, *J*<sub>A</sub>=6.7Hz), 3.71 (2H, t, ArC-CH<sub>2</sub>CH<sub>2</sub>OH, *J*<sub>A</sub>=6.7Hz), 3.82 (3H, s, OMe), 6.36-6.65 (2H, m, 2×Ar-CH), 8.09 (1H, br s, NH).

<sup>13</sup>C NMR (75 MHz, CDCl<sub>3</sub>) δ: 11.7 (Indole Ar-Me), 19.7 (Ar-Me), 28.6 (ArC-CH<sub>2</sub>CH<sub>2</sub>OH), 55.4 (OMe), 64.2 (ArC-CH<sub>2</sub>CH<sub>2</sub>OH), 101.1 (Ar-CH), 108.5 (ArC-

CH<sub>2</sub>CH<sub>2</sub>OH), 120.8 (Ar-CH), 122.2 (Ar-C-Me), 125.8 (Ar-C), 128.0 (Ar-C), 132.2 (Indole Ar-C), 144.05 (Ar-C-OMe).

### 3-(2-Azidoethyl)-7-methoxy-2,4-dimethyl-1H-indole (131)



#### Method 1

2-(7-methoxy-2,4-dimethyl-1H-indol-3-yl)-ethanol (**130**) (40 mg, 0.195 mmol), tetrahydrofuran (5 mL) and methanesulfonyl chloride (46 mg, 31  $\mu$ L, 0.402 mmol, 2.1 eq) were placed in a round bottomed flask and cooled (0 °C). Triethylamine (44 mg, 63.3  $\mu$ L, 0.430 mmol) was added dropwise over 30 mins before the reaction was allowed to warm slowly (25 °C) and then stirred overnight (14 hrs). The resulting mixture was diluted with water (5 mL) and sodium hydrogen carbonate (12.5 mg, 0.149 mmol) before sodium azide (31mg, 0.477 mmol) was added and the biphasic reaction mixture was heated to distil off the tetrahydrofuran before refluxing overnight (14 hrs). After cooling the mixture was extracted with chloroform (5  $\times$  5 mL) and the combined organic fractions were dried over magnesium sulphate, vacuum filtered and volatiles removed *in vacuo* yielding a dark brown oil (14 mg, 31 %).<sup>210</sup>

Analysis of the crude mixture by NMR, TLC and mass spectrometry detected none of the desired product. Further analysis of the isolated fractions by TLC, mass spectrometry and <sup>1</sup>H NMR revealed a mixture of unidentifiable compounds and confirmed no presence of the desired azide compound.

## Method 2

2-(7-methoxy-2,4-dimethyl-1H-indol-3-yl)-ethanol (**130**) (76.8 mg, 0.350 mmol), tetrahydrofuran (10 mL) and methanesulfonyl chloride (92 mg, 62  $\mu$ l, 0.804 mmol 2.3 eq) were placed in a round bottomed flask, cooled (0 °C) and stirred. Triethylamine (88 mg, 126.6  $\mu$ l, 0.860 mol) was added dropwise over 30mins before the reaction was allowed to warm slowly to room temperature (25 °C), stirring throughout. The reaction was monitored by TLC until no starting material remained. The mixture was diluted with water (10 mL) and the resultant clear solution evaporated to anhydrousness before dimethylformamide (10 mL) and sodium hydrogen carbonate (25 mg, 0.298 mmol) were added. Then sodium azide (62 mg, 0.954 mmol) was added and the reaction mixture was heated to 100 °C and left stirring at this temperature overnight (12 hrs). After cooling, water (10 mL) was added and the mixture was extracted with chloroform (5  $\times$  10 mL). The combined organic fractions were dried over anhydrous magnesium sulfate, vacuum filtered and volatiles removed *in vacuo* yielding a pale brown oil. This was purified by flash column chromatography on silica gel (100 % dichloromethane) to yield 3-(2-Azidoethyl)-7-methoxy-2,4-dimethyl-1H-indole (**131**) as a colourless oil (47 mg, 55 %).<sup>210</sup>

GCMS (DCM) (EI): 28.51 min (single peak), 244 ( $M^+$ ),  $C_{13}H_{16}N_4O$  requires 244.29 ( $M^+$ )

MS (ES): 243 ( $M^-$ ),  $C_{13}H_{15}N_4O$  requires 243.29( $M^-$ )

MS (ES): 245.1400 (MH<sup>+</sup>), 243.1248 (M<sup>+</sup>), C<sub>13</sub>H<sub>16</sub>N<sub>4</sub>O requires 245.3002(MH<sup>+</sup>),  
C<sub>13</sub>H<sub>15</sub>N<sub>4</sub>O=243.2844 (M<sup>+</sup>)

IR (neat): 2095 cm<sup>-1</sup> (Azide -N<sub>3</sub>), 3381 cm<sup>-1</sup> (Indole NH)

<sup>1</sup>H NMR (300 MHz, CDCl<sub>3</sub>) δ: 2.31 (3H, s, indole ArMe), 2.52 (3H, s, Ar-Me), 3.02 (2H, t, CCH<sub>2</sub>CH<sub>2</sub>N<sub>3</sub>, J<sub>A</sub>=7.6Hz), 3.34 (2H, t, CCH<sub>2</sub>CH<sub>2</sub>N<sub>3</sub>, J<sub>A</sub>=7.6Hz), 3.83 (3H, s, OMe), 6.37-6.66 (2H, m, 2×Ar-CH), 8.00 (1H, br s, NH).

<sup>13</sup>C NMR (75 MHz, CDCl<sub>3</sub>) δ: 11.5 (Indole ArMe), 19.5 (Ar-Me), 25.3 (CCH<sub>2</sub>CH<sub>2</sub>N<sub>3</sub>), 53.1 (CCH<sub>2</sub>CH<sub>2</sub>N<sub>3</sub>), 55.4 (OMe), 101.1 (Ar-CH), 108.8 (CCH<sub>2</sub>CH<sub>2</sub>N<sub>3</sub>), 120.9 (Ar-CH), 121.7 (ArC-Me), 125.6 (ArC), 127.5 (ArC), 131.8 (Indole ArC-Me), 144.1 (ArC-OMe).

### 3-(2-Hydroxyethyl)-2,4-dimethyl-1H-indol-7-ol (**132**)



#### Method 1

To 2-(7-methoxy-2,4-dimethyl-1H-indol-3-yl)ethanol (**130**) (40 mg, 182 μmol, 1 eq) in anhydrous toluene (10 mL) was added 1,4,7,10,13,16-hexaoxacyclooctadecane (18-crown-6, 0.0962 g, 364 μmol, 2 eq). The resulting solution was agitated with a lump of potassium metal (≈ 7 mm cube) under nitrogen overnight (≈ 17 hrs). The reaction mixture was transferred to a round bottom flask containing propan-2-ol (1 mL)

by means of a long needle through a rubber septum. The reaction was then separated with hydrochloric acid (1 M, 30 mL) and diethyl ether (2 × 10 mL); the combined organic fractions were dried over anhydrous magnesium sulfate, vacuum filtered and evaporated to dryness *in vacuo*. The crude product was immediately purified by chromatography (chromatatron) (100 % chloroform increasing to 19:1 chloroform: acetonitrile)

Analysis of the crude mixture by NMR, TLC and mass spectrometry detected none of the desired product. Further analysis of the isolated fractions by TLC, mass spectrometry and <sup>1</sup>H NMR revealed a mixture of unidentifiable compounds and confirmed no presence of the desired demethylated compound.

## Method 2

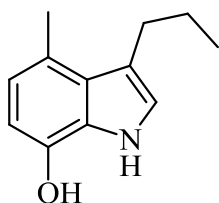
2-(7-Methoxy-2,4-dimethyl-1H-indol-3-yl)ethanol (**130**) (40 mg, 182 μmol, 1 eq) was dissolved in 1-methyl-2-pyrrolidinone (2 mL) and potassium carbonate (0.0104 g, 75 μmol, 0.15 eq) then thiophenol (0.1658 g, 154.6 μl, 1506 μmol, 3 eq) was added. This reaction mixture was then refluxed under nitrogen (200 °C, 18 hrs) before cooling, quenching with hydrochloric acid (1 M, 10 mL) and extracting with diethyl ether (3 × 10 mL). The combined organic fractions were washed with hydrochloric acid (1 M, 10 mL), dried over anhydrous magnesium sulfate, vacuum filtered and the volatiles removed *in vacuo*. The crude product was purified by flash column chromatography on silica gel (98.5: 1.5 dichloromethane: methanol) to yield 3-(2-hydroxyethyl)-2,4-dimethyl-1H-indol-7-ol (**132**) as a colourless oil (36 mg, 96 %).

MS (ES): 206 (MH<sup>+</sup>), C<sub>12</sub>H<sub>15</sub>NO<sub>2</sub> requires 206.25 (MH<sup>+</sup>)

$^1\text{H}$  NMR (300 MHz,  $\text{CDCl}_3$ )  $\delta$ : 2.31 (3H, s, Indole Ar-Me), 2.52 (3H, s, Ar-Me), 3.02 (2H, t, ArC-CH<sub>2</sub>CH<sub>2</sub>OH,  $J_{\text{A}}=6.6\text{Hz}$ ), 3.75 (2H, t, ArC-CH<sub>2</sub>CH<sub>2</sub>OH,  $J_{\text{A}}=6.6\text{Hz}$ ), 6.04 (1H, br s, OH), 6.33-6.56 (2H, m, 2 $\times$ Ar-CH), 8.31 (1H, br s, NH).

$^{13}\text{C}$  NMR (75 MHz,  $\text{CDCl}_3$ )  $\delta$ : 11.8 (Indole Ar-Me), 19.7 (Ar-Me), 28.5 (ArC-CH<sub>2</sub>CH<sub>2</sub>OH), 64.1 (ArC-CH<sub>2</sub>CH<sub>2</sub>OH), 105.7 (Ar-CH), 108.3 (ArC-CH<sub>2</sub>CH<sub>2</sub>OH), 121.0 (Ar-CH), 121.8 (Ar-C-Me), 125.3 (Ar-C), 128.6 (Ar-C), 132.4 (Indole Ar-C), 139.7 (Ar-C-OH).

#### 4-Methyl-3-propyl-1H-indol-7-ol (134)



#### Method 1

7-Methoxy-4-methyl-3-propyl-1H-indole (**112**) (101.7 mg, 500  $\mu\text{mol}$ , 1 eq) was dissolved in acetonitrile (10 mL) and iodotrimethylsilane (0.200 g, 0.142 mL, 1 mmol, 2 eq) and the mixture heated to 85°C for 6hrs under nitrogen before cooling, quenching with saturated sodium thiosulphate (20 mL) and extracting with dichloromethane (3  $\times$  20 mL). The combined organic fractions were washed with saturated sodium thiosulphate (20 mL), then water (20 mL), before anhydrous over anhydrous magnesium sulfate, vacuum filtering and the volatiles removed *in vacuo*. The crude product was immediately purified by chromatography (chromatatron) (100 % chloroform increasing to 19:1 chloroform: acetonitrile).

Analysis of the crude mixture by NMR, TLC and mass spectrometry detected none of the desired product. Further analysis of the isolated fractions by TLC, mass spectrometry and  $^1\text{H}$  NMR revealed a mixture of unidentifiable compounds and confirmed no presence of the desired demethylated compound.

A large number of further attempts following this procedure were made, each time altering one variable (e.g. temperature, time, concentration of starting materials and reagents), however none were successful.

## Method 2

7-Methoxy-4-methyl-3-propyl-1H-indole (**112**) (101.7 mg, 500  $\mu\text{mol}$ , 1 eq) in anhydrous toluene (20 mL) was added 18-crown-6 (0.264 g, 1 mmol, 2 eq). The resulting solution was agitated with a lump of potassium metal ( $\approx 7$  mm cube) under nitrogen overnight ( $\approx 17$  hrs). The reaction mixture was transferred to a round bottom flask containing isopropanol (1 mL) by means of a long needle through a rubber septum. This mixture was separated with hydrochloric acid (30 mL, 1 M) and diethyl ether ( $2 \times 20$  mL). The combined organic fractions were dried over anhydrous magnesium sulfate, filtered and evaporated to anhydrousness *in vacuo*. The crude was filtered, volatiles removed *in vacuo* and the crude product (0.100 g, 106 %) immediately purified by chromatography (chromatatron) (100 % chloroform increasing to 19: 1 chloroform: acetonitrile) to yield 4-methyl-3-propyl-1H-indol-7-ol (**134**) as off-white crystals (0.052 g, 55 %).<sup>214</sup>

## Method 3

7-Methoxy-4-methyl-3-propyl-1H-indole (**112**) (101.7 mg, 500  $\mu\text{mol}$ , 1 eq) was dissolved in 1-methyl-2-pyrrolidinone (1 mL) and potassium carbonate (0.0104 g,

75  $\mu\text{mol}$ , 0.15 eq) followed by thiophenol (0.1658 g, 154.6  $\mu\text{l}$ , 1506  $\mu\text{mol}$ , 3 eq). This reaction mixture was heated to reflux (210  $^{\circ}\text{C}$ ) for 18 hrs under nitrogen before cooling, quenching with hydrochloric acid (10 mL, 1 M) and extracting with diethyl ether (3  $\times$  10 mL). Combined organic fractions were washed with hydrochloric acid (10 mL, 1 M), dried over magnesium sulphate, filtered and volatiles removed *in vacuo*. The crude product was purified by column chromatography (100 % chloroform increasing to 19:1 chloroform: acetonitrile) to yield 4-methyl-3-propyl-1H-indol-7-ol (**134**) as off-white crystals (0.062 g, 66 %)

Melting Point: 131-132  $^{\circ}\text{C}$

GCMS (DCM) (EI): 15.55 min (single peak), 189 ( $\text{M}^+$ ),  $\text{C}_{12}\text{H}_{15}\text{NO}$  requires 189.25 ( $\text{M}^+$ )

MS (ES): 190.1228 ( $\text{MH}^+$ ),  $\text{C}_{12}\text{H}_{15}\text{NO}$  requires 190.1161 ( $\text{MH}^+$ )

IR (neat): 3418  $\text{cm}^{-1}$  (N-H indole)

$^1\text{H}$  NMR (300 MHz,  $\text{CDCl}_3$ )  $\delta$ : 0.95 (3H, t, ArC- $\text{CH}_2\text{CH}_2\text{CH}_3$ ,  $J_{\text{A}}=7.4\text{Hz}$ ), 1.63 (2H, sex, ArC- $\text{CH}_2\text{CH}_2\text{CH}_3$ ,  $J_{\text{A}}=7.4\text{Hz}$ ), 2.55 (3H, s, Ar- $\text{Me}$ ), 2.79 (2H, td, ArC- $\text{CH}_2\text{CH}_2\text{CH}_3$ ,  $J_{\text{A}}=7.4\text{Hz}$ ,  $J_{\text{B}}=0.7\text{Hz}$ ), 4.71 (1H, br s, OH), 6.33-6.57 (2H, m, 2 $\times$ Ar-CH), 6.84-6.86 (1H, m, indole Ar-CH), 7.17 (1H, br s, NH)

$^{13}\text{C}$  NMR (75 MHz,  $\text{CDCl}_3$ )  $\delta$ : 14.1 (ArC- $\text{CH}_2\text{CH}_2\text{CH}_3$ ), 19.6 (Ar- $\text{Me}$ ), 24.6 (ArC- $\text{CH}_2\text{CH}_2\text{CH}_3$ ), 29.1 (ArC- $\text{CH}_2\text{CH}_2\text{CH}_3$ ), 105.9 (Ar-CH), 118.5 (Ar-NHCHC), 120.2

(Ar-CH), 121.4 (Indole Ar-CH), 123.7 (Ar-C-Me), 126.6 (Ar-C), 127.8 (Ar-C), 139.7 (Ar-C-OH).

#### 4-Methyl-3-propyl-1H-indole-6,7-dione (**135**)



4-Methyl-3-propyl-1H-indol-7-ol (**134**) (47.3 g, 250  $\mu$ mol, 1 eq) was dissolved in acetonitrile (16 mL) to which potassium nitrosodisulfonate (0.268 g, 1 mmol) in potassium dihydrogen phosphate (0.135 g in 16 mL water, 0.062 M) was added at 0 °C under nitrogen. The resultant mixture was stirred for 15 mins at 0 °C before being allowed to warm (25 °C) and then being stirred under nitrogen (18 hrs). The reaction mixture was extracted with ethyl acetate (3  $\times$  15 mL), the organic fractions combined, dried over anhydrous magnesium sulfate and the volatiles removed *in vacuo*. The crude product was purified by flash column chromatography on silica gel (100 % ethyl acetate) to yield 4-methyl-3-propyl-1H-indole-6,7-dione (**135**) as a dark brown precipitate (0.038 g, 75 %).<sup>26</sup>

Melting Point: >230 °C

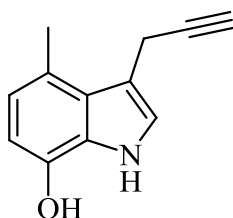
MS (ES): 202 ( $M^-$ ),  $C_{12}H_{13}NO_2$  requires 202.23 ( $M^-$ )

MS (ES): 204.1022 ( $MH^+$ ),  $C_{12}H_{13}NO_2$  requires 204.2450 ( $MH^+$ )

IR (neat): 1625  $\text{cm}^{-1}$  (Quinone C=O), 3166  $\text{cm}^{-1}$  (N-H indole)

$^1\text{H}$  NMR (400 MHz,  $\text{CDCl}_3$ )  $\delta$ : 0.95 (3H, t, C- $\text{CH}_2\text{CH}_2\text{CH}_3$ ,  $J_A=7.3\text{Hz}$ ), 1.53-1.64 (2H, m, C- $\text{CH}_2\text{CH}_2\text{CH}_3$ ), 2.24 (3H, app d,  $\text{CHC-Me}$   $J_A=1.4\text{Hz}$ ), 2.53 (2H, t, C- $\text{CH}_2\text{CH}_2\text{CH}_3$ ,  $J_A=7.7\text{Hz}$ ), 5.72 (1H, s,  $\text{CHC-Me}$ ), 6.96 (1H, s, indole Ar- $\text{CH}$ ), 10.56 (1H, br s,  $\text{NH}$ )

#### 4-Methyl-3-(prop-2-ynyl)-1H-indol-7-ol (136)



#### Method 1

7-Methoxy-4-methyl-3-(prop-2-ynyl)-1H-indole (**112**) (99.6 mg, 500  $\mu\text{mol}$ , 1 eq) was dissolved in acetonitrile (10 mL) and iodotrimethylsilane (1.001 g, 0.712 mL, 5 mmol, 10 eq). The mixture was refluxed under nitrogen (85  $^\circ\text{C}$ , 4 hrs) before cooling, quenching with saturated sodium thiosulphate (20 mL) and extracting with dichloromethane ( $3 \times 20$  mL). The combined organic fractions were washed with saturated sodium thiosulphate (20 mL), then water (20 mL) before anhydrous over anhydrous magnesium sulfate, filtering and the volatiles removed *in vacuo*. The crude product was immediately purified by chromatography (chromatatron) (100 % chloroform increasing to 19:1 chloroform: acetonitrile).

Analysis of the crude product by NMR, TLC and Mass spectrum suggested none of the desired product had been formed. Further analysis of the isolated fractions

by TLC, mass spectrometry and  $^1\text{H}$  NMR revealed a mixture of unidentifiable compounds and confirmed no presence of the desired demethylated compound.

A large number of further attempts following this procedure were made, each time altering one variable (e.g. temperature, time, concentration of starting materials and reagents), however none were successful.

## Method 2

To 7-methoxy-4-methyl-3-(prop-2-ynyl)-1H-indole (**112**) (50 mg, 0.251  $\mu\text{mol}$ ) dissolved in anhydrous dichloromethane (5 mL) at  $-78^\circ\text{C}$  and under nitrogen was added  $\text{BBr}_3\text{-CH}_2\text{Cl}_2$  (0.753 mL, 753  $\mu\text{mol}$ , 1 M, 3 eq) dropwise. The mixture was stirred at  $-78^\circ\text{C}$  for a further 15 mins after which the reaction was allowed to warm ( $25^\circ\text{C}$ ) before stirring for a further 18hrs under nitrogen. The reaction mixture was then quenched with ice water ( $\approx 100$  mL) and extracted with dichloromethane ( $3 \times 10$  mL). The combined organic fractions were further washed with water (10 mL), dried over anhydrous magnesium sulfate, vacuum filtered and the volatiles evaporated *in vacuo*.

Upon analysis of the crude product by NMR, TLC and mass spectrometry none of the desired product was found but a mixture of unidentifiable compounds had been formed. No further attempts were made to either purify or improve this experiment.

## Method 3

7-Methoxy-4-methyl-3-(prop-2-ynyl)-1H-indole (**112**) (99.6 mg, 500  $\mu\text{mol}$ ) was dissolved in 1-methyl-2-pyrrolidinone (1 mL) and potassium carbonate (0.0104 g, 75  $\mu\text{mol}$ , 0.15 eq) before adding thiophenol (0.1658 g, 154.6  $\mu\text{l}$ , 1506  $\mu\text{mol}$ , 3 eq) and the mixture refluxed under nitrogen ( $210^\circ\text{C}$ , 18 hrs) before cooling, quenching with hydrochloric acid (10 mL, 1 M) and extracted with diethyl ether ( $3 \times 10$  mL). The

combined organic fractions were washed with hydrochloric acid (10 mL, 1 M), dried over anhydrous magnesium sulfate, vacuum filtered and volatiles removed *in vacuo*. The crude product was purified by column chromatography (100 % chloroform increasing to 19:1 chloroform: acetonitrile).

Analysis of the crude product by NMR, TLC and mass spectroscopy showed none of the desired product had formed. Further analysis of the isolated fractions by TLC, mass spectroscopy and  $^1\text{H}$  NMR revealed a mixture of unidentifiable compounds and confirmed no presence of the desired demethylated compound.

Further attempts at following this procedure were made, each time altering one variable (e.g. temperature, time, concentration of starting materials and reagents), however none were successful.

#### Method 4

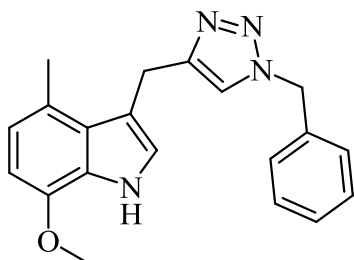
To 7-methoxy-4-methyl-3-(prop-2-ynyl)-1H-indole (**112**) (99.6 mg, 500  $\mu\text{mol}$ , 1 eq) in anhydrous toluene (20 mL) was added 18-crown-6 (0.264 g, 1 mmol, 2 eq). The resulting solution was agitated with a lump of potassium metal ( $\approx 7$  mm cube) under nitrogen overnight ( $\approx 17$  hrs). The reaction mixture was transferred to a round bottom flask containing propan-2-ol (1 mL) by means of a long needle through a rubber septum. The reaction was separated with hydrochloric acid (30 mL, 1 M) and diethyl ether ( $2 \times 20$  mL), before the combined organic fractions were dried over magnesium sulphate, vacuum filtered and evaporated to anhydrousness *in vacuo*. The crude product was immediately purified by chromatography (chromatatron) (97:3 dichloromethane: acetonitrile).

Analysis of the crude mixture by NMR, TLC and mass spectrometry detected none of the desired product. Further analysis of the isolated fractions by TLC, mass

spectrometry and  $^1\text{H}$  NMR revealed a mixture of unidentifiable compounds and confirmed no presence of the desired demethylated compound.

Further attempts at this procedure were made, each time altering one variable (e.g. time, concentration of starting materials and reagents), however none were successful.

### 3-((1-Benzyl-1H-1,2,3-triazol-4-yl)-methyl)-7-methoxy-4-methyl-1H-indole (137)



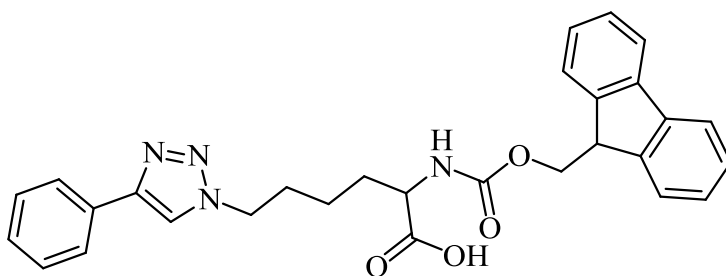
To a stirred solution of 7-methoxy-4-methyl-3-(prop-2-ynyl)-1H-indole (**127**) (0.020 g, 100  $\mu\text{mol}$ , 1 eq) (in methanol (1 mL) making a 0.1 M solution) was added (azidomethyl)benzene (14.6 mg, 110  $\mu\text{mol}$ , 1.1 eq) (in methanol (1.1 mL), making a 0.1 M solution). Copper sulphate (7.98 mg, 50  $\mu\text{mol}$ , 0.5 eq, 0.5 mL, 0.1 M in methanol) was added followed by the quick addition of sodium ascorbate (19.8mg, 100 $\mu\text{mol}$ , 1eq). The reaction was left to stir until TLC showed complete consumption of the 7-methoxy-4-methyl-3-(prop-2-ynyl)-1H-indole, the volatiles were removed *in vacuo*. The resultant material was diluted with ethyl acetate (10 mL) and separated with ammonia (0.5 M, 3  $\times$  10 mL). The organic layer was subsequently separated with several portions of aqueous sodium ethylenediaminetetraacetic acid (6  $\times$  15 mL, 4.016 $\times 10^{-3}$  M), solution followed by acidified brine solution. The combined organic fractions were dried over anhydrous magnesium sulfate and volatiles evaporated *in vacuo* to yield 3-

((1-benzyl-1H-1,2,3-triazol-4-yl)-methyl)-7-methoxy-4-methyl-1H-indole (**137**) as a crude pale yellow oil (19.6 mg, 59 %).<sup>234</sup>

Mass Spectrum (ES): 333 (MH<sup>+</sup>), 331 (M<sup>-</sup>), C<sub>20</sub>H<sub>20</sub>N<sub>4</sub>O requires 332.4

Mass Spectrum (ES): 333.1705 (MH<sup>+</sup>), C<sub>20</sub>H<sub>20</sub>N<sub>4</sub>O requires 333.17154 (MH<sup>+</sup>)

**2-(((9H-Fluoren-9-yl)methoxy)carbonylamino)-6-(4-phenyl-1H-1,2,3-triazol-1-yl)hexanoic acid (138)**



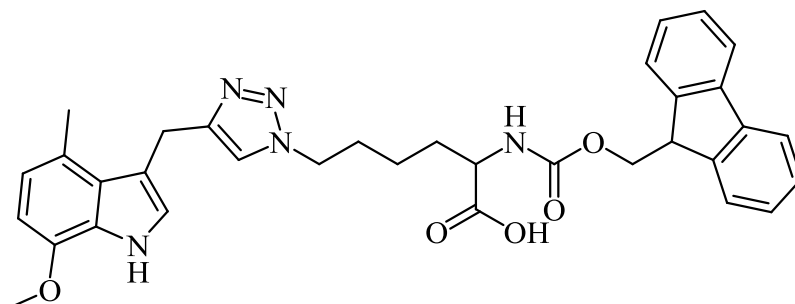
To a stirred solution of ethynylbenzene (0.0102 g, 100  $\mu$ mol, 1 eq) (in methanol (1 mL) making a 0.1M solution) was added 2-(((9H-fluoren-9-yl)-methoxy)-carbonylamino)-6-azidohexanoic acid (43.4 mg, 110  $\mu$ mol, 1.1 eq, 1.1 mL, 0.1 M in methanol). Copper sulphate (7.98mg, 50 $\mu$ mol, 0.5eq, 0.5 mL, 0.1 M in methanol) was then added followed by quick addition of sodium ascorbate (19.8 mg, 100  $\mu$ mol, 1 eq). The reaction was left to stir until TLC showed complete consumption of ethynylbenzene, volatiles were removed *in vacuo*. The resultant material was diluted with ethyl acetate (10 mL) and separated with ammonia (0.5 M, 3  $\times$  10 mL). The organic layer was subsequently separated with aqueous sodium ethylenediaminetetraacetic acid solution (6  $\times$  15 mL, 4.016 $\times$ 10<sup>-3</sup> M) followed by

acidified brine solution. The combined organic fractions were dried over anhydrous magnesium sulfate and volatiles evaporated *in vacuo* to yield crude 2-(((9H-fluoren-9-yl)methoxy)carbonylamino)-6-(4-phenyl-1H-1,2,3-triazol-1-yl)hexanoic acid (**138**) (17.9 mg, 36 %).<sup>234</sup>

Mass spectrum (ES): 497 (MH<sup>+</sup>), 495 (M<sup>-</sup>), C<sub>29</sub>H<sub>28</sub>N<sub>4</sub>O<sub>4</sub> requires 496.2

Mass spectrum (ES): 497.2173 (MH<sup>+</sup>), C<sub>29</sub>H<sub>28</sub>N<sub>4</sub>O<sub>4</sub> requires 497.2189 (MH<sup>+</sup>)

**2-(((9H-Fluoren-9-yl)methoxy)carbonylamino)-6-(4-phenyl-1H-1,2,3-triazol-1-yl)-hexanoic acid (140)**



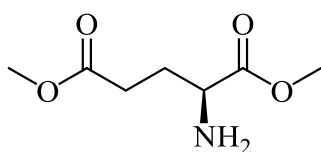
Tris-(Benzyltriazolylmethyl)amine (0.058 g, 110  $\mu$ mol, 1.1 eq) in methanol (1.1 mL) was added to copper sulphate (16 mg, 100  $\mu$ mol, 1 eq), the resulting suspension was placed in a sonicator for approximately 15mins until all the copper had dissolved and was in solution. To a stirred solution of 7-methoxy-4-methyl-3-(prop-2-ynyl)-1H-indole (**127**) (0.020 g, 100  $\mu$ mol, 1 eq, 1 mL, 0.1 M in methanol) was added 2-(((9H-fluoren-9-yl)methoxy)carbonylamino)-6-azidohexanoic acid (43.4 mg, 110  $\mu$ mol, 1.1 eq, 1.1 mL, 0.1 M in methanol). The complexed copper tris-(Benzyltriazolylmethyl)-amine was then added followed by quick addition of sodium

ascorbate (39.6 mg, 200  $\mu\text{mol}$ , 2 eq). The reaction was left to stir until TLC showed complete consumption of 7-methoxy-4-methyl-3-(prop-2-ynyl)-1H-indole (**127**). The resultant material was diluted with ethyl acetate (10 mL) and separated with ammonia (0.5 M,  $3 \times 10$  mL). The organic layer was subsequently separated with ethylenediaminetetraacetic acid solution ( $6 \times 15$  mL,  $4.016 \times 10^{-3}$  M) solution followed by brine solution acidified with hydrochloric acid. The combined organic fractions were dried over anhydrous magnesium sulfate and volatiles evaporated *in vacuo* to yield crude 2-(((9H-Fluoren-9-yl)-methoxy)-carbonylamino)-6-(4-phenyl-1H-1,2,3-triazol-1-yl)-hexanoic acid (**140**) (10.1 mg, 17 %).<sup>234</sup>

Mass Spectrum (ES): 592 (M<sup>-</sup>), C<sub>34</sub>H<sub>35</sub>N<sub>5</sub>O<sub>5</sub> requires 593

Mass Spectrum (ES): 594.2743 (MH<sup>+</sup>), C<sub>34</sub>H<sub>35</sub>N<sub>5</sub>O<sub>5</sub> requires 594.2716 (MH<sup>+</sup>),

### Dimethyl-2-aminopentanedioate



To a stirred suspension of L-glutamic acid (1.47 g, 10 mmol) in anhydrous methanol (33 mL, 0.3 M) in an ice bath was slowly added iodotrimethylsilane (5.6 mL, 44 mmol, 4.4 equiv). The ice bath was removed after the addition was complete and the reaction stirred overnight (12 hrs) until TLC analysis showed complete conversion. All volatile materials were removed *in vacuo*, the oily residue dissolved in water (30 mL) and this solution made just basic by dropwise addition of aqueous sodium hydroxide (25

%). The aqueous solution was extracted with ethyl acetate ( $3 \times 30$  mL), all organic extracts combined, dried over anhydrous magnesium sulfate and the solvent removed *in vacuo* to yield crude dimethyl-2-aminopentanedioate as a clear colourless oil (1.621 g, 93 %). The crude material was then purified by flash column chromatography on silica gel (20:80 ethyl acetate: petroleum ether (40/60 °C)) to yield dimethyl-2-aminopentanedioate as a clear colourless oil (1.362 g, 78 %).

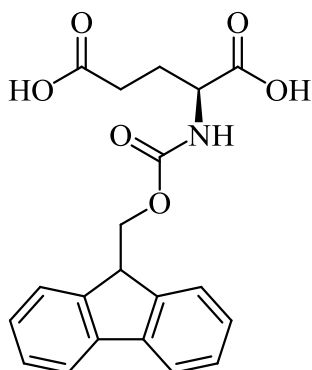
MS (ES): 176 ( $\text{MH}^+$ ),  $\text{C}_7\text{H}_{13}\text{NO}_4$  requires 176.09 ( $\text{MH}^+$ )

MS (ES): 176.0926 ( $\text{MH}^+$ ),  $\text{C}_7\text{H}_{13}\text{NO}_4$  requires 176.0923 ( $\text{MH}^+$ )

IR (neat):  $1729\text{ cm}^{-1}$  (C=O), absence of (O-H)

$^1\text{H}$  NMR (300MHz,  $\text{CD}_3\text{OD}$ )  $\delta$ : 1.45 (2H, s, C-NH<sub>2</sub>), 1.57-1.71 (1H, m, CH<sub>2</sub>CH<sup>1</sup>H<sup>2</sup>CHNH<sub>2</sub>), 1.81-1.94 (1H, m, CH<sub>2</sub>CH<sup>1</sup>H<sup>2</sup>CHNH<sub>2</sub>), 2.28 (2H, app t, CH<sub>2</sub>CH<sup>1</sup>H<sup>2</sup>CHNH<sub>2</sub>), 3.29 (2H, dd, CH<sub>2</sub>CH<sup>1</sup>H<sup>2</sup>CHNH<sub>2</sub>,  $J_A = 8.2\text{Hz}$ ,  $J_B = 5.3\text{Hz}$ ), 3.48 (3H, s, MeOOCCH<sub>2</sub>CH<sup>1</sup>H<sup>2</sup>CHNH<sub>2</sub>), 3.53 (3H, s, NH<sub>2</sub>CHCOOMe).

$^{13}\text{C}$  NMR (75 MHz,  $\text{CDCl}_3$ )  $\delta$ : 29.5 (CH<sub>2</sub>CH<sub>2</sub>CHNH<sub>2</sub>), 30.1 (CH<sub>2</sub>CH<sub>2</sub>CHNH<sub>2</sub>), 51.4 (MeOOCCH<sub>2</sub>CH<sub>2</sub>CHNH<sub>2</sub>), 51.8 (NHCHCOOMe), 53.5 (CH<sub>2</sub>CH<sub>2</sub>CHNH<sub>2</sub>), 173.3 (NHCHCOOMe), 175.9 (MeOOCCH<sub>2</sub>CH<sub>2</sub>CHNH<sub>2</sub>).

**2-((9H-fluoren-9-yl)-methoxy)-carbonylamino)-pentanedioic acid**

L-Glutamic acid (0.772 g, 5.25 mmol) was suspended in water (12.5 mL) and sodium hydrogen bicarbonate (0.882g, 10.5 mmol, 2eq) added with stirring before being cooled over an ice bath. (9H-Fluoren-9-yl)methyl-2,5-dioxopyrrolidin-1-yl carbonate (2.656 g, 7.875 mmol, 1.5 eq) in *para*-dioxane (12.5 mL) was then added slowly. The resultant mixture was stirred at 0°C for 1hr and allowed to warm to room temperature (25 °C) overnight (14hrs) before water was added (25 mL) and the aqueous layer extracted twice with diethyl ether (50 mL) followed by ethyl acetate (50 mL). The remaining aqueous phase was acidified to a pH of 2 by addition of concentrated hydrochloric acid and the aqueous suspension further extracted with ethyl acetate (50 mL). The organic extract was washed with brine (50 mL) then water (50 mL), and anhydrousing over anhydrous anhydrous magnesium sulfate. The combined organic phases were concentrated *in vacuo* and the crude material purified by flash column chromatography on silica gel (40:60 ethyl acetate: petroleum ether (40/60 °C)) to yield 2-((9H-fluoren-9-yl)-methoxy)-carbonylamino)-pentanedioic acid as a white solid (1.419 g, 73 %).

Melting point: 183-185 °C

MS (ES): 370 ( $\text{MH}^+$ ) and 368(MH),  $\text{C}_{20}\text{H}_{19}\text{NO}_6$  requires 370.37 ( $\text{MH}^+$ ) and 368.37 (MH)

IR (neat):  $1693\text{ cm}^{-1}$  (C=O)  $3300\text{ cm}^{-1}$  (N-H)

$^1\text{H}$  NMR (300MHz,  $\text{CD}_3\text{OD}$ )  $\delta$ : 1.85-2.02 (1H, m,  $\text{CH}_2\text{CH}^1\text{H}^2\text{CHNH}_2$ ), 2.12-2.26 (1H, m,  $\text{CH}_2\text{CH}^1\text{H}^2\text{CHNH}_2$ ), 2.42 (2H, app t,  $\text{CH}_2\text{CH}^1\text{H}^2\text{CHNH}_2$ ,  $J_A = 7.4\text{Hz}$ ), 4.18-4.27 (2H, m,  $\text{CH}_2\text{CH}^1\text{H}^2\text{CHNH}_2$  and  $\text{CH}_2\text{CH}^1\text{H}^2\text{CHNH}_2$ ), 4.35 (2H, br d,  $\text{CH}_2\text{CH}^1\text{H}^2\text{CHNH}_2$ ,  $J_A = 7.5\text{Hz}$ ), 7.28-7.89 (8H, m, Ar-H).

$^{13}\text{C}$  NMR (75 MHz,  $\text{CD}_3\text{OD}$ )  $\delta$ : 27.9 ( $\text{CH}_2\text{CH}^1\text{H}^2\text{CHNH}_2$ ), 31.2 ( $\text{CH}_2\text{CH}^1\text{H}^2\text{CHNH}_2$ ), 48.7 (Fmoc,  $\text{CH}_2\text{CH}^1\text{H}^2\text{CHNH}_2$ ), 54.7 ( $\text{CH}_2\text{CH}^1\text{H}^2\text{CHNH}_2$ ), 68.0 (Fmoc,  $\text{CH}_2\text{CH}^1\text{H}^2\text{CHNH}_2$ ), 120.9 (Fmoc,  $\text{CHArC}-\text{CH}$ ), 126.3 (Fmoc,  $\text{ArCH}$ ), 128.2 (Fmoc,  $\text{ArCH}$ ), 128.8 (Fmoc,  $\text{ArCH}$ ), 142.6 (Fmoc,  $\text{Ar}-\text{C}-\text{CH}$ ), 145.2 (Fmoc,  $\text{Ar}-\text{C}-\text{CH}$ ), 158.7 (Fmoc,  $\text{NH}-\text{CO}-\text{OCH}_2$ ), 175.4 ( $\text{NHCHCOOH}$ ), 176.4 ( $\text{NHCHCH}_2\text{CH}_2\text{COOH}$ ).

## References

- (1) Wong, C.; Whitesides, G. M. In *Enzymes in Synthetic Organic Chemistry*; Elsevier Science Ltd.: 1995; Vol. Tetrahedron Organic Chemistry Series 12, pp 371.
- (2) Wolfenden, R.; Snider, M. J. *Acc. Chem. Res.* 2001, *34*, 938.
- (3) Pauling, L. *Chem. Eng. News* 1946, *24*, 1375.
- (4) Gandour, R. D.; Schowen, R. L. In *Transition States for Biochemical Processes*; Plenum Press: New York, 1978; pp 77.
- (5) Garcia-Viloca, M.; Gao, J.; Karplus, M.; Truhlar, D. G. *Sci.* 2004, *303*, 186.
- (6) Tsai, C. J.; Jordan, K. D. *J. Phys. Chem.* 1993, *97*, 11227.
- (7) Ma, B.; Kumar, S.; Tsai, C. -.; Hu, Z.; Nussinov, R. *J. Theo. Biol.* 2000, *203*, 383.
- (8) Villa, J.; Warshel, A. *J. Phys. Chem. B* 2001, *105*, 7871.
- (9) Miller, B. G.; Wolfenden, R. *Annu. Rev. Biochem.* 2002, *71*, 847.
- (10) Wu, N.; Moi, Y.; Gaoi, J.; Pai, E. F. *Proc. Natl. Acad. Sci. USA.* 2000, *97*, 2017.
- (11) Warshel, A.; Strajbl, M.; Villa, J.; Florian, J. *Biochem.* 2000, *39*, 14728.
- (12) Radzicka, A.; Wolfenden, R. *Sci.* 1995, *267*, 90.
- (13) Metzler, D. E.; Metzler, C. M. In *Biochemistry: The Chemical Reactions of Living Cells*; Harcourt: USA, 2001; Vol. 2, pp 945.
- (14) Nilsson, U.; Meshalkina, L.; Lindqvist, Y.; Schneider, G. *J. Biol. Chem.* 1997, *272*, 1864.
- (15) Dyda, F.; Furey, W.; Swaminathan, S.; Sax, M.; Farrenkopf, B.; Jordan, F. *Biochem.* 1993, *32*, 6165.
- (16) Ciszak, E. M.; Korotchkina, L. G.; Dominiak, P. M.; Sidhu, S.; Patel, M. S. *J. Biol. Chem.* 2003, *278*, 21240.

- (17) Salisbury, S. A.; Forrest, H. S.; Cruse, W. B. T.; Kennard, O. *Nature* 1979, 280, 843.
- (18) McIntire, W. S. *Annu. Rev. Nutr.* 1998, 18, 145.
- (19) McIntire, W. S.; Wemmer, D. E.; Chistoserdov, A.; Lidstrom, M. E. *Sci* 1991, 252, 817.
- (20) Chen, L.; Mathews, F. S.; Davidson, V. L.; Huizinga, E. G.; Vellieux, F. M. D.; Duine, J. A.; Hol, W. G. J. *FEBS Lett.* 1991, 287, 163-166.
- (21) Chen, L.; Mathews, F. S.; Davidson, V. L.; Huizinga, E. G.; Vellieux, F. M. D.; Hol, W. G. J. *Proteins.* 1992, 14, 288.
- (22) Govindaraj, S.; Eisenstein, E.; Jones, Limei. H. S. U.; Sanders-Loehr, J.; Chistoserdov, A.; Davidson, V. L.; Edwards, S. L. *J. Bacteriol.* 1994, 176, 2922.
- (23) Davidson, V. L.; Brooks, H. B.; Graichen, M. E.; Jones, Limei. H. S. U.; Hyun, Y. L. *Method Enzymol* 1995, 258, 176.
- (24) McIntire, W. S. *Method Enzymol* 1995, 258, 149.
- (25) Tanizawa, K. *J. Biochem.* 1995, 118, 671.
- (26) Itoh, S.; Takada, N.; Ando, T.; Haranou, S.; Huang, X.; Uenoyama, Y.; Ohshiro, Y.; Komatsu, M.; Fukuzumi, S. *J. Org. Chem.* 1997, 62, 5898.
- (27) Reid Bishop, G.; Brooks, H. B.; Davidson, V. L. *Biochem.* 1996, 35, 8948.
- (28) Zhu, Z.; Davidson, V. L. *J. Bio. Chem.* 1998, 273, 14254.
- (29) Husain, M.; Davidson, V. L. *J. Bio. Chem.* 1985, 260, 14626.
- (30) Reid Bishop, G.; Davidson, V. L. *Biochemistry (N. Y. )* 1995, 34, 12082-12086.
- (31) Hyun, Y.; Davidson, V. L. *Biochemistry (N. Y. )* 1995, 34, 12249-12254.
- (32) Husain, M.; Davidson, V. L. *J. Bacteriol.* 1987, 169, 1712.
- (33) Iwaki, M.; Yagi, T.; Horiike, K.; Saeki, Y.; Ushijima, T.; Nozaki, M. *Arch. Biochem. Biophys.* 1983, 220, 253.

- (34) Roujeinikova, A.; Scrutton, N. S.; Leys, D. *J. Bio. Chem.* 2006, *281*, 40264.
- (35) Masgrau, L.; Roujeinikova, A.; Johannissen, L. O.; Hothi, P.; Basran, J.;  
Ranaghan, K. E.; Mulholland, A. J.; Sutcliffe, M. J.; Scrutton, N. S.; Leys, D. *Sci*  
2006, *312*, 237.
- (36) Chen, L.; Durley, R.; Poliks, B. J.; Hamada, K.; Chen, Z.; Scott Mathews, F.;  
Davidson, V. L.; Satow, Y.; Huizinga, E. *Biochem.* 1992, *31*, 4959.
- (37) Hyun, Y. L.; Davidson, V. L. *Biochem.* 1995, *34*, 816.
- (38) Itoh, S.; Takada, N.; Haranou, S.; Ando, T.; Komatsu, M.; Ohshiro, Y.;  
Fukuzumi, S. *J. Org. Chem.* 1996, *61*, 8967.
- (39) Chen, L.; Doi, M.; Durley, R. C. E.; Chistoserdov, A. Y.; Lidstrom, M. E.;  
Davidson, V. L.; Mathews, F. S. *J. Mol. Biol.* 1998, *276*, 131-149.
- (40) Pearson, A. R.; Marimanikkuppam, S.; Li, X.; Davidson, V. L.; Wilmot, C. M. *J.*  
*Am. Chem. Soc.* 2006, *128*, 12416.
- (41) Wang, Y.; Li, X.; Jones, L. H.; Pearson, A. R.; Wilmot, C. M.; Davidson, V. L. *J.*  
*Am. Chem. Soc.* 2005, *127*, 8258-8259.
- (42) Wilmot, C. M.; Davidson, V. L. *Cur. Op. Chem. Bio.* 2009, *13*, 469.
- (43) Chen, L.; Mathews, F. S.; Davidson, V. L.; Tegoni, M.; Rivetti, C.; Rossi, G. L.  
*Protein Sci.* 1993, *2*, 147.
- (44) Itoh, S.; Ohshiro, Y. *Method Enzymol* 1995, *258*, 164.
- (45) Huizinga, E. G.; Zanten, B.; Van Duine, J.; Jongejan, J. A.; Huitema, F.; Wilson,  
K. S.; Hol, W. G. J. *Biochem.* 1992, *31*, 9789.
- (46) Ohshiro, Y.; Itoh, S. *Pure Appl. Cem.* 1994, *66*, 753.
- (47) Anthony, C. *Biochem. J.* 1996, *320*, 697.
- (48) Brooks, H. B.; Jones, L. H.; Davidson, V. L. *Biochem.* 1993, *32*, 2725.
- (49) Hyun, Y. L.; Davidson, V. L. *Biochim. Biophys. Acta. BBA* 1995, *1251*, 198.

- (50) Davidson, V. L. *Biochem. J.* 1989, 261, 107.
- (51) Kenny, W. C.; McIntire, W. S. *Biochem.* 1983, 22, 3858.
- (52) Durley, R.; Chen, L.; Mathews, F. S.; Lim, L. W.; Davidson, V. L. *Protein Sci.* 1993, 2, 739.
- (53) Romero, A.; Nar, H.; Huber, R.; Messerschmidt, A.; Kalverda, A. P.; Canters, G. W.; Durley, R.; Mathews, F. S. *J. Mol. Bio.* 1994, 236, 1196.
- (54) Jørgensen, L. E.; Ubbink, M.; Danielsen, E. *J. Bio. Inorg. Chem.* 2004, 9, 27.
- (55) Chen, L.; Mathews, F. S.; Davidson, V. L.; Huizinga, E. G.; Vellieux, F. M. D.; Hol, W. G. J. *Protien Struct. Func. Bioinfor.* 1992, 14, 288.
- (56) Brooks, H. B.; Davidson, V. L. *Biochem.* 1994, 33, 5696.
- (57) Itoh, S.; Ogino, M.; Haranou, S.; Terasaka, T.; Ando, T.; Komatsu, M.; Ohshiro, Y.; Fukuzumi, S.; Kano, K.; Takagi, K.; Ikeda, T. *J. Am. Chem. Soc.* 1995, 117, 1485.
- (58) Hauge, H. G. *J. Bio. Chem.* 1964, 239, 3630.
- (59) Westerling, J.; Frank, J.; Duine, J. A. *Biochem. Biophys. Res. Comm.* 1979, 87, 719.
- (60) Davidson, V. L. *Adv. Protein. Chem.* 2001, 58, 95.
- (61) Anthony, C.; Ghosh, M.; Blake, C. C. F. *Biochem. J.* 1994, 304, 665.
- (62) Itoh, S.; Fukui, Y.; Ogino, M.; Haranou, S.; Komatsu, M.; Ohshiro, Y. *J. Org. Chem.* 1992, 57, 2788.
- (63) Itoh, S.; Ogino, M.; Fukui, Y.; Murao, H.; Komatsu, M.; Ohshiro, Y.; Inoue, T.; Kai, Y.; Kasai, N. *J. Am. Chem. Soc.* 1993, 115, 9960.
- (64) Satoh, A.; Kim, J.; Miyahara, I.; Devreese, B.; Vandenberghe, I.; Hacisalihoglu, A.; Okajima, T.; Kuroda, S.; Adachi, O.; Duine, J. A.; Van Beeumen, J.; Tanizawa, K.; Hirotsu, K. *J. Bio. Chem.* 2002, 277, 2830.

- (65) Murakami, Y.; Yoshimoto, N.; Fujieda, N.; Ohkubo, K.; Hasegawa, T.; Kano, K.; Fukuzumi, S.; Itoh, S. *J. Org. Chem.* 2007, 72, 3369-3380.
- (66) Wang, S. X.; Nakamura, N.; Murei, M.; Klinman, J. P.; Sanders-Loehr, J. *J. Bio. Chem.* 1997, 272, 28841.
- (67) Frebort, I.; Pec, P.; Luhovfi, L.; Toyama, H.; Matsushita, K.; Hirota, S.; Kitagawa, T.; Ueno, T.; Asano, Y.; Kato, Y.; Adachi, O. *Biochim. Biophys. Acta.* 1996, 1295, 59.
- (68) Nakamura, N.; Matsuzaki, R.; Choi, Y.; Tanizawa, K.; Sanders-Loehr, J. *J. Bio. Chem.* 1996, 271, 4718.
- (69) Schwartz, B.; Olgin, A. K.; Klinman, J. P. *Biochem.* 2001, 40, 2954.
- (70) Stites, T. E.; Mitchell, A. E.; Rucker, R. B. *J. Nutrition* 2000, 130, 719.
- (71) Eliot, A. C.; Kirsch, J. F. *Annu. Rev. Biochem.* 2004, 73, 383.
- (72) Toney, M. D. *Arch. Biochem. Biophys.* 2005, 433, 279.
- (73) Schulman, M. P.; Richert, D. A. *J. Bio. Chem.* 1957, 226, 181.
- (74) Klawans, H. L.; Ringel, S. P.; Shenker, D. M. *J. Neurol. Neurosurg. Psychiat.* 1971, 34, 682.
- (75) Hashemi, M. M.; Ahmadi Beni, Y. *J. Chem. Research* 1998.
- (76) Zimmer, H.; Lankin, D. C.; Horgan, S. W. *Chem. Rev.* 1971, 71, 229.
- (77) McIntire, W. S. *J. Bio. Chem.* 1987, 262, 11012.
- (78) Backes, G.; Davidson, V. L.; Huitema, F.; Duine, J. A.; Sanders-Loehr, J. *Biochem.* 1991, 30, 9201.
- (79) Itoh, S.; Taniguchi, M.; Takada, N.; Nagatomo, S.; Kitagawa, T.; Fukuzumi, S. *J. Am. Chem. Soc.* 2000, 122, 12087.
- (80) Itoh, S.; Mure, M.; Ogino, M.; Ohshiro, Y. *J. Org. Chem.* 1991, 56, 6857.
- (81) Mure, M.; Klinman, J. P. *J. Am. Chem. Soc.* 1993, 115, 7117.

- (82) Mure, M.; Unman, J. P. *J. Am. Chem. Soc.* 1995, *117*, 8698.
- (83) Murakami, Y.; Tachi, Y.; Itoh, S. *Eur. J. Org. Chem.* 2004, 3074.
- (84) Hothi, P.; Roujeinikova, A.; Abu Khadra, K.; Lee, M.; Cullis, P. M.; Leys, D.; Scrutton, N. S. *Biochem.* 2007, *46*, 9250.
- (85) Hothi, P.; Lee, M.; Cullis, P. M.; Leys, D.; Scrutton, N. S. *Biochem.* 2008, *47*, 183.
- (86) Kraut, J. *Sci* 1988, *242*, 533.
- (87) Kurz, J. L. *J. Am. Chem. Soc.* 1963, *85*, 987.
- (88) Wolfenden, R. *Nature* 1969, *223*, 704.
- (89) Wolfenden, R. *Acc. Chem. Res.* 1972, *5*, 10.
- (90) Sutcliffe, M. J.; Scrutton, N. S. *Phil. Trans. R. Soc. Lond. A.* 2000, *358*, 367.
- (91) Snider, M. J.; Wolfenden, R. *Biochem.* 2001, *40*, 11364.
- (92) Wolfenden, R. *Biophys. Chem.* 2003, *105*, 559.
- (93) Wolfenden, R. *Nature* 1969, *223*, 704.
- (94) Campbell, I. D.; Jones, R. B.; Kiener, P. A.; Richards, E.; Waley, S. G.; Wolfenden, R. *Biochem. Biophys. Res. Comm.* 1978, *83*, 347.
- (95) Wolfenden, R. *Annu. Rev. Biophys. Bioeng.* 1976, *5*, 271.
- (96) Buchowiecki, M.; Vaniček, J. *J. Chem. Phys.* 2010, *132*, 194106.
- (97) Marcus, A. R.; Sutin, N. *Biochim. Biophys. Acta.* 1985, *811*, 265.
- (98) Basran, J.; Patel, S.; Sutcliffe, M. J.; Scrutton, N. S. *J. Bio. Chem.* 2001, 276, 6234.
- (99) Bruno, W. J.; Bialek, W. *Biophys. J.* 1992, *63*, 689.
- (100) Scrutton, N. S. *Biochem. Soc. Trans.* 1999, *27*, 767.
- (101) Devault, D. *Q. Rev. Biophys.* 1980, *13*, 387.
- (102) Scrutton, N. S.; Basran, J.; Sutcliffe, M. J. *Eur. J. Biochem.* 1999, *264*, 666.

- (103) Miyashita, O.; Axelrod, H. L.; Onuchic, J. N. *J. Bio. Phys.* 2002, 28, 383.
- (104) Hopfield, J. J. *Proc. Natl. Acad. Sci. USA.* 1974, 71, 3640.
- (105) Bahnson, B. J.; Klinman, J. P. *Method Enzymol.* 1995, 249, 373.
- (106) Grant, K. L.; Klinman, J. P. *Biochem.* 1989, 28, 6597.
- (107) Cha, Y.; Murray, C. J.; Klinman, J. P. *Science* 1989, 243, 1325.
- (108) Jonsson, T.; Edmondson, D. E.; Klinman, J. P. *Biochem.* 1994, 33, 14871.
- (109) Jonsson, T.; Glickman, M. H.; Sun, S.; Klinman, J. P. *J. Am. Chem. Soc.* 1996, 118, 10319.
- (110) Kohen, A.; Jonsson, T.; Klinman, J. P. *Biochem.* 1997, 36, 2603.
- (111) Swain, G.; Stivers, E. C.; Reuwer Jnr, J. F.; Schaad, L. J. *J. Am. Chem. Soc.* 1958, 80, 5885.
- (112) Schneider, M. E.; Stern, M. J. *J. Am. Chem. Soc.* 1972, 94, 1517.
- (113) Sumi, H.; Ulstrup, J. *Biochim. Biophys. Acta.* 1988, 955, 26.
- (114) Kramers, H. A. *Physica* 1940, 7, 284.
- (115) Basran, J.; Sutcliffe, M. J.; Scrutton, N. S. *Biochem.* 1999, 38, 3218.
- (116) Borgis, D.; Hynes, J. T. *J. Chem. Phys.* 1991, 94, 3619.
- (117) Antoniou, D.; Schwartz, S. D. *Proc. Natl. Acad. Sci. USA.* 1997, 94, 12360.
- (118) Suárez, A.; Silbey, R. *J. Chem. Phys.* 1991, 94, 4809.
- (119) Alberty, W. J.; Knowles, J. R. *Biochem.* 1976, 15, 5631.
- (120) Nambiar, K. P.; Stauffer, D. M.; Kolodziej, P. A.; Benner, S. A. *J. Am. Chem. Soc.* 1983, 105, 5886.
- (121) Rodgers, J.; Femec, D. A.; Schowen, R. L. *J. Am. Chem. Soc.* 1982, 104, 3263.
- (122) Klinman, J. P. *Trends Biochem. Sci.* 1989, 14, 368.
- (123) England, P. M. *Biocem.* 2004, 43, 11623.

- (124) Heckler, T. G.; Chang, L.; Zama, Y.; Naka, T.; Chorghade, M. S.; Hecht, S. M. *Biochem.* 1984, *23*, 1468.
- (125) Noren, C. J.; Anthony-Cahill, S. J.; Griffith, M. C.; Schultz, P. G. *Science* 1989, *244*, 182.
- (126) Bain, J. D.; Glabe, C. G.; Dix, T. A.; Chamberlin, A. R. *J. Am. Chem. Soc.* 1989, *111*, 8013.
- (127) Stryer, L. In *Biochemistry - Fourth Edition*; 1995, pp 1064.
- (128) Dougherty, D. A. *Science* 1996, *271*, 163.
- (129) Zhong, W.; Gallivan, J. P.; Zhang, Y.; Li, L.; Lester, H. A.; Dougherty, D. A. *Proc. Natl. Acad. Sci. USA.* 1998, *95*, 12088.
- (130) Gallivan, J. P.; Dougherty, D. A. *Proc. Natl. Acad. Sci. USA.* 1999, *96*, 9459.
- (131) Lundblad, R. L. In *Chemical Reagents for Protein Modification - Third Edition*; 2005; , pp 313.
- (132) Wang, L.; Brock, A.; Herberich, B.; Schultz, P. G. *Science* 2001, *292*, 498.
- (133) Chin, J. W.; Ashton Cropp, T.; Christopher Anderson, J.; Mukherji, M.; Zhang, Z.; Schultz, P. G. *Science* 2003, *301*, 964.
- (134) Hahn, M. E.; Muir, T. W. *Trends Biochem. Sci.* 2005, *30*, 26.
- (135) Merrifield, R. B. *J. Am. Chem. Soc.* 1963, *85*, 2149.
- (136) Cemazar, M.; Craik, D. J. *J. Pept. Sci.* 2008, *14*, 683.
- (137) Knorr, R.; Trzeciak, A.; Bannwarth, W.; Gillessen, D. *Tet. Lett.* 1989, *30*, 1927.
- (138) Guillier, F.; Orain, D.; Bradley, M. *Chem. Rev.* 2000, *100*, 2091.
- (139) Jones, J. In *Amino Acid and Peptide Synthesis*; Oxford University Press: United States, 1992; , pp 82.
- (140) Hu, B.; Messersmith, P. B. *Tet. Lett.* 2000, *41*, 5795.

- (141) Greene, T. W.; Wuts, P. G. M. In *Protective Groups in Organic Synthesis - Third Edition*; John Wiley & Sons Inc.: 1999, pp 749.
- (142) Civitello, E. R.; Rapoport, H. *J. Org. Chem.* 1994, 58, 3775.
- (143) Deguest, G.; Bischoff, L.; Fruit, C.; Marsais, F. *Tetrahedron Asymmetry* 2006, 17, 2120.
- (144) Hanby, W. E.; Waley, S. G.; Watson, J. *J. Chem. Soc.* 1950, 3239.
- (145) Bredenkamp, M. W.; Holzapfel, C. W.; van Zyl, W. J. *Synth. Comm.* 1990, 20, 2235.
- (146) Hu, T.; Panek, J. S. *J. Am. Chem. Soc.* 2002, 124, 11368.
- (147) Vollhardt, K. P. C.; Schore, N. E. In *Organic Chemistry - Structure and Function*; W. H. Freeman and Company: United States of America, 1998, pp 1209.
- (148) Seyferth, D.; Menzel, H.; Dow, A. W.; Flood, T. C. *J. Organomet. Chem.* 1972, 44, 279.
- (149) Nahm, S.; Weinreb, S. M. *Tet. Lett.* 1981, 22, 3815.
- (150) Sibi, M. P. *Org. Prep. Proceed. Int.* 1993, 25, 15.
- (151) Mentzel, M.; Hoffmann, H. M. R. *J. Prakt. Chem.* 1997, 339, 517.
- (152) Trost, B. M.; Fleming, I. In *Comprehensive Organic Synthesis - Selectivity, Strategy & Efficiency in Modern Organic Chemistry*; Elsevier: 2005; Vol. 8 - Reduction, pp 1143.
- (153) Mukaiyama, T.; Araki, M.; Takei, H. *J. Am. Chem. Soc.* 1973, 95, 4763.
- (154) Meyers, A. I.; Comins, D. L. *Tet. Lett.* 1978, 19, 5179.
- (155) Kende, A. S.; Scholz, D.; Schneider, J. *Synth. Comm.* 1978, 8, 59.
- (156) Sato, F.; Inoue, M.; Oguro, K.; Sato, M. *Tet. Lett.* 1979, 20, 4303.
- (157) White, J. M.; Tunoori, A. R.; Georg, G. I. *Chem. Innov.* 2000, 30, 17.

- (158) Clayden, J.; Greeves, N.; Warren, S.; Wothers, P. In *Organic Chemistry*; 2009, pp 1511.
- (159) Singh, J.; Satyamurthi, N.; Aidhen, I. S. *J. Prakt. Chem.* 2000, 342, 340.
- (160) Han, K.; Kim, M. *Lett. Org. Chem.* 2007, 4, 20.
- (161) Raghurani, T.; Vijaysaradhi, S.; Singh, I.; Singh, J. *Synth. Comm.* 1999, 29, 3215.
- (162) Levin, J. I.; Turos, E.; Weinreb, S. M. *Synth. Comm.* 1982, 12, 989.
- (163) Padrón, J. M.; Kokotos, G.; Martín, T.; Markidis, T.; Gibbons, W. A.; Martín, V. *S. Tetrahedron Asymmetry* 1998, 9, 3381.
- (164) White, C. G. H.; Tabor, A. B. *Tetrahedron* 2007, 63, 6932.
- (165) Rodriguez, M.; Taddei, M. *Synthesis* 2005, 493.
- (166) Furniss, B. S.; Hannaford, A. J.; Smith, P. W. G.; Tatchell, A. R. In *Vogel's Textbook of Practical Organic Chemistry*; Longman Group UK Limited: 1989; , pp 1514.
- (167) Joshi, A. V.; Baidoosi, M.; Mukhopadhyay, S.; Sasson, Y. *Organic Process Research & Development* 2003, 7, 95.
- (168) Vogel, A. I. In *Vogel's textbook of practical organic chemistry*; 1989.
- (169) Cadogan, J. I. G.; Molina, G. A. *J. Chem. Soc. Perkin Trans. I* 1973, 541.
- (170) Doyle, M. P.; Dellaria Jr., J. F.; Siegfried, B.; Bishop, S. W. *J. Org. Chem.* 1977, 42, 3494.
- (171) Hylarides, M. D.; Mettler Jr., F. A.; patent number 4,577,046; 1986.
- (172) March, J. In *Advanced Organic Chemistry*; John Wiley & Sons: 1985; , pp 1346.
- (173) Magee, M. D.; Walker, S. *Can. J. Chem.* 1971, 49, 1106.
- (174) Bredikhin, A. A.; Vul'fson, S. G.; Vereshchagin, A. N. *Rus. Chem. Bull.* 1981, 30, 2255.
- (175) Lucas, H. J.; Liu, Y. *J. Am. Chem. Soc.* 1933, 55, 1271.

- (176) Sigma-Aldrich Company Ltd. MSDS Phenylhydrazine.  
<http://www.sigmaaldrich.com/catalog/DisplayMSDSContent.do> (accessed October 18th, 2010).
- (177) Blaikie, K. G.; Perkin, W. H. *J. Chem. Soc. Trans.* 1924, 125, 296.
- (178) Cacchi, S.; Fabrizi, G. *Chem. Rev.* 2005, 105, 2873.
- (179) Li, J. J.; Gribble, G. W. In *Palladium in Heterocyclic Chemistry - A Guide for the Synthetic Chemist*; Elsevier: 2007; pp 638.
- (180) Watanabe, Y.; Yamamoto, M.; Shim, S. C.; Miyanaga, S.; Mitsudo, T. *Chem. Let.* 1980, 9, 603.
- (181) Douglas, A. W. *J. Am. Chem. Soc.* 1979, 101, 5676.
- (182) Fahey, D. *J. Chem. Soc. Chem. Commun.* 1970, 417.
- (183) Fahey, D. R. *J. Organomet. Chem.* 1971, 27, 283.
- (184) Kim, T.; Choi, K.; Lee, K.; Park, D.; Jin, M. Y. *Polym. Bull.* 2000, 44, 55.
- (185) Cotton, F. A.; Wilkinson, G. In *Basic Inorganic Chemistry*; John Wiley & Sons, Inc.: 1976; pp 579.
- (186) McMurry, J. In *Organic Chemistry - International Student Edition*; 2004; pp 1176.
- (187) Jain, S.; Hiran, B. L.; Bhatt, C. V. *E-Journal Chem.* 2009, 6, 237.
- (188) Piancatelli, G.; Scettri, A.; D'Auria, M. *Synthesis* 1982, 245.
- (189) Kolb, H. C.; Sharpless, K. B. *Drug Discov. Therapeutics* 2003, 8, 1128.
- (190) Kolb, H. C.; Finn, M. G.; Sharpless, K. B. *Angew. Chem. Int. Ed.* 2001, 40, 2004.
- (191) Wangler, C.; Schirmacher, R.; Bartenstein, P.; Wangler, B. *Curr. Med. Chem.* 2010, 17, 1092.
- (192) Tornøe, C. W.; Christensen, C.; Meldal, M. *J. Org. Chem.* 2002, 67, 3057.

- (193) Rostovtsev, V. V.; Green, L. G.; Fokin, V. V.; Sharpless, K. B. *Angew. Chem. Int. Ed.* 2002, *41*, 2596.
- (194) Huisgen, R. *Proc. Chem. Soc.* 1961, 357.
- (195) Michael, A. *J. Prakt. Chem.* 1893, *48*, 94.
- (196) Rodionov, V. O.; Fokin, V. V.; Finn, M. G. *Angew. Chem. Int. Ed.* 2005, *44*, 2210.
- (197) Meldal, M.; Tornøe, C. W. *Chem Rev* 2008, *108*, 2952.
- (198) Stanley, N. J.; Sejer Pedersen, D.; Nielsen, B.; Kvist, T.; Mathiesen, J. M.; Bräuner-Osborne, H.; Taylor, D. K.; Abell, A. D. *Bioorg. Med. Chem. Lett.* 2010, *20*, 7512.
- (199) Moses, J. E.; Moorhouse, A. D. *Chem. Soc. Rev.* 2007, *36*, 1249.
- (200) Franke, R.; Doll, C.; Eichler, J. *Tet. Lett.* 2005, *46*, 4479.
- (201) Sun, X.; Stabler, C. L.; Cazalis, C. S.; Chaikof, E. L. *Bioconjugate Chem.* 2006, *17*, 52.
- (202) Dawson, P. E.; Muir, T. W.; Clark-Lewis, I.; Kent, S. B. H. *Sci.* 1994, *266*, 776.
- (203) Speers, A. E.; Cravatt, B. F. *Chem. Biol.* 2004, *11*, 535.
- (204) Speers, A. E.; Cravatt, B. F. *ChemBioChem* 2004, *5*, 41.
- (205) Chang, P. V.; Prescher, J. A.; Sletten, E. M.; Baskin, J. M.; Millera, I. A.; Agard, N. J.; Lo, A.; Bertozzi, C. R. *Proc. Natl. Acad. Sci. USA.* 2010, *107*, 1821.
- (206) Agard, N. J.; Prescher, J. A.; Bertozzi, C. R. *J. Am. Chem. Soc.* 2004, *126*, 15046.
- (207) Prescher, J. A.; Bertozzi, C. R. *Nat. Chem. Biol.* 2004, *1*, 13.
- (208) Ma, D.; Lu, X. *Tetrahedron* 1990, *46*, 6319.
- (209) Huckstep, M.; Taylor, R. J. K. *Synthesis* 1982, 881.
- (210) Susumu, K.; Uyeda, H. T.; Medintz, I. L.; Pons, T.; Delehanty, J. B.; Mattoussi, H. *J. Am. Chem. Soc.* 2007, *129*, 13987.

- (211) Jung, M. E.; Lyster, M. A. *J. Org. Chem.* 1977, 42, 3761.
- (212) Jung, M. E.; Lyster, M. A. *J. Chem. Soc., Chem. Commun.* 1978, 315.
- (213) Parmar, A. Model Chemistry of Tryptophan Tryptophylquinone Cofactor, University of Leicester, 2009.
- (214) Ohsawa, T.; Hatano, K.; Kaydh, K.; Kotabe, J.; Oishi, T. *Tet. Lett.* 1992, 33, 5555.
- (215) Nayak, M. K.; Chakraborti, A. K. *Tet. Lett.* 1997, 38, 8749.
- (216) Sims, P. *J. Chem. Soc.* 1959, 1959, 3648.
- (217) Carnahan Jr., J. C.; Closson, W. D.; Ganson, J. R.; Juckett, D. A.; Quaal, K. S. *J. Am. Chem. Soc.* 1976, 98, 2526.
- (218) Ornelas, C.; Broichhagen, J.; Weck, M. *J. Am. Chem. Soc.* 2010, 132, 3923.
- (219) Lallana, E.; Fernandez-Megia, E.; Riguera, R. *J. Am. Chem. Soc.* 2009, 131, 5748.
- (220) Chan, T. R.; Hilgraf, R.; Sharpless, K. B.; Fokin, V. V. *Org. Lett.* 2004, 6, 2853.
- (221) Díez, R.; Badorrey, R.; Díaz-de-Villegas, M. D.; Gálvez, J. A. *European Journal of Organic Chemistry* 2007, 2114.
- (222) Cavero, M.; Hobbs, A.; Madge, D.; Motherwell, W. B.; Selwood, D.; Potier, P. *Bioorg. Med. Chem. Lett.* 2000, 10, 641.
- (223) Demir, A. S.; Sesenoglu, O.; Aksoy-Cam, H.; Kaya, H.; Aydogan, K. *Tetrahedron: Asymmetry* 2003, 14, 1335.
- (224) Pettit, G. R.; Nelson, P. S. *J. Org. Chem.* 1986, 51, 1282.
- (225) Sobolev, I. *J. Org. Chem.* 1961, 26, 5080.
- (226) Koshi, K.; Shimizu, M. *Chem. Pharm. Bull.* 1968, 16, 2343.
- (227) Yoshida, S.; Watanabe, T.; Sato, Y. *Bioorg. Med. Chem.* 2007, 15, 3515.
- (228) Gopalsamy, A., *J. Med. Chem.* 2004, 47, 6603.

- (229) Fischer, A.; Fyles, D. L.; Henderson, G. N.; Mahasay, S. R. *Can. J. Chem.* 1986, 64, 1764.
- (230) Nozoe, T.; Takase, K.; Yasunami, M.; Ando, M.; Hiroaki, S.; Imafuku, K.; Yin, B.; Honda, M.; Goto, Y.; Hanaya, T.; Hara, Y.; Yamamoto, H. *Bull. Chem. Soc. Jpn.* 1989, 62, 128.
- (231) Padwa, A.; Kulkarni, Y. S.; Zhang, Z. *J. Org. Chem.* 1990, 55, 4144.
- (232) Hamano, H.; Nagata, K.; Fukada, N.; Shimotahira, H.; Ju, X.; Ozoe, Y. *Bioorg. Med. Chem.* 2000, 8, 665.
- (233) Deaton, K. R.; Gin, M. S. *Org. Lett.* 2003, 5, 2477.
- (234) Shah, J.; Khan, S. S.; Blumenthal, H.; Liebscher, J. *Synthesis* 2009, 3975.

## 7. Appendix

### 7.1. Appendix 1 – X-ray Crystal Data

#### 7.1.1. 5-benzyl-1-methyl-2-(tert-butoxycarbonylamino)-pentanedioate

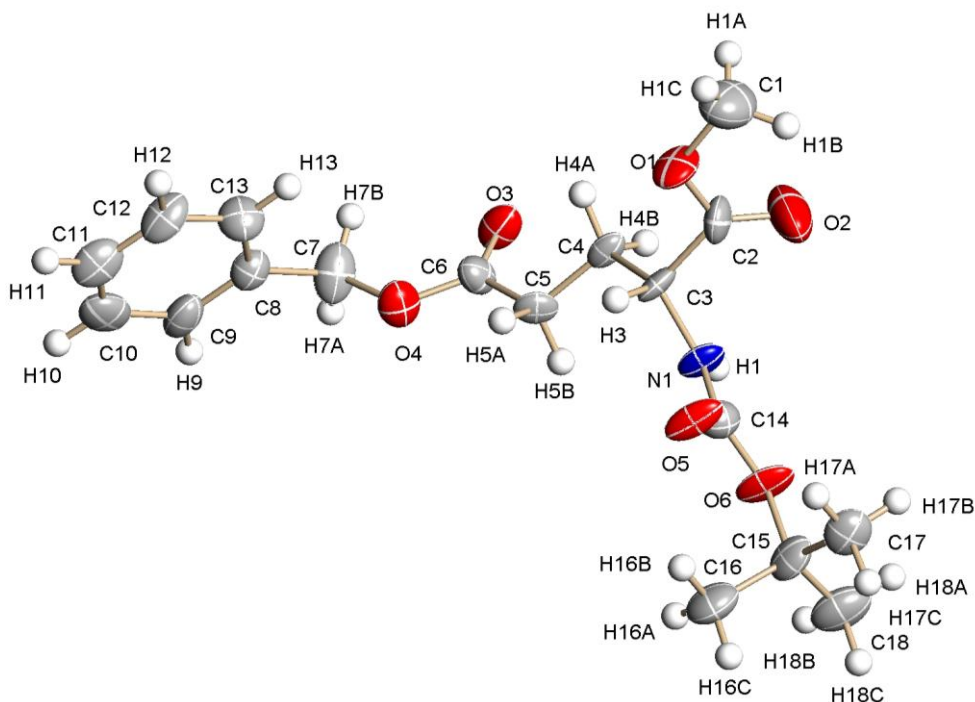
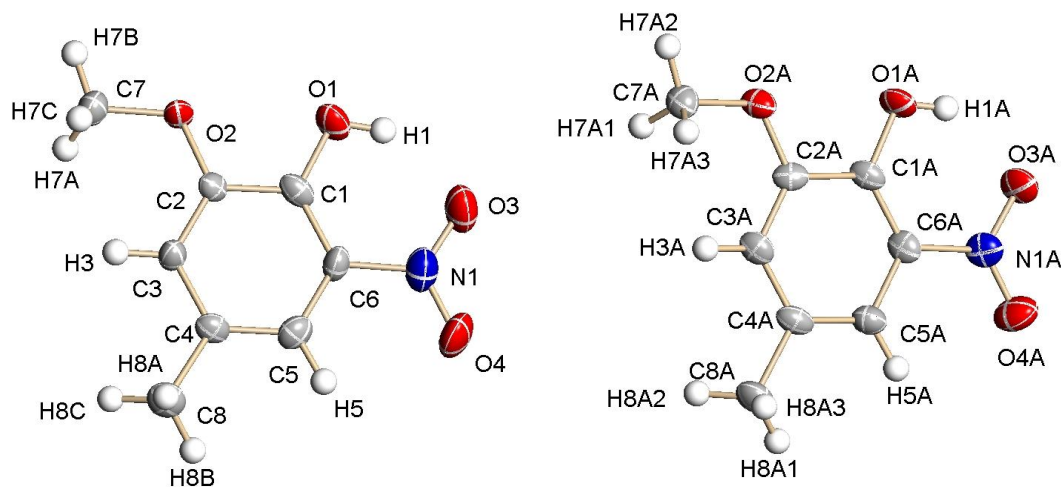


Figure shows 50% displacement ellipsoids. There is intermolecular hydrogen bonding; hydrogen bonds with  $H \dots A < r(A) + 2.000$  Angstroms and  $\langle DHA \rangle > 110$  deg.

Identification code	07033
Empirical formula	C <sub>18</sub> H <sub>25</sub> N O <sub>6</sub>
Formula weight	351.39
Temperature	150(2) K
Wavelength	0.71073 Å
Crystal system	Orthorhombic
Space group	P2(1)2(1)2(1)

Unit cell dimensions	$a = 5.161(2) \text{ \AA}$	$\alpha = 90^\circ$ .
	$b = 10.196(4) \text{ \AA}$	$\beta = 90^\circ$ .
	$c = 36.773(15) \text{ \AA}$	$\gamma = 90^\circ$ .
Volume	$1935.0(14) \text{ \AA}^3$	
Z	4	
Density (calculated)	$1.206 \text{ Mg/m}^3$	
Absorption coefficient	$0.090 \text{ mm}^{-1}$	
F(000)	752	
Crystal size	$0.32 \times 0.18 \times 0.08 \text{ mm}^3$	
Theta range for data collection	$1.11$ to $25.00^\circ$ .	
Index ranges	$-6 \leq h \leq 6$ , $-12 \leq k \leq 12$ , $-43 \leq l \leq 43$	
Reflections collected	13706	
Independent reflections	3392 [R(int) = 0.1943]	
Completeness to theta = $25.00^\circ$	99.8 %	
Absorption correction	None	
Refinement method	Full-matrix least-squares on $F^2$	
Data / restraints / parameters	3392 / 0 / 231	
Goodness-of-fit on $F^2$	1.111	
Final R indices [ $I > 2\sigma(I)$ ]	$R1 = 0.1236$ , $wR2 = 0.2708$	
R indices (all data)	$R1 = 0.1868$ , $wR2 = 0.3037$	
Absolute structure parameter	0(5)	
Extinction coefficient	$0.018(5)$	
Largest diff. peak and hole	$0.374$ and $-0.355 \text{ e.\AA}^{-3}$	

**Table 5:** Crystal data and structure refinement for 07033.

7.1.2. 2-Methoxy-4-methyl-6-nitrophenol

Figures show 50% displacement ellipsoids. Shown are the two unique molecules in the unit cell. There is intramolecular hydrogen bonding; hydrogen bonds with  $H..A < r(A) + 2.000$  Angstroms and  $\langle DHA \rangle > 110$  deg.

Identification code	08063	
Empirical formula	C <sub>8</sub> H <sub>9</sub> N O <sub>4</sub>	
Formula weight	183.16	
Temperature	150(2) K	
Wavelength	0.71073 Å	
Crystal system	Monoclinic	
Space group	P2(1)/n	
Unit cell dimensions	$a = 3.8394(10)$ Å	$\alpha = 90^\circ$ .
	$b = 26.437(6)$ Å	$\beta = 94.414(5)^\circ$ .
	$c = 16.170(4)$ Å	$\gamma = 90^\circ$ .
Volume	$1636.4(7)$ Å <sup>3</sup>	
Z	8	

Density (calculated)	1.487 Mg/m <sup>3</sup>
Absorption coefficient	0.121 mm <sup>-1</sup>
F(000)	768
Crystal size	0.16 x 0.14 x 0.08 mm <sup>3</sup>
Theta range for data collection	1.48 to 25.00°.
Index ranges	-4<=h<=4, -31<=k<=31, -19<=l<=19
Reflections collected	11637
Independent reflections	2896 [R(int) = 0.1194]
Completeness to theta = 25.00°	99.9 %
Absorption correction	Empirical
Max. and min. transmission	0.9904 and 0.9809
Refinement method	Full-matrix least-squares on F <sup>2</sup>
Data / restraints / parameters	2896 / 0 / 241
Goodness-of-fit on F <sup>2</sup>	1.050
Final R indices [I>2sigma(I)]	R1 = 0.0779, wR2 = 0.1493
R indices (all data)	R1 = 0.1546, wR2 = 0.1749
Largest diff. peak and hole	0.287 and -0.236 e.Å <sup>-3</sup>

**Table 6:** Crystal data and structure refinement for 08063.

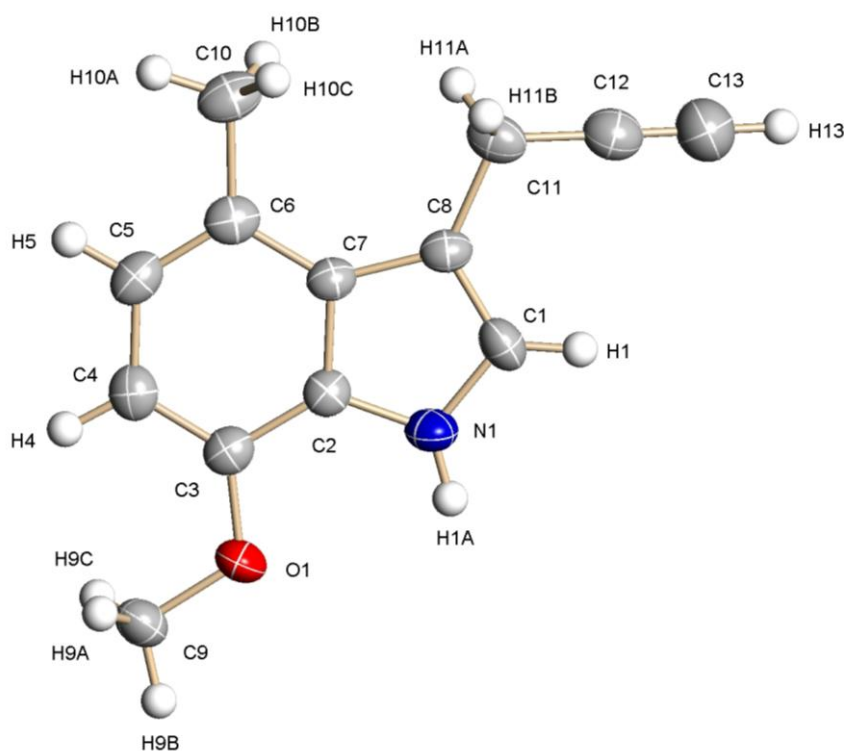
7.1.3. 7-methoxy-4-methyl-3-(prop-2-ynyl)-1H-indole

Figure shows 50% displacement ellipsoids.

Identification code	10023	
Empirical formula	C <sub>13</sub> H <sub>13</sub> N O	
Formula weight	199.24	
Temperature	150(2) K	
Wavelength	0.71073 Å	
Crystal system	Orthorhombic	
Space group	Pccn	
Unit cell dimensions	a = 15.976(4) Å	α = 90°.
	b = 18.599(5) Å	β = 90°.
	c = 7.0681(18) Å	γ = 90°.
Volume	2100.2(9) Å <sup>3</sup>	

Z	8
Density (calculated)	1.260 Mg/m <sup>3</sup>
Absorption coefficient	0.080 mm <sup>-1</sup>
F(000)	848
Crystal size	0.18 x 0.09 x 0.07 mm <sup>3</sup>
Theta range for data collection	2.19 to 24.99°.
Index ranges	-18<=h<=18, -22<=k<=22, -8<=l<=8
Reflections collected	14048
Independent reflections	1853 [R(int) = 0.2184]
Completeness to theta = 24.99°	99.9 %
Absorption correction	Empirical
Max. and min. transmission	0.969 and 0.329
Refinement method	Full-matrix least-squares on F <sup>2</sup>
Data / restraints / parameters	1853 / 0 / 138
Goodness-of-fit on F <sup>2</sup>	0.846
Final R indices [I>2sigma(I)]	R1 = 0.0594, wR2 = 0.0981
R indices (all data)	R1 = 0.1554, wR2 = 0.1217
Largest diff. peak and hole	0.168 and -0.152 e.Å <sup>-3</sup>

**Table 7:** Crystal data and structure refinement for 10023.

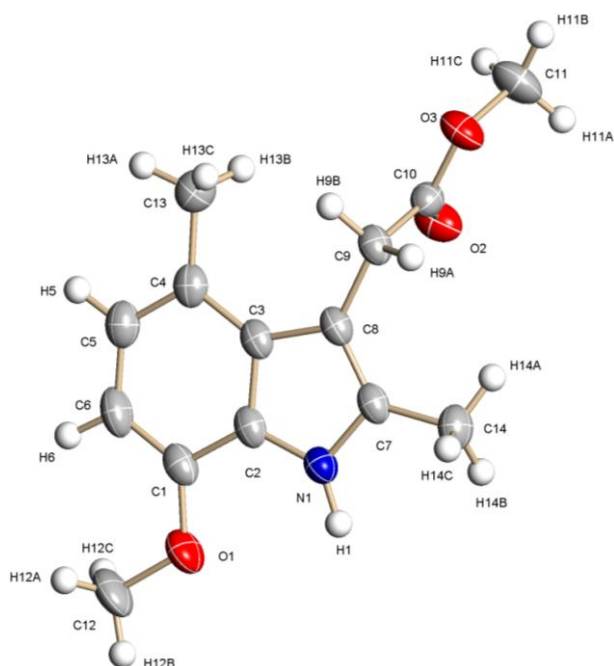
7.1.4. Methyl-2-(7-methoxy-2,4-dimethyl-1H-indol-3-yl)-acetate

Figure shows 50% displacement ellipsoids. There is intermolecular hydrogen bonding; hydrogen bonds with  $H \cdots A < r(A) + 2.000$  Angstroms and  $\langle DHA \rangle > 110$  deg.

Identification code	10064	
Empirical formula	C <sub>14</sub> H <sub>17</sub> N O <sub>3</sub>	
Formula weight	247.29	
Temperature	150(2) K	
Wavelength	0.71073 Å	
Crystal system	Monoclinic	
Space group	P2(1)/n	
Unit cell dimensions	$a = 10.378(7)$ Å	$\alpha = 90^\circ$ .
	$b = 8.135(6)$ Å	$\beta = 102.259(12)^\circ$ .
	$c = 15.460(11)$ Å	$\gamma = 90^\circ$ .
Volume	$1275.4(16)$ Å <sup>3</sup>	

Z	4
Density (calculated)	1.288 Mg/m <sup>3</sup>
Absorption coefficient	0.091 mm <sup>-1</sup>
F(000)	528
Crystal size	0.43 x 0.29 x 0.22 mm <sup>3</sup>
Theta range for data collection	2.17 to 24.99°.
Index ranges	-12<=h<=12, -9<=k<=9, -18<=l<=18
Reflections collected	8782
Independent reflections	2241 [R(int) = 0.0536]
Completeness to theta = 24.99°	99.9 %
Absorption correction	Empirical
Max. and min. transmission	0.969 and 0.585
Refinement method	Full-matrix least-squares on F <sup>2</sup>
Data / restraints / parameters	2241 / 0 / 167
Goodness-of-fit on F <sup>2</sup>	1.041
Final R indices [I>2sigma(I)]	R1 = 0.0497, wR2 = 0.1231
R indices (all data)	R1 = 0.0613, wR2 = 0.1292
Largest diff. peak and hole	0.232 and -0.178 e.Å <sup>-3</sup>

**Table 8:** Crystal data and structure refinement for 10064.